AD

USAAMRDL TECHNICAL REPORT 71-33

HELICOPTER AURAL DETECTABILITY

By

J. B. Ollerhead

July 1971

EUSTIS DIRECTORATE
U. S. ARMY AIR MOBILITY RESEARCH AND DEVELOPMENT LABORATORY
FORT EUSTIS, VIRGINIA

CONTRACT DAAJ02-69-C-0083
WYLE LABORATORIES
HAMPTON, VIRGINIA

Unclassified

Security Classification

DOCUMENT CONTROL DATA - R & D

(Security classification of title, body of abstract and indexing annotation must be entered when the overall report is classified)

1. ORIGINATING ACTIVITY (Corporate author)	2a. REPORT SECURITY CLASSIFICATION
Wyle Laboratories Hampton, Virginia	Unclassified
	2b. GROUP

3. REPORT TITLE

HELICOPTER AURAL DETECTABILITY

4. DESCRIPTIVE NOTES (Type of report and inclusive dates)

Final Report

5. AUTHOR(S) (First name, middle initial, last name)

John B. Ollerhead

6. REPORT DATE	7a. TOTAL NO. OF PAGES	7b. NO. OF REFS
July 1971	196	81

8a. CONTRACT OR GRANT NO.	9a. ORIGINATOR'S REPORT NUMBER(S)
DAAJ02-69-C-0083	USAAMRDL Technical Report 71-33
b. PROJECT NO. Task 1F162204A14235	
c.	9b. OTHER REPORT NO(S) (Any other numbers that may be assigned this report)
d.	WR 71-3

10. DISTRIBUTION STATEMENT

Approved for public release; distribution unlimited.

11. SUPPLEMENTARY NOTES	12. SPONSORING MILITARY ACTIVITY
	Eustis Directorate U. S. Army Air Mobility Research & Development Laboratory, Ft. Eustis, Va.

13. ABSTRACT

The principal objective of this study is to develop the methodology for the prediction of helicopter aural detection thresholds from measured or estimated parameters of significance. The subjective aspects of helicopter noise are discussed. A review is presented of the effects of atmospheric and terrain features upon the observed sound, and of the limitations in the measurement and analysis of helicopter noise. An experimental program is described, in which a group of subjects listened to a large number of synthetic and recorded helicopter sounds inside a specially designed acoustic chamber. Through these experiments, a model for calculating aural detection thresholds is developed, tested, and found to be accurate to within ±4dB. Appendices to the report include detailed instructions for applying several versions of the developed method and also provide simplified procedures for estimating propagation losses.

DD FORM 1 NOV 68 1473 REPLACES DD FORM 1473, 1 JAN 64, WHICH IS OBSOLETE FOR ARMY USE.

Unclassified

Security Classification

DISCLAIMERS

The findings in this report are not to be construed as an official Department of the Army position unless so designated by other authorized documents.

When Government drawings, specifications, or other data are used for any purpose other than in connection with a definitely related Government procurement operation, the United States Government thereby incurs no responsibility nor any obligation whatsoever; and the fact that the Government may have formulated, furnished, or in any way supplied the said drawings, specifications, or other data is not to be regarded by implication or otherwise as in any manner licensing the holder or any other person or corporation, or conveying any rights or permission, to manufacture, use, or sell any patented invention that may in any way be related thereto.

DISPOSITION INSTRUCTIONS

Destroy this report when no longer needed. Do not return it to the originator.

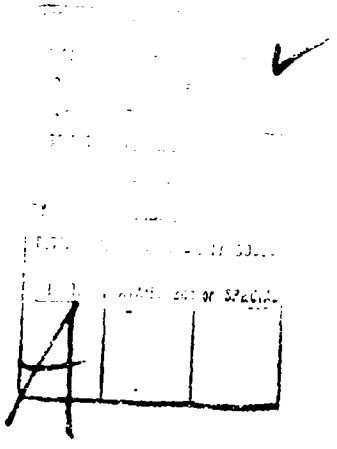

14. KEY WORDS	LINK A		LINK B		LINK C	
	ROLE	WT	ROLE	WT	ROLE	WT
Noise						
Helicopter Noise						
Aural Detectability						

DEPARTMENT OF THE ARMY
U. S. ARMY AIR MOBILITY RESEARCH & DEVELOPMENT LABORATORY
EUSTIS DIRECTORATE
FORT EUSTIS, VIRGINIA 23604

The objective of this program was twofold. The first was to analyze, identify, and analytically define those parameters which contribute to the subjective characteristics of helicopter noise. The second was to develop a practical method for predicting the detectability threshold of helicopter noise from measurable characteristics of the signature and the ambient conditions.

This report has been reviewed by the Eustis Directorate, U. S. Army Air Mobility Research and Development Laboratory. The report is considered to be technically sound and to meet the objective for this program. The report is published for the dissemination of information and appropriate application.

The technical monitor for this contract was Mr William E. Nettles, Aeromechanics Division.

Task 1F162204A14235
Contract DAAJ02-69-C-0083
USAAMRDL Technical Report 71-33
July 1971

HELICOPTER AURAL DETECTABILITY

Final Report

Wyle Research Staff Report WR 71-3

By

J. B. Ollerhead

Prepared by

Wyle Laboratories
Hampton, Virginia

for

EUSTIS DIRECTORATE
U.S. ARMY AIR MOBILITY RESEARCH AND DEVELOPMENT LABORATORY
FORT EUSTIS, VIRGINIA

ABSTRACT

Because of their high-level and characteristic noise signatures, helicopters suffer the tactical disadvantage that they can be heard at very great distances and efforts to reduce this detection range are continuing. Extensive research into helicopter noise generation mechanisms has now made it possible to estimate the radiation with some confidence at the design stage. Unfortunately, sound propagation and aural detection, factors of equal importance to the military problem, have not been understood to the same extent. Consequently, the principal objective of this experimental program was to develop the methodology for the prediction of helicopter aural detection thresholds from measured or estimated parameters of significance.

Following a discussion of the subjective aspects of helicopter noise generation, the effects of atmospheric and terrain features upon the observed sound are reviewed. Limitations in the measurement and analysis of helicopter noise are also examined. A review of research into the mechanisms of human aural detection gives the background to the experiments in which a group of subjects listened to a large number of synthetic and recorded helicopter sounds inside a specially designed acoustic chamber. Through these experiments, a model for calculating aural detection thresholds was developed, tested, and found to be accurate to within ± 4 dB. Appendices to the report include detailed instructions for applying several versions of this method and also provide simplified procedures for estimating propagation losses.

FOREWORD

The work reported herein was performed by Wyle Laboratories Research Staff under Contract DAAJ02-69-C-0083 (Task 1F162204A14235) for the Eustis Directorate, U. S. Army Air Mobility Research and Development Laboratory, Fort Eustis, Virginia. The work was carried out under the technical cognizance of Mr. William E. Nettles of the AMRDL staff.

This report describes the work of many members of Wyle Laboratories Research Staff. In particular the author wishes to acknowledge the considerable efforts of Mr. B. D. Adcock, who designed and developed the data acquisition system and computer analysis procedures described in Appendix II; Dr. R. J. Cunitz, Staff Sensory Psychologist, who evolved the experimental design; Mr. R. B. Boulay, who was responsible for execution of the experimental program; Mr. L. C. Sutherland, who reviewed the sound propagation mechanisms and prepared Section 2.3 and Appendix I of this report; and Mr. A. C. Jolly, who developed methods for the digital generation of acoustic stimuli.

Wyle Laboratories is also indebted to the U. S. Air Force Flight Dynamics Laboratory and Mr. D. L. Smith for making available a large number of helicopter noise recordings and to the National Aeronautics and Space Administration, Langley Research Center, Dynamics Loads Division and Mr. D. Hilton for similar services.

Figure 23 is included by special permission of John Wiley and Sons, Inc. of New York, N. Y.

TABLE OF CONTENTS

TABLE OF CONTENTS (Continued)

TABLE OF CONTENTS (Continued)

TABLE OF CONTENTS (Continued)

ILLUSTRATIONS

LIST OF TABLES

LIST OF SYMBOLS

Note: The following symbols are defined according to their general use in the main text of the report. Other symbols and all those used in the Appendices are used only locally and are defined where they first occur.

a	attenuation, dB/1000 ft
a_n, b_n	cosine and sine harmonic components of n-th sound harmonic
f	frequency, Hz
f_o	fundamental frequency, Hz
n	harmonic number, 1/3-octave frequency band number
p, $p(t)$	fluctuating pressure (sound pressure), lb/ft^2
$\overline{p^2}$	mean square pressure, $(lb/ft^2)^2$
p_o	pressure oscillation amplitude, lb/ft^2
p_f	filtered pressure signal, lb/ft^2
p_{rms}	root mean square pressure, lb/ft^2
t	time, sec
$w(f)$	power spectral density of random noise, (pressure^2/Hz)
A_g	ground attenuation, dB/1000 ft
A'_n	absolute threshold level for tones or critical bands of noise, dB
$E(p^2)$	expected value of mean square pressure, (lb/ft^2)
L	sound pressure level of just audible tone, dB
L_n	measured signal threshold level in n-th 1/3-octave band, dB
L_{n_c}	"theoretical" signal threshold level in n-th 1/3-octave band, dB

LIST OF SYMBOLS (Continued)

L'_n	signal threshold level in n-th critical band, dB
M	Mach number
M_n	band masking level, dB
M'_n	critical band threshold level, dB
N	total number of frequency bands
N_R	rotational speed, rpm
N_s	power spectral density level of just audible noise, dB
N_3	1/3-octave band level of just audible noise, dB
R	relative humidity, %
SR	slant range, ft
SPL	sound pressure level
T	averaging time, sec
T	temperature, ^{o}F
T_o	fundamental period, sec
T'_n	combined critical band threshold level, dB
β	elevation angle, degrees
σ_{p^2}	standard deviation of mean square pressure fluctuations (lb/ft^2)
σ_{EA}	standard deviation of excess absorption, dB
Δf	bandwidth, Hz
$\Delta f'$	critical bandwidth, Hz
Δf_3	1/3-octave bandwidth, Hz

1.0 INTRODUCTION

The military value of helicopters for tactical and surveillance missions is reduced by their high-level and very characteristic noise signatures. In many situations a helicopter can be heard approaching from distances between 5 and 10 miles, which at helicopter speeds gives several minutes warning to the enemy. The chances of survival in such situations can be low, and aircrews have learned to take advantage of natural acoustic barriers to minimize this audible warning.

The fact is that noise generated by a helicopter represents a very tiny fraction of its total power expenditure, typically around one tenth of one percent, and it is very difficult to manipulate such a small energy dissipation through aircraft design. Nevertheless, many years of research has led to a fairly clear understanding of helicopter noise generation mechanisms with the result that it is now possible, in principle at least, to exercise some degree of control over the noise characteristics at the design stage.

Unfortunately, the modern helicopter has evolved through a process of aerodynamic and mechanical refinement to the extent that most changes which are desirable for noise reduction purposes generally involve some performance penalty or high manufacturing costs. Such compromises are usually unacceptable, and mainly for this reason helicopters are still noisy. The fact remains, however, that for certain missions, it is most likely that there are potentially beneficial tradeoffs to be made between performance and detection distance. For example, a 6 dB noise reduction could reduce detection distance by half. If this could be achieved for a speed reduction of even 25 percent, a one-third reduction of warning time would result. Obviously, considerably better figures than these may be anticipated.

The difficulty in evaluating such possibilities lies in establishing a realistic relationship between noise reduction at the source and detection distance. Helicopter noise is surprisingly complex and so too, to an even greater degree, is human perception of noise. Unfortunately, although many of the factors which contribute to community annoyance by aircraft noise have been the subject of extensive research, most of the findings are not applicable to the aural detection problem which involves much lower sound intensities. The main study of helicopter detectability was made by Loewy[1] in 1963, and his paper is still the standard reference on the subject.

Whatever the trade-off between noise and performance, it is important that performance penalties are minimized. Without accurate aural detection criteria there is always the danger that emphasis might be addressed at reducing noise in the wrong way. For example, there would be little point in silencing a tail rotor if the main rotor could be heard at greater distances in the first place. With reliable criteria, on the other hand, analytical studies could be made of all operational aspects of specific noise control procedures.

The main objective of the present study is to develop improved criteria for defining helicopter aural detectability thresholds. Consideration is given to the source characteristics, the effects of sound propagation through the air and over ground cover, human hearing acuity, and the ambient noise environment. A comprehensive experimental program was conducted to establish and validate a new threshold prediction procedure, which is described with full instructions for its use in Appendix IV.

Because helicopter noise is so complex, because in the past there has been considerable disagreement between different sources of acoustic data, and because potential sources of error are many, the application of acoustic analysis techniques to helicopter noise have also been reviewed. Attention is confined to the principles involved rather than to hardware details, but it is hoped that the material in Section 2.0 will contribute to a clearer understanding of the data requirements. Section 3.0 is devoted to the human hearing mechanism, and Sections 4.0 and 5.0 describe the experimental program undertaken. The report is concluded in Sections 6.0 and 7.0 by a summary of the major conclusions and a number of recommendations for future research.

2.0 HELICOPTER NOISE ANALYSIS AND PERCEPTION

2.1 FREQUENCY-TIME RELATIONSHIPS

When an observer hears a helicopter approaching, he is sensing fluctuations of the atmospheric pressure at the position of his ears. A microphone (i.e., a sensitive pressure transducer) may also be used to monitor these fluctuations, and if its voltage output is displayed as a function of time on an oscillograph or oscilloscope, patterns such as those shown in Figure 1 will be observed. The mean value of the pressure is the atmospheric ambient, and the oscillations about it are due to wave propagation from pressure disturbances caused by the helicopter (and any other sources in the vicinity). The character of the sound, as judged by the listener, is entirely dependent upon the manner in which the pressure varies with time, and Figure 1 illustrates a number of helicopter noise signatures which vary considerably in their subjective characteristics. The hearing process will be described in some detail in Section 3.0; it is sufficient to state here that the ear is an extremely sensitive pressure sensor with a working dynamic range of over 1,000,000:1.

Tones

The simplest form of acoustic signal is a tone which has a purely sinusoidal pressure time history. Provided the signal is continuous, that is, it repeats itself precisely from cycle to cycle ad infinitum, it can be adequately and conveniently represented in either the time or frequency domain, as shown in Figure 2.

The left-hand diagram shows the function $p_o \sin 2\pi f_c t$ plotted against time in the range $0 < t < T_o$, where T_o is the period of the signal equal to the reciprocal of the frequency f_o. The right-hand diagram is a frequency coordinate f_o. A pure tone is amplitude p_o at the frequency coordinate f_o. A pure tone is rarely, if ever, heard in practice; the closest approximation would be generated by a tuning fork or, electronically, by an oscillator/loudspeaker combination. The frequency of this sound has a first-order influence on its subjective pitch (although other factors, which will not be discussed here, also affect this attribute). Middle C on the piano keyboard, for example, has a frequency of 256 Hz, and octave intervals represent doubled or halved frequencies. This illustrates the relevance of the frequency transformation in psychoacoustics. A tone is observed as a continuous sound, not as a fluctuating quantity, and is described subjectively in terms of both its pitch and its level, the latter being dependent upon the pressure amplitude p_o. Tones with different pitches are easily distinguished by a human observer, and his hearing system is capable of very selective frequency discrimination.

It is a simple matter to measure graphically both the amplitude and frequency of the signal from a pressure time history diagram. However, it is not normally convenient to perform this analysis, and direct-reading analog instruments are available to

analyze the electrical output from a microphone. In order to eliminate the rapid fluctuations from the signal, it is necessary to take a time average. Since the time average of an acoustic pressure fluctuation is, by definition, zero, the signal is first squared to eliminate the negative portion. The mean squared pressure for a tone can thus be obtained by integrating over exactly one period as follows:

$$\overline{p^2} = \frac{1}{T_o}\int_0^{T_o}\left[p_o \sin 2\pi f_o t\right]^2 dt \qquad (1)$$

$$= \frac{p_o^2}{2}$$

The square root of this quantity provides a value which is directly proportional to the pressure amplitude known as the root mean square (rms) pressure

$$p_{rms} = \frac{p_o}{\sqrt{2}}$$

However, since the mean square pressure is proportional to acoustic power or intensity it is normally preferred to the rms pressure in acoustic analysis. Also, because of the very large pressure range of practical interest, it has become an accepted practice to express sound pressures on a logarithmic scale. The Sound Pressure Level (SPL) of a sound in decibels (dB) is written

$$SPL = 10 \log_{10}\left(\frac{\overline{p^2}}{p_o}\right) = 20 \log_{10}\left(\frac{p_{rms}}{p_o}\right) \text{ dB} \qquad (2)$$

where p_o is a standard reference pressure of 2×10^{-5} newtons/meter^2. This particular reference was chosen because it is in the region of the threshold of audibility for a 1000 Hz tone. Throughout this report SPLs in dB are referenced to this quantity unless otherwise stated.*

*Strictly speaking, the decibel notation should always be accompanied by a statement defining the reference. The latter has been dropped herein because of the frequent use of dB and the unwieldiness of 2×10^{-5} N/M^2.

If, in Equation (1), the period T_o is not known, a close approximation to $\overline{P^2}$ can be obtained by integrating over a period which is large compared with T_o since

$$\overline{p^2} = \lim_{T \to \infty} \frac{1}{T} \int_0^T p_o \sin 2\pi f_o t \qquad (3)$$

In practice this approximation is a very good one, provided T is more than about 3 times greater than T_o. An instrument which performs (approximately) the operation described by Equation (3) (and takes the square root) upon an electrical signal is called an rms detector. Analog instruments usually contain a voltage squaring circuit and an RC (resistance-capacitance) averaging circuit which, for sinusoidal signals at least, gives an output signal closely proportional to p_{rms}. If T is not large compared with T_o, then the output voltage merely fluctuates about the rms value. The limitations of this device for some complex sounds more typical of helicopter noise are described in Section 2.4.

General Periodic Signals

Although the sine wave or tone is of somewhat academic interest as an acoustic signal per se, it is of great importance in the capacity of a component of more complex signals. Any harmonic function, that is, one which repeats itself precisely and regularly during successive equal time intervals, can be exactly represented as the sum of a number (sometimes infinite) of sine and cosine components of the fundamental frequency and its harmonics. (The n-th harmonic is the component with a frequency n times the fundamental or a period of T_o/n.)

That is

$$p(t) = \sum_{n=1}^{\infty} (a_n \cos 2\pi n f_o t + b_n \sin 2\pi n f_o t) \qquad (4)$$

or

$$p(t) = \text{Real Part of} \left[\sum_{n=1}^{\infty} A_n e^{i2\pi n f_o t} \right] \qquad (5)$$

where the A_n are complex.

Periodic sound is commonplace in our mechanized world. Practically any device which utilizes rotating or reciprocating machinery and operates continuously generates harmonic sound: piston engines, compressors, circular saws, electric motors and,

of particular relevance here, propellers and rotors all generate acoustic waveforms which are periodic in nature. That this is true of helicopters may be seen in Figure 1. Generally speaking, the more discontinuous the waveform, the more harmonic components the signal contains. A square wave, for example, contains all odd-numbered harmonics, while a repetitive spike contains all harmonics with equal amplitudes. More realistic sounds contain a finite number of harmonics which generally decay in amplitude with harmonic number. The more pulsatile the sound is, the more harmonics it will contain. This may be seen in Figure 3, which shows some oscilloscope records of a computer generated waveform. The period of this signal is 100 msec (i.e., a fundamental frequency of 10 Hz), and the signal was reproduced for analysis by a magnetic tape recorder which resulted in some distortion. However, the waveforms do clearly illustrate the effect of an increasing number of harmonics. All in-phase (cosine) harmonics were included, and the amplitudes were inversely proportional to the square root of harmonic number; that is, they decayed in amplitude at the rate of 3 dB per octave. The signals contain, respectively, the first 5, 10, 20, 40 and 80 harmonics of the fundamental leading toward a very spiked waveform for the highest number. Subjectively, this sound consisted of a train of pulses which increased in sharpness with a definite cracking sensation in the case of 80 harmonics.

Similar trends may be noted in Figure 4, which demonstrates the effect of harmonic decay, i.e., the rate at which successive harmonics diminish in amplitude. Each signal contains the first 20 cosine harmonics, but the harmonic decay rates are, from top to bottom, 0, 3, 6, 9 and 12 dB per octave. The sharpness of the spike diminishes at the higher decay rates.

The phase between harmonics also has a bearing on the waveform as Figure 5 shows. The six different waveforms differ only in interharmonic phase (defined by the relative proportions of the sine and cosine components), although the phase difference between adjacent harmonics (i.e., between the 1st and the 2nd, the 2nd and the 3rd, and so on) is constant in each case. The values of this phase difference are 0°, 10°, 20°, 30°, 60° and 90° for the six diagrams. Although the harmonic energies of the signals are identical, the nature of the waveform appears to vary significantly and could create an impression that the harmonic energy distribution differed from case to case.

Regardless of phase, the mean square pressure of a harmonic signal is equal to the sum of those of the individual components; in other words, the energies add as follows:

$$\overline{p^2} = \sum_{n=1}^{N} \overline{p_n^2} = \tfrac{1}{2} \sum_{n=1}^{N} \overline{p_n^2} \qquad (6)$$

where $\overline{p_n^2} = a_n^2 + b_n^2$

and N is the total number of harmonics. However, it may be noted from Figure 5 that the magnitude of the peak pressure varies with interharmonic phase. The crest factor of a signal is the ratio of the peak amplitude to the rms amplitude, and since, as we shall see, the crest factor of a sound has considerable significance in acoustic analysis, phase is also important from this standpoint.

The frequency diagram of a harmonic signal is called a line spectrum since it consists of a number of vertical lines, one for each harmonic. For its complete definition, a harmonic waveform in fact requires two such diagrams, either one each for the cosine and sine components or an amplitude spectrum coupled with a spectral representation of harmonic phase. For most purposes, phase is ignored and the mean square value of each frequency component is plotted in an energy spectrum.

An rms detector by itself cannot, of course, provide any information regarding the harmonic composition of a periodic signal. To obtain this, the signal must be examined with a frequency selective filter which is able to discriminate between one harmonic and another. In its simplest form, a "band pass" filter is a tuned circuit which responds to excitation in a narrow frequency range. An ideal filter is one which passes all energy within a defined frequency interval and rejects all energy outside this band. Although such characteristics cannot be achieved in practice, modern filter technology is such that active devices approaching the ideal, with "skirts" that fall off at 60 dB/octave and more, are possible. Filter bandwidths (defined as the frequency interval between the 3 dB-down points) of practically any value can be selected, although their use is subject to many practical constraints as we shall see. For harmonic sound, a very narrow filter can be used in conjunction with an rms detector to accurately measure any number of individual components. To discriminate between adjacent components (of equal amplitude), it is only necessary that the filter bandwidths is less than the frequency difference between the components. If the components differ in amplitude, it is necessary to examine the filter characteristics in some detail to determine whether individual ones could be isolated.

Random Noise

Although sources of harmonic noise are common, most sound has a random nature such that its time history fluctuates in an unpredictable and irregular manner. Like most random functions, however, such noise is normally the result of a constrained process and is amenable to measurement or specification in a statistical sense. Noise whose long-term rms level does not vary is called "stationary." That is, a stationary random noise is one whose sound pressure randomly fluctuates about a zero mean in such a way as to maintain a constant rms level. The degree of stationarity is really related to the time over which the rms level has been averaged since, in general, it will always fluctuate if the averaging time is short enough. In the normally accepted sense "stationarity" assumes a very long averaging time.

Because it fluctuates randomly, random noise, unlike periodic sound, contains energy over a continuous frequency range. This can be understood by considering that a random time history never repeats itself and therefore has an infinitely long period. Its fundamental frequency is thus zero, implying that its Fourier components have zero frequency intervals between them. On the other hand, to keep the total energy in the signal finite, these harmonics must have zero amplitude. To avoid this impasse, the concept of Power Spectral Density (PSD) is introduced which, as its name implies, describes the distribution of power density (in pressure^2/Hz) as a continuous function of frequency. If the power spectral density function is w(f), the mean squared sound pressure level is

$$\overline{p^2} = \int_0^\infty w(f)\, df \tag{7}$$

The subjective quality of a stationary random noise depends, of course, on the distribution of w(f). A frequently used concept is that of "white" noise, an idealized signal with uniformly distributed energy, i.e., a constant value of w(f) and a normal (gaussian) pressure amplitude distribution. White noise, or its approximation produced by an electronic noise generator, sounds like the hiss of escaping steam, but the sensation, because of the dynamic characteristics of the hearing mechanism, is essentially dominated by the high frequency components. Jet exhaust noise is also a wideband random noise, but its spectrum, instead of being flat, tends to rise from low frequencies to peak in the region from 100 to 250 Hz and decay from there at the rate of 6 dB or more per octave. At very great distances, most of the high-frequency energy is absorbed and jet noise sounds rather like a dull rumble, a typical characteristic of low-frequency random noise which is spread over a range of frequencies. As the bandwidth of random noise is reduced, the waveform, as might be expected, tends to become more sinusoidal in appearance. However, the amplitude of this wave fluctuates in a random manner, and the smaller the bandwidth, the greater the excursions become. This in fact is the major difficulty associated with the analysis of random noise.

In order to measure the distribution of power spectral density (PSD) with frequency, we can use a filter/rms detector to measure the energy in any particular passband and obtain an estimate of PSD by dividing the result by the bandwidth. Provided the true PSD does not vary significantly over the filter frequency range, the result will be a good approximation; i.e.,

$$w(f) \approx \frac{1}{\Delta f \cdot T} \int_{t-T}^{t} p_f^2\, dt \tag{8}$$

where p_f is the filter output signal and the squaring/time integration is the rms detection (although the square root is not required). A typical result of this process is sketched in Figure 6. The upper trace shows the time history of narrow-band noise (or the output of a narrow-bandpass filter applied to wideband noise). After squaring and averaging this signal, an rms detector output would appear like that in the lower sketch, where measured mean square pressure, depending on the averaging time, follows the rise and fall in the pressure envelope, fluctuating about the expected or true, long-time average value $E(p^2)$. The error between the measured and the true values decreases with increased averaging time, and it is necessary to understand the relationship in order to make an adequate compromise between analysis time and accuracy. The standard deviation of these fluctuations, σ_{p^2}, can be shown (e.g., Reference 2) to be a simple function of the averaging time, T, and the bandwidth of the noise (or the filter) Δf:

$$\frac{\sigma_{p^2}}{E(p^2)} = \frac{1}{\sqrt{\Delta f . T}} \qquad (9)$$

The actual distribution of the error is the chi-square (X^2) distribution of classical statistical theory, and tables of its values have been used to prepare Figure 7 which shows the 80% confidence limits associated with any single sound pressure level measurement made with a combination of bandwidth Δf Hz and averaging time T seconds. The limits show the range, relative to the measured value SPL, within which there is an 80% probability that the true mean SPL lies. This figure can be used to select the bandwidth required to achieve a given accuracy. For example, to achieve an accuracy of ± 1 dB, the product $\Delta f \cdot T$ must be approximately 40 or greater. For a bandwidth of 5 Hz, an averaging time of 8 seconds is required, implying, for the frequency range 0 to 10,000 Hz, a total analysis time of $8 \times 1000 = 8000$ seconds if each band is analyzed consecutively. On the other hand, a bandwidth of 100 Hz would reduce this to 40 seconds, showing the importance of choosing the coarsest bandwidth consistent with adequate resolution. In general, if the signal is known to have a fairly smooth, slowly varying PSD function, a coarse bandwidth may be used. If the PSD varies rapidly, as is the case for any signal which contains harmonic spikes, a much narrower bandwidth is required.

The above technique is called constant bandwidth analysis and is used whenever detailed spectral resolution is required. A more commonly used method in acoustic work is known as constant percentage bandwidth analysis, a technique based on the fact that whereas narrow bandwidth resolution is normally required at low frequencies, increasingly less resolution is acceptable at higher frequencies. This is because narrow bands are generally required to identify the presence of discrete frequency spikes, or concentrations of energy in a very narrow range of frequencies. Since such components normally occur at integral multiples of a fundamental frequency f_o, the

spacing between spikes is also f_o. Thus, constant-percentage filters, whose bandwidths are proportional to their center frequencies can isolate harmonics with a degree of resolution which is independent of the fundamental frequency. The most commonly used filters have octave and 1/3 octave bandwidths, although other popular instruments use 1/2 octave, 1/10th octave, and 6% and 1% bandwidths. Preferred center frequencies for the octave and 1/3 octave center frequencies have been agreed upon internationally and are used throughout this report. The upper band frequency limit of an octave filter is twice the lower limit, whereas the ratio for 1/3 octave bands, of which there are three per octave, is $\sqrt[3]{2} = 1.26$. The corresponding bandwidths are 0.707 and 0.231 times the center frequency, respectively.

The application of these analysis techniques to helicopter noise is discussed in detail in Section 2.4.

2.2 HELICOPTER NOISE SOURCES

It is not the intention here to treat helicopter noise generation in depth. For detailed treatments of the subject, including methods for the prediction of source characteristics, the reader is referred to references 3 through 13. However, it is necessary to relate the subjective characteristics of the radiated sound to the underlying source mechanisms, and the major sources will be reviewed in turn.

The main sources of helicopter noise are the rotors and the engines, in that order. The engine exhaust is a predominant component in the noise of piston-engine machines, being a highly pulsatile sound with considerable harmonic content. However, most modern helicopters use turbine engines which radiate a combination of periodic and random noise, the former from compressor and turbine components and the latter mainly from the turbulent exhaust flow. Jet exhaust noise, described previously, has a broadband random spectrum which tends to be distributed over higher frequencies as the exhaust nozzle dimensions get smaller or the flow velocity higher. A distinctive feature of jet exhaust noise is that the greatest part of the energy radiates at acute angles to the flow, i.e., generally in an aft direction. Compressor noise, on the other hand, tends to radiate forward from the engine intake and is caused by the rotation of the compressor blades and their interactions with unsteady wakes. Again, frequency depends upon engine size; normally the fundamental is above 1 or 2 kHz and for the small turbines typical of small helicopters, it can approach the upper end of the audible frequency range (~15 kHz). In any event, the higher harmonics of compressor noise approach or exceed this limit and are thus inaudible. For this reason, compressor noise sounds pure-tone like, being the characteristic whistle of turbine engines. Gearbox noise, also significant at short distances from the helicopter, could be described similarly. However, both components are normally small at large distances from the helicopter because of atmospheric and other absorption effects, which are discussed in Section 2.3.

This brings us to the rotors, which generate the characteristic noise of helicopters. Rotor noise generation mechanisms have been the subject of extensive research, with the result that, qualitatively if not quantitatively, the processes involved are reasonably well understood. There is a tendency for acousticians to divide rotor noise into three specific categories: rotational noise, broadband (or "vortex") noise, and blade slap.

Rotational Noise

Rotational noise has a periodic waveform and is the "thumping" or pulsatile component with a fundamental equal to the Blade Passage Frequency (BPF),

$$f_o = 60\, N_R B, \text{ Hz} \qquad (10)$$

where N_R is the rotor rpm and B is the number of blades. Many harmonics of the fundamental are normally present, but in most helicopters, the energy in the fundamental harmonic of the main lifting rotor(s) dominates the spectrum. However, since the BPF is low, typically in the range 10-20 Hz, the fundamental itself does not contribute much to the perceived noise. Rotational noise itself results from two distinct actions, one of which is referred to as thickness noise and is related to the periodic displacement of air particles as the blade passes. The other more important mechanism is the action of aerodynamic forces acting on the blades, which, when they move or fluctuate in level, generate noise.

The most straightforward case, studied by Gutin[13], is that of the steady thrust and drag forces. These components oscillate backward and forward and from side to side relative to an observer who is some distance away from the rotor and in doing so radiate sound waves toward him. Because these motions are not exactly sinusoidal, Fourier harmonics of the rotational frequency are generated and blade symmetry causes all harmonics which are not multiples of the number of blades to cancel each other out. Probably of greater importance, however, is the action of unsteady revolution to revolution, which by the very nature of rotor aerodynamics they are constrained to do, they also generate harmonic noise in a very efficient manner. Again, these periodic forces move toward and away from the observer as the blades rotate; consequently, he hears a variation of frequency from any airload harmonic due to the Doppler effect. Because many airload harmonics exist and because each generates a range of acoustic harmonics, the net result is the radiation of a very wide range of discrete frequency components. These harmonics are clearly evident in the narrow band analysis of helicopter noise shown in Figure 8. Also, the importance of the periodic component to the acoustic waveform may be seen in Figure 9, which records the waveform at various instants during the approach of a UH-1F helicopter at an altitude of 1000 ft and a speed of 60 kt. At the farthest distance, the profile is dominated by the main rotor noise; but as it approaches, an increasing "ripple" due to the higher frequency tail rotor may be noticed.

The magnitude of the periodic noise and the frequency distribution of the harmonic energy are largely controlled by the rotor design, particularly by its total lift, number of blades, disc loading, and above all the tip speed. The acoustic power radiation increases very rapidly with this parameter, and the harmonic energy becomes more and more significant as the blade tip speed approaches high subsonic Mach numbers. This is purely a Doppler effect. As a periodic noise source approaches a listener, both the amplitude and frequency of the observed pressure wave increase by the factor $(1 - M)^{-1}$ where M is the source Mach number in the direction of the listener. In the case of a rotating source, M oscillates periodically about zero; as its amplitude approaches unity, a very great frequency and pressure range amplification occurs. The result, as shown in Figures 3 and 4, is for the impulsiveness of the waveform to increase, eventually reaching a condition which is known as "blade slap." This should be termed "high-speed blade slap" to distinguish it from a second and more common condition which sounds very similar but has its roots in a totally different mechanism. This is "wake interaction slap" and is caused by an impulsive aerodynamic load fluctuation experienced when a blade passes through the vortex wake trailing from another blade. This commonly occurs with tandem-rotor helicopters where the two rotors interact, but it can also happen for single main rotors in conditions of low inflow; for example, during a descent or landing flare. Examples of pressure waveforms for varying degrees of blade slap are shown in Figure 10 obtained from the recording of a single flyover of a CH-47A helicopter. A comparison of this development with Figures 3 through 5 indicates a gradual increase in the higher harmonic content of the signal.

Broadband Noise

Progressing to higher frequencies in the rotor noise spectrum of Figure 8, we see that the harmonic spikes gradually merge into a humped region of the spectrum which has been termed "vortex" noise. Previously thought to dominate the noise down to fairly low frequencies, recent research[14] has indicated that harmonic components can control the spectrum level of frequencies up to and above the 60th harmonic of the BPF, even at low tip speeds. Nevertheless, the signal becomes increasingly random at higher frequencies and reflects the turbulent instability of the flow conditions at high Reynolds numbers. The precise origins of these broadband components are still being investigated, but it is clear that blade surface pressure fluctuations induced by both boundary layer, shed vorticity and flow turbulence contribute to this radiation. For present purposes, it is sufficient to consider that an airfoil moving steadily through the air radiates stationary random noise such as that represented by the spectrum sketch in Figure 11. Now, in much the same way that harmonic pressure fluctuations on a rotating blade are observed by a stationary observer to generate a range of frequencies, so the observed spectrum of a rotating random source is observed to oscillate in level and frequency as shown in Figure 12. This periodic spectral transformation is the familiar "swishing" effect associated with the sound of rotors at close range. Very approximately, both frequency and overall sound pressure

oscillate between limits given by the ratio $(1 + M)/(1 - M)$, where M is the maximum source Mach number component in the direction of the observer. The following ranges are of significance (where the subscripts "max" and "min" denote maxima and minima in the observed values):

$$\frac{\overline{p}_{max}}{\overline{p}_{min}} \sim \frac{1 + M}{1 - M} \tag{11}$$

$$\frac{\overline{p^2}_{max}}{\overline{p^2}_{min}} \sim \left(\frac{1 + M}{1 - M}\right)^2 \tag{12}$$

$$\frac{\Delta f_{max}}{\Delta f_{min}} \sim \left(\frac{1 + M}{1 - M}\right) \tag{13}$$

(Here Δf is the observed bandwidth of the noise radiated by a fixed source energy bandwidth).

$$\frac{(\overline{p^2}/\Delta f)_{max}}{(\overline{p^2}/\Delta f)_{min}} \sim \frac{1 + M}{1 - M} \tag{14}$$

Note that although the total sound pressure level fluctuates by $10 \log_{10}\left(\frac{1 + M}{1 - M}\right)^2$ dB, the PSD level changes by only $10 \log_{10}\left(\frac{1 + M}{1 - M}\right)$ dB. If the source spectrum is flat, this change would be observed in any frequency band. Figure 13 shows the waveforms of "pink" noise* modulated harmonically in the range 0 - 12 dB. This corresponds to values of M between 0 and 0.33. If the spectrum is not flat, as for example

* Pink noise has a constant spectrum level as measured by a constant percentage bandwidth analyzer.

indicated in Figure 11, then considerably greater fluctuations could be observed at a single frequency due to the absolute frequency oscillations. It must be remembered that these cyclic modulations are, in fact, superimposed upon modulations which already exist due to the random nature of the sound, and for this reason they tend to be obscured as shown in Figure 13. Whether or not the amplitude variations are perceived as harmonic modulations or not depends upon the bandwidth of the noise and the frequency and depth of the modulation.

2.3 HELICOPTER NOISE PROPAGATION

The noise generation characteristics of a helicopter are a function of its flight configuration and ambient atmospheric conditions. However, the sound observed at any point on the ground is very greatly influenced by the sound propagation path along which acoustic energy is dissipated by a variety of mechanisms. The effect of propagation upon the observed signature is dependent upon (a) atmospheric conditions, (b) the position of the source relative to the ground, and (c) the ground features adjacent to the sound path. The propagation losses can be classified in terms of these factors as follows:

Spreading Losses:

(a) Uniform spherical spreading (Inverse Square Law) losses

(b) Nonuniform spreading

- reflection by finite boundaries
- refraction by nonuniform atmosphere
- diffraction (scattering) by nonstationary atmosphere

Absorption Losses:

(a) Absorption by atmosphere

- classical absorption
- molecular relaxation absorption

(b) Absorption by ground and ground cover

Each of these effects, any one of which may predominate depending upon atmospheric and ground cover conditions, is reviewed briefly in this section. Also, more detailed analytical considerations, together with specific methods for predicting propagation losses for the purposes of estimating helicopter detectability range are presented in Appendix I.

Spreading Losses

(a) Uniform Spherical Spreading - In an ideal medium the total sound power radiated from a point source through an expanding spherical wave front remains constant so that sound pressure levels are reduced 6 dB each time the distance from the source doubles. Deviations from this rule occur for finite-size sources at small source-to-receiver distances where the physical dimensions of the source region are comparable to the propagation path length. However, for the propagation path lengths to be considered here, this "near field" effect is not significant, and uniform spreading loss can be computed by the simple 6-dB loss per doubling of distance from the source. This loss is independent of frequency.

(b) Reflection by Boundaries - If the source is within a few (say less than 10) wavelengths of the ground, sound reflection effects will affect propagation characteristics. These include amplifications (a) due to an effective increase in source power when the height is small compared with a wavelength, and (b) due to the interference between the direct and reflected signals. Variations in the far-field sound levels of up to 6 dB are possible.

(c) Refraction by Nonuniform Atmosphere - Atmospheric wind velocity and temperature gradients change the directionality characteristics of a source by bending the sound rays as illustrated in Figure 14. As noted in Figure 14a, a "shadow zone" is formed in the presence of a negative vertical velocity of sound gradient caused by vertical changes in either wind speed or velocity. Conversely, a positive vertical velocity of sound gradient, Figure 14b, will cause the sound rays to be bent back toward the ground, resulting in a phenomenon known as "focusing." In the case of a negative temperature gradient, the shadow zone is in the shape of a circle with the source as center; however, in the presence of wind, the shadow zone is as illustrated in Figure 14c. Here the shadow zone begins upwind and has a boundary shape as indicated in the figure. Downwind, however, there can be "focusing" of the sound rays similar to that shown in Figure 14b. Theoretical methods for predicting the effects of refraction are well developed (e.g., reference 15). However, these require detailed definition of the atmospheric distribution of meteorological parameters and are thus not convenient for practical studies of helicopter detectability. Also, two points of practical significance should be mentioned. The first is that refraction effects are not strongly dependent upon frequency and are insignificant for elevation angles greater than about 10 degrees. The second is that operational use can be made of strong negative temperature gradients over a site which cause upward refraction of sound and reduce detection range. Such conditions are prevalent in the later hours of daylight. The opposite situation during the early hours of the day causes sound to propagate over exceptionally large ground distances.

(d) Scattering by Nonstationary or Turbulent Atmosphere - Turbulence scattering is another important source of atmospheric attenuation for low-frequency sound. It does not involve a dissipation of sound energy, but a redirection of it. Its principal effect, on a directional sound field, is to equalize acoustic energy propagating in all directions at large distances from the source. This is a direct result of the scattering of the sound field by the nonuniform sound velocity distributions in atmospheric turbulence. Thus, a highly directional sound profile can be gradually rounded out, tending to a nondirectional pattern at great distances from the source. This scattering or redistribution of sound energy is, in fact, the basis for a finite limitation in the excess attenuation in a shadow zone discussed in the previous paragraph. In the frequency range of 60-100 Hz, the observed scattering loss coefficient for ground-to-ground propagation of sound is of the order of 0.4 dB/1000 ft. This appears to be a characteristic frequency range for maximum scattering attenuation for ground-to-ground propagation. However, it is not possible to make detailed quantitative estimates of this scattering attenuation within the present state of the art, so that reliance must be placed on experimental data. Such data indicate the combined effect of refraction and scattering losses for propagation at low elevation angles of the source. Empirical prediction methods which account for these combined effects are presented in Appendix I.

Atmospheric Absorption Losses

Atmospheric absorption losses have two basic forms: (1) classical losses associated with the change of acoustical energy (or kinetic energy of molecules) into heat by fundamental gas transport properties of a gas, and (2) for polyatomic gases, relaxation losses associated with the change of kinetic or translational energy of the molecules into internal energy within the molecules themselves. A detailed review of atmospheric absorption losses is contained in Reference 16.

Of the two forms of absorption loss, molecular or relaxation loss is far more important at lower frequencies. This component depends on frequency, temperature, and humidity content and, in the critical frequency range, is primarily due to vibration relaxation enhanced by the presence of water molecules. Until recently, the significance of nitrogen as the principal contributor to this loss was not recognized so that previous comparisons of theory and experiment, based only on relaxation of oxygen molecules were in substantial disagreement[17,18]. Figure 15 illustrates a typical comparison of laboratory measurements and theoretical predictions. By including relaxation of nitrogen in the theoretical predictions, substantial improvement is obtained in the agreement between theory and experiment. To avoid total reliance upon this laboratory data, allowing for real atmospheric nonuniformities, a practical approach has been based upon correlating theoretical predictions (using meteorological conditions measured on the ground) with field measurements of atmospheric absorption losses. A number

of field investigations have been made of air absorption losses for aircraft noise over nearly vertical propagation paths. Typical results, from References 19 and 20, are shown in Figure 16. This figure also shows the predicted values for the absorption loss coefficient, a, in dB/1000 ft based on the refined theoretical methods summarized in Appendix I and/or weather conditions measured at the ground. The observed difference between prediction and field measurements of the absorption coefficient is attributed primarily to the fact that surface conditions are only an approximation to the actual nonuniform structure of the atmosphere. However, when vertical profiles for weather data have been examined, it has been found that surface measurements of temperature and humidity are reasonably accurate predictors for the average temperature and humidity in the first 1000 ft above the ground. Thus, for detection studies, surface conditions for temperature and humidity are considered to be adequate for prediction of atmospheric absorption losses for low-flying helicopters.

Absorption Losses by Ground Surfaces and Ground Cover

The vast majority of field measurements of sound propagation losses have been made over horizontal propagation paths with ground surface conditions ranging from hard concrete to thick dense jungle. As indicated earlier, the effect of refraction on sound propagation is particularly important for near-horizontal propagation paths. Thus, field measurements are not a reliable source of data for isolating effects of ground cover unless great care has been taken in the experiment to remove any effects associated with weather. Also, it is necessary to consider propagation over very long path lengths. Field measurements which combine these two features in the experimental plan -- careful accounting for weather effects, and propagation over long distances -- are very limited. Applicable results, from References 21 through 24, are summarized in Figure 17. It is apparent that ground absorption effects can increase the excess absorption very substantially over that due to atmospheric absorption alone. For purposes of estimating maximum detection range, it may be assumed that the minimum loss for very small elevation angles of the source ($< 10^{\circ}$) will be due to scattering losses from turbulence near the ground. This minimum excess attenuation for ground-to-ground propagation is defined in Appendix I.

Summary of Prediction Methods

Engineering prediction methods for estimating propagation losses for a wide range of weather and ground conditions are given in detail in Appendix I. These methods are based on a critical analysis of available theory and data on the phenomena outlined in the preceding paragraphs. For preliminary estimates of detectability range, the following expressions may be used. The first covers the case where the propagation angle β (between horizontal and sound propagation path) is greater than 10 degrees. The second applies to cases where this angle is less than 10 degrees. The predicted propagation loss is based on the approximation that the loss at 250 Hz is a valid measure for initial estimates of detectability range.

Elevation Angle Greater than 10 Degrees:

(a) For $R(T + 40) \geq 500$

where R = Relative Humidity, % and T = Temperature, ^{o}F

$$\alpha \simeq 0.6 \left[\frac{R(T + 40)}{1000}\right]^{-0.4} \text{ dB/1000 ft.} \tag{16a}$$

(b) For $R(T + 40) < 500$

$$\alpha \simeq 0.1 + 0.7 \left[\frac{R(T + 40)}{500}\right] \text{ , dB/1000 ft.} \tag{16b}$$

Elevation Angle Equal to or Less than 10 Degrees:

Add to loss determined by Equation (16), the fixed attenuation loss given by

$$A_g = 10\, e^{-\sqrt{\tan 3\beta}} \text{ , dB} \tag{17}$$

where β = elevation angle, degrees.

The actual propagation losses experienced at a given site will be subject to considerable variation due to variations in weather conditions. An approximate indication of the magnitude of this variation is provided by the following expression based on unpublished Wyle Laboratories data. The latter comprises a statistical analysis from over 2000 aircraft noise measurements over a range of 700 to 3200 feet.

$$\sigma_{EA} = 1.3 + 0.3 \left[\frac{SR}{1000}\right] \text{ , dB} \tag{18}$$

where σ_{EA} = standard deviation in excess absorption over slant range (SR), feet

2.4 HELICOPTER NOISE ANALYSIS

The proper way to analyze helicopter noise depends entirely upon the purpose for which the analysis is being performed. In general, there are two basic reasons for measuring helicopter noise characteristics: first, as part of research and development investiga-

tions of source mechanisms and, second, in order to derive information for use in studies of the effects of helicopter noise, for example, upon communities which are exposed to it. The requirements are likely to be more stringent in the first case than in the second. For research purposes, the greatest possible resolution and accuracy will be required. Data requirements might, for example, include individual harmonic amplitudes of rotational noise (possibly including phase) and the power spectral density of random components, all specified as functions of flight configuration and position. On the other hand, the effects of noise are not normally dependent upon such details, as we shall see, and it generally is adequate to determine much broader features using fairly coarse filter bandwidths, for example. However, over and above the basic requirements, the practical complexity of performing these measurements must be considered. Invariably, the experimenter must make a very difficult choice between resolution, accuracy and analysis time.

Noise Recording

Thus far it has been assumed that suitable records of helicopter noise pressure time histories are available for analysis. Whereas these are best obtained as the direct voltage output from a microphone system in the field, this approach is normally impractical or impossible because of the time required to perform the analysis. Thus it is necessary to acquire a permanent record of this voltage on a magnetic tape recorder.

The ideal recording system would meet the following requirements:

a) Frequency response flat between 0 and 20,000 Hz

b) Working dynamic range of 120 dB+

c) Crest factor capacity of 15 dB+

d) Zero frequency (tape speed) error

The second of these is considerably beyond the present state of the art. Direct-record, audio tape recorders (which record a voltage proportional to the sound pressure) can reach a 60-dB signal-to-noise ratio, but their frequency response is poor compared with that of an FM (frequency modulation) machine. Also, their transient response (to rapidly changing SPLs) appears to present a problem for helicopter noise recording. An FM tape recorder (which records a carrier signal whose frequency is varied by an amount proportional to the pressure signal) can meet the frequency response requirement but has a poor dynamic range of less than 45 dB. Allowing an adequate margin for high crest factor tolerance, this is reduced to a practical value of 25 - 30 dB. This puts a big demand upon the signal conditioning system, which must be designed to maintain the tape recorder input voltage within a narrow operating range, yet at all times meet rigorous calibration requirements.

Finally, commonly used general-purpose, high-quality microphones are normally deficient at frequencies below 20 Hz. Special purpose systems are required which use an FET preamplifier stage to overcome a low-frequency problem. Microphones are available which come close to meeting all the requirements described above, but only for a particular orientation. All microphones tend to be highly directional at high frequencies and must be arranged with considerable care.

The problems of helicopter noise measurement have been investigated in a parallel project, and the detailed findings have been reported by Brown[25].

Spectrum Analysis

The principles of spectrum analysis are well established and are documented in many texts (e.g., Reference 2). However, an application of these techniques to helicopter noise is not straightforward because of its unusual composition of random and periodic noise. Analysis requirements for these components tend to conflict, and significant errors are likely if due attention is not given to each. The bandwidth/averaging time requirements for stationary random noise were discussed in Section 2.2, and it remains to examine the measurement of mean square levels for tones.

The mean squared sound pressure of a sinusoidal signal is

$$\overline{p^2} = \frac{1}{T_o} \int_0^{T_o} (p_o \cos \omega t)^2 \, dt \qquad (19)$$

where $\omega = 2\pi f_o$ and T_o is exactly one period $= 2\pi/\omega$ seconds. (Equivalent to Equation 1).

A mean-square detection circuit computes a running estimate of this value, which is

$$\overline{p_m^2} = \frac{p_o^2}{T} \int_{t-T}^{t} \cos^2 \omega t$$

$$= \frac{p_o^2}{2} \left[1 + k \cos (2\omega t + \phi)\right] \qquad (20)$$

where T is the averaging time of the circuit and

$$k = \frac{\sin \omega T}{\omega T} \qquad (21)$$

That is, the output of the measuring device oscillates about the true mean square value

$\overline{p^2} = \overline{p_o^2}/2$ with an amplitude $k(\overline{p^2})$ and a frequency 2ω radians/sec. Thus, the limits of the error associated with the instantaneous measurement $\overline{p_m^2}$ are

$$\overline{p^2}\left(\frac{1+|k|}{1}\right) \text{ dB} \quad \text{and} \quad \overline{p^2}\left(\frac{1}{1-|k|}\right) \text{ dB} \tag{22}$$

Figure 18 shows the sound pressure level error limits corresponding to Equation (22) as a function of T/T_o. Only the envelope of the possible error is shown; its actual value oscillates with time t and drops to zero at all integral multiples of $0.5\ T_o$. The figure shows that the accuracy is better than ± 1 dB for $T/T_o > 0.8$ and better than ± 0.5 dB for $T/T_o > 1.33$. That is, provided the averaging time is greater than one and one-third periods of the frequency of the tone to be measured, the measured mean square level will be within 0.5 dB of the true value. It is most important to note, however, that this statement is true only for a single tone. The errors associated with the rms detection of harmonic complex will be considered separately below.

Comparing the requirements for random and sinusoidal noise at a frequency of 10 Hz (typical of a main rotor BPF) using, for example, a 5-Hz filter bandwidth, it is clear that the tone requires considerably less averaging time for an accuracy of ± 1 dB (.08 seconds) than does random noise (8 seconds).

A hovering helicopter radiates noise which is essentially stationary at any fixed microphone location. Provided no excessive level fluctuations occur due to propagation irregularities, and a sufficient length of record is available, any degree of spectral analysis can be applied. For high resolution, a narrow bandwidth tracking filter can be slowly swept through the frequency range at a rate which is compatible with the required averaging time. If, at the low frequencies, only harmonic information is required, a low averaging time is acceptable. If the random "noise floor" levels between the spikes are required, then a longer averaging time and correspondingly lower sweep rate is called for as specified by Figure 7. In any event, at sufficiently high frequencies, typically above 300 Hz or so, the random components of the signal become important and the sweep rate must be reduced or a wider bandwidth selected. The latter alternative is unavoidable if modulation amplitudes are required. Suppose, for example, we wish to examine a 10-Hz modulation of the random noise and the modulation depth (i.e., the ratio of the peak level to the trough level) is 6 dB. To detect this variation, the averaging time T must be substantially less than the modulation period T_o, say, 20 msec. To discriminate the periodic modulations, they should be significantly greater than the random level

fluctuations. To keep the latter to a level of + 1 dB requires the product $\Delta f \cdot T$ to be greater than around 40. Thus, a bandwidth of 40/.02 = 2000 Hz would be required. This reveals the difficulty of measuring modulation depth unless it is very large.*

The net result of these requirements is that a detailed narrow-band analysis of helicopter noise (in real time) can take several hours to accomplish. When this is multiplied by the number of positions necessary to define the spatial characteristic of the sound field, the total analysis time expands to days or weeks.

If the signal is nonstationary, as in the case of an aircraft flyby, an additional constraint is that the averaging time T should be small compared with time scale of the signal change. This is required for two reasons. First, because the source is moving, and it is normally desirable to measure the signature at some fixed direction of radiation relative to the aircraft; second, because if the signal characteristics change appreciably during the averaging time, the measurement will be erroneous. The extensive subject of nonstationary data analysis is beyond the scope of this study, but some simple examples usefully illustrate the problem.

The orientation problem increases in severity as flight-speed increases and microphone distance decreases. Accepting an angle of 5° to be a limit upon the change of position of the helicopter with respect to the microphone, the averaging time for a speed of 100 kt and a distance of 200 feet should not exceed 100 msec. This in turn would require a bandwidth limit of 400 Hz for the analysis of random noise with a +1 dB accuracy. Note that in the case of a helicopter approaching the microphone, this constraint is considerably relaxed. Theoretically at least, only the change in sound pressure level with distance need be considered. Neglecting excess attenuation, a 1-dB change in level corresponds to a 20% reduction in distance. For a distance of 2000 ft, and an approach speed of 100 kt, this criterion could be met by an averaging time of 2.4 seconds. In practice of course, short period fluctuations of much greater than 1 dB will be observed due to propagation effects.

The spectrum analysis problem is best described with reference to a sinusoidal signal. For a moving source, both frequency and amplitude are observed to change due to the Doppler effect. If a Fourier analysis is attempted with respect to a fixed period, spurious frequencies are introduced because the signal is non-sinusoidal. This problem can be overcome by transforming the data to a re-

* The required information is better extracted by "ensemble averaging" over many successive modulation periods. However, this technique requires the precise definition of the modulation cycles.

tarded or source time-frame but this operation is beyond the capabilities of conventional instrumentation and in any case requires a precise knowledge of the aircraft position and propagation effects. Instead, it is more common to select bandwidths and averaging time to best compromise resolution and accuracy.

For many reasons, 1/3 octave band filters frequently provide a good compromise to these requirements. They are sufficiently narrow at low frequencies to allow identification of the first few harmonics and increase in bandwidth rapidly enough to provide statistical confidence at the higher frequencies of the random components (assuming a constant averaging time). A sufficiently small number (33) of adjacent bands cover the entire audible frequency range of interest (12.5 to 20,000 Hz) to allow the practical use of a bank of parallel filters and, finally, as will be seen later in the report, provide a useful analogy to the hearing mechanism. For these reasons, 1/3 octave analysis is very widely used in the aircraft noise field.

However, for helicopter noise, 1/3-octave band analysis is not without its problems. Figure 19 shows the waveforms from the outputs of a number of 1/3 octave filters applied to recordings of two helicopters. Those on the left-hand side were obtained from that of a CH-47A tandem-rotor machine approaching the microphone at 100 kt in a blade slap condition (as evidenced by the pulsatile pressure signature at the top of the page). The right-hand diagrams correspond to an HH-43B helicopter (twin meshing rotors) hovering at an altitude of 50 feet at a distance of 200 ft from the microphone. This particular sound includes considerable high frequency energy as evidenced by the large amplitudes associated with the 500, 1000, and 2000 Hz bands. Amplitude modulation is apparent in all bands although the envelopes have an irregular appearance at the higher frequencies. Turning to the CH-47A record, we see that all filters display regular periodic type waveforms which are very pulsatile (high crest factor) at the higher frequencies. In particular, the band at 125 Hz, which is centered on the 12th harmonic of the BPF (11 Hz) and thus encompasses the 11th, 12th and 13th harmonics, shows a very severe modulation. It is interesting to compare these diagrams with Figure 20, which shows similar results for a synthetic waveform containing 100 harmonics of a 20 Hz fundamental. The harmonics decay at 3 dB/octave. The strong similarity implies a similar harmonic composition, and the amplitude modulations result purely from the interaction of the finite number of components within the filter bandwidth. It may be seen that the more components there are within a band, the more impulsive the wave envelope becomes.

It has been found that these waveforms which have theoretical crest factors of up to 9 dB present difficulty to analog rms detection circuits. Figure 21, for example, shows two 1/3 octave analyses of a similar signal with a 10-Hz fundamental performed with a B&K 3332 spectrometer/graphic level recorder combination. The first plot, made with a lower limiting frequency (LLF) setting of 2 Hz, is accurate, as

verified by narrow-band analysis of the spectrum.* The second, with a 10-Hz LLF, exhibits extremely large errors of 25 dB and above at the higher frequencies. The error is greater than that attributable to an inadequate averaging time as indicated by Figure 22, which was obtained numerically for the ideal 1/3 octave band centered on the 20th harmonic (very similar results were also obtained for the 40th harmonic). The graph shows the ratio of the maximum measured level to the true level as a function of averaging time (expressed as a multiple of the fundamental period T_o). Only the upper limit is represented, and it might be expected that the level recorder pen would maintain a position near this level. However, it turns out that the capacitors in the averaging circuits do not hold their voltages between successive pulses if the averaging time is of the order of this interval or less; they consequently record an excessively low value. The rule appears to be that the averaging time should be significantly greater than the lowest fundamental period present, regardless of whether or not this component is required in the analysis. The practical significance of this problem is largely related to the number of harmonics which can be discretely identified in the spectrum, since the error becomes serious only at high frequencies. Analyses of typical helicopter recordings showed discrepancies of only 4-5 dB in the mid-frequency range, although greater ones are clearly conceivable.

It is appropriate here to note that crest factors exceeding 9 dB can be handled only by the highest quality analog detectors since intricate circuitry is required to perform the squaring process. In general, these devices are not designed to accommodate crest factors in excess of 5 dB.

Real-Time Analyzers

Many instrument manufacturers are now marketing high-speed spectrum analysis devices known collectively as "real-time analyzers." These instruments use digital logic or a combination of digital and analog techniques to perform and record the results of spectral analysis at a very high rate. The highest rate possible normally depends upon the method used to display or store the data, but typically they are capable of generating several spectra per second. The use or details of these machines will not be described here except to state the reminder that they are subject to the same principles and restrictions that have been discussed. Their major advantages over the "old fashioned" procedures are that they allow simultaneous analysis of actual or effective filter outputs and provide the data in a convenient form for presentation or further analysis. Also, those units which perform digital rms averaging

* The lower limiting frequency setting controls an initial stage of time integration (a second is introduced by limits set on the pen writing speed) where the time constant is approximately equal to the reciprocal of LLF.

may be expected to provide greater accuracy for high crest factor signals. Many of these devices are ahead of the state of the art in the theory of acoustic analysis and their true value will emerge with the passing of time.

3.0 AURAL DETECTION AND THE HUMAN HEARING SYSTEM

3.1 THE AUDITORY MECHANISM

The human hearing unit consists of three main divisions as illustrated in Figure 23, adapted from Reference 26. These are the outer, middle and inner ears. The outer ear contains the visible portion, the pinna, which in humans is fairly ineffective but has some small effect in focussing incident sound waves upon the entrance to the auditory canal. The auditory canal is essentially a straight tube, about 25 mm long and 7 mm in diameter. Its inner end is closed by the eardrum or drum membrane, and the tube thus has a quarter-wave resonance around 3000 Hz. At this resonance, the sound pressure level at the eardrum is some 10 dB greater than that at the entrance to the canal and because the resonance curve is fairly broad, the dimensions of the canal have an important influence upon hearing sensitivity over a wide frequency range above 1 kHz.

The drum membrane has the shape of a shallow cone with its apex pointing toward the middle ear which contains the three ossicles, the hammer (malleus), the anvil (incus), and the stirrup (stapes). This system of bones and ligaments mechanically transmits the induced vibrations of the eardrum to the inner ear. The pressure in the middle ear, which is filled with air, is equalized to that of the atmosphere through the Eustachian tube, a cavity connecting it to the throat which is momentarily opened by the act of swallowing.

The footplate of the stirrup covers an opening into the inner ear known as the oval window. It is in fact hinged to one side of this window and is free to rock back and forth to transmit pressure waves into the inner ear.

The purpose of the middle ear appears to be to match the impedance of the air in the auditory canal to that of the liquid in the cavity of the inner ear. The inner ear itself has three parts: the vestibule or entrance chamber which contains the oval window and a second sealed opening known as the round window; the semicircular canals; and the cochlea. The semicircular canals are connected with the sense of balance and play no role in the hearing mechanism. The cochlea, however, contains the auditory nerve endings and other structures whose function is to translate mechanical motions into neural stimuli and as such is of major interest in the studies of the detection process.

The cochlea, named after the snail shell, is a coiled tube with a total length of about 31 mm which makes approximately 2-3/4 turns. Its mean diameter is about 1.5 mm and the tube narrows somewhat irregularly towards a point at its closed end.

The cochlear tube is divided longitudinally into two channels known as the upper and lower galleries by a rather complicated partition as shown in the cross-sectional view in Figure 24. This partition extends from the base of the cochlea almost to the apex but leaves a small orifice, the helicotrema, connecting the fluid in the two galleries (Figure 25). One reason for this passage is to protect the delicate membranes of the partition from possible damage by static pressure differentials. The partition, in fact, contains two membranes, Reissner's membrane and the basilar membrane, which enclose a duct containing a thick gelatinous fluid. Reissner's membrane does not appear to play any role in the hearing process other than to restrain the fluid. The basilar membrane, which on the other hand most definitely does, is connected to a bony shelf on one side of the cochlear tube and the spiral ligament on the other. The bony shelf is quite rigid and protrudes into the cochlea by an amount which decreases toward the apex (Figure 25). Thus, the basilar membrane actually increases in width from the base to the apex of the cochlea.

When the stapes is excited by very low frequency sound, the incompressible fluid oscillates between the upper and lower galleries through the helicotrema, the fluctuations in the lower gallery being accommodated by deformations in the diaphragm of the round window (Figure 25). At higher frequencies, however, the fluid inertia prevents this orifice flow and instead, deformations of the basilar membrane occur. This deformation is sensed by the Organ of Corti which transmits the information through the auditory nerve to the brain. The Organ of Corti is attached to the upper surface of the basilar membrane and traverses its entire length (Figure 24). It forms a termination to the auditory nerve which enters the cochlea alongside the bony shelf and contains more than 20,000 hair cell sensing elements. These protrude from its upper surface to connect with the tectorial membrane, a fairly rigid element extending from the bony shelf. When the basilar membrane distorts, these hair cells are put into tension, and in much the same way as a piezo-electric transducer, generate small electrical voltages known as cochlear potentials.

Many theories have been put forward to explain the dynamics of the cochlear system and many experimental simulations have been attempted. However, due to the extremely complex structure of the real system, many details are imperfectly understood. For present purposes, a simple explanation is adequate to introduce the concepts of auditory frequency selectivity which are fundamental to presently accepted theories of the hearing process. This model is illustrated in Figure 25, which shows a diagrammatic representation of the cochlea and basilar membrane. As noted previously, except at very low frequencies, antiphase vibrations of the oval and round windows are possible because deformations of the basilar membrane allow the necessary fluid motion. These deformations are highly localized for a fixed frequency input as seen in Figure 26, which is a sketch of the longitudinal distortions of the membrane for a 1000 Hz tone. The entire cycle is illustrated in 8 diagrams at 45° intervals through the 360° period. As might be expected, the higher the frequency, the closer the

disturbed area comes to the base of the cochlea until, at the upper end of the audible frequency range, the motions are immediately adjacent to the base.

3.2 HEARING PERFORMANCE

The most important index of hearing performance, insofar as the present study is concerned, is the threshold of audibility, that is the sound pressure level of the sound which is just audible to the human observer in silence. From a physical point of view it is thought that at levels below the threshold, the generation of neural impulses in the Organ of Corti is nil. When the acoustic stimulation slightly exceeds threshold level, neuron generation is activated and a finite signal is transmitted to the brain. The threshold level is strongly dependent upon frequency and, as might be expected, varies substantially from listener to listener. Figure 27 shows a number of determinations of the audibility function for pure tones. The considerable variation in these curves may be attributed to different listeners, different experimental techniques and most particularly, different methods of presenting the sound (earphones, one ear, two ears, free field, etc.). This point will be discussed later. For the moment the discrepancies are not important. What matters is the indication of the associated ranges of frequency and level. The upper frequency limit of the audible range exceeds 10 kHz and, depending upon age (the threshold at high frequencies normally increases fairly rapidly with age) and hearing acuity, can be as high as 25 kHz. The lower limit is somewhat difficult to define. Normally thought to be around 20 Hz, some experiments indicate that sound is audible at frequencies almost down to zero, provided the level is high enough. What always casts some doubt upon these measurements is the difficulty of avoiding harmonic distortion when generating low frequency sounds. This opens up the possibility that it is second or higher harmonics rather than the fundamental which are heard. Nevertheless, experiments conducted in this study with a very low-distortion system have shown that sound is definitely audible at 10 Hz.

The most remarkable feature of the hearing system is its enormous dynamic range which exceeds the performance of most electronic measuring equipment by a large margin. In the frequency range 1 - 5 kHz, minimum perceptible intensities can be as low as 10^{-16} watts/cm^2, at which level the vibration amplitude of the eardrum is approximately one-tenth the diameter of the hydrogen molecule. (If the hearing were any more sensitive we would be able to hear the hissing of air molecules due to thermal agitation.) At the other end of the scale, the system is limited by tickle, discomfort, and pain caused by excessive motions of the eardrum and ossicles. These limits, some of which are also indicated in Figure 27, are somewhat difficult to specify because of subjective adaptation to high intensities, but they are sufficiently high to be beyond the range of normal experience. The total dynamic range of hearing in the vicinity of 1000 Hz is approximately 120 dB.

At levels between these extremes, sound is observed to exhibit varying degrees of quietness, loudness or noisiness. Considerable research has been devoted to the problem of defining these subjective quantities in terms of measurable characteristics of the sound. This has led to the development of such indices as loudness level (in phons), weighted sound pressure levels (in dBA, dBN, etc.), and perceived noise level (in PNdB). These quantities are derived by procedures which take account of many important psychosensory features of the hearing process. However, despite their obvious association with present considerations, these procedures are concerned with sound intensities well above threshold and, as such, are in no way applicable to the aural detection problem.

3.3 THE CRITICAL BAND CONCEPT

His pioneering studies of auditory performance and considerations of cochlear dynamics discussed in Section 3.1 led Fletcher[27] to propose the concept of the critical band. This notion is based upon the fact that a single frequency tone excites a finite region of the basilar membrane (as shown in Figure 26) so that the excitation regions of tones closely spaced in frequency overlap. Thus, if a second tone is added, it attempts to stimulate a region of the basilar membrane which is already in motion due to the first. In the simplest possible sense, the "critical bandwidth" is the frequency separation of two tones whose excitation regions do not overlap to any significant degree.

Nearly forty years of research (References 27 to 44) have shown that the critical band hypothesis gives a satisfactory explanation for most of the observed characteristics of the hearing mechanism. These include:

1. The masking of tones by random noise and the masking of noise by tones
2. The growth of subjective loudness with bandwidth for both tone complexes and random noise
3. The frequency selectivity of the ear and pitch discrimination
4. The relationships between absolute thresholds for pure and finite bandwidth sounds
5. Phase discrimination

The only major source of disagreement between researchers is the exact dimensions of the critical bands themselves. As in all psychoacoustic measurements, confidence intervals are large and the results appear very sensitive to experimental technique.

The early measurements of Fletcher and Munson[28] were based upon two assumptions:

(a) If a tone and wideband random noise are played simultaneously, and the level of the tone is adjusted until it is just barely audible, then only the random noise energy contained within the critical band centered at the tone frequency is effective in masking the tone

(b) At the just masked level, the energy in the critical band is equal to that of the tone

In fact, his experiments were based upon the second assumption which enabled him to compute the critical bandwidth as a function of the tone/noise ratio directly as

$$10 \log_{10} \Delta f' = L - M_S \tag{23}$$

where L is the level of the tone at threshold and M_S is the spectrum level (PSD) of the masking noise in the vicinity of the tone frequency. This second assumption in fact imposes a specific definition upon Fletcher's critical band function which is shown in Figure 28 and has caused later researchers to refer to it as a "critical ratio." Its actual variation with frequency was confirmed by the remarkably similar results of Hawkins and Stevens[31], obtained many years later and shown for comparison in Figure 28.

More direct investigations of the first assumption (a) have been performed by Fletcher[27], Schafer, et al[32], Bilger and Hirsch[35], and Greenwood[37,38], and although all confirmed that noise outside a certain critical bandwidth became rapidly less effective in masking a tone, there is disagreement in the measurements of the bandwidth. De Boer[40] reviewed these and other studies and concluded that the critical band cannot be accurately determined solely from masking experiments because the band limits are too imprecisely defined. This is seen to be the case in De Boer's compilation of data which is reproduced in Figure 29. The plot shows, for tones around 1000 Hz, different measurements of the tone-to-noise ratio for different noise bandwidths. Fletcher's model is shown for comparison. Possibly for this reason Zwicker, Flottorp and Stevens[36] turned their attention to the role of critical bandwidth in loudness summation, performing experiments to measure the increase of loudness with bandwidth. The sounds studied included both bands of noise and groups of tones and in both cases they were able to clearly show that, for bandwidths (or frequency spacings) up to a certain limit, the loudness remains constant. Beyond this limit loudness increases. They then compared their results with critical bands derived in different ways. Of particular relevance here, they first compared absolute thresholds for single and multiple tones to show that, up to a certain number of components (i.e., up to a certain bandwidth), the overall level of the just detectable complex remains constant. When this limit is exceeded the detection level increases. Secondly, the masking of bands of noise placed midway between two tones (essentially the inverse of Fletcher's experiments) was studied. Finally, they included data on the perception of inter-

tone phase perception resulting from amplitude and frequency modulation of tones. This showed that phase effects were only important for tones within a critical band. In general, they found close agreement between all these various results and were able to recommend with some confidence, a revised critical band function, although of similar shape to Fletcher's curve, turned out to be approximately $2\frac{1}{2}$ times larger (see Figure 28).

The recommendation of Zwicker et al went unchallenged until 1961, when Greenwood[37], as a result of his earlier masking experiments[38], a study of optical measurements of the basilar membrane, and some early psychophysical measurements, presented a revised critical bandwidth curve which is also shown in Figure 28. In deriving this new result, Greenwood consolidated earlier beliefs[36] that critical bandwidths represent equal distances along the basilar membrane (approximately 1 mm) and the frequency intervals over which the inner ear performs a spacial integration. In fact, his results agree fairly closely with those of Zwicker et al[36] in the mid-frequency range, but diverge at high and, more significantly, at low frequencies. In the latter regard, it should be noted that Greenwood's curve appears to take account of the only published data at frequencies below 100 Hz.

3.4 TEMPORAL EFFECTS

Evidence that the ear possesses frequency filtering abilities was discussed in the previous section. In a further analogy with acoustic data analysis methods, it is of distinct interest to hypothesize that the auditory signal processing system includes an equivalent of the rms detection circuit. The notion that such processing takes place is perfectly consistent with observations of the perception of fluctuating signals (e.g. beats and other modulated sounds) and several investigators (e.g. References 42 through 44) have attempted to measure the appropriate time constant. However, different sources of data conflict, with averaging times between 5 msec and 200 msec having been suggested. As with other characteristics, it seems that a precise value depends almost entirely upon the type of experiment used to determine it. In general, a value between 100 and 200 msec seems to be discussed most frequently.

3.5 SUMMARY

For the purposes of the present study the following observations, based on a review of relevant research into the functioning of the hearing mechanism, seemed to be important:

1. Absolute threshold data for pure tones are plentiful and in sufficient agreement to define an appropriate "average" value.

2. The "critical band" concept appears well founded, well supported and is central to modern auditory theory. A model of the aural detection process must be based upon its existence, but there is some disagreement regarding the form of the critical band function.

3. Most research has, of necessity, been confined to relatively simple acoustic stimuli such as tones and narrow bands of noise. Little data are available on more complex sounds such as those associated with helicopters.

4.0 EXPERIMENTAL PROGRAM

The main purpose of this study is to develop methods for calculating the aural detection ranges of helicopters. To do this it is necessary to: (a) specify an analytical/empirical model of the aural detection process and (b) define its applicability and accuracy. This section describes the experimental study which was conducted for these purposes.

4.1 EXPERIMENTAL REQUIREMENTS

An accurate, practical and useful method for estimating the aural detection thresholds of helicopter sounds should take account of all variables which are known to be of first-order importance to the problem. These include the acoustic characteristics of the helicopter, the effects of propagation over long distances on the observed sound, the ambient noise environment in the vicinity of the observer, and finally, the hearing acuity of the observer himself.

It is obviously desirable for each variable to be specified in terms of quantities which can be conveniently measured, or more importantly from a design standpoint, estimated. Of equal importance is the need to recognize the degree of accuracy with which each can be specified. Although it is evident that the psychoacoustic variables themselves have wide confidence intervals, there is little point in demanding greater resolution than can be expected of the physical inputs. In this section each of the main factors are examined in the light of these requirements and for their applicability to a potential model.

Source Radiation

At the present time, the state of the art in helicopter noise estimation for design purposes is such that the first few (<12) harmonics of rotor noise can be estimated with reasonable confidence ($\pm$ 2 - 3 dB) and the remainder of the spectrum with somewhat lesser accuracy ($\pm$ 5 dB). The spectral details, associated with these estimates, in terms of energy distribution, can be predicted fairly well but phase information, which has an important bearing on the pulsatile nature of the total sound, is beyond the present state of the art. It may be confidently expected that as knowledge advances, improvements in all areas will be forthcoming, but the very nature of the problem suggests that definition of high-frequency spectral details will always be difficult. This is particularly true of such transient phenomena as blade slap.

Helicopter noise can be measured with as much accuracy as the instrumentation will allow. Modern techniques can provide very high quality data provided very rigorous experimental procedures are followed. In practice it is difficult to maintain

ideal conditions and instrumentation limitations make themselves felt. Measurements at long distances from the helicopter are extremely sensitive to environmental conditions while short range measurements present problems with nonstationarity.

Taking all these factors into account it would seem that source noise should be measured or estimated in terms of 1/3 octave band spectrum levels. This bandwidth is sufficiently narrow to allow fairly detailed spectral resolution, particularly being close to the critical bandwidth over a wide frequency range (Figure 28), and yet wide enough to avoid serious errors due to nonstationarity in the analysis of flyover data. Also, the reduction of design predictions to this format is fairly convenient. Furthermore, commercial analysis equipment for this purpose is readily available in a wide variety of forms.

In addition to frequency selectivity, there is the question of time averaging. A judgement on an appropriate analysis time constant must be made on the basis of both psychoacoustic considerations and the significance of short-time scale signal fluctuations such as blade passage modulation.

Propagation

The effects of the atmosphere and the terrain are of profound importance to the aural detectability problem, particularly the latter in the case of low-flying aircraft. Unfortunately, although atmospheric absorption can be estimated with some reliability, very little is presently known about terrain effects. Also of probable significance are the effects of random signal level fluctuations due to atmospheric inhomogeneities and other causes. Although unpredictable, these are always present and, like other propagation effects, will eventually become better documented. Some account of their influence is thus considered desirable.

Masking Noise

Masking noise may of course be specified in practically any terms, depending upon what is known about the ambient noise in a particular environment. In general, it seems unlikely that there would be any necessity to be more specific than an octave band level spectrum; but again, for flexibility, the model should accommodate a 1/3-octave band level definition. The effects of temporal variations of level could be considered, but lack of detailed knowledge would probably render this superfluous in the majority of applications.

Human Observer Characteristics

Hearing acuity varies significantly from person to person and also from community to community and must be included in the model as a variable. For convenience it should be appropriate to include this variable as pure tone absolute threshold function.

Specific Objectives

In the light of the foregoing considerations, the experimental program was divided into two phases with the following objectives:

Phase I: To provide the necessary supporting data to establish an adequate analytical model of the aural detection process. Subsidiary goals of the Phase I tests were specifically:

1. To develop a reliable experimental technique
2. To measure absolute and masked thresholds for tones, tonal complexes and bands of noise, both stationary and modulated
3. To investigate the critical band concept as applied to detection of helicopter noise.

Phase II: To test and or refine the model through application to actual helicopter sounds.

4.2 EXPERIMENTAL METHOD

Psychophysical Test Procedure

Although an audibility threshold is defined as that specific level at which finite neural activity is stimulated, it is not possible to measure the threshold level with the precision that this description implies because of a difference between the levels at which the stimulus is definitely audible and definitely inaudible. The magnitude of this difference is a function of many factors, including whether or not the signal is increasing or decreasing in level, its duration, the degree of concentration of the subject, whether or not he is warned of the signal's existence, what to listen for, and so on. Many techniques have been established for the measurement of audibility thresholds and a choice between them inevitably rests upon the desired compromise between accuracy and speed; as in most measurements, higher precision generally requires more time.

In the psychophysical method which was originally proposed for the present study, subjects were to listen to a helicopter sound that was gradually increasing in intensity and were to respond when they first detected the sound. Unfortunately, this method suffers from two well-known types of error often observed in psychophysical experiments; errors of anticipation and errors of habituation. The former refers to the tendency of subjects to consistently respond too early, i.e., below their actual detection threshold, and the latter refers to the tendency of subjects to wait too long before reporting their detection of the stimulus, i.e., they respond well

above their detection threshold. These errors are typically cancelled out by presenting both increasing and decreasing stimulus intensity sequences: a procedure which requires a relatively large number of trials with each stimulus to be effective and which, conceptually, at least, does not fit the field detection situation. The original technique, therefore, could not be counted on to yield reliable results. Furthermore, it was very inefficient; each threshold determination would probably require at least 10 separate threshold determinations.

The standard psychophysical Method of Adjustment appeared to provide a satisfactory balance between the requirements of reliability and efficiency. A pilot test of the Method of Adjustment was performed with eight subjects. Each subject adjusted a logarithmic potentiometer to control the headphone (TDH-39) level of a computer-simulated helicopter sound spectrum which was repeatedly "turned on" for approximately 1.75 seconds and "off" for approximately 0.5 seconds. Subjects manipulated the potentiometer until they were satisfied that the sound was just at their detection threshold. They then brought the signal to suprathreshold levels and repeated the adjustment procedure for a total of 20 threshold estimates for each subject. Thresholds estimated varied over a 22 dB range for the eight subjects. An individual subject was, however, quite reliable at picking and remaining with a particular threshold value from trial to trial. The average standard deviation of the subjects around their own mean thresholds was 1.7 dB. This small amount of variability indicated that the Method of Adjustment could provide a reliable indication of detection thresholds for complex acoustic stimuli.

Although the method appeared to be very reliable, it soon became clear that it would be too time consuming to investigate the large number of different helicopter sound characteristics that contribute to detection. Each adjustment required between 30 and 60 seconds. Thus, if thresholds were to be found for only 100 different stimuli, and each threshold estimate were composed of only 10 different adjustments/subject, each subject would have to make 1000 adjustments requiring a total of 500 to 1000 minutes (8 to 16 hours for this limited number of stimulus values).

An alternative approach was required because considerably more than 100 data points/subject were desired. Von Békésy[45] described an audiometric technique for determining pure-tone thresholds as a continuous function of frequency, which used a modified Method of Adjustment. The technique has been favorably evaluated by Hirsch[46], who found that it was a quick and reliable means of obtaining auditory thresholds across an entire audible frequency spectrum. Békésy's audiometer consists of a variable-frequency oscillator that is coupled mechanically to a rotary drum on which is mounted an audiogram blank. The listener controls the direction of an attenuator motor, continuously adjusting the signal level between the points where it becomes audible and then inaudible. A writing device inscribes the amount of attenuation on the vertical axis of the audiogram blank so that the result is a continuous line that moves up and down between points of audibility and inaudibility as a

function of frequency. The Békésy method may be classified as a modified Method of Adjustment, which is reliable and yields a large number of threshold determinations in a short time.

The methodology used for the Békésy audiometer was, therefore, suited to the present task and the entire experiment was designed around its use. The test signals were recorded on analog magnetic tape or generated in such a way that the stimulus parameter under study, normally frequency, was varied slowly with time. A pure tone audiogram, for example, was obtained during a 5 minute frequency sweep from 12 Hz to 12,000 Hz. Whatever the signal, the subject, who was able to control the signal level, was asked to continually adjust it to the just-audible point for the entire test duration. The control and data acquisition system developed for this purpose is described below.

Control and Data Acquisition System (DAS)

In order to obtain a statistically adequate number of measurements for the range of variables envisaged, it was clear from the outset that some form of automated test procedure would be required to obtain them reliably and accurately. Accordingly, a significant proportion of the effort during this project was directed toward the development of an automatic test control and data handling system for large-scale Békésy audiometry.

The system was centered around a 120-dB, continuously variable attenuator, which controlled the level of the stimulus sound being presented to the subject. The setting of the attenuator was controlled by a bi-directional electric motor, which was in turn controlled by the subject. The tracking rate of the attenuator was 2 dB per second in either direction.

The subject listened to the stimulus sounds inside an acoustic test chamber. He was furnished with a simple hand-held pushbutton cord switch and instructed to push down the button as long as he was able to hear the stimulus, releasing it when the signal became inaudible. Pushing the button drove the attenuator in the direction of increasing attenuation and releasing it caused the sound level to increase again.

During the course of the test the automatic data system sampled the position of the attenuator setting at intervals of approximately one second, recording these data on punched paper tape. These were subsequently subjected to computer analysis by programs which converted the punched numbers to sound pressure levels and related these levels to the temporally varying characteristics of the stimulus sounds. The results were made available as listings or plots of the means and deviations of the threshold levels, either for individual subjects or as average results for an entire test jury. An example plot is shown in Figure 30.

The data system and associated software have been described in detail by Adcock[47]. The main design features of the system together with operation and calibration procedures and data analysis methods are described in Appendix II to this report.

Test Environment

It was originally intended to present all stimuli to the subjects in a totally progressive wave environment in Wyle Laboratories' 1500-cu ft progressive wave chamber, which has been described in References 48 through 51. However, recent experience in another project[50] revealed a serious difficulty in maintaining a known stimulus level at the subjects' ears at frequencies above 1 kHz. This problem is caused by head diffraction patterns which vary between subjects and with head orientation. Accordingly, it was decided to avoid this problem through the use of wide-frequency-range headphones. At the same time, the possible importance of total body exposure at low frequencies was recognized and to retain the effect of nonauditory stimulation, the tests were performed inside a newly developed low-frequency progressive wave chamber. A crossover network was used so that the test subject seated in the working section of this facility was totally exposed to frequencies below 65 Hz generated by loudspeakers while listening to higher frequencies through high-quality binaural headphones.

A cutaway view of the acoustic chamber in Figure 31 shows its three sections. The first is a 1300-cu ft loudspeaker enclosure containing four 30-inch-diameter Electrovoice W30 speakers. These generate a test sound pressure level in excess of 120 dB at frequencies down to less than 10 Hz. To damp out resonances, two wedges containing 170 lb of low-density glass fibers are installed in this enclosure. The speakers are mounted in a reinforced wooden baffle and are driven by the parallel 190 watt channels of a Crown DC-300 solid-state amplifier. The total system has a very low harmonic distortion of less than 0.3% at levels less than 100 dB. The middle test section, which is 10 ft long x 8 ft wide x 7 ft high, can accommodate four seated subjects, although the present adjustment tests involved only one subject at a time. Behind the working section and designed to absorb the total speaker power output of more than 50 acoustic watts, are four 20 ft long fiberglass wedges, each spanning the full height of the chamber and expanding to a maximum width of 2 ft at the rear wall. In all the facility is 50 ft long and is constructed of 12-in-thick concrete to provide high attenuation of external noise.

The headphones used were the newly available Koss ESP-9 electrostatic units which have a nominal frequency response ($\pm$ 5 dB) of 10 - 18,000 Hz. To minimize self-generated noise, the AC-powered voltage source was replaced for the tests by a dry cell to maintain the polarization voltage of 500 volts. The E-9 energizer was driven by a single 20-watt channel of a Crown D-40 solid-state amplifier, like the

DC-300 an extremely stable, wide-dynamic range-amplifier with excellent frequency response characteristics.

Figure 32 is a schematic diagram of the entire sound generation and instrumentation system. The frequency characteristics of the system, as measured in a Koss B&K 6-cc coupler using a $\frac{1}{2}$-in.B&K 4133 microphone, are presented in Figure 33. These calibrations were performed at a sound pressure level of approximately 100 dB. The overall response curves, one for each earphone, are presented in Figure 33 (a), and the lower diagram (b) shows the separate free field (loudspeaker) and pressure field contributions (headphones). It should be noted that in the loudspeaker frequency range, the headphone coupler arrangement is totally transmissive since precisely the same function is measured both with the headphones removed and with the microphone removed from the coupler. Details of the calibration procedures used are described in Appendix II.

4.3 PHASE I TESTS

The main purpose of the Phase I tests was to validate the experimental procedures and equipment and to investigate certain aspects of aural detection of relevance to the helicopter problem which do not appear to have been covered in previous research. Specifically, these included measurements of absolute and masked thresholds for tones, bands of noise, both stationary and harmonically modulated, and finite bands of multiple harmonic noise. The precise combinations of signals and noise included are presented in Section 5.0. Altogether, more than two hundred and fifty individual tests were run over a period of 2 months for a total test duration of approximately 65 hours (including Phase II).

Subjects

Initial Phase I tests were repeated with five subjects. However, experience showed that equally consistent data could be obtained with three trained subjects selected from Wyle Laboratories engineering staff, so to cover the maximum ground in the time available, the bulk of the experiments were performed with three subjects. The absolute audibility function for pure tones averaged over these three subjects showed good agreement with a variety of previous determinations taken from the literature. This comparison is discussed in Section 5.0; it suffices here to state that the agreement was sufficiently close for the subjects to be regarded as having normal hearing acuity.

Signal Generation

Early experiments caused abandonment of the original plan to perform all experiments using a remote controlled tape reproducer as a signal source. This was due to problems associated with the extraordinary dynamic range of the ear as

witnessed by the threshold contours of Figure 27. Very simply, it was discovered that "tape hiss" was considerably more audible than the signal for tones and other sounds with low frequencies and this problem required major alterations to both the equipment and the test plan.

All pure-tone thresholds were obtained by what was effectively a standard Békésy audiometric procedure using the BFO as a signal source with direct input to the DAS amplifier. The automatic sweep facility of this oscillator was used to vary the frequency at a rate of 0.83 octave per minute in the range of 10 Hz to 12.5 kHz.

Stationary random noise was investigated in octave or 1/3-octave bandwidths by on-line filtering of pink noise reproduced from an FM tape recording (see Figure 32). During the test, the tape was played continuously into the stepping filter of the B&K 2112 Audio Frequency Spectrometer which was automatically switched from band to band at 0.83 octave per minute between 12.4 Hz and 10 kHz (1/3- octaves) or between 16 Hz and 8 kHz (octaves).

The same technique was also used to generate modulated random noise and multiple harmonic noise. The modulated noise was initially recorded on FM tape by modulating the same source of pink noise with an electro-optical amplitude modulator. This unit was driven by a modulating signal from an HP 650 A oscillator. Modulation depths* of up to 12 dB and frequencies of up to 40 Hz were applied to pink noise signals with energy between 10 and 12,500 Hz. Some oscilloscope records of these signals were shown in Figure 13. The harmonic sounds containing one hundred harmonics and fundamental frequencies of 10, 20 and 40 Hz were generated digitally by an XDS Sigma V computer, converted to analog form by a high-speed digital to analog recorder and recorded on an Ampex AG 500 1/4-inch direct record tape machine.

Test Procedures

Test participation demands considerable concentration on the part of the test subject, so to avoid fatigue, test runs were limited to the shortest possible duration. For this reason all preliminary checks and setup procedures were completed before the subject entered the test chamber. Upon entering, the subject was seated and warned of an imminent start by the test controller. A two-way intercom was installed, and the controller was able to hear the subject at all times when a test was in progress. The subject himself could monitor the progress of the test by watching a slave console which relayed the status of the DAS. Illumination of an amber "STANDBY" lamp

* Defined in terms of the peak to trough rms levels.

indicated that the DAS was readied and the test could commence at any time. When the display switched to "READY" (also amber), the system was energized and the attenuator motor was running. At this time, the subject should have been wearing his headphones and begin to perform his test function. When a green "RUN" lamp lit, data was being acquired. The simultaneous illumination of a red "LIMIT" lamp warned that the attenuator had reached the end of its travel and had thus automatically switched off the motor. This situation could only be remedied by the controller as described in Appendix II, and to be sure that the abort had come to his attention the subject was asked to advise the controller whenever the red lamp was lit. At the end of the run the display switched from "RUN" to "STANDBY" at which point the subject was usually asked to relax and leave the chamber.

Should an abnormal situation arise during a run, the subject could operate a guarded "ALARM" switch on the panel which lit a warning lamp on the main control console and also automatically shut down the test. For cases of extreme emergency, a switch was also installed within reach of the subject which cut off the electrical supply to the audio power amplifiers. This precaution was taken to protect the subject in the event of a signal runaway. However, no abnormal situations were experienced at any time during the program.

Typical Phase I tests lasted between 5 and 10 minutes. In every case, the first 60 seconds of the stimulus signal was maintained constant to allow the subject to acclimatize himself and to give the motor time to move the attenuator to the vicinity of the appropriate working range. Similarly, the final stimulus signal was maintained for an additional 30 seconds as a check that the subject had indeed tracked his threshold accurately and was still concentrating at the end of the test. For wide frequency range sweeps, the 100 dB dynamic range of the system was insufficient to give a reasonable chance of avoiding running out of attenuator range. This problem was remedied by inserting an optional 30-dB attenuator into the system at the DAS output. The procedure for using this was to hold the frequency sweep in the vicinity of 400 Hz for a period of 20 seconds. During this time, the attenuator was switched into the circuit, leaving the subject sufficient time to adjust to a new attenuator setting before continuing the sweep.

4.4 PHASE II TESTS

The purpose of this second series of tests was to provide comprehensive experimental confirmation of the validity of the aural detectability criteria for practical application. The experiment was designed around the Békésy audiometric procedure but involved the use of recorded helicopter sounds in place of the "artificial" stimuli used previously and a wide range of ambient noise spectra.

The helicopter noise recordings were obtained from the U. S. Air Force Flight Dynamics Laboratory, the Acoustics Branch of NASA Langley Research Center Dynamics Loads Division, and from Wyle Laboratories' magnetic tape library. Many signals were examined for their ability to meet the following criteria listed: in order of importance)

1. Good signal-to-noise ratio and signal quality;

2. Freedom from wind noise, insect sounds, bird calls, vehicle movements, voices, and other spurious sounds;

3. Long duration and steadiness;

4. A diversity of source characteristics;

5. Large distance between source and microphone.

In fact, these requirements were difficult if not impossible to meet collectively, and in almost all cases a compromise of some kind was necessary. Probably of most significance in this regard is that it was generally criterion number 5 that suffered, and most of the sounds selected were recorded at distances substantially less than detection range. The 21 signals selected for study are listed in Table I.

Most of the original recordings were made on wide-frequency-range FM equipment, and the initial intention was to use an FM reproducer to generate the test stimuli in order to include the frequencies below 20 - 25 Hz. Unfortunately, severe problems were encountered with the PS-207 remote operation facility which could not be overcome during the available test period. Accordingly, it was necessary to copy data to a direct record system for reproduction according to the arrangement shown in Figure 32.

Because of the finite travel rate of the DAS attenuator, any sudden, large changes of level essentially cause the loss of threshold data while the potentiometer travels to its new equilibrium problem. To minimize the occurence of such discontinuities, the 21 signals were copied in sequence onto a master test tape through an amplifier whose gain was continually adjusted to maintain an approximately constant overall level.

The 1/3-octave band levels were read at 15-second intervals from time history analyses of this tape made with a 300-msec averaging time (see Section 5.4). These histories were further averaged by eye to smooth out low-period random fluctuations for a total effective averaging time of the order of 10 seconds.

The tape, which was initiated and terminated by 60 seconds and 30 seconds respectively of a 100-Hz control tone for setup and calibration purposes, lasted about

TABLE I. SOUND RECORDINGS USED IN PHASE II TESTS

Ident. No.	Helicopter Type	Flight Configuration	Estimated Ground Distance ft.	Signal Duration sec.
1	CH-47B	Hover in ground-effect	200	57
2	UH-1B	Hover and approach	5,000	61
3	UH-1B	Hover in ground-effect	600	70
4	CH-47B	Hover in ground-effect	300	94
5	UH-1B	Hover in ground-effect	2,500	53
6	HH-43B	Hover in ground-effect	200	25
7	HH-43B	Hover at 50 ft altitude	200	23
8	HH-43B	Hover at 200 ft altitude	200	20
9	HH-43B	Hover at 500 ft altitude	200	29
10	CH-47A	Flyover at 1100 ft, 100 kt	from 10,000	62
11	CH-47A	Flyover at 750 ft, 100 kt	from 6,000	37
12	CH-47A	Flyover at 450 ft, 100 kt	from 6,000	37
13	CH-47A	Flyover at 250 ft, 100 kt	from 6,000	36
14	QH-50	Flyover at 125 ft, 30 kt	from 4,000	80
15	QH-50	Flyover at 1000 ft, 40 kt	from 3,500	51
16	YOH-6	Flyover at 500 ft, 100 kt	from 10,000	57
17	YOH-6	Hover at 500 ft	200	36
18	CH-3E	Flyover at 1000 ft, 60 kt	from 8,000	85
19	CH-3E	Hover at 500 ft	200	39
20	UH-1F	Flyover at 1000 ft, 60 kt	from 9,000	91
21	UH-1B	Ground run	50	81

23 minutes. The entire tape was played for each test in combination with one of eight different ambient masking sounds (including "zero" ambient for the determination of absolute thresholds). These ambient sounds all comprised gaussian random noise with spectrum levels designed to provide the severest possible test of the analytical threshold model. Only two spectrum shapes were involved: flat "pink" noise and noise whose 1/3-octave band level decayed at the rate of 6 dB per octave. These sounds were recorded on two separate tapes which were reproduced at different levels to obtain the specified conditions.

To provide improved statistical reliability in these main tests, ten subjects were used. These were all men in their twenties and early thirties who were selected from approximately thirty applicants on the basis of acceptable hearing ability. No related experience was required and, in an attempt to derive realistic results typical of "untrained" listeners in the tactical situation, no extensive training was given. Each subject was paid for his services and participated in each of the eight test runs described above. In addition, sine sweep audiograms were measured on a number of occasions. Because of the long duration of these tests, each subject was allowed at least 30 minutes' rest period between successive tests.

The written instructions given to the subjects are presented in Appendix III. The participants were given ample time to study these and to ask any questions to satisfy themselves and the Test Director that they fully understood what was required. In addition they were allowed short practice runs. It should be noted that the instructions made specific reference to aircraft sounds. This was felt to be important after preliminary tests revealed that a difference normally existed between the level at which an unspecified stimulus difference was detected and the level at which the signal was recognized as the sound of a helicopter.

5.0 RESULTS AND DISCUSSION

The experimental data presented in Sections 5.1 and 5.2 were read from the computer plots such as shown in Figure 30. Curves were fitted through the average threshold points by eye, and from it values were read and tabulated at 1/3-octave intervals. The data points shown in the various figures are these 1/3-octave values. All results are averaged for the same three experienced subjects and it should thus be noted that each 1/3-octave data point effectively represents the contributions of approximately 45 individual measurements. The variability of these individual measurements, due to both the differences between subjects and the adjustment oscillation, had an average standard deviation of approximately 4 dB. However, deviations tended to increase to around twice this value at frequencies above 4000 Hz.

5.1 ABSOLUTE THRESHOLD DETERMINATIONS

The absolute threshold of audibility for a pure tone is shown in Figure 34 as a function of frequency. Two sets of data are plotted, measured on two occasions separated by several weeks, which indicate the degree of repeatability obtained. Very small differences are observed at frequencies below 2000 Hz, but discrepancies are apparent at higher frequencies. This reflects the increased data scatter at high frequencies referred to above and is probably attributable to the difficulties of accurately establishing the true sound pressure level in this region (see the headphone response diagram, Figure 33).

A best-fit curve has been faired through the data points for use as a basic pure-tone reference in subsequent discussions. The slight hump in the curve around 80 - 100 Hz is purely a function of the stimulus presentation system as Figure 35 reveals. This compares the thresholds measured in three ways: with headphones only, with loudspeakers only, and with both headphones and loudspeakers connected through a 65-Hz crossover network. The loudspeaker-alone data is practically undistinguishable from the "combined" curve, but a marked increase in the threshold level may be seen for the headphone presented sound. This difference, with a maximum of 12 dB at 25 - 31.5 Hz, is probably due to the different methods by which the sound pressure levels were measured and the fact that the headphone levels differ between the coupler used for calibration purposes and the normal head fitting position due to leakage through the seal. The rapid convergence of the two curves above 63 Hz suggests that a higher frequency crossover would have been more appropriate, but the choice is not considered detrimental since the findings of the study are based upon relative threshold measurements.

The pure-tone function is compared with previous threshold determinations in Figure 36. Fletcher and Munson[28] measured the average threshold of eleven subjects in 1933 using headphones, and this curve has been and continues to be widely used

and quoted. Their curve agrees closely with present data in the mid-frequency range (63 - 1000 Hz), although differences at higher frequencies become quite large. The second curve, which demonstrates the increase of threshold level with increasing age, is due to Robinson and Dadson[34], who performed a painstaking experiment with 90 subjects to determine threshold levels for totally free field exposure (Minimum Audible Field). The derived levels are those measured at the center of the head position in the absence of the subject, and this will account to some extent for the lower threshold evident in the 20-year-old curve around 4000 Hz. As Wiener[52] has shown, sound diffraction patterns around the head cause an increase in sound pressure level at the entrance to the ear, relative to that in the undisturbed field, by 10 or more dB at frequencies above 1000 Hz. At frequencies below 1000 Hz, the Robinson and Dadson data is considerably lower than the other curves and is probably due to differences in subject performance and extra-auditory effects not present with headphone stimulation. At very low frequencies the curves tend to converge, although the previous curves terminate at 25 Hz. One of the few previous studies of very low frequency noise was performed by Von Békésy in 1936, and a report in Reference 53 explains that this curve corresponds to the Minimum Audible Pressure measured at the eardrum. In any event, this data is rather higher in level than that from the other sources. As noted previously, the subtle differences between the various results are of no concern here since the only requirement was to determine all thresholds in the same way to provide comparative results for difference sound sources.

The absolute threshold for 1/3-octave bands of stationary random noise is compared with the pure-tone curve in Figure 37. Again two separate sets of data are shown, and the same comments regarding agreement apply. The differences between the two curves are small but consistent. At low frequencies the noise threshold is lower than the tone threshold, whereas at frequencies above 1000 Hz the converse is true. It is likely that the low-frequency difference is related to the fact that low-frequency narrow bands of random noise differ from pure tones mainly in that their rms levels vary with time. In fact, subjectively, a low-frequency band of noise sounds precisely like a tone with the same center frequency whose intensity fluctuates in a random manner. Based on the analysis presented in Section 2.1, Figure 38 has been prepared to show the level in dB relative to the true, long time averaged level, which is exceeded by a narrow band of noise for 10% of the time. An averaging time of 200 msec was assumed to be typical of the hearing system as discussed in Section 3.4. If it is appropriate to suppose that a listener can detect the most intense 10% of the signal, then the fact that the curve of Figure 38 agrees closely with the difference between the tone and 1/3-octave noise thresholds in Figure 40 supports the value of 200 msec for the averaging time for the hearing system. However, the choice is arbitrary, and a higher percentage would imply a smaller averaging time.

The difference between the two curves at high frequencies is largely a critical bandwidth effect. Accepting that the pure-tone curve is also correct for critical

bands of noise (since both sounds stimulate the same region of the basilar membrane), the fact that the 1/3-octave bandwidths are greater than critical bandwidths at high frequencies explains the increase in threshold level. This is discussed further in Section 5.3.

Also shown in Figure 37 is the 1/3-octave band spectrum of the ambient noise in the test chamber. Measurements above 160 Hz are uncertain due to inherent microphone noise, but levels are generally more than 10 dB below the threshold level.

The thresholds measured for octave bands of noise are presented in Figure 39 in comparison with both the tone and the 1/3-octave curves. Similar comments are applicable to the tone versus noise comparison, although the differences are smaller at low frequencies and greater at high frequencies. This is precisely as might be expected. Because of the increased bandwidth, the rms level fluctuations are decreased at low frequencies, as shown by the octave band curve in Figure 38; whereas, the increased difference at high frequencies reflects the higher octave/critical bandwidth ratio.

The results of various degrees of amplitude modulation of the random noise are shown in the 1/3-octave band thresholds plotted in Figure 40, where the curve for stationary noise is also included. The modulations were all impressed at a frequency of 10 Hz, typical of helicopter main rotor blade passage frequencies, and at levels of 3, 6 and 9 dB (corresponding to peak-to-trough pressure ratios of 1.4, 2 and 2.8 respectively). Although some slight differences may be observed, there are no obvious trends, and it is felt that these cannot be regarded as significant, particularly at the high frequencies. It should be noted that these modulation depths are equivalent, in the case of rotor broadband noise, to tip Mach numbers of 0.17, 0.33, and 0.47, which are perhaps rather low, but were restricted by the capacity of the modulator available. The corresponding peak-to-mean sound pressure level ratios (crest factors) are computed to be 1.2, 2.2 and 2.9 dB respectively.

Absolute thresholds were also measured for 1/3-octave bands of harmonic noise with fundamental frequencies of 10, 20 and 40 Hz respectively. The signals were generated with zero interharmonic phase, but instrumentation response may be expected to have a significant effect upon the observed phase differences. In each case the test included the 1/3-octave bands covering the range between the 3rd and 100th harmonics of the fundamental. The three sets of results are compared with the pure-tone threshold in Figure 41. Only slight differences between the various data may be noted, and again these are somewhat random. This is almost certainly true between 50 and 160 Hz where the low-frequency bands pass signals which are essentially sinusoidal with only very slight amplitude variations due to interharmonic beating (see Figure 20). The differences above 1000 Hz, where the threshold should be influenced by the critical band effect, are too small to warrant much discussion. Of particular significance here is that the outputs of the higher

frequency bands are essentially highly modulated (Figure 20) with crest factors of as much as 9 dB. The amount of modulation perceived will be highly dependent upon aural averaging time as indicated by Figure 22, which shows the peak-to-mean SPL ratio as a function of this factor. If, as has been suggested by studies of amplitude modulated random noise[44], the averaging time is much less than 100 msec, then for the 10-Hz signal, a listener would hear intermittent levels considerably in excess of the rms levels indicated in Figure 41. It is quite likely, therefore, that these observed level fluctuations depress the threshold (just as do the random fluctuations in low-frequency bands of noise) below the value which might be expected on a critical band basis. However, even though the modulations are very apparent in all bands, the auditory averaging time and consequently the depth of the perceived modulations are unknown. It can be stated that the apparent perceived modulation diminishes as the modulation (fundamental) frequency increases, a fact which again points to the role of auditory temporal averaging.

5.2 MASKED THRESHOLD DETERMINATIONS

In order to investigate the masking effects of ambient noise, similar experiments were repeated in which the signals were mixed with wideband noise which was essentially flat as measured by a constant-percentage bandwidth analyzer. The masking of pure tones by this noise at two levels is illustrated in Figure 42. The broken lines show both the absolute threshold for pure tones and the 1/3-octave band levels of the masking noise. It is apparent that the low-frequency thresholds are controlled by the absolute hearing ability, whereas the high frequency thresholds are controlled by the presence of the masking noise. Although there are some differences between the threshold signal-to-noise ratios at the two levels, an attempt has been made to minimize these differences in the fixed curves. It may be seen that the level of the just-audible tone decreases, relative to the 1/3-octave band level of the ambient, as frequency increases, being typically 10 dB below it at the high frequencies. It is interesting to compare Figure 42 with the results of Hawkins and Stevens[31], which are reproduced in Figure 43. Figure 43 shows masked tone thresholds for four different masking levels of "white" noise. Although their data extends down only to a frequency of 100 Hz, they bear a good resemblance to the present ones, although detailed inspection reveals some notable differences in the mid-frequency range.

Results for 1/3-octave bands of noise, both stationary and modulated, are presented in Figure 44. It may be seen that in the region where the masking noise is well above absolute threshold, the differential threshold is roughly constant at about - 5 dB. In other words, the band of noise is just detectable when the existing level of noise in that band is raised by 1 dB (since the addition of two uncorrelated signals which differ in level by 5 dB gives a combined level 1 dB greater than that of the highest level). In terms of the auditory mechanism it can be stated that a noise signal

is audible in an ambient noise when the combined critical band level is increased by 1 dB. This is greater than the generally accepted just noticeable difference (JND) of 0.5 dB (which is produced by a noise 9 dB less than ambient).

Use of the critical band concept leads to an explanation of the difference between the masked threshold for tones and bands of noise which is evident in Figure 44. Since we may assume that the tone is also audible when it raises the combined critical band level by 1 dB, the above ratio gives a direct measure of the critical bandwidth. Use will be made of this in Section 5.3.

In Figure 45 the results for the masking of octave bands of noise are presented. These are entirely consistent with the 1/3-octave band data since the 1/3-octave band components of the just-masked octave bands lie approximately 5 dB below ambient 1/3-octave band levels.

Figure 46 compares the masked thresholds for tones and 1/3-octave bands of harmonic noise; again, as in the case of abolute thresholds, the two curves are essentially coincident. In this case, however, it is clear that the threshold for filtered harmonic noise is decidedly lower than that for 1/3-octave bands of random noise. It can only be concluded that this difference is attributable to the high modulation level in the case of the harmonic complexes. Depending upon averaging times, the peak-to-mean SPLs for these signals can be as high as 9 dB (Figure 22) and substantially greater than those associated with the modulated noise signals studied (up to 3 dB).

5.3 AUDITORY FREQUENCY AND TEMPORAL RESOLUTION

Critical Bands

It is clear from the results plotted in Figure 44 that the "critical ratio" measured by Fletcher and Munson and later by Hawkins and Stevens (see Figure 28) is a function of two parameters. It first depends upon the width of the critical band, the discriminatory filter of the hearing mechanism, and secondly, the minimum perceptible differences in the critical band level caused by the addition of the tone. The factor of 2.5 noted by Zwicker et al.[36] between their critical band function and the "critical ratio" is in fact the just-noticeable signal increment which, expressed in logarithmic units, is 4 dB. This corresponds closely to the value of 5 dB observed directly for bands of noise in Figures 44 and 45*. Figure 44 can also be used to obtain a direct measure of the critical bandwidth by equating the energy in the just-audible tone to that in the critical bandwidth of the just-audible noise; i.e., since

*But see paragraph 5.5

$$L = N_s + 10 \log_{10} \Delta f' \tag{24}$$

where L is the SPL of the just-audible tone, N_s is the PSD of the just-audible noise signal, and $\Delta f'$ is the critical bandwidth. Since $N_s = N_3 - \Delta f_3$, where the subscript 3 denotes 1/3-octave quantities, then

$$10 \log_{10} \Delta f' = L - N_3 + 10 \log_{10} \Delta f_3 \tag{25}$$

The critical band function derived in this way is compared with those of Zwicker et al. and Greenwood in Figure 47.

The same equation (25) should be true whether the threshold is a masked threshold or an absolute threshold (in quiet). It has therefore been applied to the data from Figures 40 and 42 to obtain further estimates of the critical bandwidth function, which are presented in Figure 50.

The three curves are perhaps more notable for their differences than their similarities, a fact which corroborates the conclusions of Swets et al.[39], De Boer[40], and others, that critical bandwidths are very difficult to measure, being a function of the measurement method, the assumed filter function, and many other psychosensory variables. On the other hand, the results do at least straddle the previously obtained values, tending to favor that due to Greenwood[37]. Because of this, the fact that Greenwood did use measurements made at low frequencies and because his function has a convenient and simple mathematical description, it seems most appropriate to rely upon it for an aural detection model.

Multiband Detection

An important question which arises in the practical application of threshold data for tones and narrow bands of noise is whether the simultaneous detection of more than one band or frequency component influences the combined threshold level. To investigate this problem, a test was performed to measure the masked threshold level of a noise signal which varied in bandwidth steps between one single 1/3 octave (centered at 500 Hz) and 13 bands covering the range 125 to 2000 Hz. The spectrum of the signal was adjusted so that each band was equally detectable according to the finding that the differential threshold for bands of noise is - 5 dB. The results, illustrated diagrammatically in Figure 48(a), demonstrated that the masked threshold decreased at a slow rate as the number of just-detectable bands increased. The rate from Figure 48(b) is approximately - N/4 dB where N is the number of bands. Although this data is very limited, it does suggest that the depression of the threshold by multiple band detection is a small effect since in general it is likely that detection will be confined to a relatively small region of the frequency spectrum.

Averaging Time

Although the literature cites auditory averaging times between 10 msec and 200 msec, several considerations suggest that a value nearer to the latter is probably more accurate. The first evidence is described in Section 5.1 in connection with the different threshold levels for low-frequency bands of noise. The second is related to the fact that level fluctuations in bands of noise become less perceptible as frequency increases. For 1/3-octave bands of gaussian random noise, the transition from unsteady to steady sound occurs around 4000 Hz. For octave bands it occurs at a little lower frequency. Naturally, this is a highly subjective phenomenon, and the above statement is based upon very few observations, but it does agree with the peak-to-steady rms data presented in Figure 38 for a 200 msec averaging time. The curves for octave and 1/3-octave bands of noise cross the 0.5-dB just-noticeable difference line around the above-mentioned frequencies. In a similar way, the perception of amplitude modulations in filtered harmonic noise decreases as modulation frequency increases. The 40-Hz modulation frequency used in the experiments appeared to approach the limit of perception. This would seem unlikely if the averaging time were 10 msec (i.e., 0.25 x modulation period), giving a peak-to-true level ratio of around 5 dB. For similar reasons, the agreement between both absolute and masked thresholds for filtered harmonic noise would probably diverge widely if the averaging time were very small.

5.4 MODEL FOR HELICOPTER AURAL DETECTABILITY

The experimental results presented in the previous sections provide the basis for calculating the aural detectability of helicopter noise in the light of the following conclusions:

1) It is reasonable to assume that a unique absolute audibility threshold function exists which is the same for constant-amplitude tones and for critical bands of random-noise where the latter should ideally be measured as the 90th percentile level obtained from the output of a sound pressure level detector with an averaging time of around 200 msec.

2) High levels of amplitude modulation do appear to cause an increase in signal detectability. Although random signals with amplitude modulations of up to 3 dB peak-to-average SPL (corresponding to 9 dB peak-to-trough SPL) did not reveal this increase, modulations as high as 9 dB in the case of filtered harmonic noise did indicate a noticeable lowering of the threshold. Again, it seems that peak sound pressure levels recorded by a system with a 200-msec averaging time are appropriate for the specification of detection level.

3) The critical band function established by Greenwood provides a convenient explanation for the observed differences between both masked and absolute thresholds of the various sounds studied.

4) At levels well above the absolute threshold, a narrow-band signal is audible in a noise background when the combined level of any critical band is increased by 1 dB., i.e., when the critical band level of the signal is increased to within 5 dB of that of the masking noise.

5) Simultaneous detection of many adjacent frequency bands causes a small depression of the threshold. However, the effect is sufficiently small to be ignored for practical purposes.

6) In the presence of masking noise, the combined threshold level may be calculated by (decibel) addition of the absolute threshold for tones and the critical band masking level.

Since measuring instruments incorporating critical band filters cannot be obtained commercially, it is necessary in practice to use filters that can yield an adequate approximation to the critical band spectrum. One-third octave band filters are most convenient for this purpose, although other bandwidths can be used with greater or lesser accuracy.

In any event, to compute the audibility threshold level of a helicopter noise spectrum in a particular ambient noise environment, it is necessary (a) to convert the ambient noise data to the form of a critical band spectrum, (b) to define a critical band masking level which is 5 dB less than the critical band ambient spectrum, (c) to combine an appropriate absolute threshold of hearing with the masking level (by decibel addition) to establish a combined threshold function, (d) to convert the helicopter noise data to a critical band spectrum, and finally, (e) to adjust the overall level of this spectrum to the highest value at which no critical band level exceeds the combined threshold level.

When computing a detection distance, step (e) is a lengthy process because the observed helicopter spectrum changes its frequency dependence with distance due to sound absorption. It thus becomes necessary either to examine the variation of each individual critical band level with distance to determine which one is critical, or to estimate a detection distance, compute the difference between the signal and the combined threshold and iterate toward an exact solution based on the magnitude of the error.

Detailed procedures for the calculation of both detection thresholds and detection distances, together with methods for converting both octave and 1/3-octave band data to critical band spectra are presented in Appendix IV. The next section includes

the results of the Phase II experiments and demonstrates the level of accuracy which may be expected of these procedures.

5.5 APPLICABILITY OF THRESHOLD PREDICTION PROCEDURES

Figure 49 shows the eight ambient noise conditions established for the eight tests which comprised the Phase II experiments. The lowest ambient (Test 1) is the noise floor of the test chamber and corresponds to "quiet" conditions. The remaining masking noises were mixed with the signal and generated by the loudspeakers and headphones. The broken line superimposed on these profiles is the average pure-tone since inspection of individual results indicated that two of the original ten subjects performed very poorly (unacceptably high standard deviations of their threshold levels). Even for the remaining eight, the standard deviation of the threshold (as previously defined) was approximately 10 dB.

The eight combined critical band thresholds computed from the data shown in Figure 49 by the method described in Appendix IV, Method A, are presented in Figure 50. Note that the two lowest ambient levels cause only a very small deviation from the absolute tone threshold (lowest curve).

The 1/3-octave band spectrum of the helicopter recording was measured (for all frequencies between 12.5 Hz and 10,000 Hz) at 15-second intervals throughout its length and digitized for computer analysis. The absolute threshold level of the signal was computed in each case by applying the measured attenuation level averaged for all eight subjects. Each spectrum level corrected in this way for overall level and for the system frequency response was converted to an equivalent critical band level by the method of Appendix IV, Method A. The differences between the estimated threshold level L_{n_e} and the actual threshold level L_n in each band at all instants of time were analyzed to derive the results presented in Figures 51 through 58 and Tables II and III. Figures 51 through 58 show (in 1/3-octave rather than critical band levels) the distributions of the measured threshold band levels about the theoretical values. Three curves are shown in each figure which correspond to the 75th, 92nd and 97.5th percentiles of the measured level distributions. These are levels exceeded by the measured threshold band levels 2.5%, 8% and 25% of the time respectively. These diagrams show very clearly that the theoretical threshold levels are exceeded, at some part of the audible frequency range, for around 25% of the time. Of direct interest is the average differences between the measured and theoretical threshold levels.

This information is listed in Table II in terms of the average for each individual test and the grand average for all tests. Two errors (differences) are analyzed: the

TABLE II. ANALYSIS OF THE THRESHOLD PREDICTION ERRORS

TEST NO.	Error $L = \sum_{dB} (L_n - L_{n_e})^*$		Error $L_{min} = (L_n - L_{n_e})_{min}$	
	mean	std. devn.	mean	std. devn.
1	+4.8	2.4	+1.5	3.0
2	+5.3	2.5	+2.5	3.0
3	+4.4	2.9	+1.2	3.2
4	+6.0	3.5	+2.7	3.5
5	+3.3	2.8	+0.1	3.2
6	+2.2	2.9	-1.4	3.1
7	+3.6	3.4	+0.8	3.7
8	+2.0	4.0	+0.3	4.6
ALL	+4.0	3.6	+1.0	3.9

*L_n = measured threshold level; L_{n_e} = theoretical threshold level.

minimum error $L_{min} = (L_n - L_{n_e})_{min}$, which is the minimum difference between the measured and theoretical levels found in any of the 30 frequency bands at one instant of time, and composite error $\sum L = \sum_{dB} (L_n - L_{n_e})$, the decibel sum of all 30 differences at one instant of time. The latter is effectively the total intensity level of the signal relative to the threshold level.

The grand average errors are +1.0 dB and +4 dB respectively. In other words, the helicopter sounds were just detectable, on the average, when an individual critical band level increased to 1 dB above the theoretical combined threshold*, or when the decibel sum of such differences reached a value of 4 dB. The associated standard deviations of 3.9 dB and 3.6 dB suggest, in fact, that the second criterion is a little more consistent. However, the increase in practical complexity does not seem justified by the small reduction in variability. Furthermore, the average minimum difference, L_{min}, seems to be more consistent from test to test, i.e., as the ambient level varies, than does $\sum L$ (intertest standard deviations of the mean are 1.3 dB and 1.5 dB respectively). The standard deviations of between 3 and 4 dB seem satisfactory in light of the subjective variability of approximately 7 dB, the average standard deviation for this experiment. Also, it is unlikely that the acoustic stimuli, both signal and noise, could ever be specified with greater accuracy; indeed for most applications it is probable that significantly larger errors might be expected.

It is of interest to examine the frequency distribution of the minimum error L_{min} presented for each test in Table III. For the lowest threshold levels (1), (2), and (7), which would be encountered in practice only in the quietest forest or jungle environments, detections are confined to a limited band of mid-frequencies. This is also clearly illustrated in Figures 51 and 52. As the ambient level of the "flat" ambient noise is increased (Tests 3 through 6), there is a noticeable shift of the most frequent detection bands to lower frequencies, as might be expected. When the "sloping" ambient noise is used in Test 8, the combined threshold curve slopes at practically the same rate as the typical helicopter noise spectrum and indicates that detections occur over a wide range of frequencies.

In the interpretations of these results, it is most important to recognize that the sounds studied were selected to include as wide a range of objective and subjective characteristics as possible. For the most part they are not typical of the sound observed at distances of tens of thousands of feet typical of helicopter detection ranges. In

* A possible explanation for this 1 dB increment is that it is the margin required for the listener to identify the sound as that of a helicopter (see Section 4.5).

TABLE III. PERCENTAGE DISTRIBUTION OF DETECTION BANDS

TEST NO.	CRITICAL BAND CENTER FREQUENCY																							
	50	63	80	100	125	160	200	250	315	400	500	630	800	1,000	1,250	1,600	2,000	2,500	3,150	4,000	5,000	6,300	8,000	10,000
1								2	13	13	14		30	14	8	8								
2								2	17	13	14		30	13	5	8								
3					2	2		6	22	23	9	5	20	5	2	3		2						
4			2	2	6	9	8	17	14	23		5	5	2		2		2				2	2	2
5			5	3	27	16	19	8	3	13			2	2		2						2	2	
6	6	5	9	13	47	5	6	2		2				2									2	
7					3			3	13	16	2	2	25	13	8	17								
8		3	6		3				5	9		3	13	5	2	13	6	2	6		2	2	5	16

retrospect, it is perhaps unfortunate that the choice of signals and the unavoidable change from FM to direct record/reproduction equipment were jointly responsible for a shift of emphasis to higher frequencies. The Phase I results certainly permit confidence that the low frequency threshold functions are accurate, but further research is required to specify the magnitude and applicability of critical band functions in that region with more precision.

A comparison of Figures 49 and 36 reveals that the average pure-tone threshold for the subjects who participated in the tests is rather higher than the free field threshold for the 20-year old men studied by Robinson and Dadson[34]. For general application, it is recommended that the free-field curve measured by Robinson and Dadson be used because (a) it is directly applicable to the case of helicopter detection conditions (at least in open country), and (b) it was obtained in experiments involving a large number of subjects. For convenience, the data from Reference 34 has been extrapolated down to 12.5 Hz on the basis of the present results and tabulated in Appendix IV.

6.0 CONCLUSIONS

Helicopter noise is an unusually complex combination of periodic and random sound. The periodic components, which contain multiple harmonics of the rotor blade passage frequencies, dominate the frequency spectrum below about 300 - 400 Hz. At higher frequencies, the noise has a broadband random nature but is periodically modulated im amplitude at the blade passage frequency. The problems of propagation, measurement and analysis peculiar to this kind of noise have been reviewed and an extensive laboratory experiment has been conducted to investigate aural detection mechanisms. The major conclusions are summarized below under the appropriate subheadings.

6.1 PROPAGATION

1) The effects of a uniform atmosphere on helicopter sound propagation are dominated by relaxation losses which can be defined analytically with considerable accuracy. Methods are provided for this purpose which may be confidently used to predict attenuation as a function of frequency for air-to-ground propagation angles greater than about 10 degrees (measured from the ground plane).

2) The effects of ground surfaces, ground cover, and atmospheric inhomogeneities become important at propagation angles of less than 10 degrees. These effects are substantially less predictable because (a) many of the fundamental mechanisms are poorly understood and (b) the parameters themselves are difficult to define in an operational situation. However, empirical results are presented which allow at least order-of-magnitude predictions to be made.

6.2 DATA ACQUISITION

1) For research purposes, a wide frequency range capability is required of the measurement and recording instrumentation. In particular, the system should have a good response down to 5 Hz or less. This can be achieved only with high quality condenser microphones used in conjunction with FET-type preamplifiers and a wide-frequency-range FM tape recorder (0 - 20 kHz response).

2) The major difficulty with recording instrumentation lies not in the frequency response performance, but in dynamic range, the critical item being the FM tape recorder. At best these recorders have signal-to-noise ratios of 45 dB. High crest factors and an adequate working tolerance reduce this to about

30 dB for the peak sound pressure level during a flyover. This compares very poorly with the 120-dB range of the human ear. Also, working systems must be designed with special attention to signal conditioning with a variable gain capability to make the best possible use of the 30-dB range.

6.3 DATA ANALYSIS

1) For most applications, helicopter sound recordings must be analyzed to define the frequency distribution of acoustic energy. An appropriate procedure for spectral analysis must be selected to compromise the requirements of resolution, accuracy, and speed. For either periodic or random noise, the requirements are well defined. The need to consider both in the case of helicopter noise imposes twofold constraints on the selection.

2) For harmonic noise, a narrow filter bandwidth is required, preferably considerably less than the fundamental frequency of interest (which is equal to the interharmonic spacing). The averaging time of the rms detection should be greater than 1.33 periods of the component under analysis for an accuracy of $\pm$ 0.5 dB, or greater than 0.8 period for an error of less than $\pm$ 1 dB.

3) For random noise, the error increases as the product bandwidth x averaging time decreases. For an accuracy of $\pm$ 1 dB, this value should exceed 40; for $\pm$ 0.5 dB, products greater than 200 are necessary. If the modulation amplitudes are required, the averaging time must be very small (typically 20 msec) so that they can be detected only by very coarse filters, unless provision is made to average a series of modulation cycles.

4) For long-duration hover recordings, the main constraint upon the analysis is the physical time involved. A detailed analog narrow-band analysis, for example, can take several hours. For flyby recordings, the signal is "nonstationary", and an additional requirement is that the spectral characteristics should not change significantly during the averaging time. The selection of an averaging time must be based upon the flight configuration under study, but this consideration generally eliminates the ability to perform a narrow-band analysis at the higher frequencies. Harmonic components, however, can be extracted with reasonable accuracy using high-speed analysis equipment.

5) For general-purpose analysis of flight data, 1/3-octave analysis is recommended since it provides a reasonable compromise between resolution, accuracy and speed, it represents an adequate analog of the hearing mechanism, and it is widely available in commercial analysis systems.

6) Real-time analyzers are very useful for high-speed, large-volume acoustic data reduction and are particularly appropriate for flyby data analysis. However, care is required to meet the accuracy requirements existing for all spectrum analysis, particularly with regard to averaging time.

7) When interpreting filtered data, it is easy to confuse modulated random noise with the waveform of a group of harmonics, since both exhibit a modulation envelope with a period equal to the blade passage interval. The safest way to discriminate between them is to perform a narrow-band analysis of the filter output.

8) The accurate measurement of pulsatile sound pressure levels with high crest factors requires an elaborate rms detection circuit. Averaging times should be several times greater than modulation periods. Failure to meet this requirement can lead to severe errors in the measurement of highly modulated signals.

6.4 PERCEPTION

1) The distinctive subjective character of helicopter noise is related to its highly impulsive nature which is perceived across the entire audible frequency range.

2) The perception of the frequency of periodic, pulsatile noise is controlled by the periodicity and not by the frequency content. The apparent detection of the rotor blade passage frequency does not necessarily mean that the fundamental frequency is audible. Indeed, the apparent frequency remains unchanged even if many of the lower harmonics are removed from the signal. Even if detection levels are controlled by signal frequencies around 200 Hz, the impression remains that of a blade passage frequency disturbance.

3) The aural detectability of helicopters is dependent upon three factors: the spectral and temporal characteristics of the signal at the observer's location; his hearing acuity; and the ambient noise environments which mask the signal.

4) The critical bandwidth function, which describes the frequency selectivity of the hearing system, plays a central role in aural detectability. Measurements of this function performed as part of this study led to the adoption of Greenwood's relationship for the critical bandwidth.

5) For the purposes of aural detection analysis, helicopter noise should ideally be analyzed or specified in terms of 90th percentile critical bandwidth levels as measured with an averaging time of around 200 msec. However, this requirement is generally impractical and procedures are presented for calculating detection threshold levels from either octave or 1/3-octave band estimates of the helicopter signature and the ambient levels.

6) The 1/3-octave procedure was extensively tested in an experiment involving 21 helicopter noise recordings, 8 ambient noise spectra, and 8 subjects. The method was found to consistently predict detection thresholds to within an accuracy of $\pm$ 4 dB.

7.0 RECOMMENDATIONS

As a result of this study, it is recommended that:

1) Sound propagation at small air-to-ground elevation angles be studied in depth. Definition of small-angle attenuation presents a major problem in the estimation of aural detection distances.

2) Field experiments be performed in various terrains using real helicopters and a group of observers to verify the accuracy of the procedures presented herein for predicting aural detection threshold.

3) Further research be addressed at possible nonauditory perception of noise and the applicability of the critical band concept in the frequency region below 100 Hz. These undoubtedly have an important effect on helicopter detectability, and it was not possible during the present study to give in-depth attention to this problem.

4) Methods for recording and analyzing high crest factor signals typical of helicopter noise be investigated. Several problems encountered in this investigation indicate that very large errors are possible.

LITERATURE CITED

1. Loewy, R. G., AURAL DETECTABILITY OF HELICOPTERS IN TACTICAL SITUATIONS, Journal of the American Helicopter Society, October 1963, pp. 36-53.

2. Crandall, S. H. (Editor), RANDOM VIBRATION, Massachusetts, M.I.T. Press, 1963.

3. Cox, C. R., and Lynn, R. R., A STUDY OF THE ORIGIN AND MEANS OF REDUCING HELICOPTER NOISE, Bell Helicopter Company, TCREC Technical Report 62-73, U. S. Army Transportation Research Command, Fort Eustis, Virginia, November 1962.

4. Davidson, I. M., and Hargest, T. J., HELICOPTER NOISE, Journal of the Royal Aeronautical Society, Vol. 69, No. 653, May 1965, pp. 325-336.

5. Loewy, R. G., and Sutton, L. R., A THEORY FOR PREDICTING THE ROTATIONAL NOISE OF LIFTING ROTORS IN FORWARD FLIGHT INCLUDING A COMPARISON WITH EXPERIMENT, Journal of Sound and Vibration, Vol. 4, No. 3., November 1966, pp. 305-347.

6. Schlegel, R. G., King, R. J., and Mull, H. R., HELICOPTER ROTOR NOISE GENERATION AND PROPAGATION, Sikorsky Aircraft, USAAVLABS Technical Report 66-4, U. S. Army Aviation Materiel Laboratories, Fort Eustis, Virginia, October 1966, AD 645 884.

7. Lowson, M. V., and Ollerhead, J. B., A THEORETICAL STUDY OF HELICOPTER ROTOR NOISE, Journal of Sound and Vibration, Vol. 9, No. 2, March 1969, pp. 197-222.

8. Sharland, I. J., and Leverton, J. W., PROPELLER, HELICOPTER AND HOVERCRAFT NOISE, Chapter 9 of NOISE AND ACOUSTIC FATIGUE IN AERONAUTICS, London, John Wiley, 1968.

9. Leverton, J. W., HELICOPTER NOISE - BLADE SLAP, National Aeronautics and Space Administration Contractor Report NASA CR-1221, October 1968.

10. Wright, S. E., SOUND RADIATION FROM A LIFTING ROTOR GENERATED BY ASYMMETRIC DISK LOADING, Journal of Sound and Vibration, Vol. 9, No. 2, March 1969, pp. 223-239.

11. Sadler, S. A., and Loewy, R. G., A THEORY FOR PREDICTING THE ROTATIONAL AND VORTEX NOISE OF LIFTING ROTORS IN HOVER AND FORWARD FLIGHT, National Aeronautics and Space Administration Contractor Report NASA CR-1333, May 1969.

12. Sternfeld, H. J., Spencer, R. H., and Schaeffer, E. G., STUDY TO ESTABLISH REALISTIC ACOUSTIC DESIGN CRITERIA FOR FUTURE ARMY AIRCRAFT, Vertol Division, The Boeing Company, TCREC Technical Report 61-72, U. S. Army Transportation Research Command, Fort Eustis, Virginia, November 1962.

13. Gutin, L. Ya., ON THE SOUND FIELD OF A ROTATING PROPELLER, from Physiks Zeitschrift der Sowjetunion, Band A Heft 1, (1936), pp. 57-71, Translated as NACA TM-1195, National Advisory Committee for Aeronautics, October 1948.

14. Brown, D., and Ollerhead, J. B., PROPELLER NOISE AT LOW TIP SPEEDS, Wyle Laboratories WR 71-9, Wyle Laboratories Research Staff, Hampton, Virginia (to be published).

15. Tedrick, R. N. and Polly, R. C., A PRELIMINARY INVESTIGATION OF THE MEASURED ATMOSPHERIC EFFECTS UPON SOUND PROPAGATION, Marshall Space Flight Center Memorandum MTP-TEST-63-6, May 1963.

16. Evans, L. B., and Sutherland, L. C., ABSORPTION OF SOUND IN AIR, Wyle Laboratories WR 70-14, Wyle Laboratories Research Staff, Huntsville, Alabama, July 1970.

17. Dean, E. A., ABSORPTION OF LOW FREQUENCY SOUND IN A HOMOGENEOUS ATMOSPHERE, Schellenger Research Laboratory Report 1237, August 1959.

18. Harris, C. M., ABSORPTION OF SOUND IN AIR BELOW 1000 CPS, National Aeronautics and Space Administration Contractor Report NASA CR 237, June 1965.

19. Sabine, H. J., SOUND PROPAGATION NEAR EARTH SURFACE AS INFLUENCED BY WEATHER CONDITIONS, WADC Technical Report TR-57-353, Four Volumes, Wright A. Development Center, Dayton, Ohio, 1957-1961.

20. Anon., Society of Automotive Engineers A-21 Committee, Data Presented at Meeting of Working Group on Atmospheric Propagation, New York, June 1969.

21. Parkin, P. H., and Scholes, W. E., OBLIQUE AIR-TO-GROUND SOUND PROPAGATION OVER BUILDINGS, Acustica, Vol. 8, 1958, pp. 99-102.

22. Eyring, Carl F., JUNGLE ACOUSTICS, Journal of the Acoustical Society of America, Vol. 18, No. 2, 1946, pp. 257-270.

23. Dobbins, D. A. et al., JUNGLE ACOUSTICS I: TRANSMISSION AND AUDIBILITY OF SOUNDS IN THE JUNGLE, U. S. Army Tropic Test Center Report No. 7, October 1966, AD 647804.

24. Wiener, Francis M. and Keast, David N., EXPERIMENTAL STUDY OF THE PROPAGATION OF SOUND OVER GROUND, Journal of the Acoustical Society of America, Vol. 31, No. 6, 1959, pp. 724-733.

25. Brown, D., BASELINE NOISE MEASUREMENTS OF ARMY HELICOPTERS, Wyle Laboratories WR 71-4, Wyle Laboratories Research Staff, Hampton, Virginia, USAAMRDL Technical Report 71-36A, U. S. Army Air Mobility Research and Development Laboratory, Eustis Directorate, Fort Eustis, Virginia, (to be published).

26. Kinsler, L. E. and Frey, A. R., FUNDAMENTALS OF ACOUSTICS, New York, John Wiley, 1959.

27. Fletcher, H., AUDITORY PATTERNS, Review of Modern Physics, Vol. 12, January 1940, pp. 47-65.

28. Fletcher H. and Munson, W. A., LOUDNESS, ITS DEFINITION, MEASUREMENT AND CALCULATION, Journal of the Acoustical Society of America, Vol. 5, October 1933, pp. 82-108.

29. Fletcher, H. and Munson, W. A., RELATION BETWEEN LOUDNESS AND MASKING, Journal of the Acoustical Society of America, Vol. 9, July 1937, pp. 1-10.

30. Miller, G. A., SENSITIVITY TO CHANGES IN THE INTENSITY OF WHITE NOISE AND ITS RELATION TO MASKING AND LOUDNESS, Journal of the Acoustical Society of America, Vol. 19, July 1947, pp. 609-619.

31. Hawkins, J. E. and Stevens, S. S., THE MASKING OF PURE TONES AND OF SPEECH BY WHITE NOISE, Journal of the Acoustical Society of America, Vol. 22, January 1950, pp. 6-13.

32. Schafer, T. H., Gales, R. S., Shewmaker, C. A., and Thomsen, P. O., THE FREQUENCY SELECTIVITY OF THE EAR AS DETERMINED BY MASKING EXPERIMENTS, Journal of the Acoustical Society of America, Vol. 22, July 1950, pp. 490-496.

33. Egan, J. P. and Hake, H. W., ON THE MASKING PATTERN OF A SIMPLE AUDITORY STIMULUS, Journal of the Acoustical Society of America, Vol. 22, September 1950, pp. 622-630.

34. Robinson, D. W., and Dadson, R. S., A REDETERMINATION OF THE EQUAL LOUDNESS RELATIONS FOR PURE TONES, British Journal of Applied Physics, May 1956, pp. 166-181.

35. Bilger, R. C., and Hirsch, J. J., MASKING OF TONES BY BANDS OF NOISE, Journal of the Acoustical Society of America, Vol. 28, July 1956, pp. 623-630.

36. Zwicker, E., Flottorp, G., and Stevens, S. S., CRITICAL BANDWIDTH IN LOUDNESS SUMMATION, Journal of the Acoustical Society of America, Vol. 29, May 1957, pp. 548-557.

37. Greenwood, D. D., CRITICAL BANDWIDTH AND THE FREQUENCY COORDINATES OF THE BASILAR MEMBRANE, Journal of the Acoustical Society of America, Vol. 33, October 1961, pp. 1344-1356.

38. Greenwood, D. D., AUDITORY MASKING AND THE CRITICAL BAND, Journal of the Acoustical Society of America, Vol. 33, April 1961, pp. 484-502.

39. Swets, J. A., Green, D. M., and Tanner, W. P., ON THE WIDTH OF THE CRITICAL BANDS, Journal of the Acoustical Society of America, Vol. 34, January 1962, pp. 108-113.

40. DeBoer, E., NOTE ON THE CRITICAL BANDWIDTH, Journal of the Acoustical Society of America, Vol. 34, July 1962, pp. 985-986.

41. Bourbon, W. T., Evans, T. R., and Deatherage, B. H., EFFECTS OF INTENSITY ON CRITICAL BANDS FOR TONAL STIMULI AS DETERMINED BY BAND LIMITING, Journal of the Acoustical Society of America, Vol. 43, August 1967, pp. 56-63.

42. Zwislocki, J., THEORY OF TEMPORAL SUMMATION, Journal of the Acoustical Society of America, Vol. 32, August 1960, pp. 1046-1060.

43. Green, D. M., MASKING WITH TWO TONES, Journal of the Acoustical Society of America, Vol. 37, May 1965, pp. 802-813.

44. Dubrovskii, N. A., and Tumatrina, L. N., INVESTIGATION OF THE HUMAN PERCEPTION OF AMPLITUDE MODULATED NOISE, Journal of Soviet Physics-Acoustics, Vol. 13, No. 1, July-September 1967, pp. 41-47.

45. Von Békésy, G., A NEW AUDIOMETER, Acta. Oto Laryngol, Vol. 35, 1947, pp. 411-422.

46. Hirsch, I. J., BEKESY'S AUDIOMETER, Journal of the Acoustical Society of America, Vol. 35, September 1962, pp. 1333-1336.

47. Adcock, B. D., AN AUTOMATIC DATA SYSTEM FOR LARGE SCALE AUDIOMETRIC TESTING, Wyle Laboratories Technical Memorandum, Wyle Laboratories Research Staff, Hampton, Virginia (to be published).

48. Ollerhead, J. B., SUBJECTIVE EVALUATION OF GENERAL AVIATION AIRCRAFT NOISE, Federal Aviation Administration Technical Report NO-68-35, April 1968.

49. Adcock, B. D., and Ollerhead, J. B., EFFECTIVE PERCEIVED NOISE LEVEL EVALUATED FOR STOL AND OTHER AIRCRAFT NOISE, Federal Aviation Administration Technical Report NO-70-5, May 1970.

50. Ollerhead, J. B., THE NOISINESS OF DIFFUSE SOUND FIELDS AT HIGH INTENSITIES, Federal Aviation Administration Technical Report NO-70-3, May 1970.

51. Ollerhead, J. B., AN EVALUATION OF METHODS FOR SCALING AIRCRAFT NOISE PERCEPTION, Wyle Laboratories WR 70-17, Wyle Laboratories Research Staff, Hampton, Virginia, November 1970.

52. Wiener, F. M., ON THE DIFFRACTION OF A PROGRESSIVE SOUND WAVE BY THE HUMAN HEAD, Journal of the Acoustical Society of America, Vol. 19, No. 1, January 1947, pp. 143-146.

53. Licklider, J. C. R., BASIC CORRELATES OF THE AUDITORY STIMULUS, Chapter 25 of HANDBOOK OF EXPERIMENTAL PSYCHOLOGY, Editor S. S. Stevens, New York, John Wiley, 1966.

54. Evans, L. B., and Sutherland, L. C., ABSORPTION OF SOUND IN AIR, Wyle Laboratories WR 70-14, Wyle Laboratories Research Staff, Huntsville, Alabama, July 1970.

55. Sutherland, L. C., A REVIEW OF THE MOLECULAR ABSORPTION ANOMALY, Paper presented at the 77th Meeting of the Acoustical Society of America, Philadelphia, Pennsylvania, April 1969.

56. Society of Automotive Engineers, STANDARD VALUES OF ATMOSPHERIC ABSORPTION AS A FUNCTION OF TEMPERATURE AND HUMIDITY FOR USE IN EVALUATING AIRCRAFT FLYOVER NOISE, Aerospace Recommended Practice, ARP 866, August 1964.

57. Kneser, H. O., PHYSICAL ACOUSTICS - PRINCIPLES AND METHODS, W. P. Mason (ed.), Chapter 3, Vol. II, Part A, New York, Academic Press, 1964.

58. Herzfeld, K. F., and Litovitz, T. A., ABSORPTION AND DISPERSION IN ULTRASONIC WAVES, New York, Academic Press, 1959.

59. Hilsenrath, J., Beckett, C. W., Benedict, W. S., Fano, L., Loge, H. J., Masi, J. F., Nuttall, R. L., Touloukian, Y. S., and Woolley, H. W., TABLES OF THERMAL PROPERTIES OF GASES, National Bureau of Standards Circular 564, November 1955.

60. Knudsen, V. O., ABSORPTION OF SOUND IN AIR, OXYGEN, AND IN NITROGEN - EFFECTS OF HUMIDITY AND TEMPERATURE, Journal of the Acoustical Society of America, Vol. 5, 1933, pp. 112-121.

61. Harris, C. M., ABSORPTION OF SOUND IN AIR IN THE AUDIO-FREQUENCY RANGE, Journal of the Acoustical Society of America, Vol. 35, 1963, pp. 11-17.

62. Harris, C. M., ABSORPTION OF SOUND IN AIR VERSUS HUMIDITY AND TEMPERATURE, National Aeronautics and Space Administration Contractor Report NASA CR 647, January 1967.

63. Bauer, H. J., and Roesler, H., RELAXATION OF THE VIBRATIONAL DEGREES OF FREEDOM IN BINARY MIXTURES OF DIATOMIC GASES, IN MOLECULAR RELAXATION PROCESS, Chemical Society Special Publication No. 29, New York, Academic Press, 1966, pp. 245-252.

64. Monk, R. G., THERMAL RELAXATION IN HUMID AIR, Journal of the Acoustical Society of America, Vol. 46, 1969, pp.580-586.

65. Knudsen, V. O. and Obert, L., THE ABSORPTION OF HIGH FREQUENCY SOUND IN OXYGEN CONTAINING SMALL AMOUNTS OF WATER VAPOR OR AMMONIA, Journal of the Acoustical Society of America, Vol. 7, 1936, pp. 249-253.

66. Henderson, M. C., THERMAL RELAXATION IN N_2, O_2 and CO WITH ADMIXTURES, Paper presented at the Fourth International Congress on Acoustics, Copenhagen, August 21-28, 1962.

67. Holmes, R., Smith, F. A., and Tempest, W., VIBRATIONAL RELAXATION IN OXYGEN, Proceedings of the Physics Society, Vol. 81, 1963, pp. 311-319.

68. Knudsen, V. O., THE ABSORPTION OF SOUND IN GASES, Journal of the Acoustical Society of America, Vol. 6, No. 4, April 1935, pp.

69. Knotzel, H., THE ABSORPTION OF AUDIBLE SOUND IN AIR AND ITS DEPENDENCE ON HUMIDITY AND TEMPERATURE, Akustische Zeitschrift, September 1940, pp. 245-256.

70. Nyborg, W. L. and Mintzer, D., REVIEW OF SOUND PROPAGATION IN THE LOWER ATMOSPHERE, WADC Technical Report 54-602, Wright Air Development Center, Dayton, Ohio, May 1955.

71. Parker, J. G., EFFECT OF SEVERAL LIGHT MOLECULES ON THE VIBRATIONAL RELAXATION TIME OF OXYGEN, Journal of Chemistry and Physics, Vol. 34, No. 5, May 1961, pp. 1763-1772.

72. Henderson, M. C., Herzfeld, K. F., Bry, J., Cookley, R., and Carriere, G., THERMAL RELAXATION IN NITROGEN WITH WET CARBON DIOXIDE AS IMPURITY, Journal of the Acoustical Society of America, Vol. 45, No. 1, 1969, pp.

73. Henderson, M. C., Clark, A. V., and Lintz, P. R., THERMAL RELAXATION IN OXYGEN WITH H_2O, HDO, and D_2O VAPORS AS IMPURITIES, Journal of the Acoustical Society of America, Vol. 37, No. 3, March 1965, pp.

74. Tuesday, C. S., and Boudart, M., VIBRATIONAL RELAXATION TIMES BY THE IMPACT TUBE METHOD, Technical Note 7, Contract AF 33(038) - 23976, Princeton University, January 1955.

75. Bauer, H. J., NONLINEAR SHIFT OF RELAXATION RATES BY ADMIXTURES, Journal of the Acoustical Society of America, Vol. 44, No. 1, 1968, pp.

76. Beyer, R. T., DOUBLE RELAXATION EFFECTS, Journal of the Acoustical Society of America, Vol. 29, No. 2, February 1957, p. 243.

77. Henderson, M. C., and Herzfeld, K. F., EFFECT OF WATER VAPOR ON THE NAPIER FREQUENCY OF OXYGEN AND AIR, Journal of the Acoustical Society of America, Vol. 46, No. 3, September 1969, p. 986.

78. Piercy, J. E., ROLE OF THE VIBRATIONAL RELAXATION OF NITROGEN IN THE ABSORPTION OF SOUND IN AIR, Journal of the Acoustical Society of America, Vol. 46, No. 3, September 1969, p. 602.

79. Evans, L. B., and Sutherland, L. C., ABSORPTION OF SOUND IN AIR, Paper presented at the 80th Meeting of the Acoustical Society of America, Houston, Texas, November 1970.

80. Society of Automotive Engineers, METHOD FOR CALCULATING THE ATTENUATION OF AIRCRAFT GROUND-TO-GROUND NOISE PROPAGATION DURING TAKEOFF AND LANDING, Aerospace Information Report, AIR 923, August 1966.

81. Burkhard, M. D., Karplus, H. B., Sabine, H. J., SOUND PROPAGATION NEAR THE EARTH'S SURFACE AS INFLUENCED BY WEATHER CONDITIONS, WADC Technical Report 57-353, Part II, Wright Air Development Center, Dayton, Ohio, December 1960.

APPENDIX I
METHODS FOR CALCULATING PROPAGATION LOSSES

As discussed in Section 2.3 of the main text, appropriate methods for the calculation of propagation losses depend upon the elevation angle between the ground plane and the line joining the source and observer. If this angle is greater than approximately 10 degrees, the total attenuation is controlled by the atmospheric absorption which can be computed with some confidence by the methods described in the first section below. For elevations less than 10 degrees, attenuation is normally controlled by terrain effects, atmospheric refraction due to wind and temperature gradients, and scattering by turbulence, all of which are poorly understood and very difficult to predict. Methods for estimating the effects of ground cover and turbulence are presented in the second section below, but it is emphasized that they are based upon very fragmentary data and are subject to revision when further information becomes available.

Attenuation data for both situations are presented, for ease of reference, in tabular or graphic form.

ATMOSPHERIC LOSSES (ELEVATION GREATER THAN 10 DEGREES)

The theoretical value for atmospheric (air-to-ground) propagation losses is the sum of four components as discussed in References 54 and 55.

$$a = a_{cl} + a_{rot} + a_{vib}(O_2) + a_{vib}(N_2) \qquad (25)$$

where a_{cl} = classical losses including, for convenience, diffusion and radiation losses which are essentially negligible

a_{rot} = molecular absorprion losses for rotational relaxation of O_2 and N_2 molecules

$a_{vib}(O_2)$ = molecular absorption losses for vibrational relaxation of O_2 molecules

$a_{vib}(N_2)$ = molecular absorption losses for vibrational relaxation of N_2 molecules

Classical Plus Rotational Losses

The first two components can be lumped together since they vary in the same way with frequency and temperature in the audible frequency range. Based on a weighted average of the most accurate measurements of these two components, they may be expressed by (see Reference 55)

$$a_{cl} + a_{rot} = (4.79 \pm 0.03) \times 10^{-8} \left\{1 + 0.0017\left[\frac{t}{p^*}\right]\right\} f^2/p^*, \text{ dB/1000 ft} \qquad (27)$$

where t = temperature in degrees centigrade

f = frequency in Hz

p^* = pressure in atmospheres

The temperature correction factor is valid over a temperature range of - 40°C to + 60°C (-40°F to 140°F). It accounts for the variation in speed of sound and viscosity of air which enter into the expressions for a_{cl} and a_{rot} in exactly the same manner.

For a typical standard-day conditions at sea level,

t = 15°C (59°F) and $P^* = 1$, and

$$a_{cl} + a_{rot} = 4.86 \times 10^{-8} f^2, \text{ dB/1000 ft} \qquad (28)$$

The corresponding value from Reference 56 is $4.85 \times 10^{-8} f^2$, dB/1000 ft. The latter has essentially the same temperature variation.

Molecular Vibration Loss

For any molecular relaxation loss, the attenuation in dB/1000 ft is given by

$$a_{mol} = 2648\, \mu_{max} \frac{f_m}{c} \left[\frac{(f/f_m)^2}{1+(f/f_m)^2}\right], \text{ dB/1000 ft} \qquad (29)$$

where

μ_{max} = maximum loss in intensity per wavelength (dimensionless)

f_m = frequency of maximum loss per wavelength, Hz

f = frequency of sound, Hz

c = speed of sound, m/sec

Two variables appear in this equation which are necessary and sufficient to define a relaxation loss. As illustrated conceptually in Figure 59, these are the maximum loss per wavelength (μ_{max}) and the relaxation frequency (f_m) at which this maximum occurs. As shown in the figure, when the loss is defined in terms of attenuation per unit distance, it rises as the square of frequency below f_m and then levels off to a constant value well above the relaxation frequency. In air, this relaxation phenomenon for O_2 and N_2 molecules is catalyzed, or becomes much more efficient with the right amount of moisture content in the air. Hence, this form of attenuation is very sensitive to the absolute moisture content in the air, as can be seen from the final tabular results. Due to the dominant role played by this loss mechanism, and the previous lack of an adequate theoretical explanation for extensive experimental observations, it has been necessary to derive appropriate expressions in order to extrapolate available data to a wide variety of weather conditions.

The value of μ_{max}, for molecular relaxation loss for one gas in a mixture, is given by (Reference 57):

$$\mu_{max} = \frac{K \pi R C_i}{\left[C_v C_p (C_v - C_i)(C_p - C_i)\right]^{1/2}} \qquad (30)$$

where

R = universal gas constant

C_i = internal energy of relaxation mode

C_v, C_p = usual specific heats at constant volume and constant pressure, respectively

K = volume concentration of gas in mixture

For diatomic molecules (i.e., $-O_2$ or N_2), the internal energy for the vibrational mode is determined from basic principles (Reference 58) to be

$$C_i/R = C_p/R - 7/2 \tag{31}$$

and $$C_v = C_p - R$$

Substituting Equation 31 into the denominator of Equation 30, the true value of μ_{max} can be expressed by

$$\mu_{max} = \frac{K\, 2\pi C_i/R}{\left[35 \frac{C_p}{R}\left(\frac{C_p}{R} - 1\right)\right]^{1/2}} \tag{32}$$

In order to determine C_i/R from Equation 31, the quantity of C_p/R must be defined from very accurate gas tables (5 or more significant figures) such as given in Reference 59.

An alternate method for defining C_i to a close approximation is based on application of the Planck-Einstein equation for the internal energy of the vibration mode. This is given by

$$C_i/R = \left(\frac{\theta_i}{T}\right)^2 \frac{e^{-\theta i/T}}{\left[1-e^{-\theta_i/T}\right]^2} \tag{33}$$

where

θ_i = characteristic temperature corresponding to the particular vibration mode, °K

T = absolute temperature, °K

If the further approximation is made that $C_i/R << C_p/R$, then $C_p/R \simeq 7/2$ and Equation 32 can then be simplified to give a simple expression for μ_{max} for diatomic molecules, which is

$$\mu_{max} \simeq \frac{K\, 4\pi C_i/R}{35} \tag{34}$$

where C_i is given by Equation 33 and K is the volume concentration of the gas in the mixture.

A comparison of values for μ_{max} computed according to Equation 32 and nearly all the available experimentally determined values from the literature (References 60 through 71) is shown in Figure 60.

While the majority of the experimental points in Figure 60 of μ_{max} for O_2 lie above the theoretical line, the most recent measurements by Harris and Monk near 20°C, which are considered to be the most accurate, agree very well with the theory as given by Equation 33 and 34 with the following constants assumed for O_2 and N_2:

Oxygen, $K = 0.20953$, $\theta_i = 2239°K$ (Reference 71)

Nitrogen, $K = 0.7811$, $\theta_i = 3353°K$ (Reference 72)

Note that the above concentration constants are for dry air. It will be necessary, for final computations, to account for the effect of moisture in the air when defining μ_{max} for the general case. The moisture content is usually very small at the conditions for which μ_{max} is normally measured (i.e. - of the order of 1% or less by volume) and therefore will normally have little effect on the observed magnitude of μ_{max}. For any general weather condition, however, the effective value of μ_{max} for O_2 must be modified. Both theory and experiment show that the relaxation of H_2O molecules occurs in concert with that of O_2, both having, effectively, a common or coupled relaxation process with essentially the same relaxation frequency [73,74]. Thus, a modified μ_{max} for O_2 will be defined as

$$\mu'_{max}(O_2) = \mu_{max}(O_2) + \mu_{max}(H_2O) \qquad (35)$$

where $\mu_{max}(O_2)$ is given by Equation 34 with the concentration constant K changed to

$$K' = K(1 - h/100)$$

and h = % of H_2O molecules in the air mixture (36)

Since H_2O is a three-atom molecule, it can be shown that the value of $\mu_{max}(H_2O)$ can be given to a close approximation by (Reference 58)

$$\mu_{max}(H_2O) = \left(\frac{h}{100}\right) \frac{\pi}{12} \frac{C_i}{R} \qquad (37)$$

where the internal energy, (C_i/R) for H_2O relaxation is given by Equation 33 with a characteristic temperature (θ_i) for the dominant H_2O vibration mode equal to 2294°K (Reference 73).

It should be pointed out that it has been assumed that the relaxation loss for H_2O molecules adds, in a linear fashion, only a small additional amount to the vibrational relaxation loss predicted for O_2. It can be expected that more sophisticated prediction models may be required in the future based on the recent theoretical studies by Bauer and Roesler[63], Bauer[75], and Beyer[76], on nonlinear summation in multiple reaction mixtures. However, the predicted air absorption loss, based on the model outlined in this appendix, will be shown to provide substantial agreement with the experimental data from Harris in the low-frequency range of concern for this study.

Relaxation Frequencies

Having defined the μ_{max} parameters for air absorption, it remains only to define the relaxation frequencies. Two values are required - one for the combined vibrational relaxation of O_2 and H_2O molecules (to be labeled f_o) and one for the vibrational relaxation of N_2 (to be labeled f_n). Both of these frequencies are a function of humidity content of the air, atmospheric pressure and temperature. For convenient correlation with theory, humidity content is expressed as an absolute humidity (h) in terms of the percentage of H_2O molecules to the total number of molecules in a mixture (the mole ratio). It can be shown that h is given in terms of relative humidity, temperature and pressure by the following expressions:

$$h = \frac{P_s}{P_o} (RH), \text{ \% mole ratio} \qquad (38)$$

where

P_o = atmospheric pressure

RH = Relative Humidity, %

P_s = vapor pressure of H_2O in saturated mixture in air

The ratio P_s/P_o can be expressed by an empirical power law as a function of temperature within $\pm$ 1% over the temperature range of -40° to $+60^\circ$C.

$$\frac{P_s}{P_o} = 10^{[-2.22 + .03516t - 1.26 \times 10^{-4} t^2 + 3.44 \times 10^{-7} t^2]} \tag{39}$$

where

t = vapor (air) temperature, $^\circ$C

Early semiempirical pow r law expressions for estimating the relaxation frequency f_o for oxygen (e.g., References 61, 68, 69) have been shown by more recent theoretical studies by Henderson[77] and Monk[64] to be inadequate. Using a modification of the theoretical expression developed by Monk, the following equation has been found to provide a satisfactory fit to experimental data as shown in Figure 61.

$$f_o = \frac{P^*}{T^*} \left\{ 11 + 1750h + 61{,}400h \left[\left(\frac{1.12 + 10h}{10.4 + 10h} \right) \right] \right\} \tag{40}$$

where h is the absolute humidity given by Equation 38 and P* and T* are the atmospheric pressure and temperature relative to standard sea level pressure and 20°C, respectively.

The relaxation frequency for nitrogen in air is less well defined. In fact, it has been recognized only recently that nitrogen plays a significant role in molecular vibration loss in air[55, 78]. The few absorption measurements which have been made on pure nitrogen at audio frequencies[72, 79] indicate that the relaxation frequency in N_2 varies linearly with humidity content and has a value of about 200 Hz per one percent H_2O mole ratio at room temperature.

A relaxation frequency for nitrogen in an air mixture has been established in an indirect manner by a critical analysis of credible measurements in air, particularly those of Harris. For each set of data, the observed total air absorption loss was corrected for the "known losses" already defined (i.e., classical and rotational losses for air and vibration loss for oxygen only). The remaining anomalous absorption could then be fitted to a general curve of the type illustrated earlier in Figure 59 and the resulting value for f_n estimated. Typical results of this process, one which necessarily leads to appreciable scatter, is illustrated in Figure 62. This has led to the following tentative expression for the relaxation frequency of N_2 in air

$$f_n \simeq 450\, h \frac{P^*}{T^*} \qquad (41)$$

It should be stressed that there are ample guidelines and data available for predicting air absorption losses already published in the literature (e.g., Reference 56). However, none of these have used a completely theoretical model for their foundation and hence are suspect or potentially inadequate for estimating air absorption losses under unusual weather conditions for which experimental data are lacking, and for which helicopter detectability range may be desired.

Application

Based on the expressions outlined in this appendix, the total air absorption has been computed for a wide range of temperatures and humidities. The results are given in Table IV for frequencies at octave intervals between 32 and 8000 Hz (atmospheric attenuation at lower frequencies is negligible). Values for intermediate frequencies may be obtained by interpolation.

OTHER LOSSES (ELEVATION LESS THAN 10 DEGREES)

Ground-to-Ground Terrain Attenuation

For zero elevation angles, the total attenuation, in dB per 1000-ft distance, is given in Table V as a function of frequency and ground cover. These data were read from Figure 17 which may be used for intermediate frequencies if desired. The three terrain types included are grassland, sparse jungle and dense jungle.

Ground-to-Ground Turbulence Losses

If the ground absorption is very small, for example over a very hard, sparsely covered surface, the propagated sound will still undergo a residual attenuation due to scattering in the turbulent boundary layer near the ground. Figure 63, which is based on an analysis from Reference 80 of the experimental results in Reference 81, provides an estimate of the magnitude of this effect as a function of frequency and distance. Note that the curves give total attenuation and that this is constant at distances above 4000 ft. Propagation losses obtained from this figure should be substituted for those obtained from Table V whenever they are greater.

Effect of Elevation Angle (β)

Reference 80 suggests the following formula for estimating the effects of elevation angle upon the ground-to-ground absorption loss:

$$\Delta A_g = \Delta A_o e^{-\sqrt{\tan 3\beta}}$$

where ΔA_o = ground-to-ground attenuation for $\beta = 0$, obtained as described above

β = elevation angle of source above the ground

TABLE IV. ATMOSPHERIC ABSORPTION LOSS - DB/1000 FT

(a) FREQUENCY IN HZ = 32

TEMP	RELATIVE HUMIDITY - %						
DEG F	10	15	20	30	50	70	100
-40	.06	.06	.06	.05	.03	.02	.02
-35	.07	.06	.05	.04	.03	.02	.02
-30	.07	.06	.05	.04	.03	.02	.02
-25	.07	.06	.05	.03	.02	.02	.02
-20	.07	.05	.04	.03	.02	.02	.01
-15	.06	.05	.04	.03	.02	.02	.01
-10	.06	.04	.03	.03	.02	.02	.01
-5	.05	.04	.03	.03	.02	.02	.01
0	.05	.04	.03	.03	.02	.02	.01
5	.04	.03	.03	.02	.02	.01	.01
10	.04	.03	.03	.02	.02	.01	.01
15	.04	.03	.03	.02	.02	.01	.01
20	.04	.03	.03	.02	.01	.01	.01
25	.04	.03	.03	.02	.01	.01	.01
30	.04	.03	.03	.02	.01	.01	.01
35	.04	.03	.03	.02	.01	.01	.01
40	.04	.03	.02	.02	.01	.01	.00
45	.04	.03	.02	.02	.01	.01	.00
50	.04	.03	.02	.01	.01	.01	.00
55	.04	.03	.02	.01	.01	.01	.00
60	.03	.02	.02	.01	.01	.00	.00
65	.03	.02	.02	.01	.01	.00	.00
70	.03	.02	.02	.01	.01	.00	.00
75	.03	.02	.01	.01	.01	.00	.00
80	.03	.02	.01	.01	.00	.00	.00
85	.02	.02	.01	.01	.00	.00	.00
90	.02	.01	.01	.01	.00	.00	.00
95	.02	.01	.01	.01	.00	.00	.00
100	.02	.01	.01	.01	.00	.00	.00
105	.02	.01	.01	.01	.00	.00	.00
110	.02	.01	.01	.01	.00	.00	.00
115	.02	.01	.01	.00	.00	.00	.00
120	.01	.01	.01	.00	.00	.00	.00

TABLE IV. (CONTINUED).

(b) FREQUENCY IN HZ = 63

TEMP DEG F	RELATIVE HUMIDITY - % 10	15	20	30	50	70	100
-40	.11	.12	.13	.13	.10	.09	.06
-35	.13	.14	.14	.13	.10	.08	.06
-30	.15	.15	.15	.12	.09	.07	.05
-25	.16	.16	.14	.12	.08	.06	.04
-20	.18	.16	.14	.10	.07	.05	.04
-15	.18	.15	.13	.09	.06	.05	.04
-10	.18	.14	.12	.08	.06	.05	.04
-5	.17	.13	.10	.07	.05	.04	.04
0	.16	.12	.09	.07	.05	.04	.04
5	.14	.11	.08	.06	.05	.04	.03
10	.13	.10	.08	.06	.05	.04	.03
15	.12	.09	.07	.06	.05	.04	.03
20	.11	.08	.07	.06	.05	.04	.03
25	.10	.08	.07	.06	.05	.04	.03
30	.10	.08	.07	.06	.04	.03	.02
35	.10	.08	.07	.06	.04	.03	.02
40	.10	.08	.07	.06	.04	.03	.02
45	.10	.08	.07	.06	.04	.03	.02
50	.10	.08	.07	.05	.03	.02	.02
55	.10	.08	.07	.05	.03	.02	.01
60	.10	.08	.06	.05	.03	.02	.01
65	.10	.08	.06	.04	.03	.02	.01
70	.10	.07	.06	.04	.02	.02	.01
75	.10	.07	.05	.04	.02	.02	.01
80	.09	.07	.05	.03	.02	.01	.01
85	.09	.06	.05	.03	.02	.01	.01
90	.08	.06	.04	.03	.02	.01	.01
95	.08	.05	.04	.03	.02	.01	.01
100	.07	.05	.04	.02	.01	.01	.01
105	.07	.05	.03	.02	.01	.01	.01
110	.07	.04	.03	.02	.01	.01	.01
115	.06	.04	.03	.02	.01	.01	.00
120	.06	.04	.03	.02	.01	.01	.00

TABLE IV. (CONTINUED).

(c) FREQUENCY IN HZ = 125

TEMP DEG F	RELATIVE HUMIDITY - % 10	15	20	30	50	70	100
-40	.13	.16	.19	.23	.26	.24	.21
-35	.16	.20	.23	.27	.27	.24	.19
-30	.20	.25	.28	.30	.27	.22	.17
-25	.25	.30	.32	.32	.25	.20	.14
-20	.30	.35	.35	.32	.23	.17	.12
-15	.36	.38	.36	.30	.20	.15	.11
-10	.40	.40	.36	.27	.18	.13	.10
-5	.44	.39	.33	.24	.16	.12	.09
0	.45	.37	.30	.22	.14	.11	.09
5	.44	.34	.27	.19	.13	.10	.09
10	.42	.31	.24	.17	.12	.10	.09
15	.39	.28	.21	.16	.12	.10	.09
20	.35	.25	.19	.15	.12	.11	.09
25	.31	.22	.18	.14	.12	.11	.09
30	.28	.21	.17	.15	.12	.10	.08
35	.26	.19	.17	.15	.12	.10	.08
40	.24	.19	.17	.15	.12	.10	.07
45	.23	.19	.18	.16	.12	.09	.07
50	.22	.20	.18	.16	.11	.09	.06
55	.23	.20	.19	.16	.11	.08	.06
60	.23	.21	.19	.15	.10	.07	.05
65	.24	.22	.19	.15	.10	.07	.05
70	.25	.22	.19	.14	.09	.06	.04
75	.26	.22	.18	.13	.08	.06	.04
80	.27	.22	.18	.12	.08	.05	.04
85	.27	.21	.17	.12	.07	.05	.03
90	.27	.20	.16	.11	.07	.05	.03
95	.26	.19	.15	.10	.06	.04	.03
100	.26	.18	.14	.09	.06	.04	.03
105	.25	.18	.13	.09	.05	.04	.02
110	.24	.17	.12	.08	.05	.03	.02
115	.23	.16	.12	.08	.04	.03	.02
120	.22	.15	.11	.07	.04	.03	.02

TABLE IV. (CONTINUED).

(d) FREQUENCY IN HZ = 250

TEMP DEG F	RELATIVE HUMIDITY - % 10	15	20	30	50	70	100
-40	.14	.18	.22	.29	.41	.48	.51
-35	.18	.23	.29	.38	.50	.55	.54
-30	.23	.30	.37	.48	.59	.60	.53
-25	.29	.39	.47	.59	.65	.60	.46
-20	.38	.50	.59	.69	.67	.57	.43
-15	.48	.62	.71	.76	.65	.51	.36
-10	.60	.75	.81	.79	.59	.44	.31
-5	.74	.86	.88	.77	.52	.38	.27
0	.87	.94	.89	.71	.45	.32	.23
5	.99	.97	.86	.64	.39	.28	.22
10	1.07	.96	.80	.56	.34	.26	.21
15	1.10	.90	.71	.48	.30	.24	.21
20	1.08	.81	.63	.42	.28	.24	.22
25	1.01	.72	.55	.38	.27	.24	.23
30	.92	.64	.49	.35	.27	.25	.23
35	.83	.56	.44	.34	.28	.27	.23
40	.74	.51	.41	.33	.30	.27	.23
45	.65	.47	.39	.34	.31	.28	.23
50	.59	.44	.39	.36	.32	.28	.22
55	.55	.44	.40	.38	.33	.27	.21
60	.52	.44	.42	.40	.33	.26	.20
65	.51	.46	.45	.41	.32	.25	.18
70	.52	.49	.47	.42	.31	.24	.17
75	.54	.52	.49	.42	.30	.22	.16
80	.57	.55	.51	.42	.28	.21	.15
85	.60	.57	.52	.41	.27	.19	.13
90	.64	.59	.52	.39	.25	.18	.12
95	.68	.60	.51	.38	.23	.17	.11
100	.71	.60	.50	.36	.22	.15	.10
105	.73	.59	.48	.34	.20	.14	.09
110	.74	.58	.46	.32	.19	.13	.09
115	.74	.56	.44	.30	.18	.12	.08
120	.75	.54	.42	.28	.16	.11	.07

TABLE IV. (CONTINUED).

(a) FREQUENCY IN HZ = 500

TEMP DEG F	RELATIVE HUMIDITY - % 10	15	20	30	50	70	100
-40	.15	.19	.24	.32	.49	.63	.82
-35	.19	.25	.31	.43	.65	.83	1.02
-30	.24	.33	.41	.57	.85	1.06	1.20
-25	.31	.43	.54	.76	1.09	1.27	1.30
-20	.41	.57	.72	.99	1.33	1.42	1.30
-15	.53	.74	.94	1.25	1.52	1.47	1.20
-10	.69	.97	1.20	1.52	1.62	1.41	1.06
-5	.90	1.24	1.49	1.75	1.60	1.27	.90
0	1.15	1.54	1.78	1.88	1.49	1.10	.75
5	1.46	1.85	2.01	1.89	1.32	.94	.64
10	1.79	2.12	2.14	1.79	1.14	.79	.55
15	2.13	2.30	2.13	1.62	.97	.68	.50
20	2.41	2.34	2.02	1.42	.83	.60	.48
25	2.60	2.26	1.83	1.22	.73	.56	.47
30	2.65	2.09	1.61	1.06	.66	.54	.49
35	2.57	1.87	1.40	.92	.62	.55	.52
40	2.39	1.64	1.22	.83	.62	.58	.56
45	2.15	1.43	1.07	.77	.64	.62	.59
50	1.91	1.26	.97	.75	.68	.66	.62
55	1.68	1.13	.91	.75	.73	.70	.63
60	1.49	1.04	.88	.79	.78	.74	.63
65	1.34	.99	.89	.85	.83	.75	.62
70	1.23	.98	.92	.91	.87	.76	.60
75	1.17	1.00	.98	.98	.89	.75	.57
80	1.14	1.05	1.05	1.05	.90	.73	.54
85	1.16	1.13	1.14	1.10	.89	.70	.51
90	1.20	1.22	1.22	1.14	.87	.66	.47
95	1.28	1.31	1.30	1.16	.84	.62	.44
100	1.38	1.41	1.36	1.16	.80	.58	.40
105	1.49	1.50	1.40	1.14	.76	.54	.37
110	1.61	1.57	1.42	1.11	.72	.50	.34
115	1.73	1.62	1.42	1.07	.67	.47	.31
120	1.84	1.65	1.40	1.03	.63	.43	.28

TABLE IV. (CONTINUED).

(f) FREQUENCY IN HZ = 1000

TEMP DEG F	RELATIVE HUMIDITY - %						
	10	15	20	30	50	70	100
-40	.19	.23	.27	.36	.54	.72	.99
-35	.23	.29	.35	.48	.73	.99	1.35
-30	.28	.37	.46	.63	.99	1.34	1.80
-25	.35	.47	.60	.85	1.34	1.79	2.30
-20	.45	.62	.79	1.14	1.79	2.32	2.77
-15	.58	.81	1.05	1.52	2.33	2.86	3.08
-10	.75	1.08	1.40	2.01	2.92	3.30	3.13
-5	.98	1.42	1.84	2.60	3.46	3.50	2.93
0	1.29	1.86	2.40	3.25	3.80	3.42	2.58
5	1.68	2.42	3.07	3.88	3.87	3.12	2.19
10	2.18	3.09	3.78	4.34	3.66	2.72	1.84
15	2.80	3.84	4.44	4.52	3.27	2.30	1.54
20	3.54	4.58	4.92	4.40	2.82	1.94	1.33
25	4.35	5.18	5.11	4.04	2.40	1.65	1.18
30	5.14	5.52	4.97	3.57	2.04	1.44	1.10
35	5.60	5.52	4.59	3.08	1.76	1.31	1.08
40	6.19	5.24	4.09	2.64	1.57	1.24	1.11
45	6.25	4.76	3.56	2.29	1.45	1.24	1.17
50	5.99	4.21	3.08	2.02	1.40	1.28	1.27
55	5.51	3.67	2.68	1.83	1.41	1.37	1.38
60	4.93	3.20	2.38	1.72	1.47	1.48	1.50
65	4.35	2.81	2.16	1.69	1.58	1.62	1.60
70	3.82	2.53	2.02	1.72	1.72	1.75	1.67
75	3.37	2.33	1.97	1.81	1.88	1.87	1.71
80	3.02	2.22	1.99	1.95	2.04	1.97	1.72
85	2.77	2.19	2.07	2.12	2.19	2.03	1.69
90	2.62	2.23	2.21	2.32	2.31	2.05	1.64
95	2.55	2.34	2.39	2.52	2.39	2.04	1.56
100	2.56	2.51	2.61	2.71	2.44	1.99	1.48
105	2.65	2.72	2.85	2.88	2.44	1.92	1.38
110	2.80	2.98	3.09	3.01	2.40	1.83	1.28
115	3.02	3.25	3.33	3.10	2.34	1.73	1.18
120	3.29	3.54	3.53	3.14	2.25	1.62	1.07

TABLE IV. (CONTINUED).

(g) FREQUENCY IN HZ = 2000

TEMP DEG F	RELATIVE HUMIDITY - % 10	15	20	30	50	70	100
-40	.33	.37	.41	.50	.68	.87	1.17
-35	.37	.43	.49	.62	.88	1.16	1.59
-30	.42	.51	.60	.78	1.16	1.56	2.17
-25	.49	.62	.74	1.00	1.55	2.11	2.96
-20	.59	.76	.94	1.31	2.08	2.87	3.98
-15	.72	.96	1.21	1.73	2.81	3.86	5.13
-10	.90	1.24	1.58	2.31	3.77	5.08	6.36
-5	1.14	1.60	2.09	3.08	4.98	6.40	7.22
0	1.45	2.09	2.76	4.10	6.37	7.56	7.46
5	1.88	2.75	3.65	5.38	7.74	8.22	7.08
10	2.43	3.62	4.80	6.88	8.77	8.21	6.29
15	3.17	4.74	6.22	8.44	9.17	7.60	5.38
20	4.13	6.13	7.86	9.78	8.86	6.68	4.52
25	5.35	7.79	9.55	10.55	8.05	5.71	3.81
30	6.85	9.58	10.99	10.59	7.02	4.83	3.27
35	8.62	11.26	11.85	9.96	6.01	4.12	2.89
40	10.54	12.50	11.96	8.94	5.12	3.58	2.65
45	12.39	13.04	11.36	7.80	4.42	3.20	2.54
50	13.83	12.80	10.32	6.73	3.89	2.97	2.54
55	14.59	11.94	9.11	5.81	3.52	2.87	2.63
60	14.55	10.75	7.93	5.06	3.31	2.89	2.81
65	13.82	9.47	6.90	4.54	3.23	3.01	3.05
70	12.64	8.28	6.05	4.17	3.27	3.21	3.34
75	11.29	7.25	5.40	3.95	3.42	3.49	3.65
80	9.96	6.42	4.94	3.88	3.66	3.83	3.94
85	8.78	5.79	4.64	3.94	3.99	4.19	4.20
90	7.79	5.35	4.51	4.12	4.37	4.54	4.39
95	7.00	5.09	4.52	4.40	4.79	4.87	4.49
100	6.41	4.98	4.66	4.78	5.22	5.13	4.51
105	6.02	5.02	4.92	5.23	5.62	5.31	4.45
110	5.80	5.20	5.29	5.73	5.96	5.39	4.31
115	5.75	5.51	5.75	6.25	6.22	5.38	4.11
120	5.85	5.93	6.30	6.77	6.38	5.28	3.86

TABLE IV. (CONTINUED).
(h) FREQUENCY IN HZ = 4000

TEMP DEG F	RELATIVE HUMIDITY - % 10	15	20	30	50	70	100
-40	.88	.92	.96	1.05	1.24	1.43	1.73
-35	.92	.98	1.04	1.17	1.44	1.72	2.17
-30	.97	1.06	1.15	1.34	1.72	2.13	2.79
-25	1.05	1.17	1.30	1.56	2.12	2.72	3.69
-20	1.15	1.32	1.50	1.88	2.68	3.56	4.95
-15	1.28	1.53	1.78	2.31	3.47	4.73	6.70
-10	1.46	1.80	2.16	2.91	4.57	6.35	9.00
-5	1.70	2.18	2.68	3.75	6.09	8.52	11.77
0	2.02	2.68	3.38	4.89	8.13	11.26	14.63
5	2.46	3.37	4.35	6.45	10.78	14.35	16.84
10	3.03	4.30	5.66	8.53	13.94	17.26	17.71
15	3.80	5.54	7.41	11.23	17.25	19.18	17.09
20	4.83	7.21	9.72	14.53	20.02	19.58	15.45
25	6.19	9.40	12.66	18.18	21.49	18.53	13.42
30	7.98	12.21	16.22	21.65	21.34	16.61	11.47
35	10.31	15.67	20.16	24.15	19.86	14.44	9.81
40	13.27	19.67	23.93	25.07	17.69	12.40	8.49
45	16.90	23.81	26.80	24.35	15.39	10.69	7.51
50	21.10	27.45	28.11	22.45	13.29	9.33	6.82
55	25.55	29.84	27.70	20.01	11.54	8.31	6.40
60	29.67	30.52	25.95	17.53	10.16	7.61	6.21
65	32.73	29.53	23.46	15.29	9.13	7.18	6.23
70	34.15	27.33	20.78	13.42	8.41	6.99	6.43
75	33.79	24.67	18.27	11.93	7.98	7.01	6.79
80	32.00	21.89	16.10	10.81	7.80	7.24	7.30
85	29.36	19.34	14.31	10.02	7.85	7.64	7.91
90	26.40	17.14	12.92	9.53	8.11	8.20	8.60
95	23.51	15.34	11.89	9.31	8.56	8.89	9.30
100	20.92	13.94	11.20	9.34	9.18	9.67	9.97
105	18.72	12.91	10.80	9.60	9.95	10.50	10.54
110	16.93	12.22	10.67	10.07	10.85	11.43	10.96
115	15.54	11.83	10.81	10.74	11.81	12.07	11.18
120	14.52	11.73	11.17	11.58	12.80	12.69	11.19

TABLE IV. (CONCLUDED).

(i) FREQUENCY IN HZ = 8000

TEMP DEG F	RELATIVE HUMIDITY - % 10	15	20	30	50	70	100
-40	3.08	3.13	3.17	3.26	3.45	3.64	3.94
-35	3.13	3.19	3.26	3.39	3.65	3.94	4.39
-30	3.19	3.28	3.37	3.56	3.94	4.36	5.03
-25	3.28	3.40	3.53	3.79	4.35	4.96	5.96
-20	3.38	3.56	3.74	4.11	4.93	5.82	7.30
-15	3.52	3.77	4.02	4.56	5.74	7.05	9.24
-10	3.71	4.05	4.41	5.17	6.88	8.81	12.00
-5	3.96	4.43	4.94	6.02	8.50	11.29	15.86
0	4.28	4.95	5.66	7.21	10.77	14.77	20.99
5	4.72	5.65	6.65	8.86	13.93	19.48	27.28
10	5.31	6.60	8.00	11.13	18.25	25.52	33.96
15	6.10	7.89	9.86	14.26	23.91	32.55	39.50
20	7.15	9.63	12.39	18.50	30.87	39.52	42.28
25	8.55	11.99	15.82	24.07	38.51	44.76	41.77
30	10.43	15.17	20.39	31.06	45.50	46.86	38.76
35	12.94	19.40	26.33	39.18	50.16	45.65	34.60
40	16.27	24.91	33.72	47.51	51.39	42.14	30.33
45	20.63	31.83	42.33	54.53	49.42	37.64	26.51
50	26.27	40.26	51.33	58.66	45.39	33.14	23.35
55	33.37	49.58	59.32	59.19	40.58	29.12	20.86
60	41.92	58.79	64.71	56.60	35.85	25.78	18.99
65	51.63	66.36	66.51	52.10	31.67	23.14	17.65
70	61.64	70.88	64.85	46.87	28.18	21.12	16.79
75	70.63	71.69	60.74	41.76	25.40	19.67	16.34
80	77.09	69.23	55.41	37.18	23.28	18.72	16.27
85	80.01	64.57	49.84	33.32	21.73	18.21	16.54
90	79.28	58.91	44.62	30.18	20.71	18.11	17.11
95	75.64	53.11	40.05	27.74	20.15	18.36	17.95
100	70.24	47.73	36.22	25.91	20.02	18.96	19.02
105	64.12	43.01	33.13	24.65	20.28	19.85	20.25
110	58.04	39.04	30.72	23.89	20.91	21.00	21.56
115	52.44	35.82	28.94	23.60	21.87	22.37	22.87
120	47.54	33.30	27.72	23.74	23.13	23.88	24.06

TABLE V. TERRAIN ATTENUATION COEFFICIENTS (FROM FIGURE 17)

Frequency Hz	Attenuation - dB per 1000 ft		
	Grassland	Sparse Jungle	Dense Jungle
16	0	0	0
31.8	0	0.15	0.9
63	0.6	2.1	14
125	2.6	7.2	34
250	6.0	12	48
500	7.6	15	63
1000	6.6	21	85
2000	3.9	30	120
4000	1.5	48	170
8000	0.35	70	230

APPENDIX II
DESCRIPTION AND OPERATION OF THE AUTOMATIC DATA SYSTEM

The data system developed for the control and analysis of the aural detection experiment described in Section 4.2 of the main text were described by Adcock in Reference 47; only the essential features of the system and associated data reduction software will be described here.

Description

Particular points which were given detailed attention during the design, development and construction phases included:

- A simple, self-guiding operational procedure, in order to minimize or eliminate operator errors;
- An intricate system of safety interlocks to guard against the acquisition of bad data being acquired, either as a result of an operator error or because of the failure of some subsystem or component;
- The compression of the acquired data into a minimum quantity of punched paper tape, in order to reduce analysis time without sacrificing precision;
- Subsystem modularity, to permit simplified checkout procedures, easy maintenance, and a capability for development and modification;
- The acquisition of data in a format which would be error free, readily interpretable, and prepared for immediate computer analysis.

The location of this unit in the sound generation system may be seen in Figure 32. Its main element, with respect to the signal generation, is a Grason Stadler Model E 800-193 continuously variable 120 dB potentiometer which is used to adjust the level of the stimulus signal. Its input, taken directly from the signal source (either a tape recorder or an oscillator) is amplified by a Crown D-40 amplifier used in the capacity of an impedance matching device. It has a linear movement with a travel of 6 inches, has a flat frequency response between 10 and 10,000 Hz, and has a resolution of 0.25 dB.

The attenuator is driven, through an antibacklash rack and pinion, by a reversible motor at a rate equivalent to 2 dB/second. The position of the attenuator, and whence the signal level, is monitored by a transducer which indicates the angle

of rotation of the pinion drive shaft. This device, which is essentially a binary-masked photoelectric shaft angle transducer, comprises a 10-inch-diameter, 1.25-inch-deep Plexiglas cylinder having around its periphery an opaque binary mask made from standard 1-inch eight-hole black punched paper tape. This mask is coded in standard binary code from decimal 1 to decimal 255 and covers approximately 300 degrees of the cylinder's circumference. A high-intensity light source located inside the cylinder and an array of silicon photodiodes are arranged to sense the eight data holes and the sprocket hold in the tape. An eight-bit storage register stores the binary coded tape character and is updated whenever any digit changes value. The contents of this register are read and punched at 1.034-second time intervals (controlled by an internal clock circuit) by a Tally Model 1786 drive package driving a Model P-120 eight-hole punch. The system continuously outputs tape characters read by the photoelectric sensors. The physical separation of the characters on the cylinder and the gearing ratio are such that the interval between characters corresponds to approximately 0.4 dB.

At the start of a test, the attenuator drive motor is started and continues to run until the test is terminated, either at the end of the run or by an abort situation. The direction of rotation is controlled by the test subject with a hand-held push-button cord switch. When the button is pressed, the signal level diminishes. When it is released, the signal increases. By alternately pressing and releasing the button, the subject continually adjusts the signal level between the just-audible and just-inaudible points.

Figure 32 shows the association of the data acquisition system with the electronic and acoustic equipment, and the subject's console in the acoustic facility. The latter comprises an array of indicator lights to identify the current experimental phase and to indicate certain abnormal conditions, and an alarm switch whereby the subject may terminate the experiment in the event of an emergency.

The various built-in system functions including the manual override capabilities, safety interlocks, abort, alarm and reset capabilities, are perhaps best described by the operations required to run a typical test. These are described below in sequence with reference to Figure 64, which is a diagram of the DAS control panel.

1) The "Ready" button is pressed to prepare the system for the test. The attenuator begins to reposition itself approximately halfway through its range and the instruction lamp "Rewind" lights up.

2) The stimulus tape is rewound on the tape reproducer, or other signal sources prepared as required. When "Rewind" is hit to acknowledge the instruction, the "Rewind" lamp turns off, and the "Set I.D." lamp lights up.

3) The required test identification number (4 decibel digits) is set on the front panel thumbwheel switch. The "Set I.D." is hit to acknowledge the instruction. The "Set I.D." lamps turn off, and the "Runout" lamp turns on.

4) The "Runout" switch is temporarily depressed to run out a length of blank tape from the perforator. This serves as a delimiter between tests for the purposes of the data analysis. The "Runout" lamp turns off, and the "Punch" lamp lights up.

5) The Punch Test I.D. buttons "First" and "Second" are pressed to write the contents of the thumbwheel registers on the paper tape. "Punch" is hit to acknowledge the command, and the instruction lamp turns off.

6) When Steps 2 through 5 have been accomplished, and when the motor drive has centered itself at the midway point of the attenuator range, the "Ready" lamp is lit.

7) When the subject is ready, "Run" is hit. The motor commences driving in a direction under the control of the subject, and the tape reproducer (if used) starts playing. The data acquisition system does not, however, drive the tape perforator at this time.

8) If a tape reproducer is being used, the "Run" phase of the operation may be controlled and timed fully automatically through the use of a control tone on a second tape channel. As soon as the "Run" switch is pressed (Step 7 above), a yellow "Run" lamp will be lit on the main panel and repeated on the subject's console. When the control signal is detected from the tape reproducer, the data system is activated and the tape perforator commences punching data. The yellow "Run" lamp turns off, and a green "Run" lamp lights, which is again repeated on the subject's console. This arrangement ensures a repeatable time origin each time a given stimulus tape is played.

   If a tape reproducer is not being used as the stimulus source, or if the tape is not furnished with a control tone on another channel, a manual override is available to start the data acquisition procedure. Again, when the "Run" switch is operated, yellow "Run" lamps are lit until the "Tape Trigger Override" switch is thrown, at which time the system commences punching data and shows green "Run" indicators.

   During this period of data acquisition, the approximate setting of the attenuator is indicated by a meter in the bottom left-hand corner of the console. Two amber indicator lamps are also provided to show the

direction in which the subject is driving the attenuator at any time. By observing these instruments, the test director is able to ascertain that the experiment is progressing normally.

If the subject attempts to drive the attenuator beyond its range in either direction, an "abort" situation arises, which is handled as indicated below.

9) At the end of the recorded stimulus sound, the control tone also ends, causing the perforator to stop, switching off the tape reproducer, and reverting the system to a "Standby" mode, with yellow "Standby" lamps illuminated on the main and subject's consoles. In the event that a trigger is not being used, the "Override Trigger Signal" switch is moved to "off" at the end of the required period of time, with the same effect upon the system.

10) Return to Step 3 for the next test.

The above sequence of operations are required during a normal run. However, a number of abnormal events are provided for by the system as follows:

Low Tape -- When the tape perforator paper tape supply runs low the warning "Low Tape" lamp illuminates. In this condition the system will not ready for a new test until the paper roll has been replaced.

Operational Error -- The system will not ready unless all operations were performed in the correct sequence.

Abort -- If, for any reason, the subject tries to drive the attenuator to its limit in either direction in the course of a test, the motor automatically stops and an abort situation arises. The test operator is warned by the "Abort" lamp that the limit has been reached, and he may then either override the condition or terminate the test. By watching the direction indicator lamps and by observing the reading on the main panel voltmeter (which is scaled from 0 to 120 dB attenuation), the operator is able to decide whether to discontinue the experiment. If the direction indicator lamps show that the subject is resolutely attempting to drive the attenuator beyond its range, the operator would probably wish to abort the experiment and determine the reason for this response. If, on the other hand, the subject reverses the direction of drive almost immediately, the experiment may be continued by pressing the "Abort" switch and allowing the system to revert to normal operation. In the event that the experiment is to be terminated, pressing "Abort" and "Reset" simultaneously will bring the system into "Standby", ready for the next test.

Data Reduction

The format of the punched paper tape consists of blocks of data punched in binary integer form and separated by lengths of blank tape.

Following the blank tape, the first two non-zero characters are interpreted as the 4-decimal-digit test identification number. The remaining string of non-zero characters are read as binary integers, which represent the decimal integers 1 through 255. The output of the attenuator position transducer is therefore recorded to a precision of 1 part in 255, or about $\pm 0.2\%$, which was considered sufficient for the experiments concerned.

The data analysis was performed in two phases using two separate computer programs written for a time-sharing computer service. Access to the computer was through a Teletype ASR-33 terminal located at the test facility which allowed convenient and rapid off-line reduction of the test data. The first program served merely to read the experimental data punched by the data acquisition system, to print sufficient information for the contents to be manually checked, and to store the good records in a permanent file. The main analysis was then performed upon these files by a second, independent program. Remembering that each file represents a time history of detection level for one particular sound sequence as adjusted by one subject, options were provided to process the files in four different ways for output:

1) The results of one test for one subject could be examined, each data sample (which was originally recorded at a rate close to 1 sample/second) being listed or plotted as selected.

2) The results of one test for one subject could be analyzed, with the time axis compressed for convenience of examination if desired. In this case a group of samples could be compressed into one data point (defined by a mean and a standard deviation) for listing or plotting purposes.

3) The results of several tests, for several separate subjects or replicate tests for the same subject, could be averaged, and mean and standard deviation data presented at each time interval.

4) The results of several tests could be averaged, as in Method 3 above, with the time axis compressed also, as in Method 2. The mean and standard deviation were thus values appropriate to a number of data points taken from several tests over some finite time span.

In order to perform the analysis, the program required several sets of calibration data as follows:

1) An attenuation table comprising 255 values, in dB, corresponding to the 255 angular positions of the binary mask. This data, obtained as described under "calibration procedures," allows precise conversion of the punched data to signal levels, in dB, relative to a calibrated reference.

2) (optional) A function defining the overall system frequency response necessary to convert source level to the level experienced at the subject's ears. This is tabulated as 31 values of a correction factor, in dB, to be added to the signal level at each 1/3-octave band center frequency between 12.5 and 12,500 Hz. This function was used in the analysis of tests involving frequency as the stimulus variable. For sine sweep tests (see Section 4.4), appropriate values for the continuously varying frequency were obtained by interpolation.

3) The stimulus variable (typically frequency) as a function of time for conversion of the time variable and more convenient interpretation of the printed results. Although this function could be tabulated, it was normally generated according to an appropriate analytical relationship in a special-purpose subroutine.

The analyzed results could be output in two forms: as a printed table as shown in Table VI, and as a quick-look plot as presented in Figure 30. The listing provided a detailed tabulation of all values of the stimulus variable under study, the mean signal level and the standard deviation of the level if appropriate. The teleprinter plot has a limited resolution of 2 dB but proved to be a most convenient method of condensing the large quantities of data involved. The zero characters represent the mean threshold level, and the asterisks denote the extent of the standard deviations.

Calibration Procedures

All calibrations of the test equipment were performed using a B&K Automatic Frequency Response and Spectrum Recorder Type 3332. This general-purpose instrument combines three mechanically coupled units: a Beat Frequency Oscillator (BFO) Type 1022, an Audio Frequency Spectrometer Type 2112 and th Level Recorder Type 2305. It provides for the generation of sine waves at frequencies up to 20,000 Hz, octave or 1/3-octave spectrum analysis at frequencies down to 12.5 Hz (in conjunction with a B&K Type 1620 extension filter set), and automatic plotting of spectral and time history data. Accessories included a B&K Model 4133 ½-in. condenser microphone, a B&K 4145 1-in.condenser microphone, an HP Model 650A test oscillator to cover frequencies between 10 and 20 Hz, and a B&K Type 4220 pistonphone. These items were fully calibrated prior to the test program to laboratory standards which in turn were traceable to the National Bureau of Standards and

TABLE VI. EXAMPLE COMPUTER ANALYSIS

ANALYSIS OF 3 TESTS: 102
103
104

TIME COUNT	ELAPSED TIME	ABSOLUTE SPL DB MEAN	SIGMA	STIMULUS PARAMETER
1	2.586	66.4	5.9	.1200E 2
2	7.759	80.8	6.0	.1200E 2
3	12.931	93.1	5.1	.1200E 2
4	18.103	98.8	3.5	.1200E 2
5	23.276	101.0	3.5	.1200E 2
6	28.448	98.6	5.5	.1200E 2
7	33.621	97.5	2.1	.1200E 2
8	38.793	98.1	5.0	.1200E 2
9	43.966	96.6	3.8	.1200E 2
10	49.138	96.5	3.5	.1200E 2
11	54.310	94.8	2.7	.1200E 2
12	59.483	97.2	4.0	.1200E 2
13	64.655	96.5	4.3	.1347E 2
14	69.828	87.7	2.4	.1521E 2
15	75.000	84.9	3.6	.1709E 2
16	80.172	78.1	2.7	.1910E 2
17	85.345	79.4	3.4	.2126E 2
18	90.517	73.7	3.9	.2359E 2
19	95.690	70.7	4.3	.2608E 2
20	100.862	68.3	3.7	.2876E 2
21	106.034	64.5	4.4	.3165E 2
22	111.207	61.6	3.0	.3474E 2
23	116.379	59.9	3.6	.3807E 2
24	121.552	56.1	3.0	.4164E 2
25	126.724	55.6	3.6	.4546E 2
26	131.897	54.5	3.3	.4961E 2
27	137.069	51.0	2.5	.5404E 2
28	142.241	52.4	4.4	.5880E 2
29	147.414	52.9	2.8	.6391E 2
30	152.586	50.2	3.9	.6940E 2
31	157.759	51.3	2.6	.7531E 2

which meet Military Specification MIL-C-45662A. A full set of calibration procedures was established during the test setup phase of the study and was rigorously adhered to during the entire program. These operations are described below, according to the frequency with which they were performed, with reference to the schematic diagram of Figure 32.

Data Acquisition System:

The data system itself was calibrated in two respects, and was also used as part of the calibration procedure for the entire acoustic system. The two system calibrations are the clock pulse period, which governs the sampling rate, and the relationship between the angular position of the transducer shaft and the setting of the attenuator.

The system clock was periodically calibrated to determine the pulse period by allowing the system to punch data for a period of precisely 5 minutes as timed by a stopwatch. In many repeats of this procedure, it was found that the number of characters punched is repeatable to within a total spread of 1 count, or an accuracy of approximately 0.3%. The overall mean period was found to be $1.034 \pm 0.3\%$ seconds/count.

The relationship between the angular position of the motor/transducer/attenuator drive shaft and the setting of the attenuator in dB attenuation is mechanically fixed and theoretically invariable. If, for any reason, however, the drive system was disassembled or adjusted, or if some mechanical malfunction occurred, the system was recalibrated. In practice, the calibration was spot-checked daily. The BFO was adjusted to set up a 1-volt-rms, 500-Hz tone as input to the attenuator at point A. Using the motor drive override control, the assembly is driven to the minimum attenuation position. The graphic level recorder monitoring the crossover input voltage at C was set to a zero dB level. The chart level recorder paper drive and tape perforator were started, and the attenuator was swept from minimum to maximum attenuation. The attenuation setting was recorded as a continuous curve on the chart recorder, with each punch pulse being identified on the chart using the event marker pen. Upon reaching maximum attenuation, the motor direction was reversed to drive the attenuator back to minimum attenuation position. The curves were averaged, and the attenuation settings read for each punch pulse were recorded for correlation with the punched paper tape output.

From these results an attenuation setting in dB was obtained for each binary count, and a 255-entry table was compiled for use by the analysis program. A copy of this table was kept in the laboratory so that periodic spot checks could be made as desired.

Acoustic System - Frequency Response:

For the purpose of computing the sound pressure level at the subject's ears from the input signal level monitored by the DAS, the overall system frequency response function was required. This is the difference, in dB, between the input signal level at C (where the signal characteristics are normally measured) and the levels heard by the subject as a function of frequency. In reality, it is difficult to define or measure these levels and many conventions are practiced. For free propagating sound it is most common to specify audible level either as that measured at the entrance to the ear canal or that measured at the subject's head position when the subject is absent. From a practical standpoint, the latter definition is probably of more value since levels are normally specified or measured in a relatively free space. Depending on frequency, the two values can differ by as much as 10 dB. However, when headphones are used, there is no free field to measure. Also, the measurement of ear canal pressures presents a severe practical problem since it is very difficult to locate microphones inside the headphone cups. Instead, an "acoustic" coupler is used to simulate the human head and in which a condenser microphone is seated at the bottom of a 6-cc cavity approximating that of the outer ear. The coupler used in this study was a Koss/B&K unit specially manufactured for the ESP-9 headphones. The precision with which this coupler represents a real human head is not known, but this imposes no restriction on the validity of the results since we are only concerned with sound pressure level values measured relative to the measured absolute threshold. The only requirement is for both measurements to be made in exactly the same way.

The frequency response was thus measured using the B&K 1022 Beat Frequency Oscillator as a signal source and using a B&K 4133 microphone cartridge mounted on a B&K 2619 preamplifier inside the coupler. The pressure response of this transducer is flat between 20 Hz and 2000 Hz, with a slight roll-off beyond this range reaching 1.0 dB at 10 Hz and 5 dB at 10,000 Hz. The coupler was mounted at the subject's normal head position to properly measure the low-frequency, free field component and the absolute level was established by applying a B&K 4200 pistonphone to the microphone generating a known 124 dB at approximately 250 Hz. The "sine-sweep" calibration was always performed with all system gain and attenuation settings adjusting to give predetermined rms voltages at each point in the system. These settings were established during the system development to provide optimum signal-to-noise situations and an optimum balance between the free field and headphone signal levels. The response to a constant sinusoidal voltage, changing slowly in frequency, was shown in Figure 33(a) for each headphone cup. It will be seen that the two earphones are fairly well

balanced, the maximum difference being approximately 2 dB. It should be noted that the frequency scale is displaced by a constant 10 Hz from the printed recorder chart values. This reflects the use of the incremental frequency adjustment available on the BFO to start the sweep at 10 Hz instead of the standard 20 Hz. The linearity and frequency of the oscillator between 10 and 20 Hz was checked using a low-frequency HP 650A oscillator.

The relative contributions from the loudspeakers and the electrostatic phones to the total signal level are shown for the right ear cup in Figure 33(b). This was obtained by superimposing upon an identical curve the two sine sweep response curves with first the loudspeakers and then the headphones disconnected. Figure 33(b) shows the overall responses measured in each earphone separately.

As a second check on the system frequency variation, the response of the system signal was obtained from an Allison Random Noise Generator, shaped to an essentially flat 1/3-octave band spectrum (Figure 65a) and recorded on the Precision Instruments PS 207 FM tape recorder. This tape was used whenever required as a source of "pink" noise. With this tape as a signal source, the 1/3-octave band level spectra shown in Figure 65(b) were recorded in the earphones. The right and left ear responses are shown separately in Figures 65(b) and 65(c) which, together with Figure 33(b), clearly illustrate the uniformity of response ($\pm$ 2.5 dB between 12.5 and 12,500 Hz) and the similarity of the two earpieces. To avoid the complications introduced by interaural differences, both for the headset itself and the subjects participating in the tests, only the maximum signal occurring in either earphone is considered for calibration purposes. Likewise, threshold results are presented in the next section without regard to the ear in which the signal was detected.

Ambient Noise:

At periodic intervals, the ambient noise inside the test chamber was measured with the sensitive B&K 4145 microphone and analyzed into 1/3-octave band levels. This was done to ensure as far as possible that the noise floor was at all times less than the threshold of audibility. Typical results are presented in Section 5.1 of the main text.

Daily Calibrations:

The calibrations described above were required to set up the entire system in readiness for the tests and were only necessary following repairs or other

changes which might alter the system performance. They provided all the calibration data required for analysis of the test data. On a day-to-day basis it was normally only necessary to make fine adjustments to the various settings, to verify that no changes had occurred to the system responses and to set up specific test stimuli as follows:

The spectrometer/level recorder was calibrated for overall level by applying the 124-dB pistonphone signal to the coupler microphone. The headset was mounted on the coupler (left ear) with the unit at the normal head position, and the chamber door sealed. The oscillator frequency was checked against the 60 Hz power supply frequency and adjusted if necessary. With the DAS attenuator in the low position all voltages were checked or set at the predetermined values. A sine sweep frequency response was then recorded between 10 Hz and 20 KHz and checked by comparison with a standard calibration. In all checks performed, the errors were undiscernible. With a 1-volt, 500-Hz signal applied to the DAS input, the crossover input level (D) was recorded while driving the potentiometer to maximum (120 dB) attenuation. This was also compared with a standard, and at selected intervals the motor was stopped to check the paper tape punch output against the newer calibration. Finally, with the DAS input voltage (b) returned to zero and the attenuator still at the maximum position, a 1/3-octave analysis was made of the microphone output to ensure that no undue noise was present in the system. A further option exercised periodically was to perform an identical analysis on the right earphone.

Individual test stimuli levels were established by monitoring and adjusting the crossover input voltage to a specified level for a known signal. For recorded helicopter sounds, this was a 60-second 100-Hz tone recorded at the beginning and end of the test tape. For other wideband signals, the 500-Hz 1/3-octave band level was used. These levels were measured to the nearest 1/10th dB with the true rms voltmeter of the audiospectrometer.

APPENDIX III
WRITTEN INSTRUCTIONS GIVEN TO TEST SUBJECTS

INSTRUCTIONS -- Please read carefully.

The purpose of these tests is to determine how human listeners detect helicopter noise. The results will be used as a basis for the development of quieter helicopters.

You will be seated inside a specially designed acoustic chamber,and sounds will be presented to you through both loudspeakers and headphones. In many of the tests you will hear a uniform background noise which will remain constant throughout the test and is beyond your control. Unless otherwise instructed, your job is to listen for the sound of aircraft. When you hear an aircraft or helicopter, depress the small hand-held button and hold it down until you can definitely no longer hear the aircraft. At this point release the button. Repeat this during the entire test, continuing to depress or release the button each time you definitely can or definitely cannot hear an aircraft sound respectively.

To inform you of the test progress, we have installed a small console in front of you. Immediately before the start of each test, the amber READY light will illuminate and your control button will energize. The test is actually in progress when the green light is on during which time we are making measurements. At the end of the test the amber STANDBY light will appear and you may take off the headphones and relax to await further instructions.

You will also notice a red LIMIT lamp. If this should light up at any time -- please alert the test director via the intercom, which is always switched on. The system has been in use for many weeks and has proven to be perfectly reliable. If, however, for any reason the sound level becomes uncomfortably high and you are unable to reduce it with your button the red switch on the wall to your left may be thrown to immediately turn off all sound. The ALARM-EMERGENCY switch on the console stops the test and should be used only under extreme circumstances.

The headphones should be worn with the cable to your left ear. Please be sure to be wearing them as soon as the READY light comes on.

The tests require considerable concentration on your part, and it is important for you to rest between tests. Please notify the test personnel if you suspect your performance deteriorated at any time.

APPENDIX IV
METHODS FOR CALCULATING HELICOPTER AURAL DETECTION THRESHOLDS

Three methods for the calculation of helicopter detection thresholds are presented in this appendix. A choice among them may be made on the basis of the degree of resolution of the available input data, the computational equipment available, the accuracy required in the specific application, and the time available to perform the computations. The first method, which in general is practical only for machine computation, requires specification of the 1/3-octave band level spectra for both the helicopter noise signal and the ambient noise at the observer location. These data are converted, as accurately as possible, to critical bandwidth spectra, and the transformed signal spectrum is compared to a combined threshold function. This is the method which was tested as described in Section 5.0 of the main report. The second method is still based upon the use of 1/3-octave band level data but is simplified by the adoption of an approximate method for the inclusion of the critical bandwidth effect. It is thought that this approach will be only slightly less accurate than the first method, and yet it offers considerable simplification of the computational steps. The final version requires only octave band spectral resolution and is otherwise identical to the second method. It is probably less accurate than either of the alternatives, but it is amenable to hand calculation.

Whatever the choice, the basic calculation indicates whether the particular helicopter noise spectrum is audible in the particular masking noise and by what margin. This margin is obtained as the greatest (or least) difference between the signal and a combined threshold. The true threshold level for this particular signal spectrum can be obtained by applying the appropriate dB adjustment to reduce the above difference to zero. In general, however, a change of signal level requires an adjustment of the helicopter position, and this in turn, due to frequency dependent attenuation effects, requires a modification to the spectrum shape. In this case the threshold is best established by iteration, basing successive estimates of the correct result upon the previous error. Again, this procedure is best performed by machine calculation.

In the following instructions, frequent use is made of the summation notations $\sum_{dB}$ and $(L_1 + L_2 + \ldots)_{dB}$. These are used to denote the decibel summation of sound pressure levels according the formula

$$\sum_{n dB} (L_n) = (L_1 + L_2 + L_3 + \ldots)_{dB}$$

$$= 10 \log_{10} (10^{L_1/10} + 10^{L_2/10} + 10^{L_3/10} + \ldots)_{dB}$$

As an aid to manual calculation, a tabular method for sound pressure level summation is presented in Table VII at the end of this Appendix.

METHOD A. "EXACT" CALCULATION USING 1/3-OCTAVE BAND LEVELS

Data Required

L_n for n = 1 to 30: the 1/3-octave band levels, in dB, of the helicopter noise spectrum at the observer location for the frequencies f_n = 12.5, 16, 20, ..., 10,000 Hz (or for whatever frequency range the data are available).

M_n for n = 1 to 30: the 1/3-octave band levels of the ambient masking noise at the observer location for the same frequency range.

Method

Step 1: Convert the 1/3-octave band levels L_n and M_n to critical band levels L_n' and M_n' using the "exact" relationships described in Table VIII.

Step 2: Calculate the combined critical band threshold level T_n' at each frequency as the decibel sum of the absolute threshold A_n' (from Table IX) and the masking threshold $(M_n' - 5)$ dB; i.e.,

$$T_n' = A_n' + (M_n' - 5) \text{ dB}$$

Note that if the difference between A_n' and $(M_n' - 5)$ exceeds 13 dB, it is sufficiently accurate to put T_n' equal to the greater of A_n' and $(M_n' - 5)$.

Step 3: Subtract the combined thresholds T_n' from the critical band signal levels L_n'. If the greatest value is greater than +1 dB, it may be assumed that the signal is audible.

Example

A hypothetical example is worked in Table X. The 1/3-octave band levels of the helicopter signal and the ambient noise are listed in columns 4 and 5 and the absolute tone threshold is copied from Table IX into column 3.

Step 1 is executed in Tables XI and XII according to the instructions provided in Table II.2, and the results are transferred to columns 6 and 9 of Table X. The critical band masking level obtained by subtracting 5 dB from the ambient levels is given in column 7. The combined threshold which is the decibel summation of the absolute tone threshold (3) and the masking level (7) is tabulated in column 8. Column 10 is the detection level which is the difference between the signal level and the threshold level. Column 11 shows the audible level in each critical band (all positive values of the column 10 entry minus 1 dB).

Thus, in this example the signal is audible in the four critical bands at 50, 63, 80 and 100 Hz. The most audible band is that at 63 Hz, and the audibility threshold for the signal is 3 dB below that specified in column 4. The results of the example calculations are shown graphically in Figure 66.

METHOD B. APPROXIMATE CALCULATION BASED ON 1/3-OCTAVE BAND LEVELS*

Data Required

As in Method A, L_n and M_n for n = 1 to 30, the 1/3-octave band levels of the helicopter signal and the ambient noise.

Method

For this approach, the absolute audibility threshold has been converted to an effective 1/3-octave band level threshold A_n so that no critical band conversions are required. The computational steps required are as follows:

Step 1: Calculate the 1/3-octave band masking level by subtracting 5 dB from each of the 1/3-octave ambient noise levels.

Step 2: Establish the 1/3-octave band combined threshold by the decimal summation of absolute threshold A_n (from Table IX) and the masking level; i.e.,

$$T_n = A_n + (M_n - 5) \quad \text{dB}$$

*This method is only approximately correct for helicopter type spectra which decay fairly uniformly in the lowest bands. Errors will be greater for different type spectra.

Step 3: Compute the detection level in each band by subtracting the threshold level from the signal level.

Step 4: The audible level is the amount by which each detection level exceeds 1 dB.

Example

The previous hypothetical data is reused for this example which is worked in Table XIII. Comparing the final results with those obtained using the exact method (Table X) it may be seen that the detection levels agree to within 1 dB. This is typical of the relative accuracy which may be expected.

METHOD C. APPROXIMATE CALCULATION BASED ON OCTAVE BAND LEVELS*

Data Required

$\overline{L}_k$ and $\overline{M}_k$ for k = 1 to 8, the octave band sound pressure levels of the helicopter signal and the ambient noise in the frequency range 16 Hz to 8 kHz.

Method

The procedure is precisely the same as that for Method B above except that the equivalent octave band thresholds $\overline{A}_k$ from Table XIV are used. Again, the procedure should be restricted to helicopter type spectra.

Step 1: Calculate the octave band masking levels by subtracting 5 dB from each of the octave band ambient noise levels.

Step 2: Establish the octave band combined threshold by the decibel addition of the absolute threshold $\overline{A}_k$ and the masking level; i.e.,

$$\overline{T}_k = \overline{A}_k + (\overline{M}_k - 5) \quad \text{dB}$$

*This method is subject to the same restrictions regarding spectrum shape as Method B (q.v.).

Step 3: Compute the detection level in each band by subtracting the threshold level from the signal level.

Step 4: The audible level is the amount by which each detection level exceeds 1 dB.

Example

A complete example is worked in Table XV. The octave band levels listed in columns 3 and 5 correspond to the 1/3-octave levels presented in the previous two examples. The final result is again very similar, i.e., an audible level of 3 dB in the octave band centered on 63 Hz. This demonstrates the usefulness of this procedure.

TABLE VII. TABLE FOR THE ADDITION OF SOUND PRESSURE LEVELS (TO THE NEAREST 0,5 dB)

dB	-20	-10	-0	+10
0	.010	.100	1.00	10.00
0.5	.011	.112	1.122	11.22
1.0	.013	.126	1.258	12.58
1.5	.014	.141	1.412	14.12
2.0	.016	.159	1.585	15.85
2.5	.018	.178	1.780	17.8
3.0	.020	.200	2.00	20.0
3.5	.022	.224	2.24	22.4
4.0	.025	.251	2.51	25.1
4.5	.028	.282	2.82	28.2
5.0	.032	.316	3.16	31.6
5.5	.036	.355	3.55	35.5
6.0	.040	.398	3.98	39.8
6.5	.045	.447	4.47	44.7
7.0	.050	.501	5.01	50.1
7.5	.056	.562	5.62	56.2
8.0	.063	.631	6.31	63.1
8.5	.071	.708	7.08	70.8
9.0	.080	.794	7.94	79.4
9.5	.089	.891	8.91	89.1

Method: Subtract the decade of the highest level from all values and convert each to an energy value using the table. Convert the sum of the energies to the nearest 1/2 dB level, remembering to replace the decade.

Example: To calculate $\sum_{dB}$ (58+ 64.5+73.5 + 71.5) dB, subtract 70 from each:

8.0 (-20), 4.5 (-10), 3.5 (-0), 1.5 (-0)
Energy values: .063 + .282 + 2.24 + 1.412 = 4.01
Nearest dB level: 6.0
Add back original 70: $\sum_{dB}$ = 76.0 dB

TABLE VIII. METHOD FOR CONVERSION FROM 1/3-OCTAVE BAND TO CRITICAL BAND LEVELS

			B_{n_i} (dB)													
	i		1	2	3	4	5	6	7	8	9	10	11	12	13	14
n	f	R_n \ f	12.5	16	20	25	31.5	40	50	63	80	100	125	160	200	250
1	12.5	9.5	0	0	0	-2	-	-	-	-	-	-	-	-	-	-
2	16	8.5	0	0	0	0	-8.5	-	-	-	-	-	-	-	-	-
3	20	7.5	0	0	0	0	-1.5	-	-	-	-	-	-	-	-	-
4	25	6.5	0	0	0	0	0	-5	-	-	-	-	-	-	-	-
5	31.5	6.0	-	-9	0	0	0	0	-	-	-	-	-	-	-	-
6	40	5.0	-	-	-	-3.5	0	0	-1	-	-	-	-	-	-	-
7	50	4.0	-	-	-	-	-9	0	0	-2	-	-	-	-	-	-
8	63	3.5	-	-	-	-	-	-	-1	0	-3.5	-	-	-	-	-
9	80	3.0	-	-	-	-	-	-	-	-2.5	0	-4.5	-	-	-	-
10	100	2.0	-	-	-	-	-	-	-	-	-3.5	0	-6.5	-	-	-
11	125	1.5	-	-	-	-	-	-	-	-	-	-5	0	-	-	-
12	160	1.0	-	-	-	-	-	-	-	-	-	-	-10.5	0	-12.5	-
13	200	0.5	-	-	-	-	-	-	-	-	-	-	-	-	0	-14.5
14	250	0														
15	315	-0.5														
16	400	-0.5														
17	500	-1.0														
18	630	-1.0														
19	800	-1.5														
20	1,000	-1.5														
21	1,250	-1.5														
22	1,600	-2.0														
23	2,000	-2.0														
24	2,500	-2.0														
25	3,150	-2.0														
26	4,000	-2.0														
27	5,000	-2.0														
28	6,300	-2.0														
29	8,000	-2.0														
30	10,000	-2.0														

1) "Exact" Method:

For frequencies below 250 Hz (i.e. $n \leq 13$) the critical bandwidth is greater than the 1/3-octave bandwidth at the same center frequency so that the critical band level must be obtained by summing the total or partial energies from a number of adjacent 1/3-octave bands. The formula for this addition is

$$L'_n = \sum_{i=1}^{14}{}_{dB} \left[L_i + B_{n_i} \right] \quad \text{where } L_i = L_n \text{ for } i = n$$

(Note that the B_{n_i} are added algebraically to the L_i before the decibel summation across i).

Example: Compute the sound pressure level in the critical band centered at 40 Hz when the 1/3-octave band levels at 31.5, 40, 50 and 63 Hz are 58, 54, 53 and 50.5 dB respectively (remaining levels may be ignored):

$$L'_n = \sum_{dB} [49 + 54 + 53 + 48.5]$$

$$= 58 \text{ dB}$$

For frequencies of 250 Hz and above, the exact method is the same as the approximate method below.

2) Approximate Method:

Add algebraically the increment R_n to the 1/3-octave level L_n; i.e., $L'_n = L_n + R_n$.

TABLE IX. ABSOLUTE THRESHOLDS OF AUDIBILITY (IN QUIET) FOR PURE TONES (CRITICAL BANDS) AND 1/3-OCTAVE BAND NOISE LEVELS FOR FREE-FIELD LISTENING CONDITIONS.

(Adapted from the data of Robinson & Dadson[34])

n	f_n	A'_n	A_n	n	f_n	A'_n	A_n	n	f_n	A'_n	A_n
1	12.5	83.0	79.5	11	125	21.5	20.0	21	1,250	3.0	4.5
2	16.0	77.0	71.5	12	160	18.0	17.0	22	1,600	2.5	4.5
3	20.0	70.0	62.0	13	200	14.5	14.0	23	2,000	1.5	3.5
4	25.0	63.0	53.0	14	250	12.0	12.0	24	2,500	0.0	2.0
5	31.5	56.5	48.5	15	315	9.0	9.5	25	3,150	-2.5	-0.5
6	40.0	50.0	44.0	16	400	7.0	7.5	26	4,000	-4.0	-2.0
7	50.0	43.5	38.5	17	500	6.0	7.0	27	5,000	-1.0	1.0
8	63.0	36.5	32.0	18	630	5.0	6.0	28	6,300	5.0	7.0
9	80.0	31.0	28.0	19	800	4.0	5.5	29	8,000	14.0	16.0
10	100.0	26.0	24.0	20	1,000	4.0	5.5	30	10,000	16.0	18.0

n = Band number

f_n = Center frequency, Hz

A'_n = Tone (critical band) threshold

A_n = 1/3-octave band threshold

} to nearest 0.5 dB

Note: The 1/3-octave band thresholds A_n below 250 Hz are approximately correct for 1/3-octave band spectra which decay at 6 dB per octave, which are typical of helicopter noise. Errors will increase for different spectra. For narrow band sounds, e.g., for single 1/3-octave bands of noise below 200 Hz, the tone threshold A'_n gives the correct result.

TABLE X. WORKED EXAMPLE USING METHOD A.

1	2	3	4	5	6	7	8	9	10	11
Band Number	Band Center Frequency	Absolute Tone Threshold (From Table IX)	Helicopter Signal 1/3 OB Level (Input Data)	1/3 Octave Band Ambient Level (Input Data)	Critical Band Ambient Level (From Table XI)	Critical Band Masking Level = (6) - 5 dB	Combined Critical Band Threshold = (3) + (7) dB	Critical Band Signal Level (From Table XII)	Detection Level = (9) - (8)	Audible Level = (10) - T
n	f_n	A_n	L_n	M_n	M'_n	M'_n-5	T_n	L'_n	n	L_T
1	12.5	83	54	30	35.5	30.5	83	57	-26	-
2	16	77	52	30	36	31	77	57	-20	-
3	20	70	48	30	37	32	70	57.5	-12.5	-
4	25	63	46.5	30	36.5	31.5	63	57.5	- 5.5	-
5	31.5	56.5	44	30	36	31	56.5	52.0	- 4.5	-
6	40	50	42	30	35	30	50	48.5	- 1.5	-
7	50	43.5	40	30	34	29	43.5	45	1.5	0.5
8	63	36.5	36.5	30	33.5	28.5	37	41	4	3
9	80	31	32	30	33	28	33	36.5	3.5	2.5
10	100	26	28	30	32	27	29.5	31.5	2	1
11	125	21.5	23.5	30	31.5	26.5	27.5	26.5	- 1	-
12	160	18	18	30	31	26	26.5	19	- 7.5	-
13	200	14.5	12.5	30	30.5	25.5	26	12.5	-13.5	-
14	250	12	6	30	30	25	25	6	-19	-
15	315	9	0.5	30	29.5	24.5	24.5	0	-24.5	-
16	400	7	-9	30	29.5	24.5	24.5	-9.5	-34	-
17	500	6	-	30	29	24	24	-	-	-
18	630	5	-	30	29	24	24	-	-	-
19	800	4	-	30	28.5	23.5	23.5	-	-	-
20	1,000	4	-	30	28.5	23.5	23.5	-	-	-
21	1,250	3	-	30	28.5	23.5	23.5	-	-	-
22	1,600	2.5	-	30	28	23	23	-	-	-
23	2,000	1.5	-	30	28	23	23	-	-	-
24	2,500	0	-	30	28	23	23	-	-	-
25	3,150	-2.5	-	30	28	23	23	-	-	-
26	4,000	-4	-	30	28	23	23	-	-	-
27	5,000	-1	-	30	28	23	23	-	-	-
28	6,000	5	-	30	28	23	23	-	-	-
29	8,000	14	-	30	28	23	23.5	-	-	-
30	10,000	16	-	30	28	23	24	-	-	-

TABLE XI. METHOD A EXAMPLE: EXACT COMPUTATION OF AMBIENT NOISE CRITICAL BAND LEVELS FROM 1/3-OCTAVE BAND LEVELS.

$M_i + B_{n_i n_j}$ (B from Table III)

i		1	2	3	4	5	6	7	8	9	10	11	12	13	14	$\sum_{ab}$ =
M_i		30	30	30	30	30	30	30	30	30	30	30	30	30	30	
n	f	12.5	16	20	25	31.5	40	50	63	80	100	125	160	200	250	M'_n
1	12.5	30	30	30	28											35.5
2	16	30	30	30	30	21.5										36
3	20	30	30	30	30	28.5										37
4	25	30	30	30	30	30	25									36.5
5	31.5		27	30	30	30	30									36
6	40				26.5	30	30	29								35
7	50					27	30	30	28							34
8	63							29	30	26.5						33.5
9	80								27.5	30	25.5					33
10	100									26.5	30	23.5				32
11	125										25	30	22			31.5
12	160											19.5	30	17.5		31
13	200													30	15.5	30.5

n	14	15	16	17	18	19	20	21	22	23	24	25	26	27	28	29	30
f	250	315	400	500	630	800	1000	1250	1600	2000	2500	3150	4000	5000	6300	8000	10K
R_n	0	-0.5	-0.5	-1.0	-1.0	-1.5	-1.5	-1.5	-2.0	-2.0	-2.0	-2.0	-2.0	-2.0	-2.0	-2.0	-2.0
M_n	30	30	30	30	30	30	30	30	30	30	30	30	30	30	30	30	30
M'_n	30	29.5	29.5	29	29	28.5	28.5	28.5	28	28	28	28	28	28	28	28	28

TABLE XII. METHOD A EXAMPLE: "EXACT" COMPUTATION OF HELICOPTER SIGNAL CRITICAL BAND LEVEL FROM 1/3-OCTAVE BAND LEVELS

		$L_i + B_{n,i}$ (B from Table VIII)														
i		1	2	3	4	5	6	7	8	9	10	11	12	13	14	$\sum_{dB}$ =
L_i		54	52	48	46.5	44	42	40	36.5	32	28	23.5	18	12.5	6	
n	f	12.5	16	20	25	31.5	40	50	63	80	100	125	160	200	250	L'_n
1	12.5	54	52	48	44.5											57
2	16	54	52	48	46.5	35.5										57
3	20	54	52	48	46.5	42.5										57.5
4	25	54	52	48	46.5	44	37									57.5
5	31.5		43	48	46.5	44	42									52.0
6	40				43	44	42	39								48.5
7	50					35	42	40	34.5							45
8	63							39	36.5	28.5						41
9	80								34	32	23.5					36.5
10	100									28.5	28	17				31.5
11	125										23	23.5	10			26.5
12	160											13	18	0		19
13	200													12.5	-8.5	12.5

n	14	15	16	17	18	19	20	21	22	23	24	25	26	27	28	29	30
f	250	315	400	500	630	800	1000	1250	1600	2000	2500	3150	4000	5000	6300	8000	10K
R_n	0	-0.5	-0.5	-1.0	-1.0	-1.5	-1.5	-1.5	-2.0	-2.0	-2.0	-2.0	-2.0	-2.0	-2.0	-2.0	-2.0
L_n	0.5	-9	-	-	-	-	-	-	-	-	-	-	-	-	-	-	-
L'_n	0.5	-9.5	-	-	-	-	-	-	-	-	-	-	-	-	-	-	-

TABLE XIII. WORKED EXAMPLE USING METHOD B.

1	2	3	4	5	6	7	8
Band Number	Band Center Frequency Hz	1/3 OB Threshold (From Table IX)	Helicopter 1/3 dB Level (Input Data)	Masking Level (Input Data)	Combined 1/3 dB Threshold (= (3)+ (5) dB)	Detection Level (= (6) - (3))	Audible Level (= (7) - 1 dB)
n	f_n	A_n	L_n	M_n -5	T_n	D_n	S_n
1	12.5	79.5	54	25	79.5	-25.5	-
2	16	71.5	52	25	71.5	-19.5	-
3	20	62	48	25	62	-14	-
4	25	53	46.5	25	53	- 6.5	-
5	31.5	48.5	44	25	48.5	- 4.5	-
6	40	44	42	25	44	- 2	-
7	50	38.5	40	25	38.5	1.5	0.5
8	63	32	36.5	25	32.5	4.0	3.0
9	80	28	32	25	30	2.0	1.0
10	100	24	28	25	27.5	0.5	-
11	125	20	23.5	25	26	- 2.5	-
12	160	17	18	25	25.5	- 7.5	-
13	200	14	12.5	25	25.5	-13	-
14	250	12	6	25	25	-19	-
15	315	9.5	0.5	25	25	-24.5	-
16	400	7.5	-9	25	25	-34	-
17	500	7	-	25	25	-	-
18	630	6	-	25	25	-	-
19	800	5.5	-	25	25	-	-
20	1,000	5.5	-	25	25	-	-
21	1,250	4.5	-	25	25	-	-
22	1,600	4.5	-	25	25	-	-
23	2,000	3.5	-	25	25	-	-
24	2,500	2	-	25	25	-	-
25	3,150	-0.5	-	25	25	-	-
26	4,000	-2	-	25	25	-	-
27	5,000	1	-	25	25	-	-
28	6,300	7	-	25	25	-	-
29	8,000	16	-	25	25.5	-	-
30	10,000	18	-	25	26	-	-

TABLE XIV.
ABSOLUTE THRESHOLDS (IN QUIET) FOR OCTAVE BAND NOISE LEVELS -- FREE FIELD LISTENING

k	f_k	$\bar{A}_k$
1	16	76.5
2	31.5	53.5
3	63	37.5
4	125	24.5
5	250	17
6	500	11
7	1,000	9.5
8	2,000	7
9	4,000	3
10	8,000	12

k = Band Number

f_k = Center Frequency (Hz)

$\bar{A}_k$ = Octave Band Threshold Level (dB)

N.B. Values only valid for helicopter type spectra.

TABLE XV. WORKED EXAMPLE OF AURAL DETECTABILITY CALCULATION USING METHOD C -- OCTAVE BAND DATA

1	2	3	4	5	6	7	8
Band	Band Center Frequency (Hz)	dB Threshold (from Table IX)	Helicopter dB Level (Input Data)	dB Masking Level (Input Data)	Combined dB Threshold = (3) + (5) dB	Detection Level = (6) - (3)	Audible Level = (7) - 1
k	f_k	$\bar{A}_k$	$\bar{L}_k$	$\bar{M}_k - 5$	$\bar{T}_k$	$\bar{D}_k$	S_k
1	16	76.5	57	30	76.5	-19.5	-
2	31.5	53.5	49.5	30	53.5	- 4	-
3	63	37.5	42	30	38	4	3
4	125	24.5	29.5	30	31	- 1.5	-
5	250	17	13.5	30	39	-16.5	-
6	500	11	-9	30	30	-39	-
7	1,000	9.5	-	30	30	-	-
8	2,000	7	-	30	30	-	-
9	4,000	3	-	30	30	-	-
10	8,000	12	-	30	30	-	-

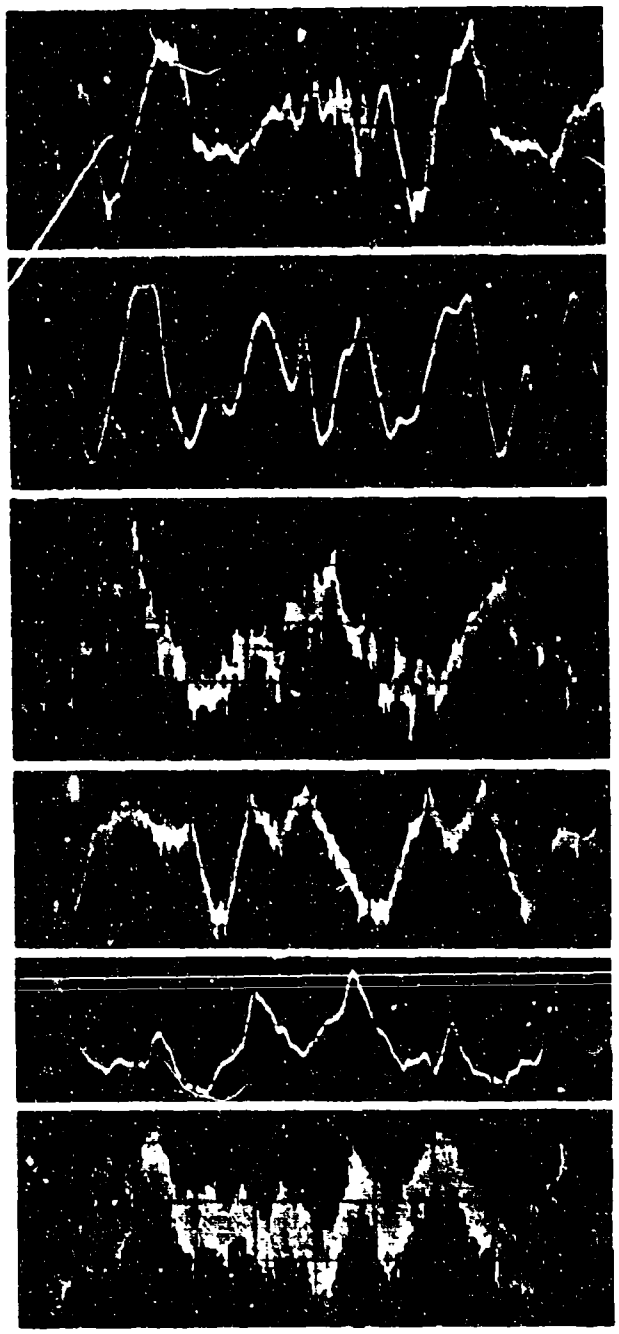

CH-47B
Hover in Ground Effect
Microphone distance ≈ 200 ft

UH-1B
Low altitude approach
Microphone distance ≈5000 ft

HH-43B
Hover at 200 ft altitude
Microphone distance ≈ 280 ft

QH-50
Flyover at 125 ft , 30 kt
Microphone distance ≈500 ft

YOH-6
Flyover at 500 ft , 100 kt
Microphone distance ≈1000 ft

UH-1B
Ground run, low power
Microphone 50 ft from tail-rotor

Figure 1. Examples of Helicopter Noise Waveforms.

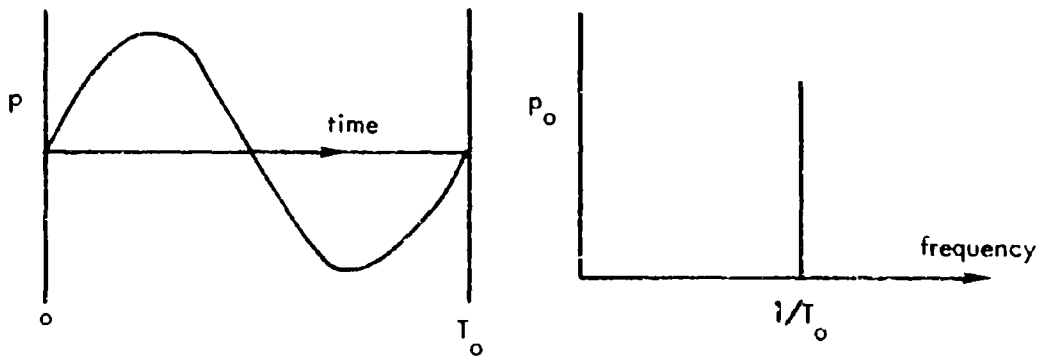

Figure 2. Time and Frequency Representations of a Sine Wave

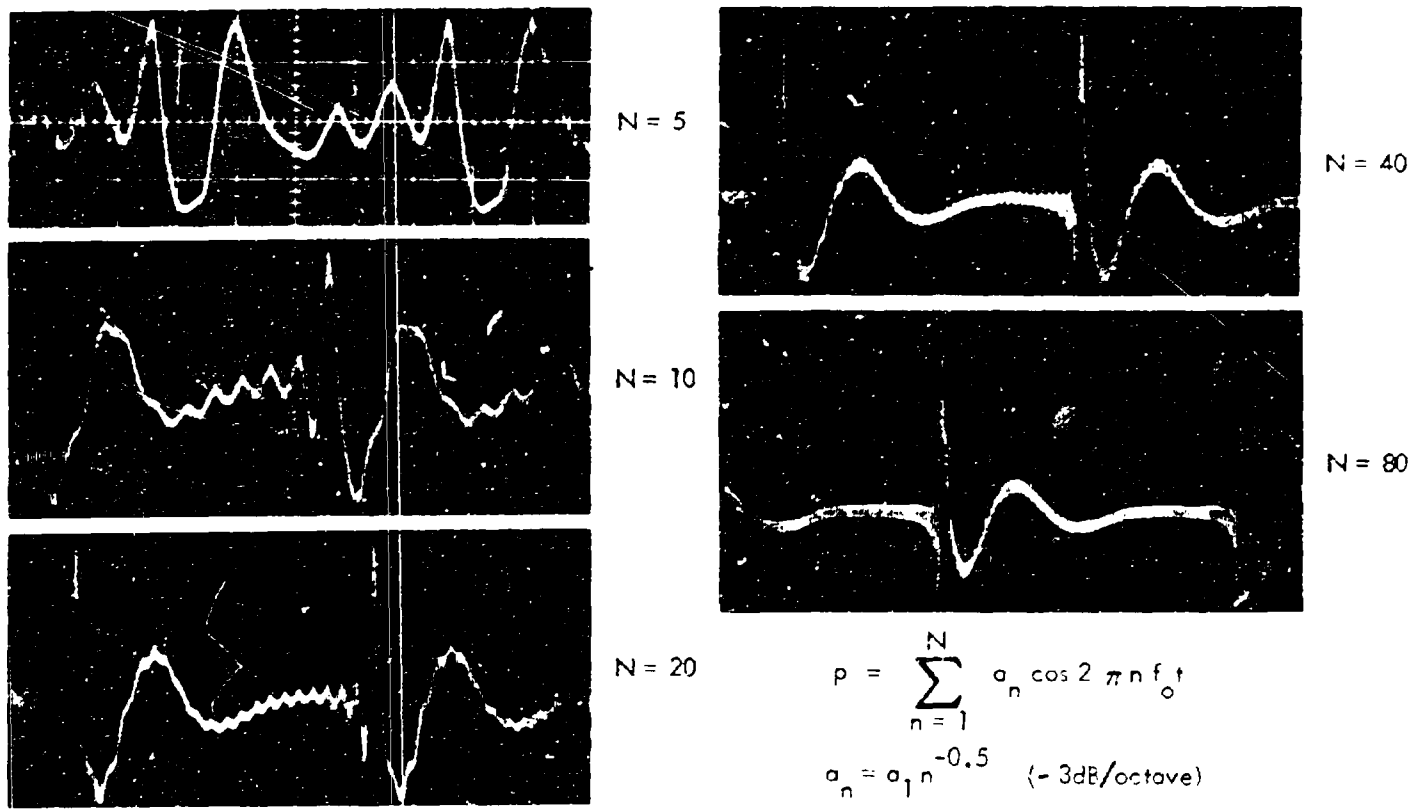

Figure 3. Waveforms of Computer Generated Periodic Sound Showing the Effect of Number of Harmonic Components.

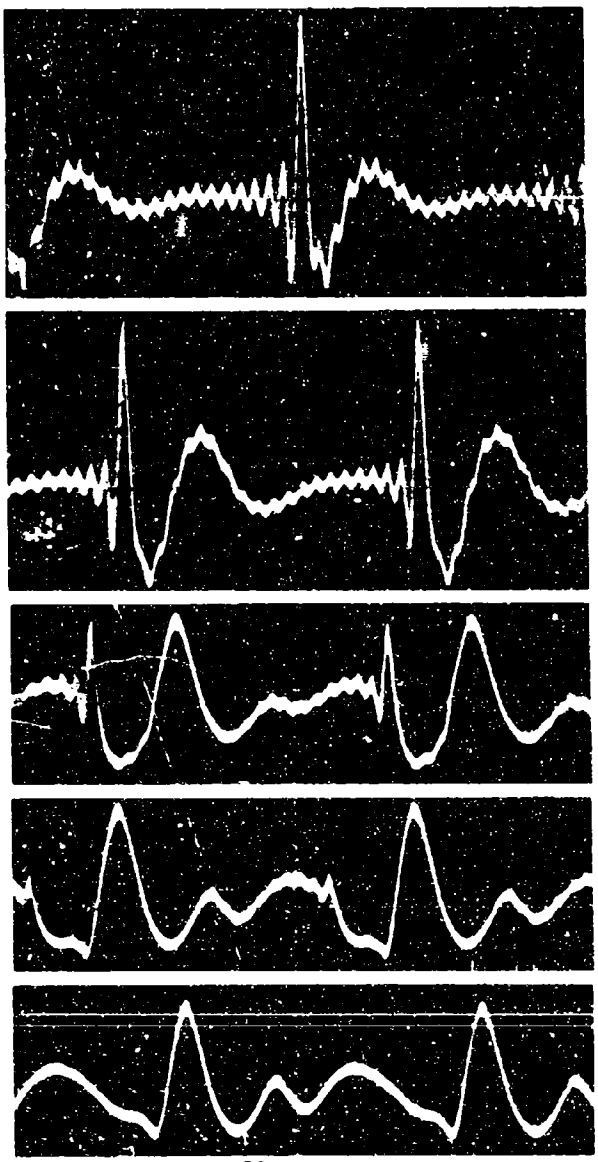

Figure 4. Waveforms of Computer Generated Sounds Showing Effect of Harmonic Amplitude Decay.

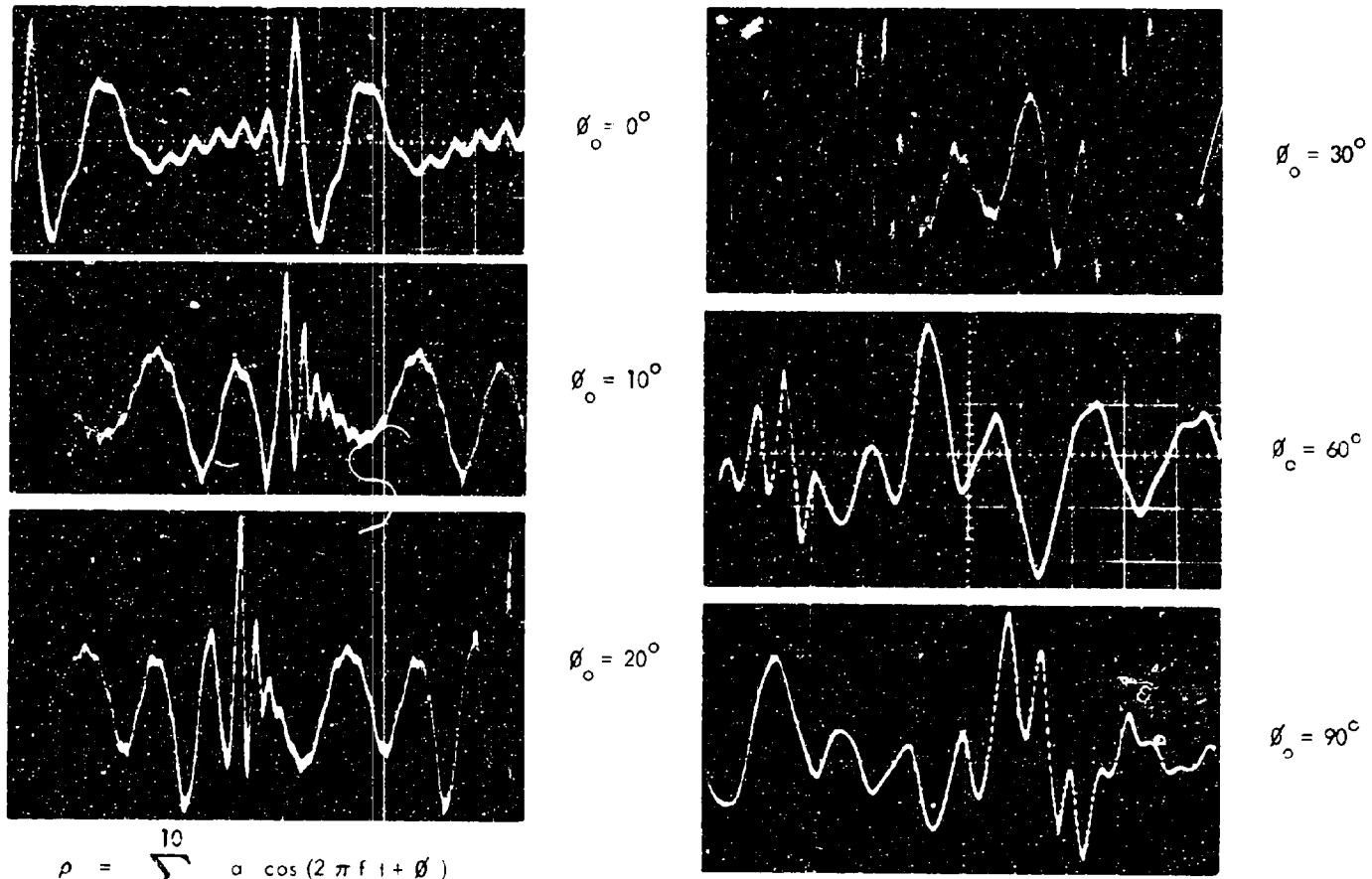

$$p = \sum_{n=1}^{10} a_n \cos(2\pi f_o t + \phi_n)$$

$$\phi_n = n\phi_o ; a_n = a_1 n^{-0.5} \text{ (-3 dB/octave)}$$

Figure 5. Waveforms of Periodic Sound Showing Effect of Interharmonic Phase.

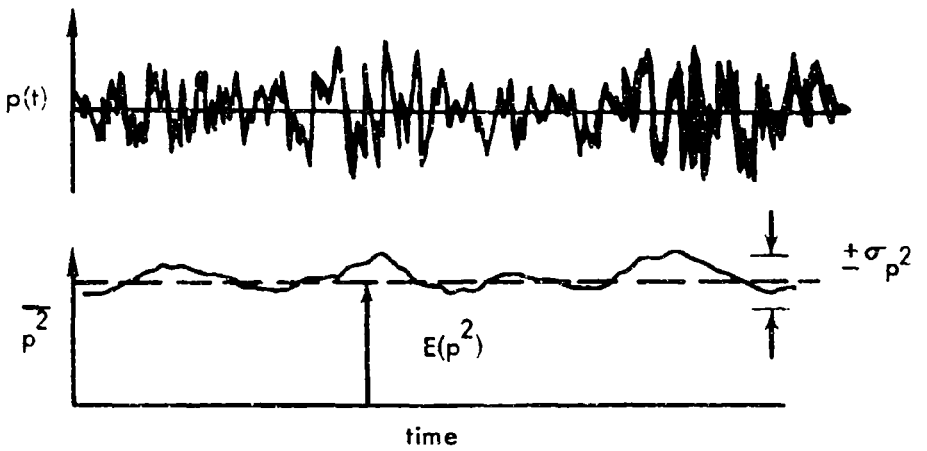

Figure 6. Fluctuation in Mean Square Value of a Random Signal.

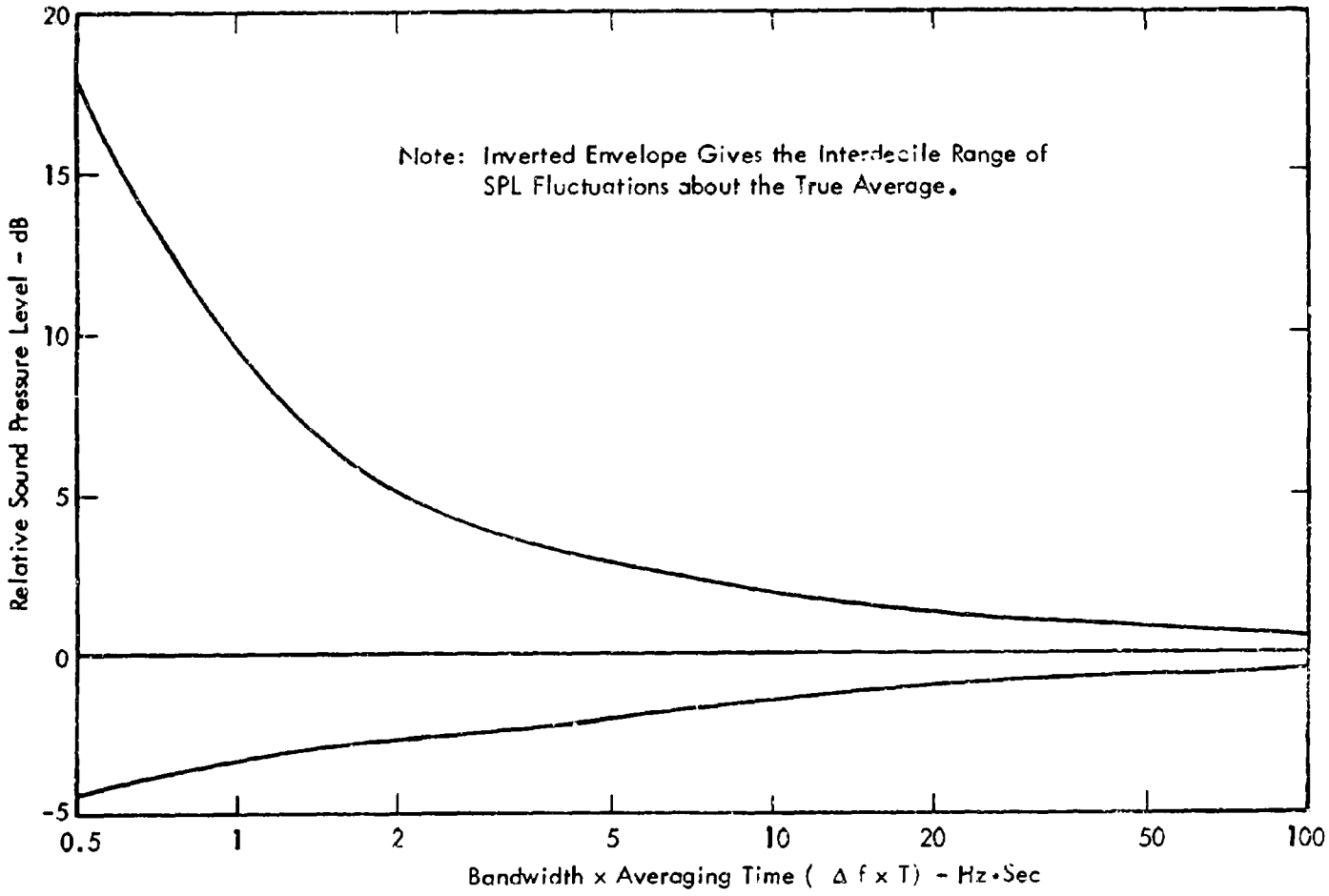

Figure 7. 80% Confidence Limits Associated with a Single SPL Measurement of a Band of Random Noise as a Function of Averaging Time and Bandwidth.

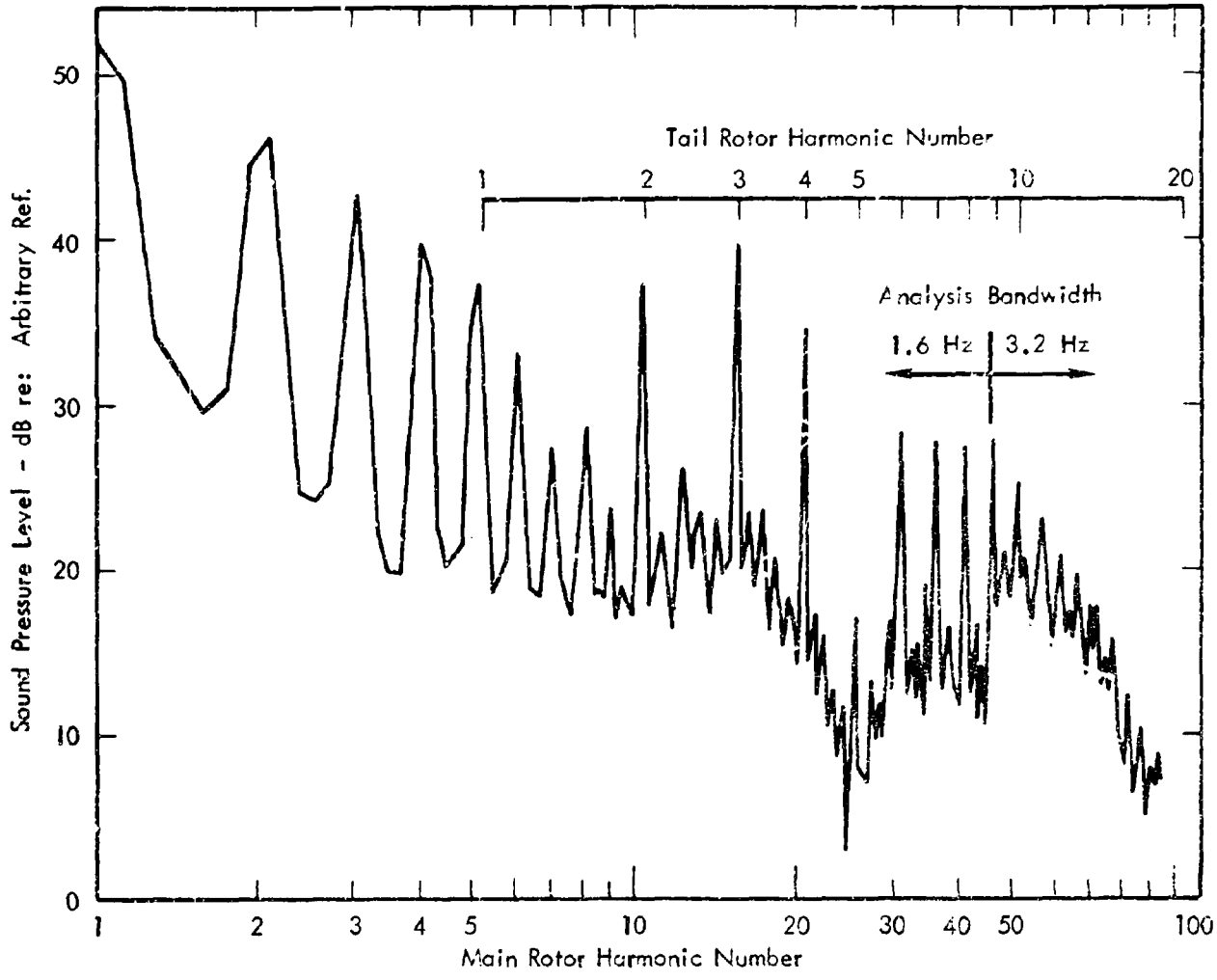

Figure 6. Narrow-Band Analysis of Helicopter Noise (UH-1B in Hover).

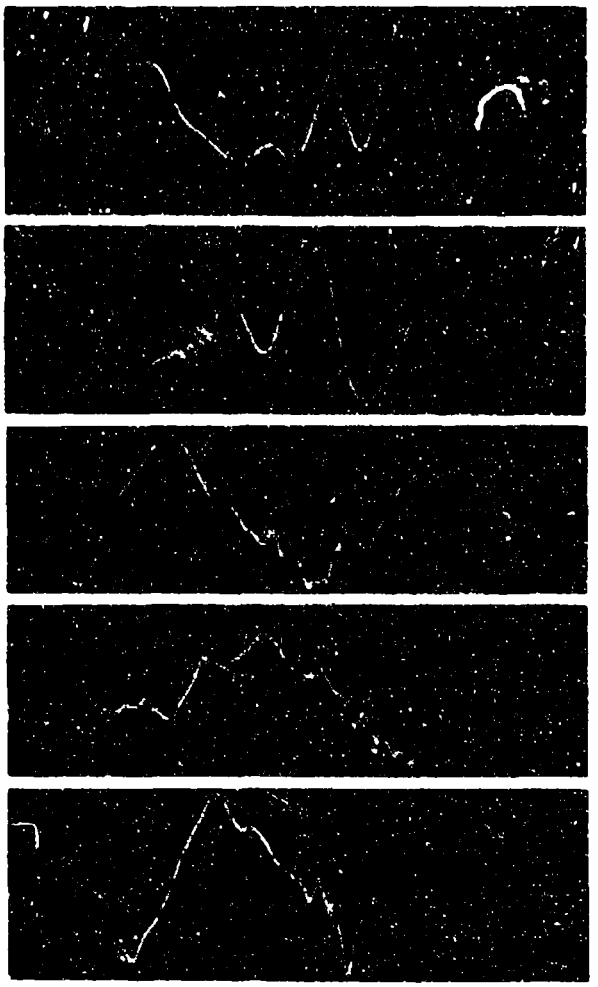

(Each diagram shows one blade passage period)

Figure 9. Waveforms Observed at Successive Times During the 60 kt Approach of a UH-1F Helicopter at 1000 ft.

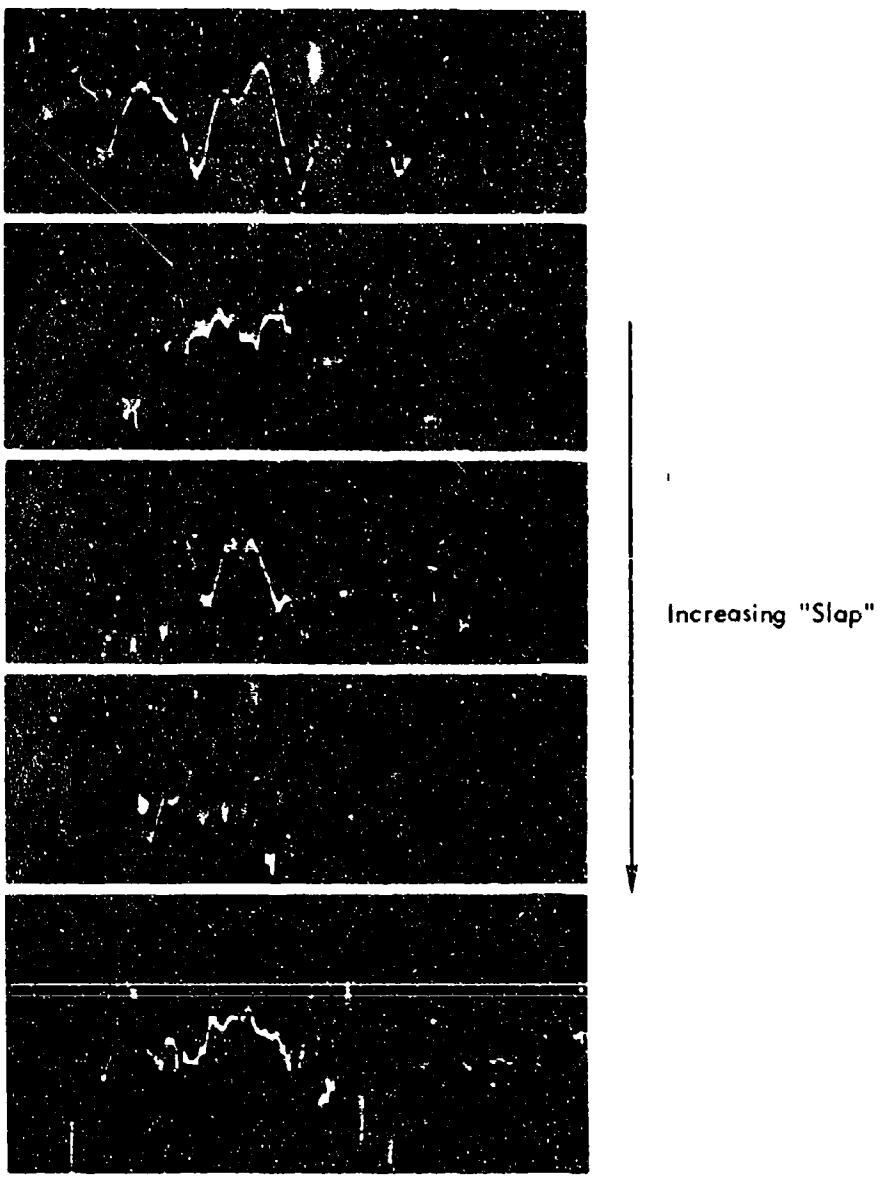

Figure 10. Waveforms Observed During the 60 kt Approach of a CH-47A Helicopter (750 ft. altitude) Showing Increasing Degrees of Blade Slap.

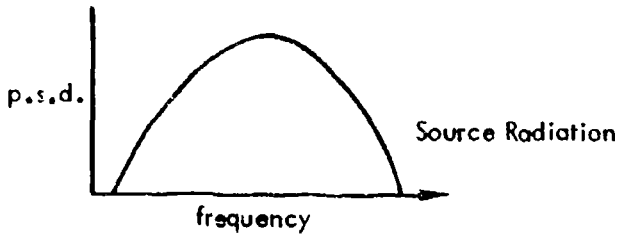

Figure 11. Conceptual Sketch of Rotor Broadband Noise Spectrum.

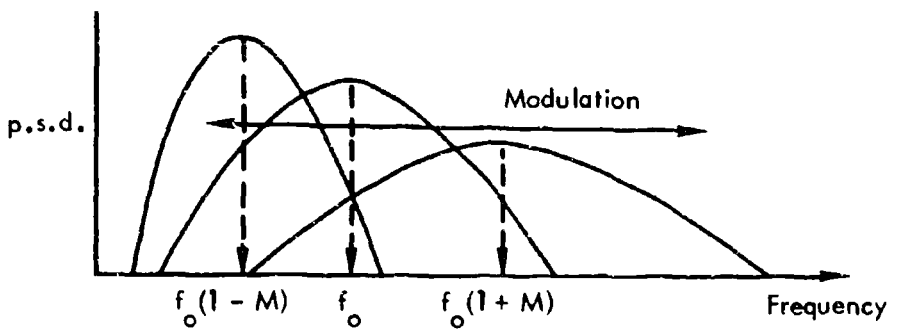

Figure 12. Modulation of Observed Broadband Noise by Rotation.

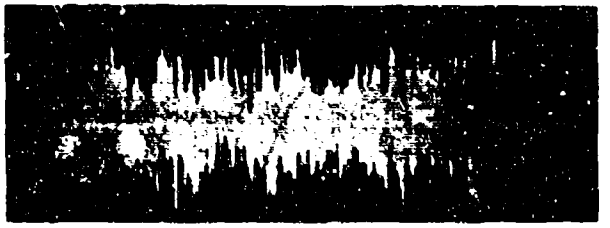

3 dB Modulation at 10 Hz

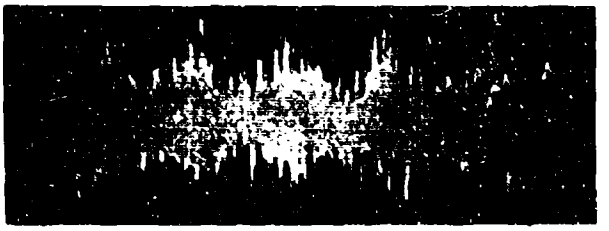

6 dB Modulation at 10 Hz

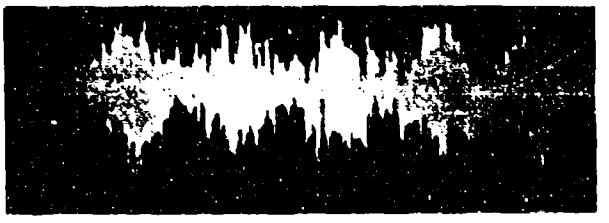

9 dB Modulation at 10 Hz

Figure 13. Waveforms of Modulated Pink Noise.

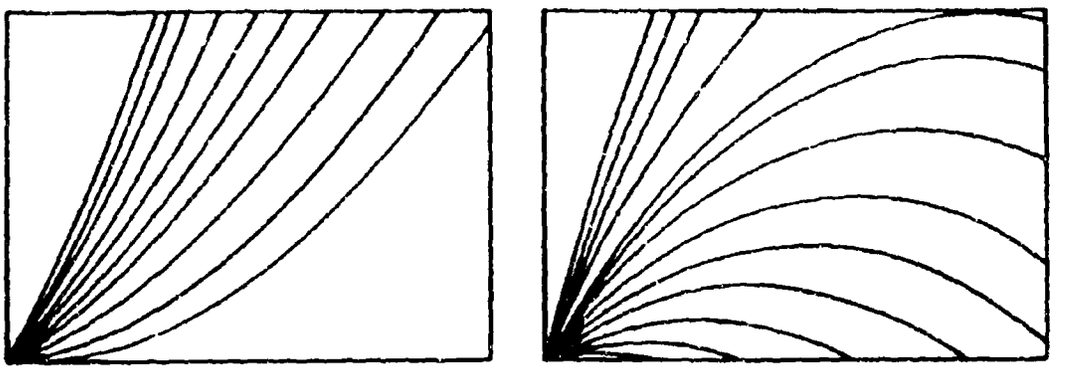

(a) Ray Paths in Air When Vertical Velocity or Temperature Gradient is Negative

(b) Ray Paths in Air When Vertical Velocity or Temperature Gradient Is Positive

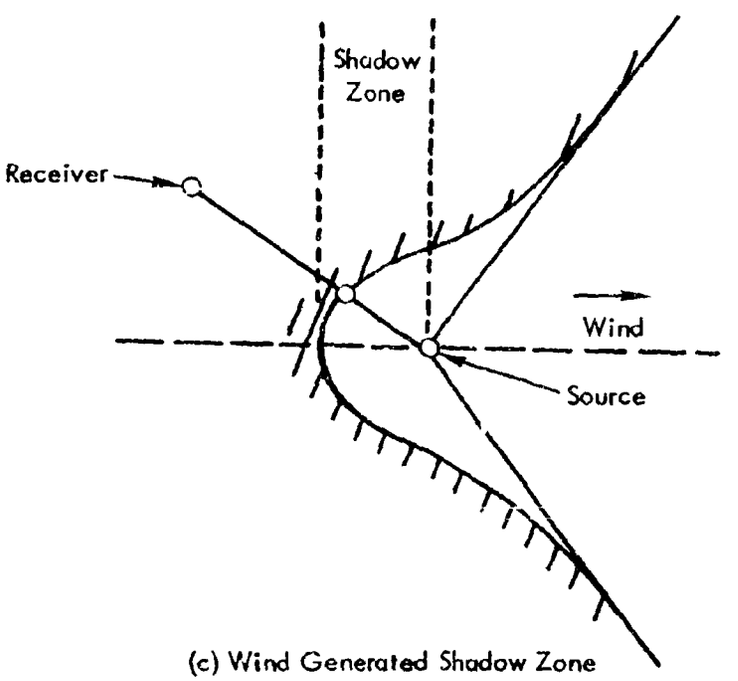

(c) Wind Generated Shadow Zone

Figure 14. Effects of Refraction on Sound Propagation.

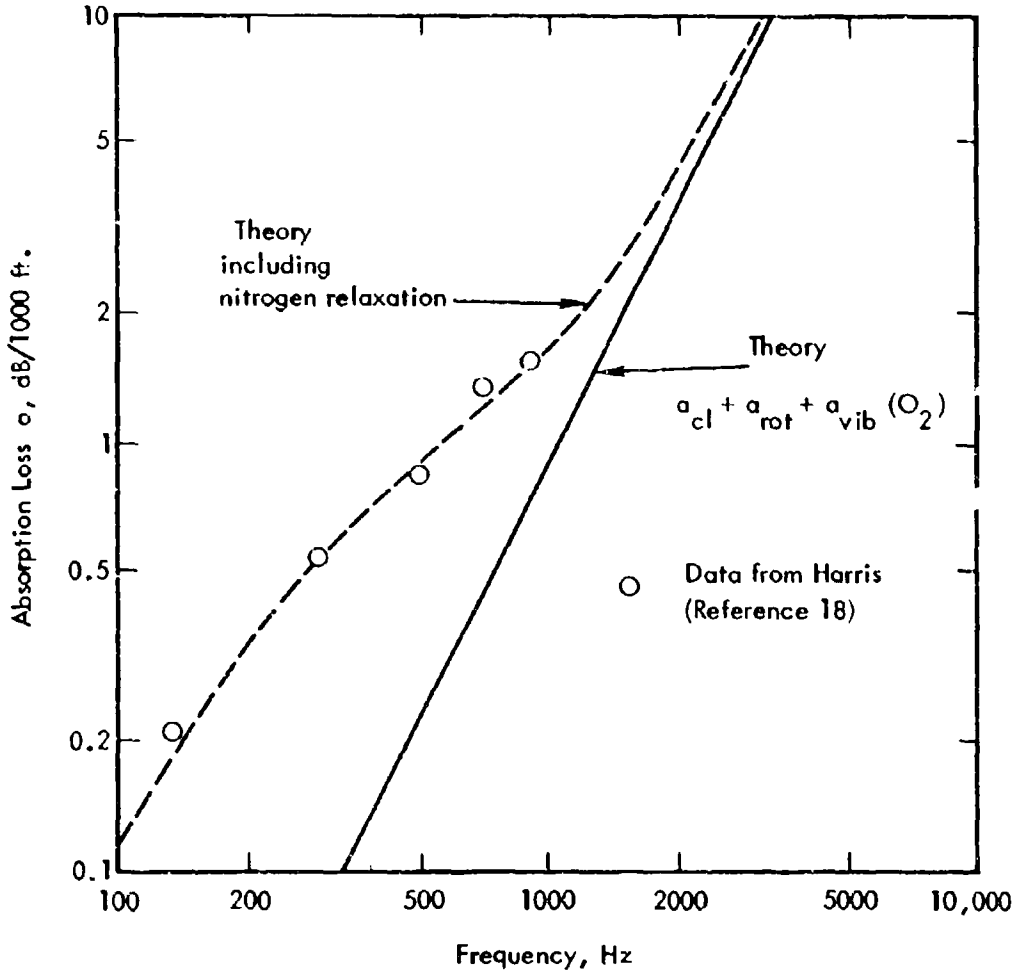

Figure 15. Comparison of Theoretical Predictions and Laboratory Measurements of Atmospheric Absorption Losses.

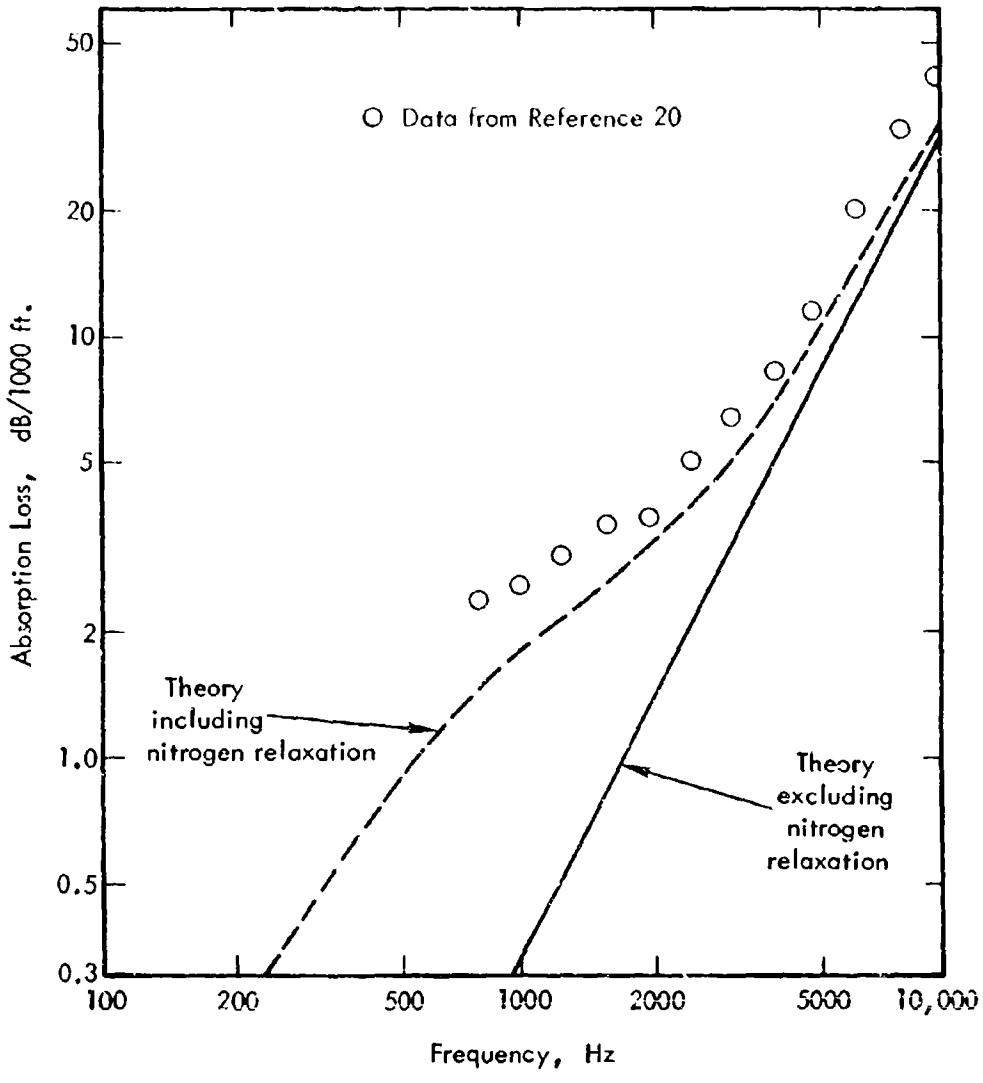

Figure 16. Comparison of Theoretical and Measured Values of Atmospheric Absorption Losses in the Field.

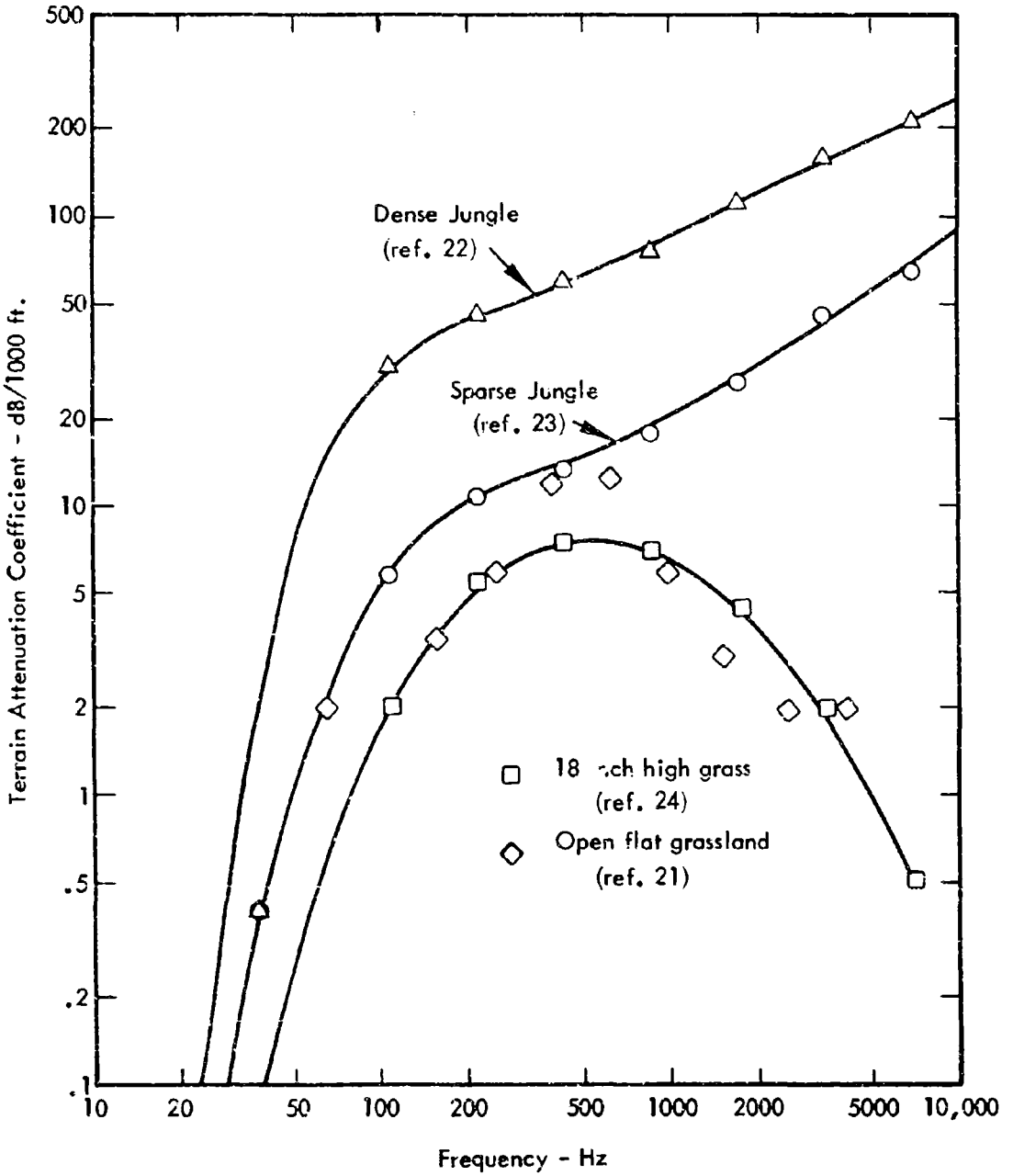

Figure 17. Absorption of Sound by Ground Cover.

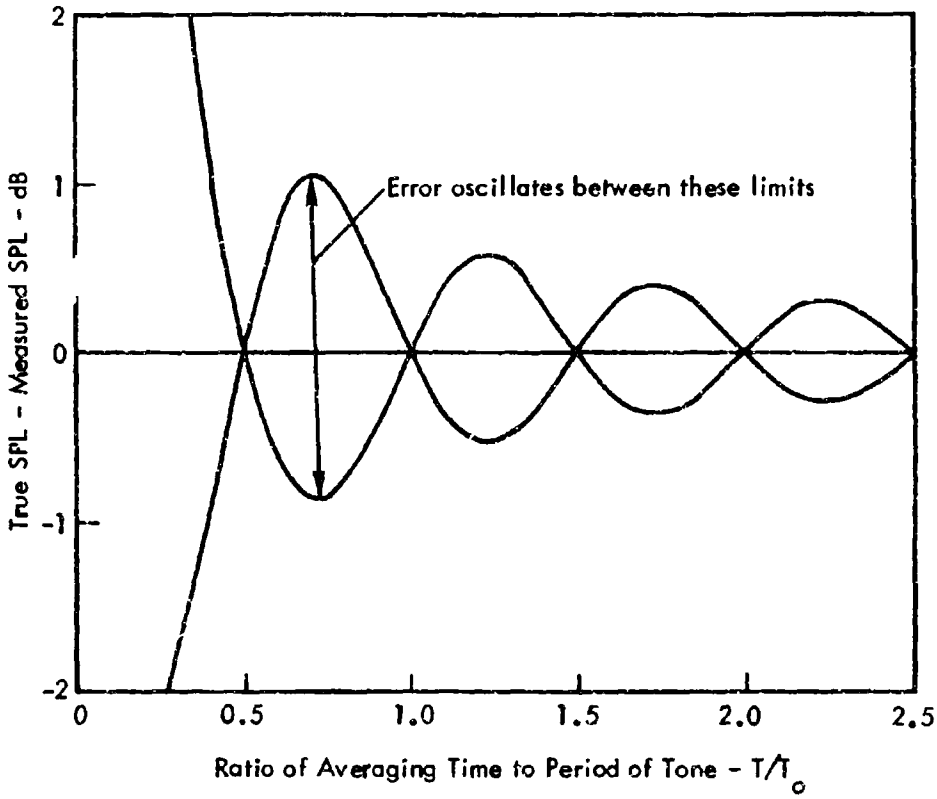

Figure 18. Error in Measured Pure-Tone Sound Pressure Level as a Function of Averaging Time.

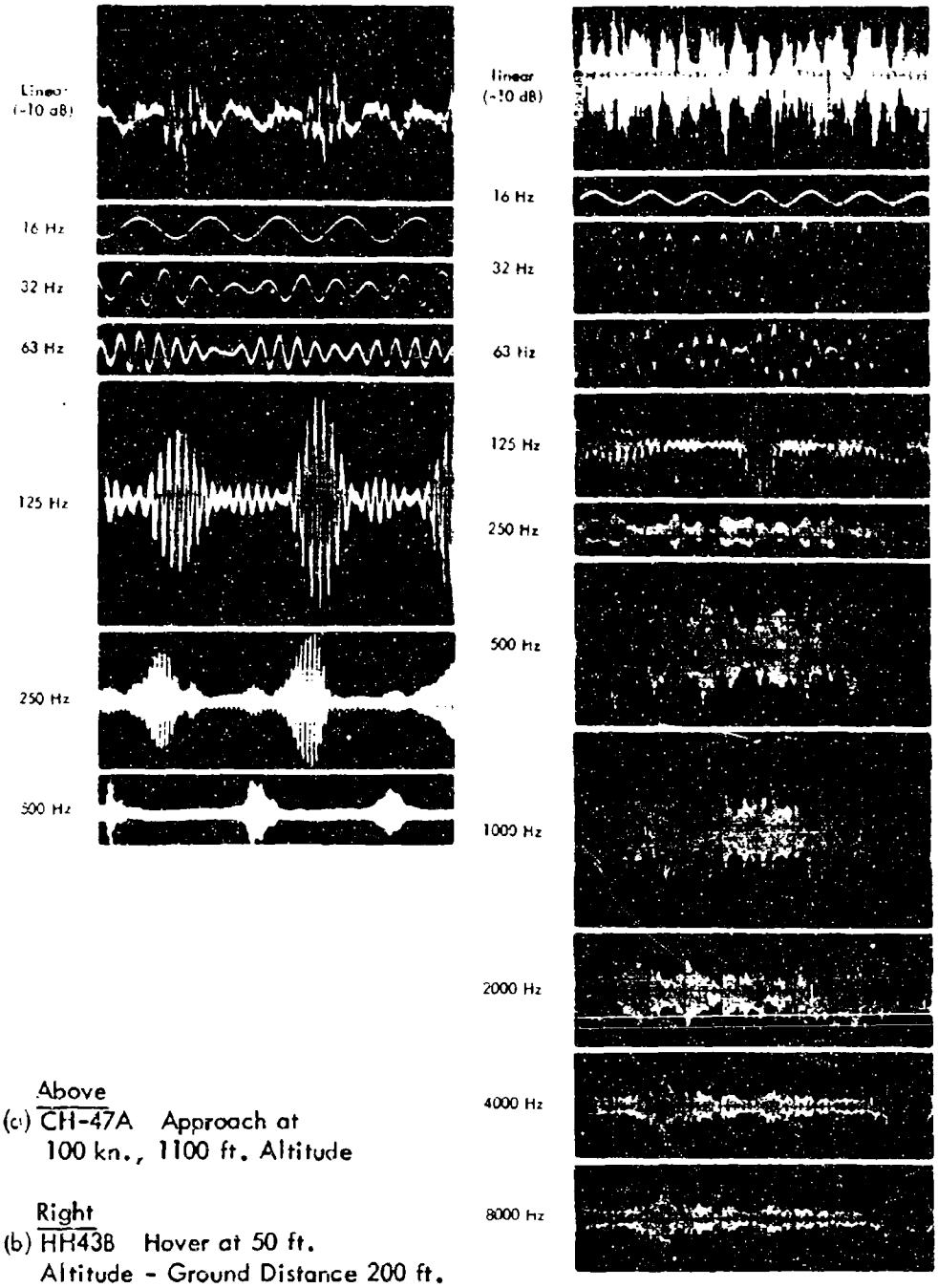

Above
(a) CH-47A Approach at
100 kn., 1100 ft. Altitude

Right
(b) HH43B Hover at 50 ft.
Altitude - Ground Distance 200 ft.

Figure 19. Waveforms of 1/3-Octave Band Filtered Helicopter Noise.

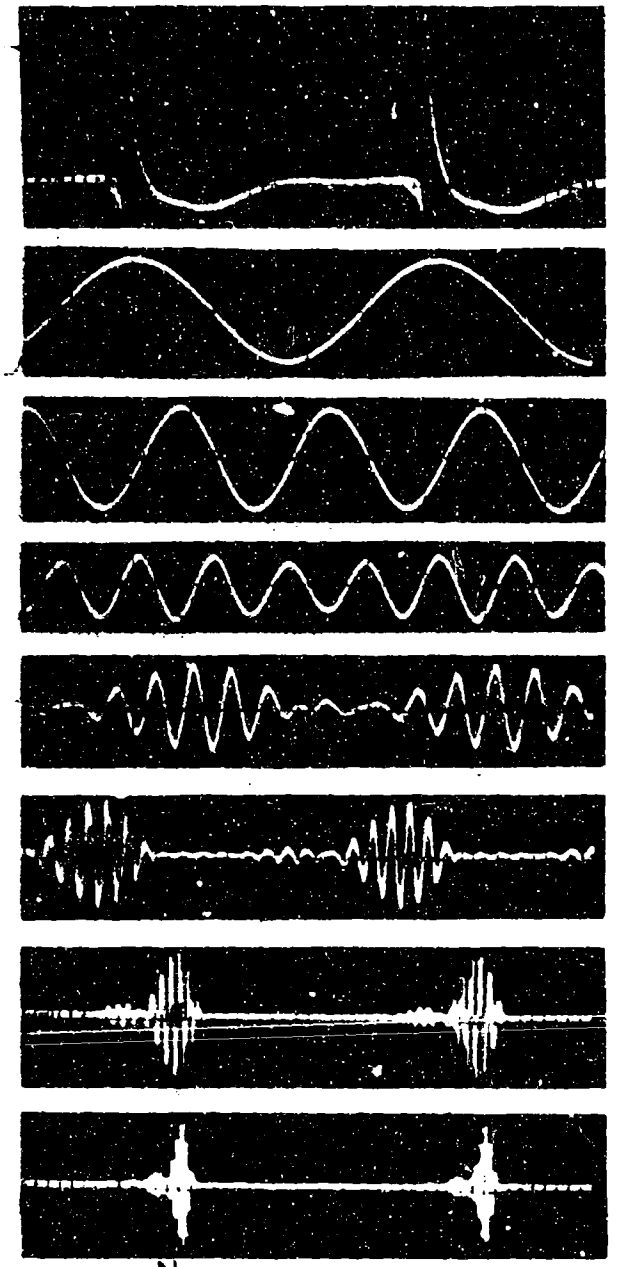

$$p = p_o \sum_{n=1}^{N} (\cos 2\pi f_o n t)/\sqrt{n} \quad ; \quad f_o = 20 \text{ Hz}$$

Figure 20. Waveforms of 1/3-Octave Filtered Harmonic Noise.

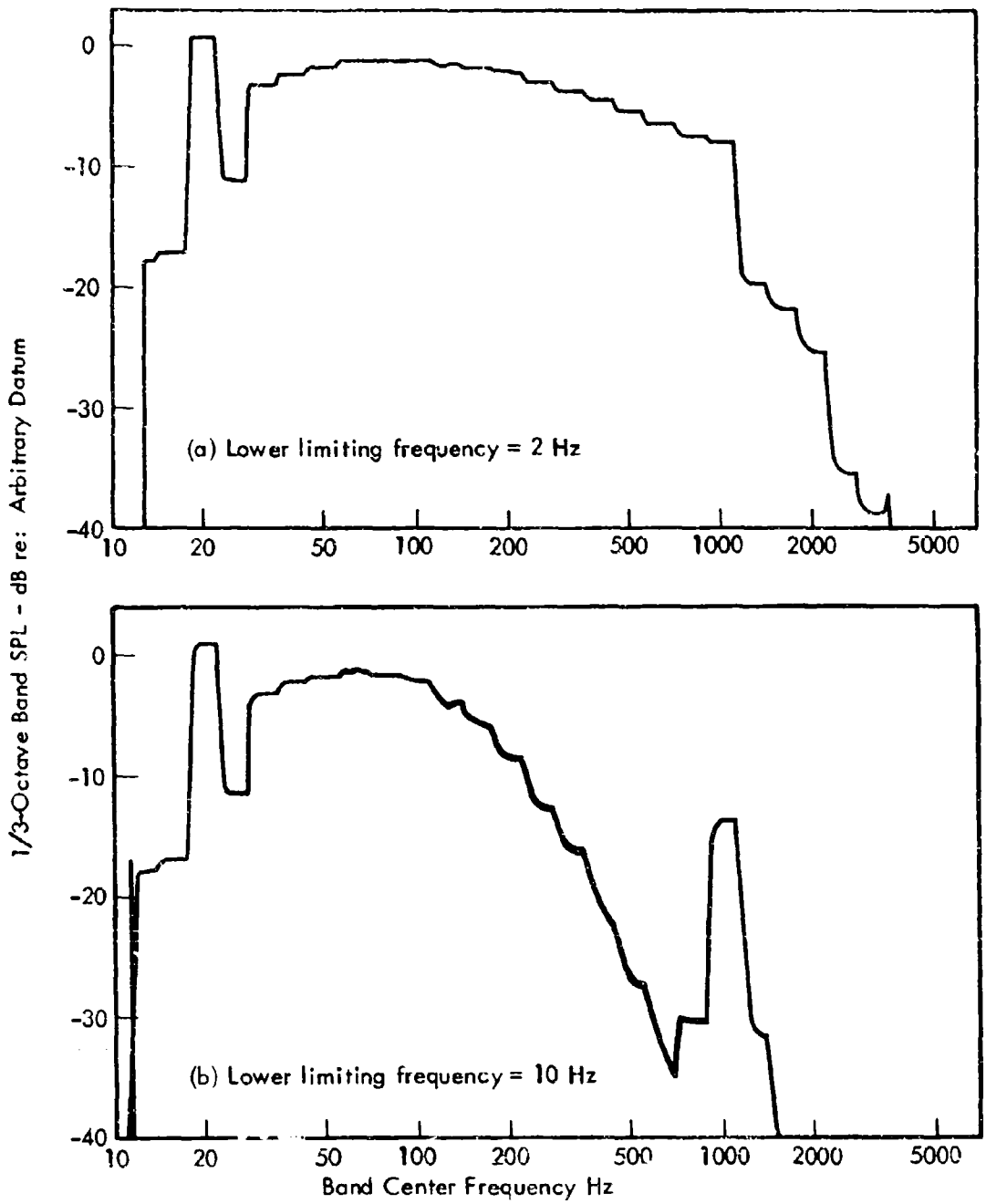

Figure 21. Effect of Averaging Time on 1/3-Octave Analysis of Harmonic Signal Containing 100 Harmonics, f_o = 20 Hz, decay = 3 dB per octave.

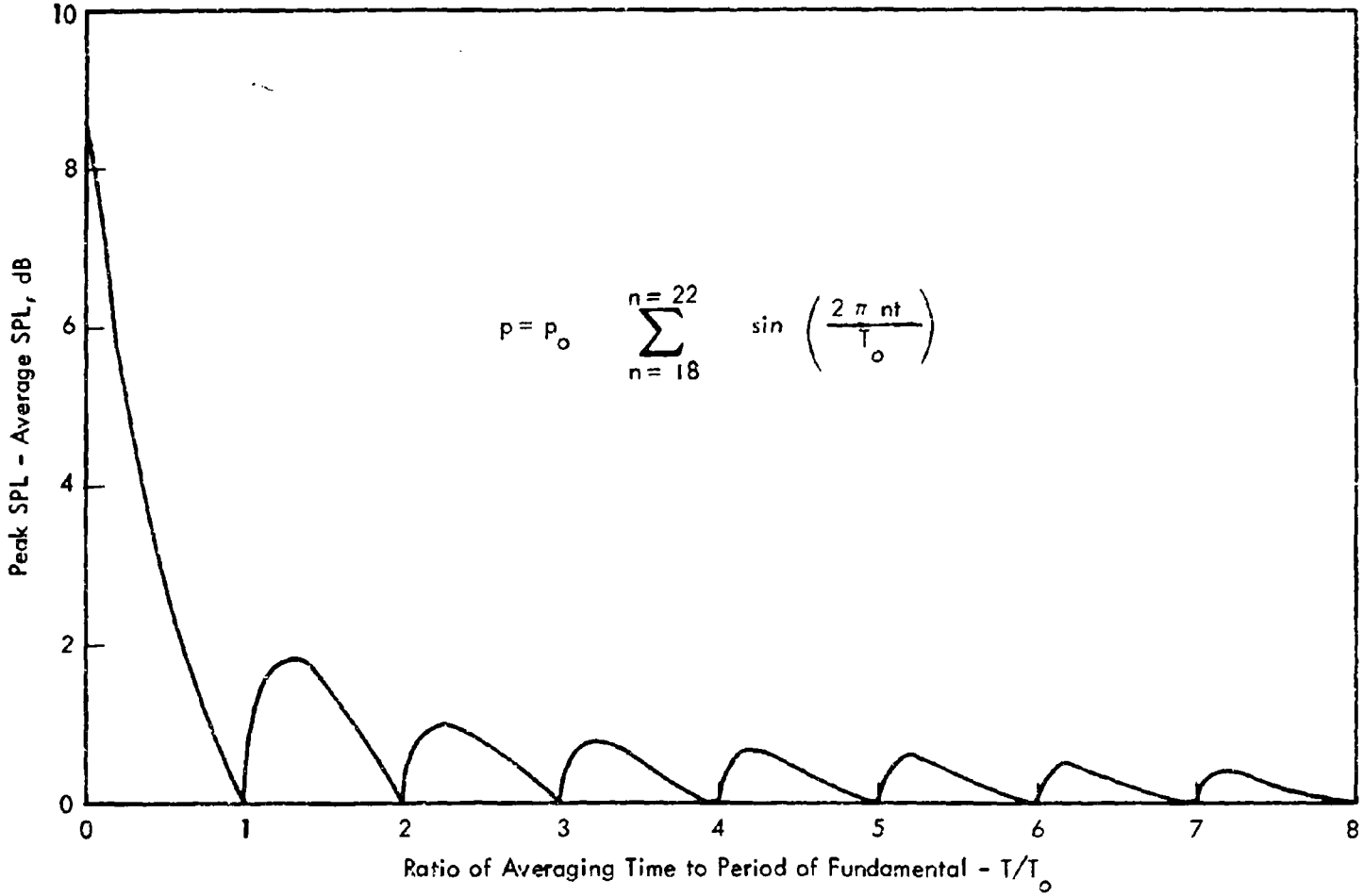

Figure 22. Peak Fluctuations in Measured SPL of Filtered Harmonic Noise as a Function of Averaging Time (1/3-Octave Centered on 20-th Harmonic).

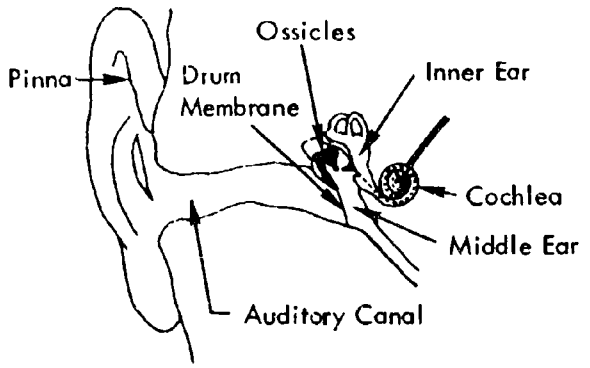

(a) Sketch of Hearing Mechanism

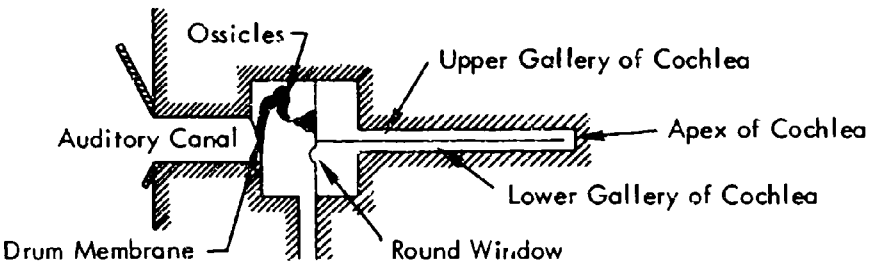

(b) Schematic Diagram of Hearing Mechanism

Figure 23. The Human Hearing Mechanism.

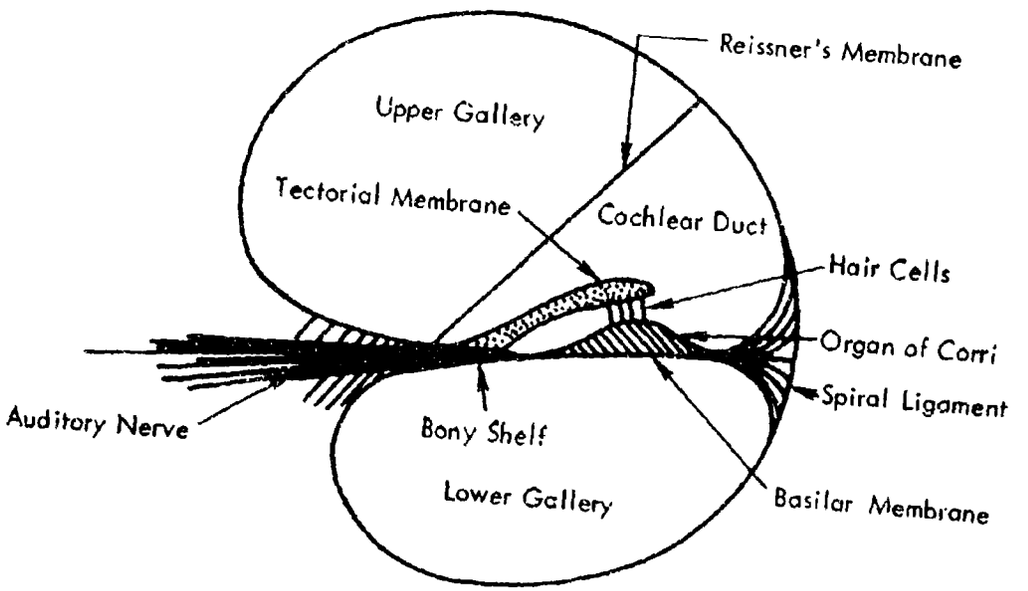

Figure 24. Cross-Section of the Cochlea.

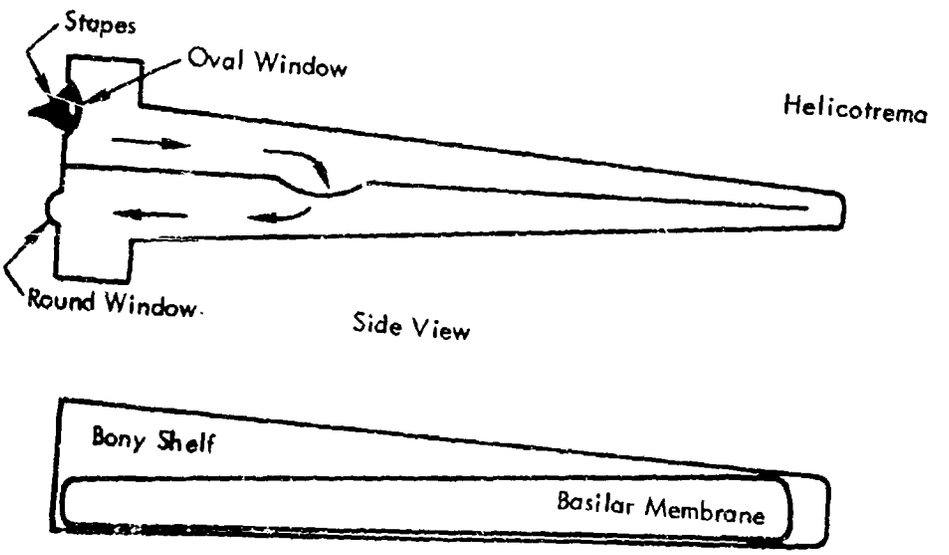

Figure 25. Diagram of Uncoiled Cochlea.

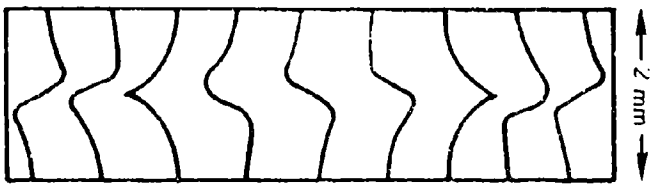

Figure 26. Deformation Patterns of the Basilar Membrane for One Cycle of a 1000-Hz Tone (at 45° Intervals).

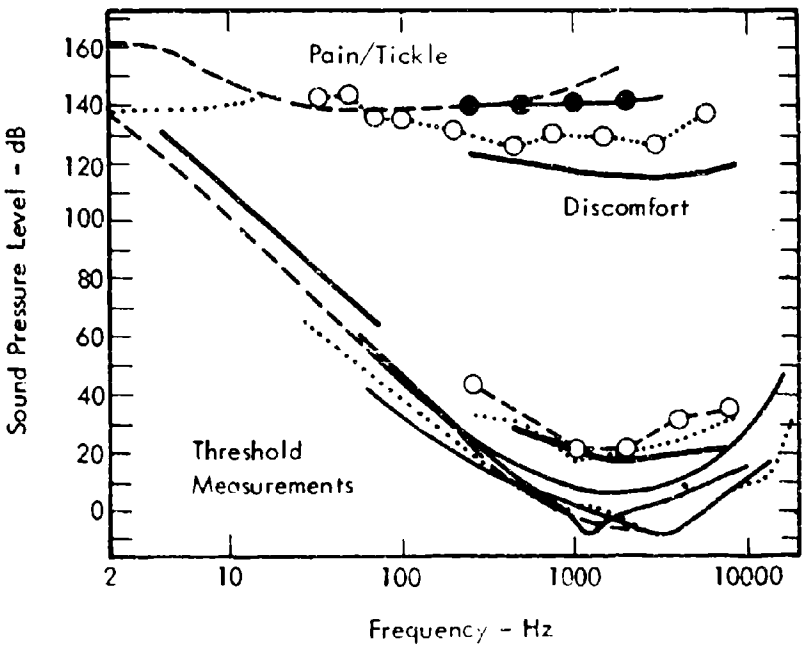

Figure 27. Various Determinations of the Threshold of Audibility and the Threshold of Feeling.

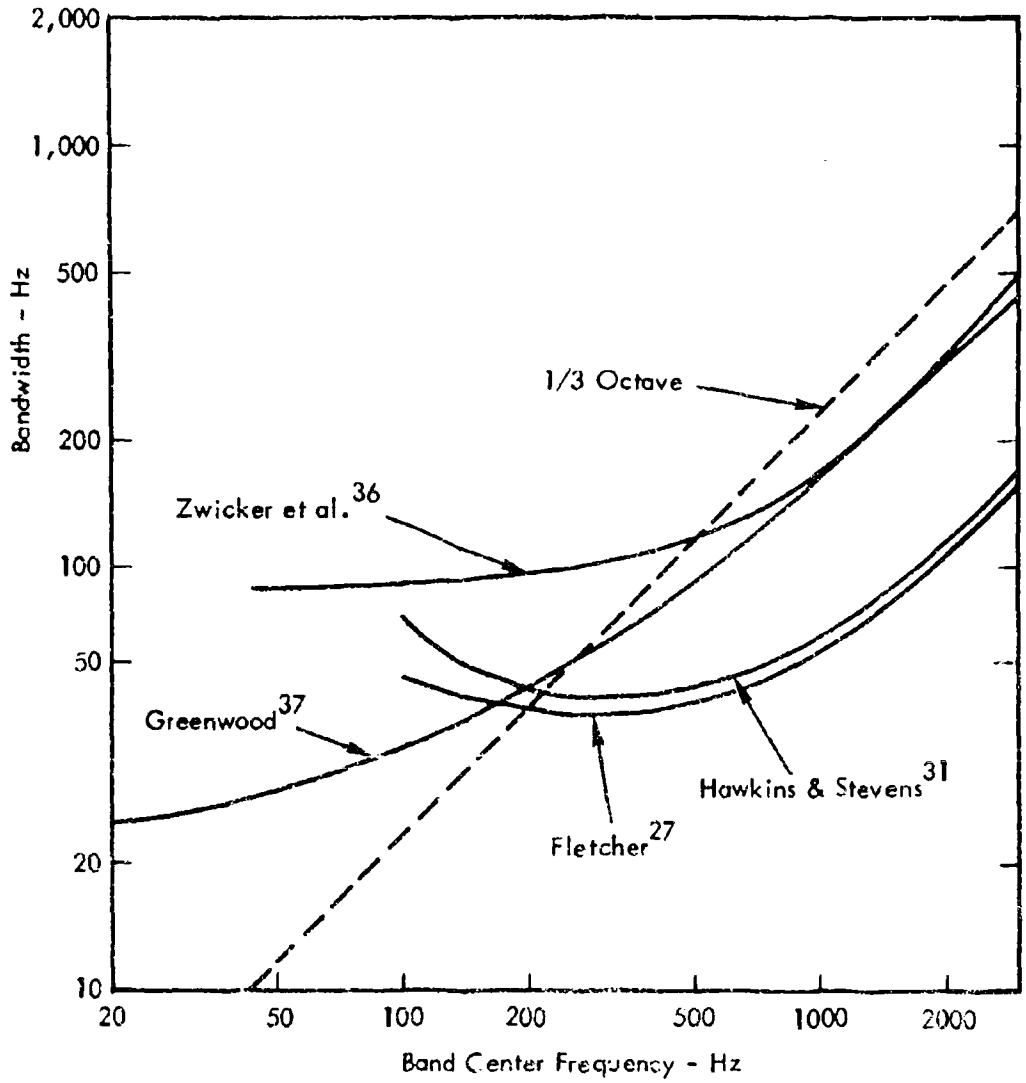

Figure 28. Comparison of Various Critical Bandwidth Measurements.

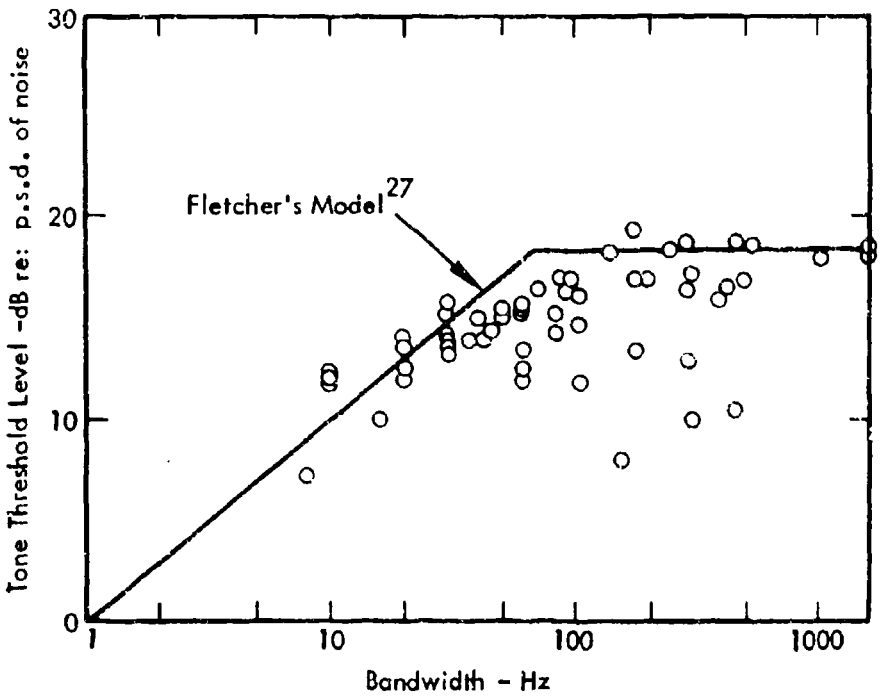

Figure 29. Typical Experimental Data on the Width of the Critical Band (from Reference 40).

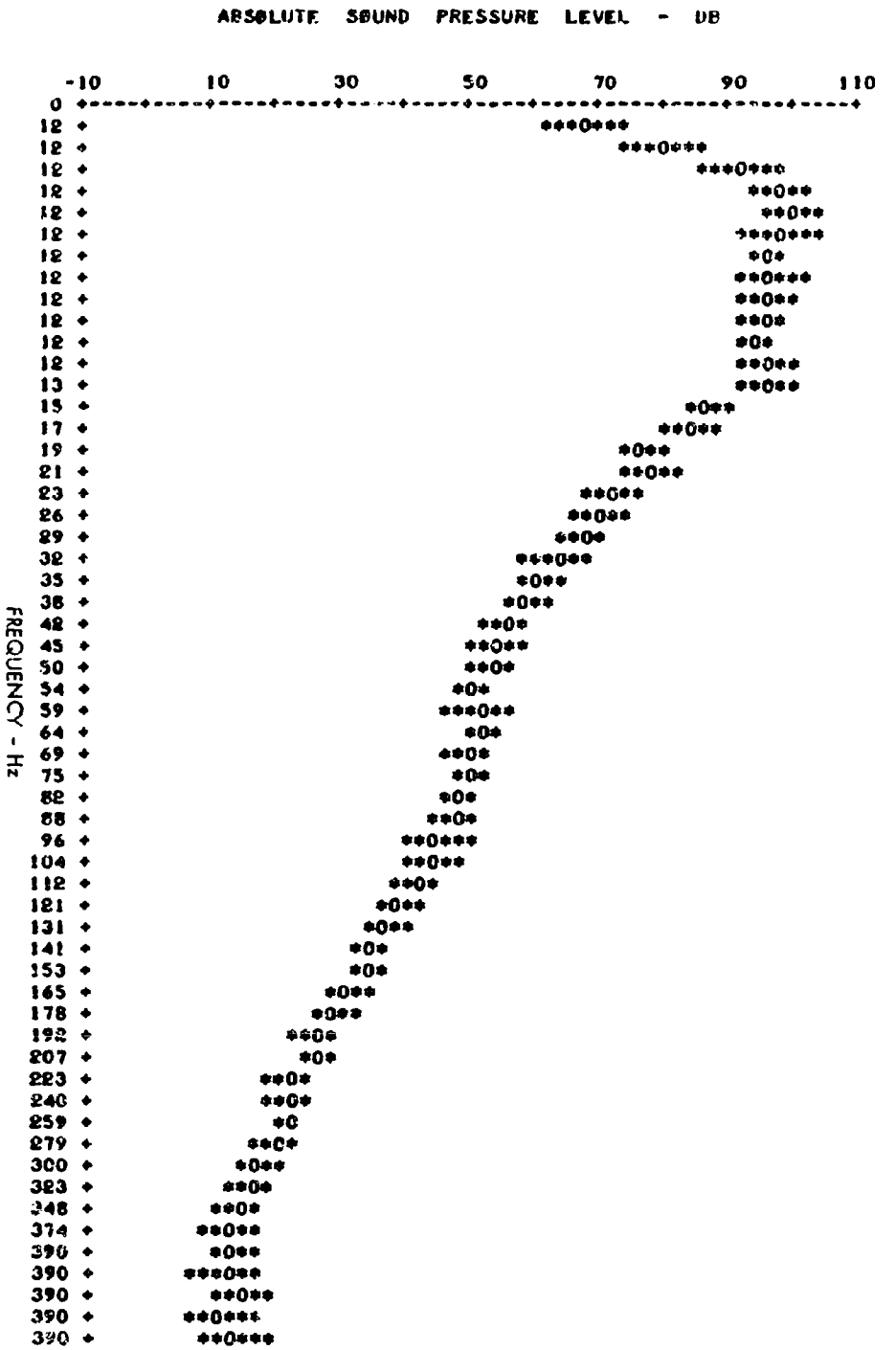

Figure 30. Example of Computer Analysis Plot.

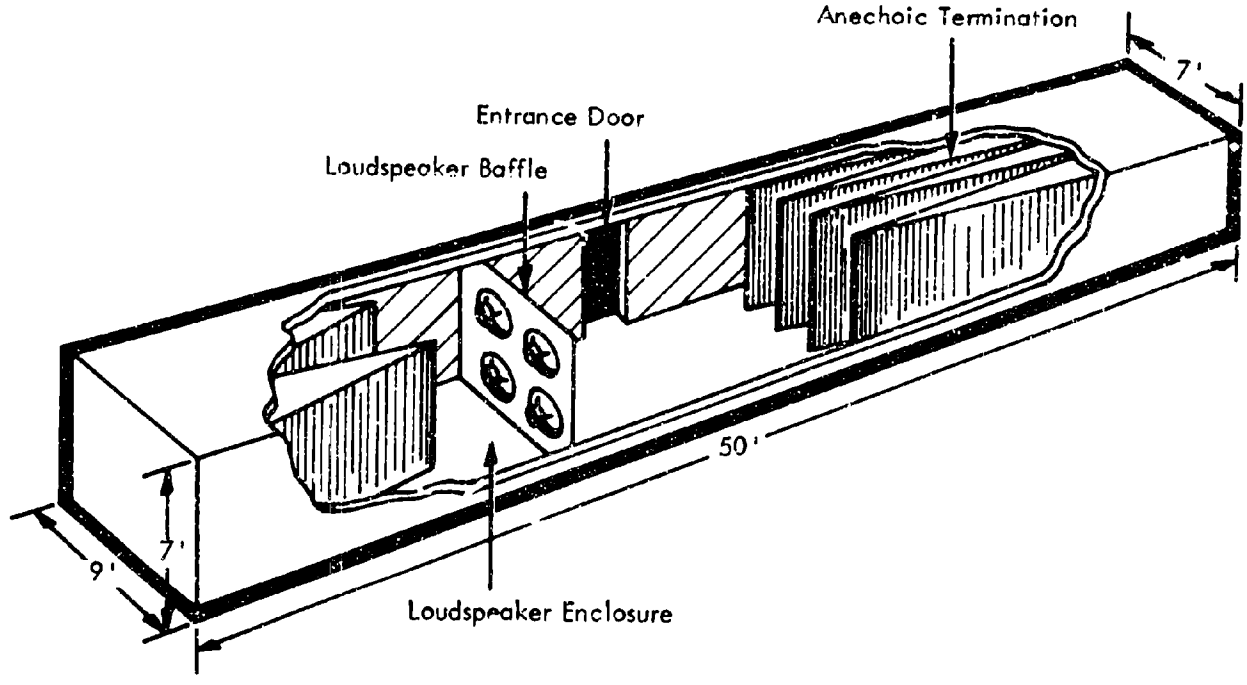

Figure 31. Progressive Wave Acoustic Chamber.

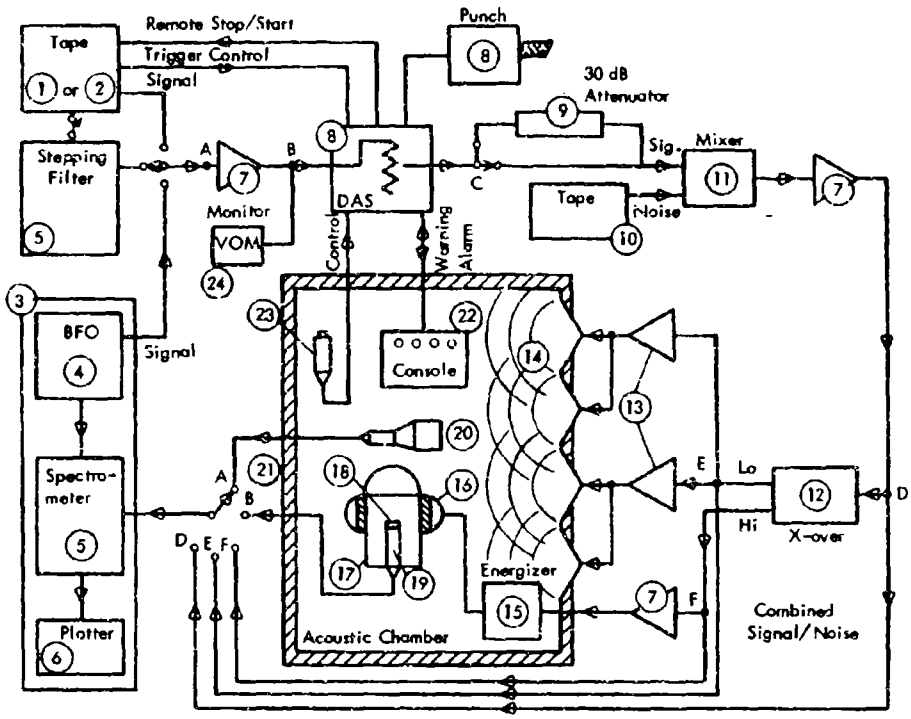

Item	Manufacturer/Model Number/Description
1.	Ampex AG 500, 2-track, ¼-inch Direct Record Tape Recorder/Reproducer
2.	Precision Instruments PS 207, 7-track, ½-inch FM Tape Recorder/Reproducer
3.	B&K 3332 Automatic Frequency Response/Spectrum Recorder (Couples 4, 5 & 6)
4.	B&K 1022 Beat Frequency Oscillator
5.	B&K 2172 Audio Frequency Spectrometer
6.	B&K 2305 Graphic Level Recorder
7.	Crown D-49 Solid State 20W Power Amplifier
8.	Wyle Automatic Control and Data Acquisition System
9.	Wyle 30 dB Attenuator
10.	Sony TC 770/2, 2-track, ¼-inch Direct Record Tape Recorder/Reproducer
11.	Wyle Signal Mixer
12.	Wyle 65 Hz Crossover Network
13.	Crown DC-300 Solid State 150W Power Amplifier
14.	Electrovoice W30 Low Frequency Loudspeaker
15.	Koss E-9 Headphone Energizer
16.	Koss ESP-9 Electrostatic Headphones
17.	Koss/B&K 6cc Earphone Calibration Coup'es
18.	B&K 4134 ½-inch Pressure Response Condenser Microphone
19.	B&K 2619 FET Preamplifier
20.	B&K 4145 1-inch Free-Field Condenser Microphone
21.	B&K AO 0029 100 ft. Extension Cable
22.	Wyle - Subject's Monitor Console
23.	Wyle - Hand-held Pushbutton
24.	Simpson Model 260 Volt/Ohm Meter

Figure 32. Detection Experiments - Test Instrumentation.

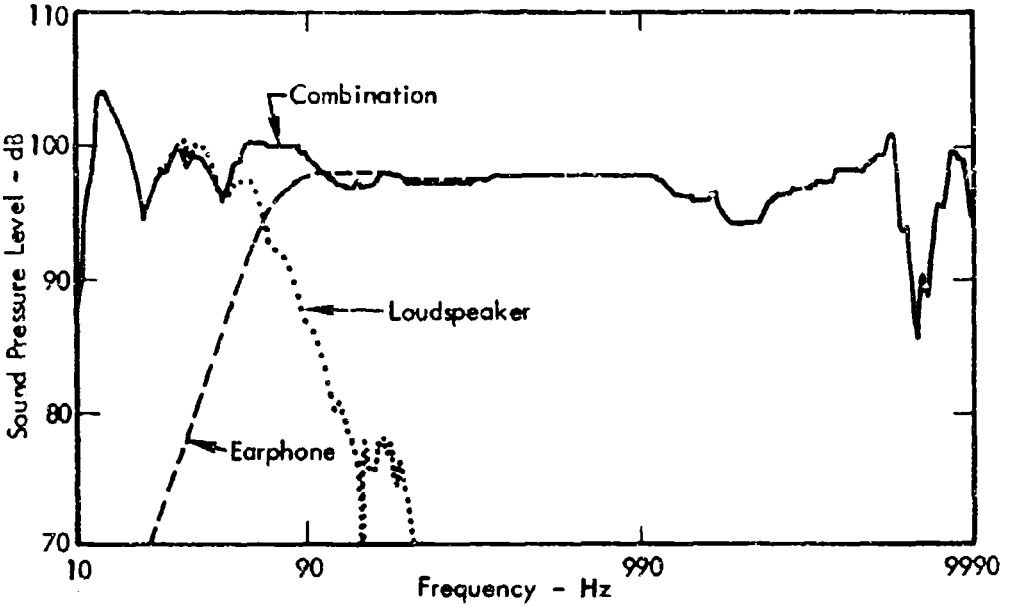

(a) Left Earphone - Showing Loudspeaker and Earphone Contribution

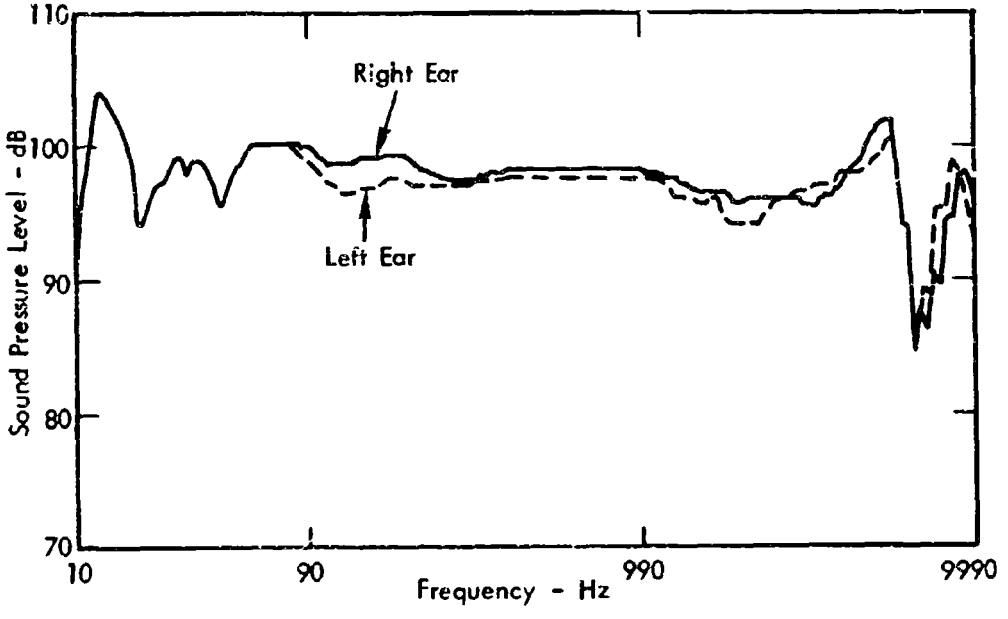

(b) Left and Right Ears

Figure 33. System Frequency Response to Sinusoidal Input.

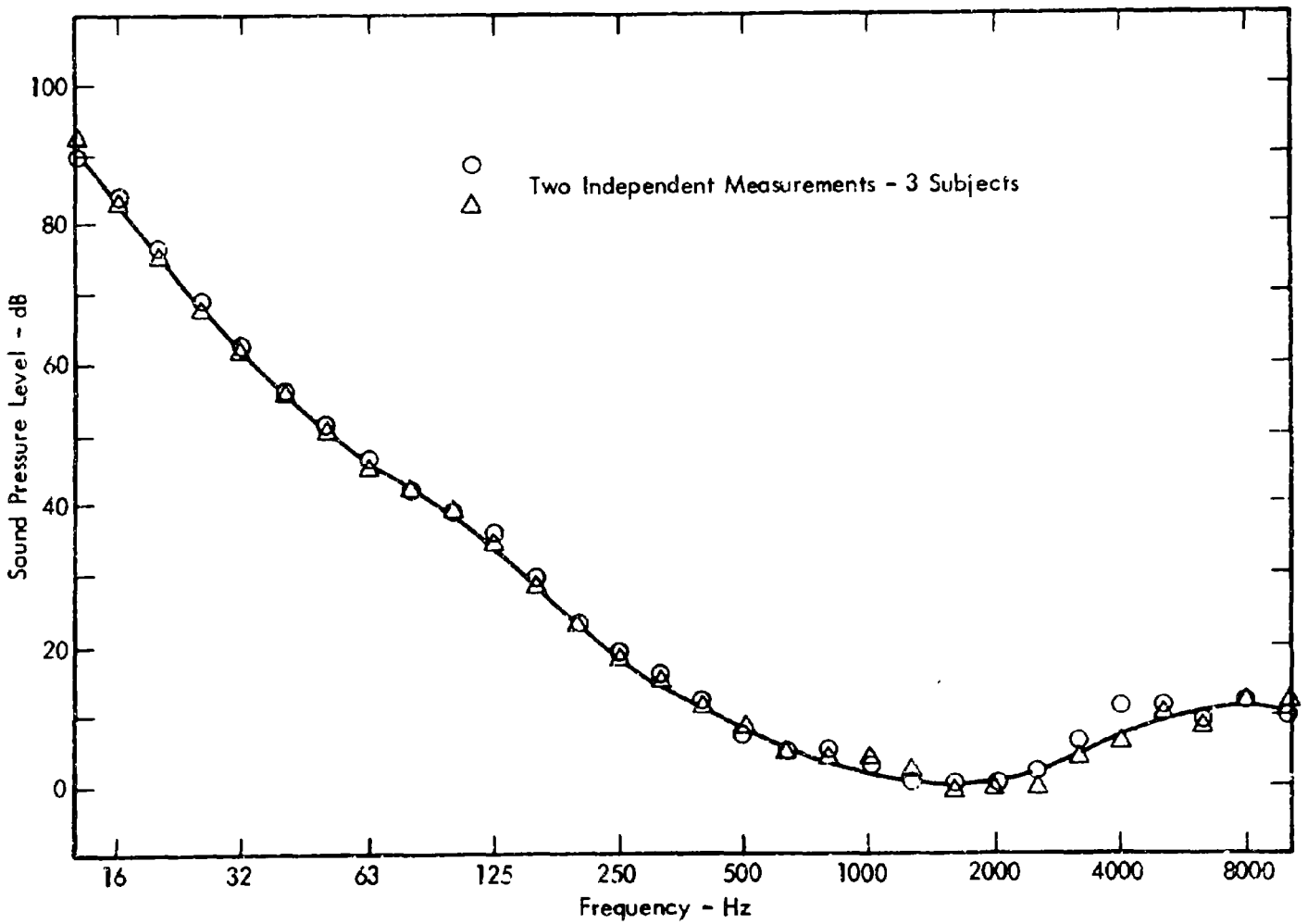

Figure 34. Absolute Audibility Threshold for Pure Tones.

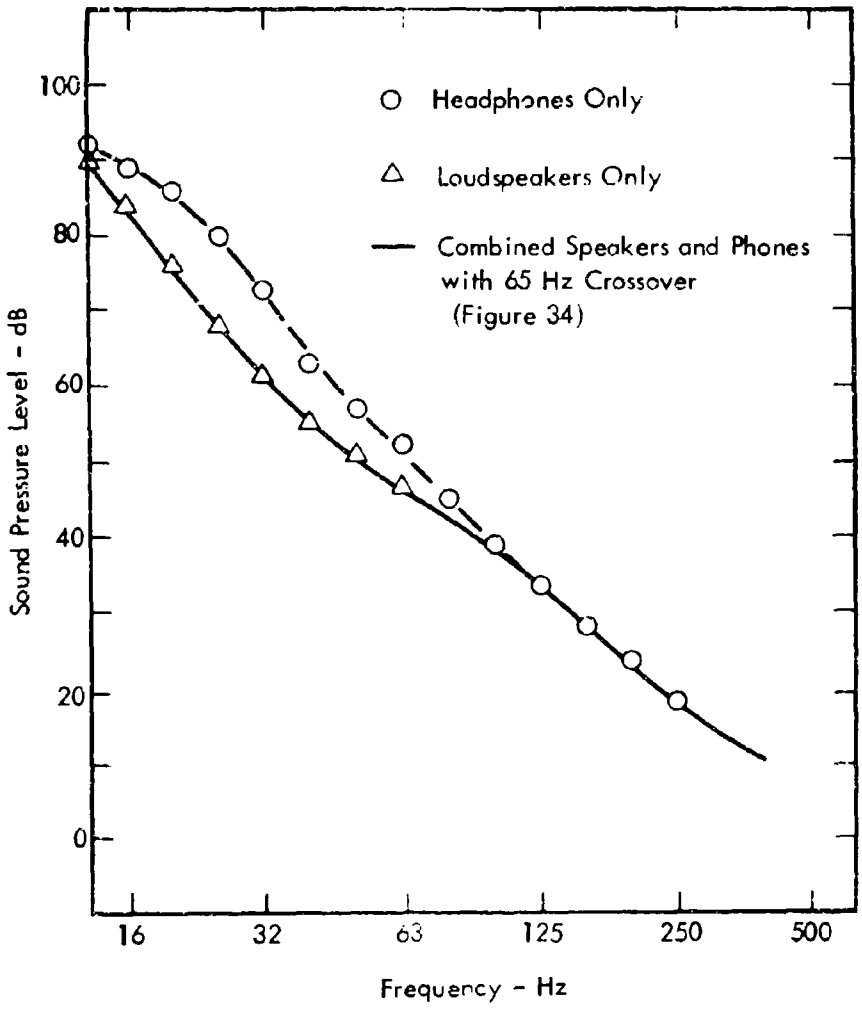

Figure 35. Comparison of Apparent Thresholds for Headphone, Loudspeaker, or Combined Presentation of Stimulus.

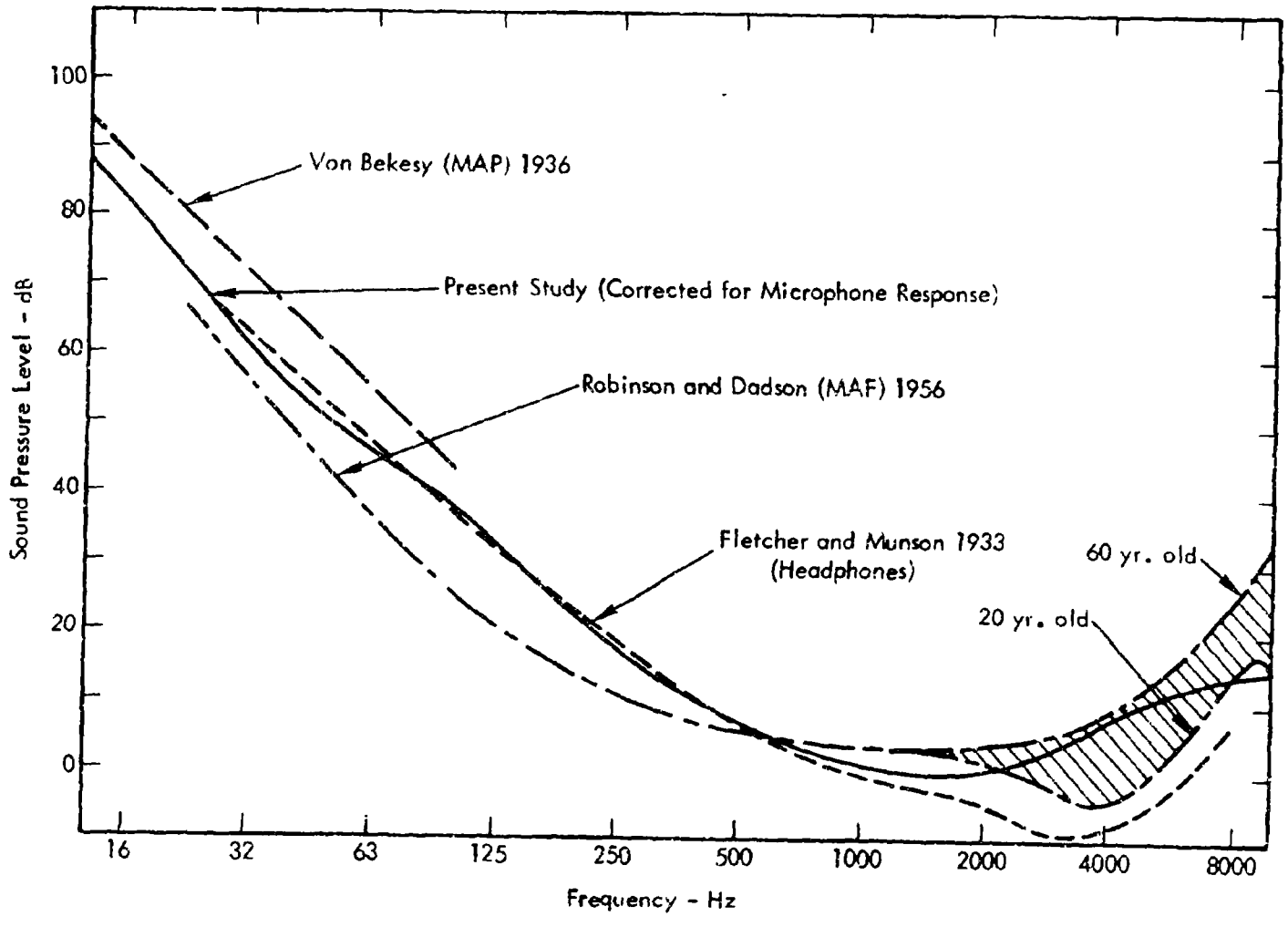

Figure 36. Comparison of Present Results with Previous Pure Tone Threshold Data.

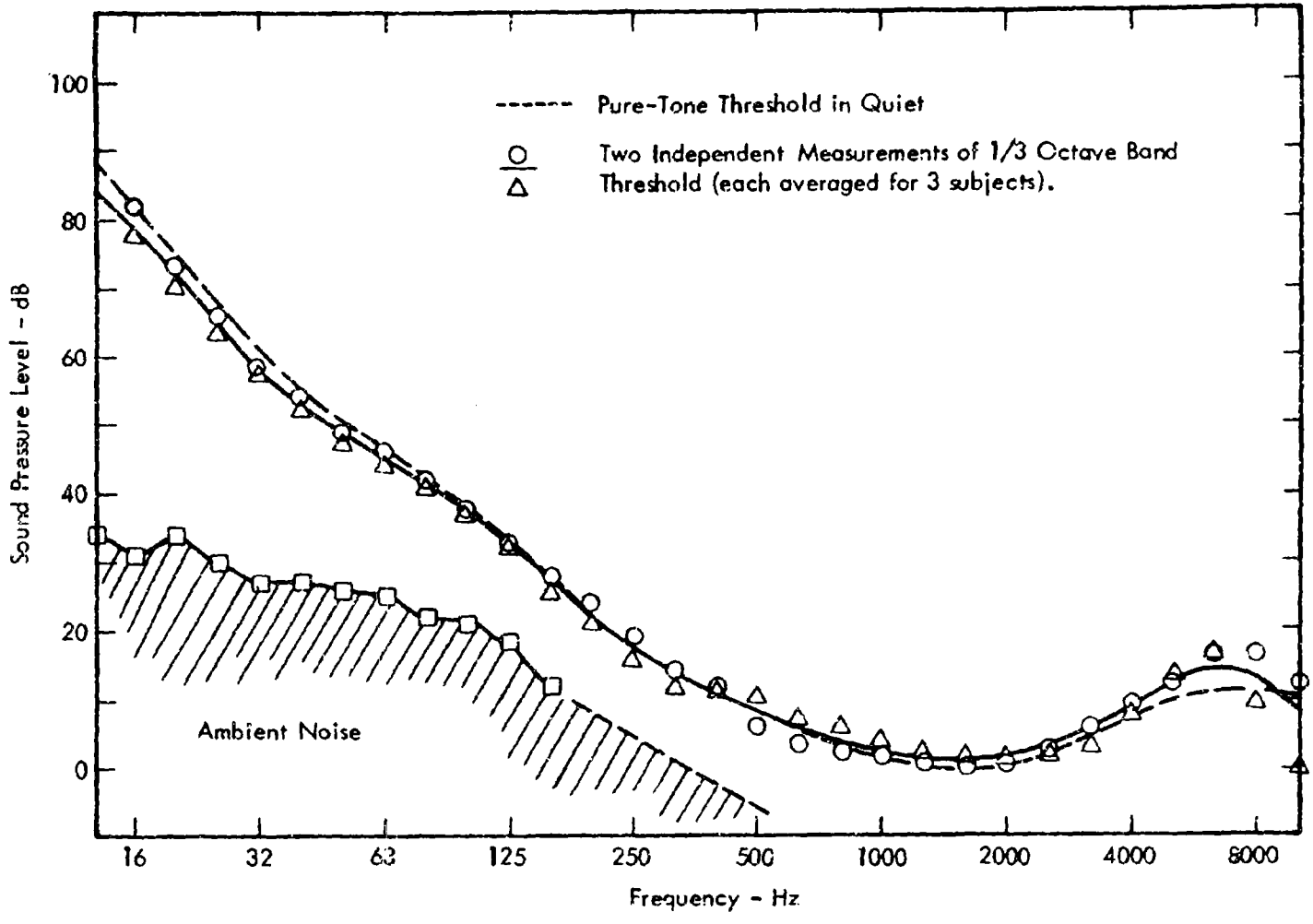

Figure 37. Audibility Threshold for 1/3-Octave Bands of Stationary Random Noise - In Quiet.

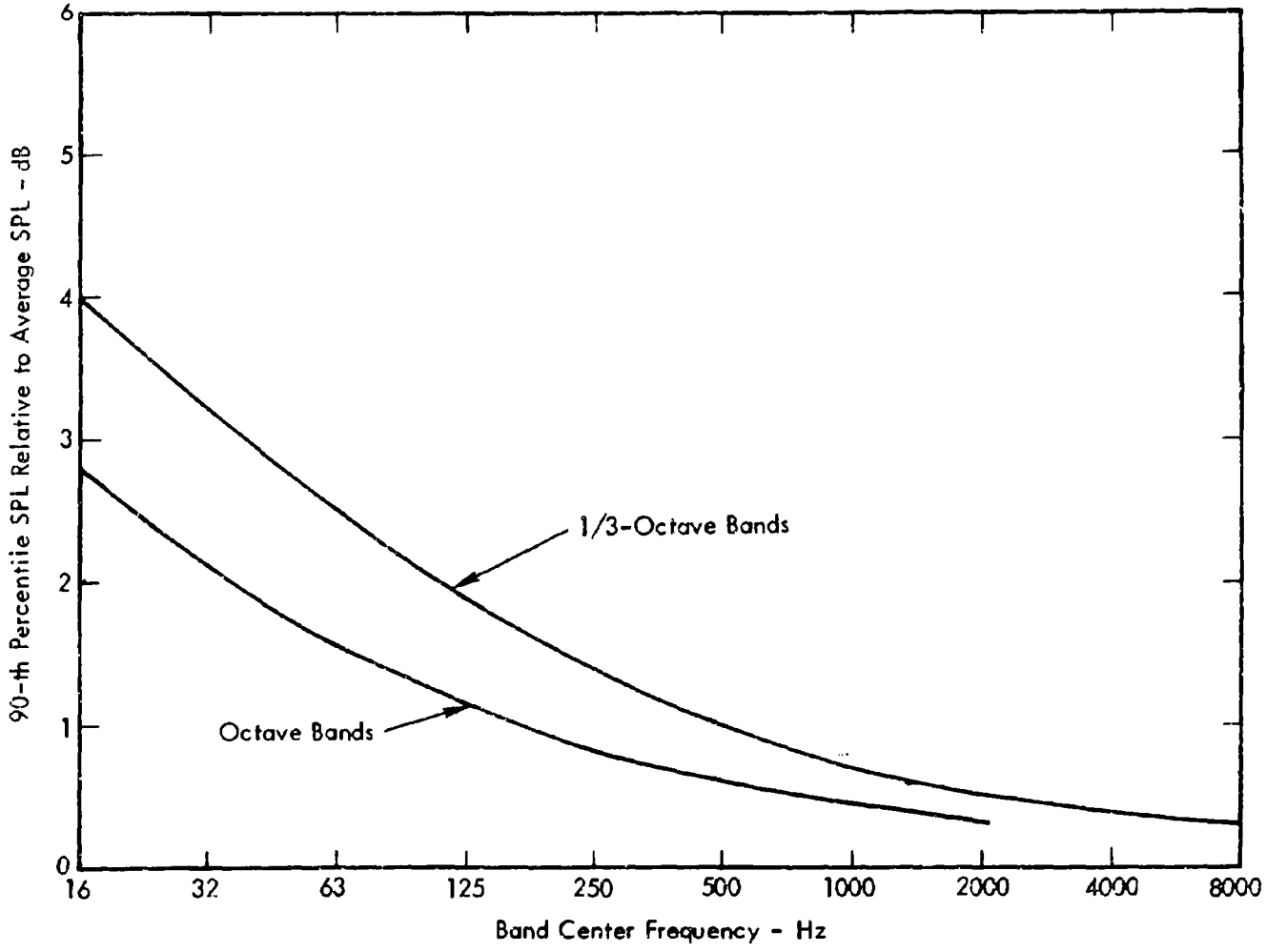

Figure 38. 90-th Percentile Levels for Bands of Random Noise with 200 msec Averaging Time.

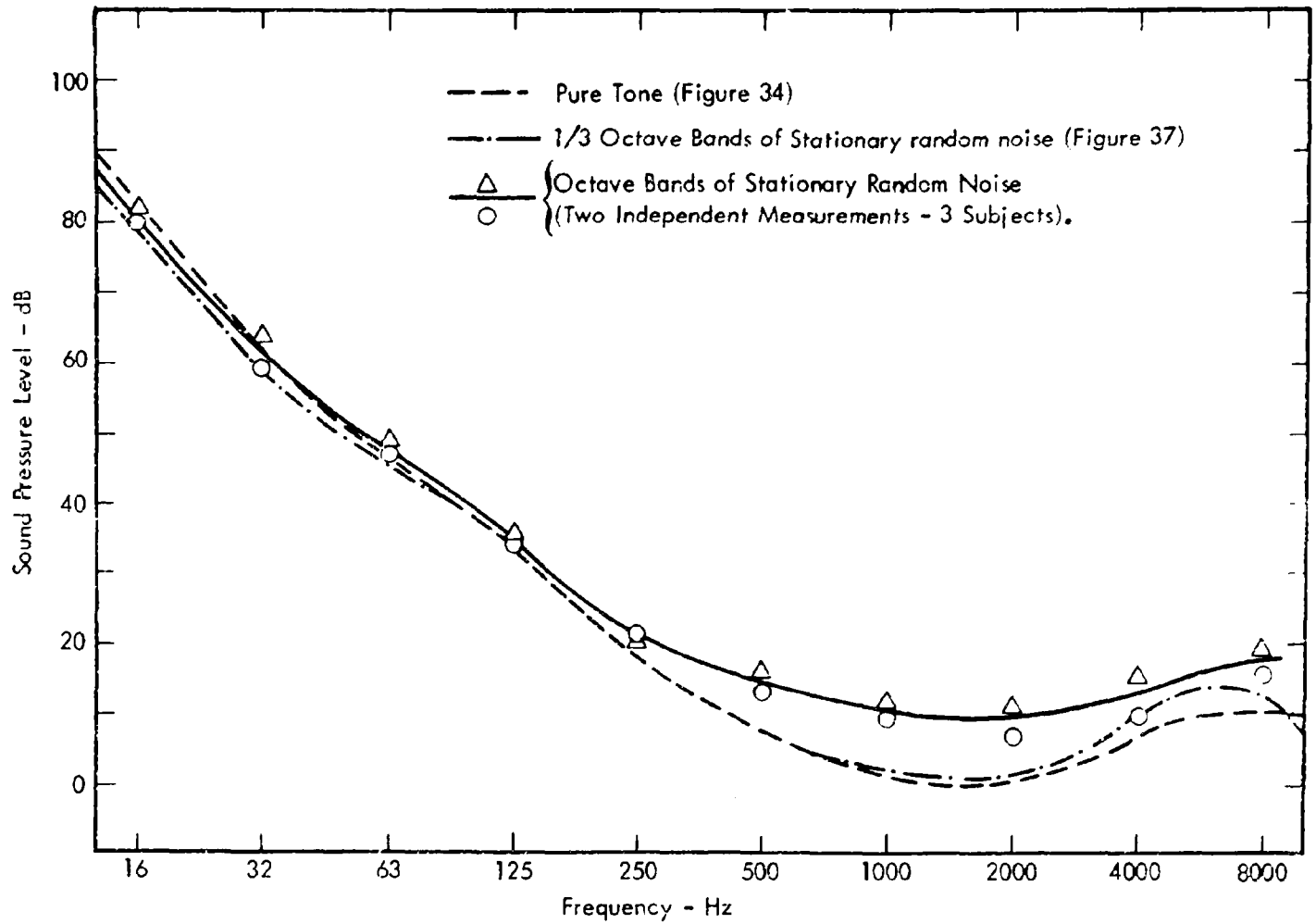

Figure 39. Audibility Thresholds in Quiet - Comparison for Tones, 1/3-Octave and Octave Bands of Stationary Noise.

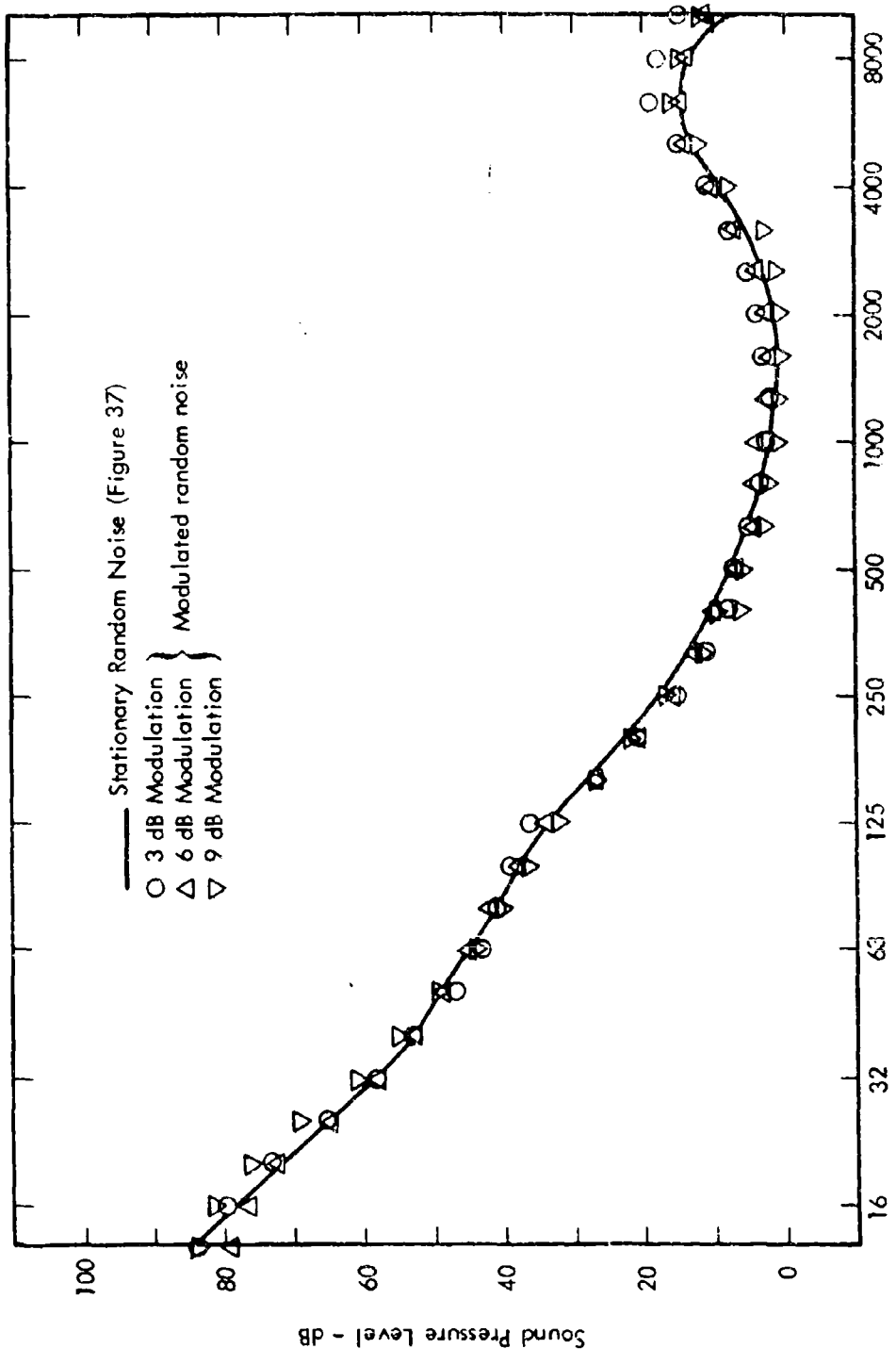

Figure 40. Audibility Thresholds for 1/3-Octave Bands of Noise - in Quiet.

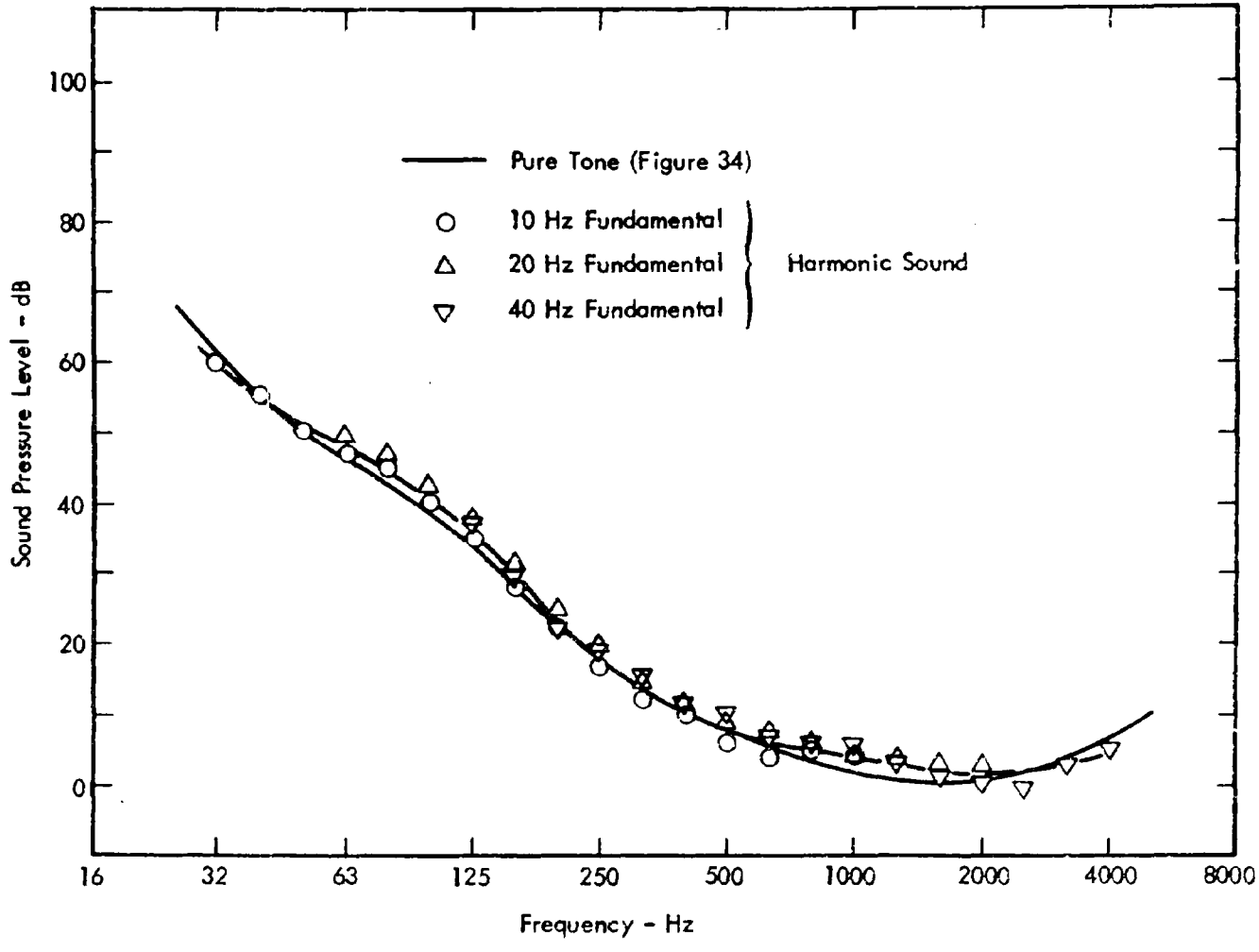

Figure 41. Absolute Audibility Thresholds for 1/3-Octave Bands of Harmonic Noise.

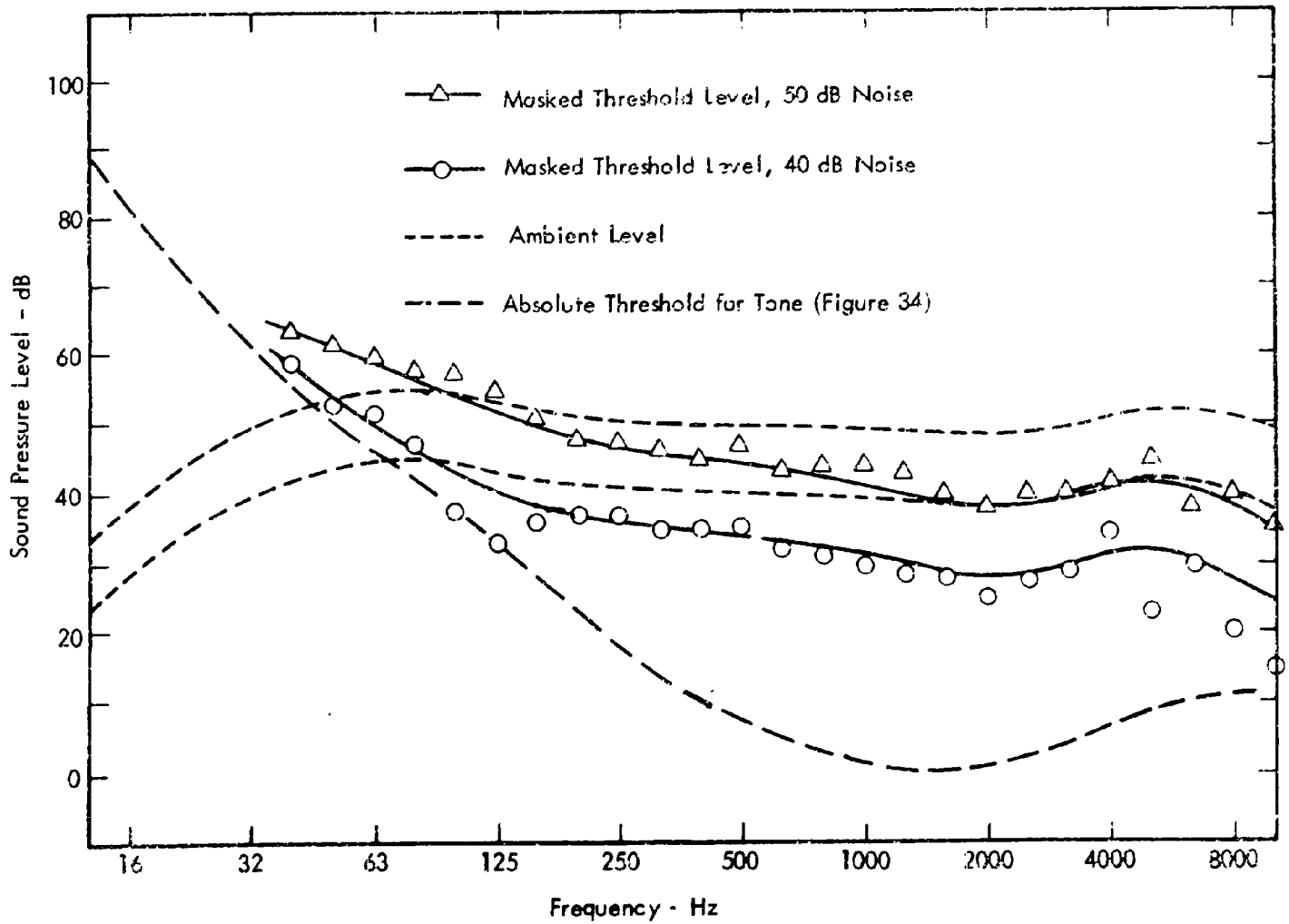

Figure 42. Masked Threshold Levels for Pure Tones.

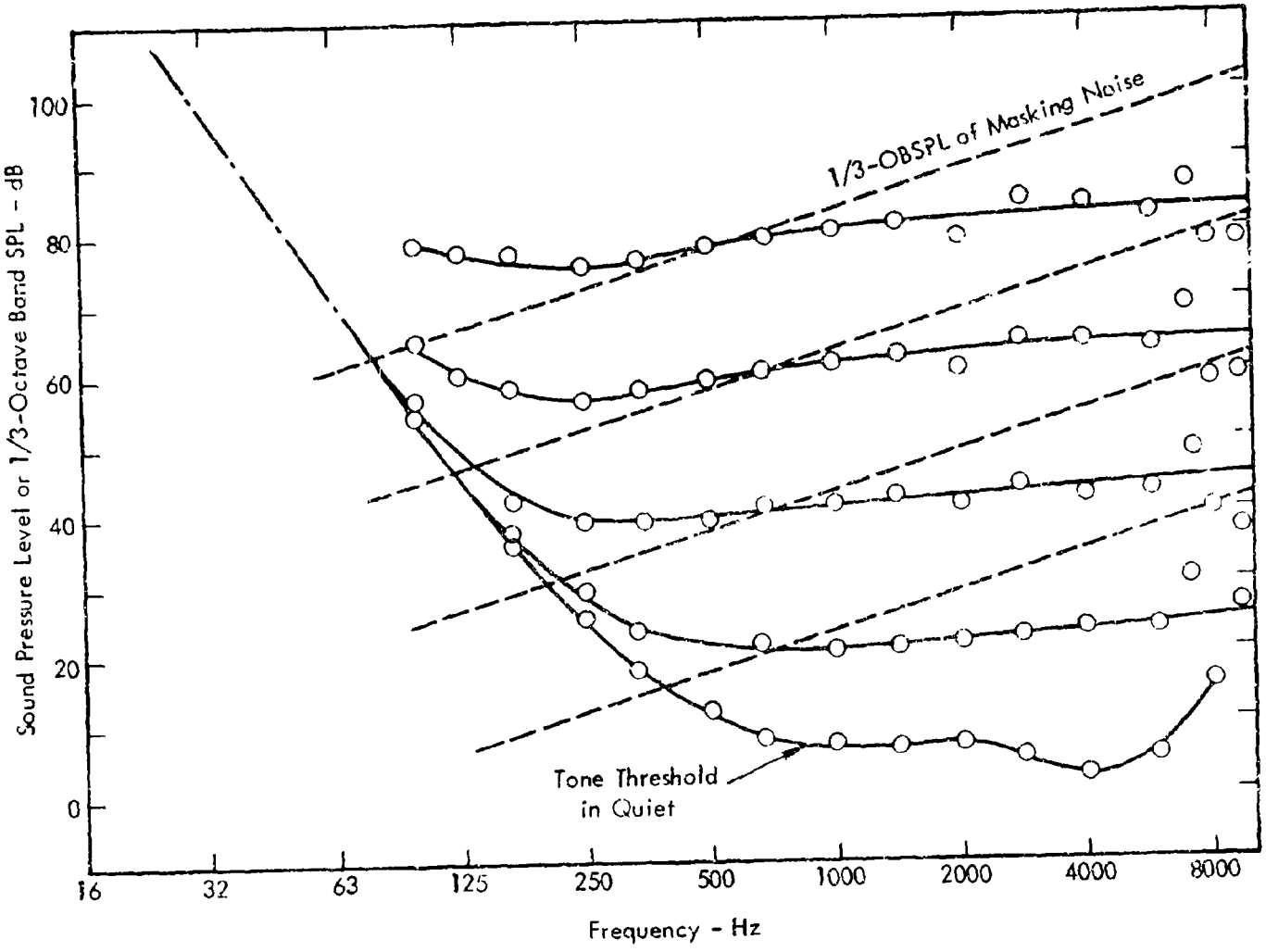

Figure 43. The Masking of Pure Tones by Wideband Noise (Data from Hawkins and Stevens[31]).

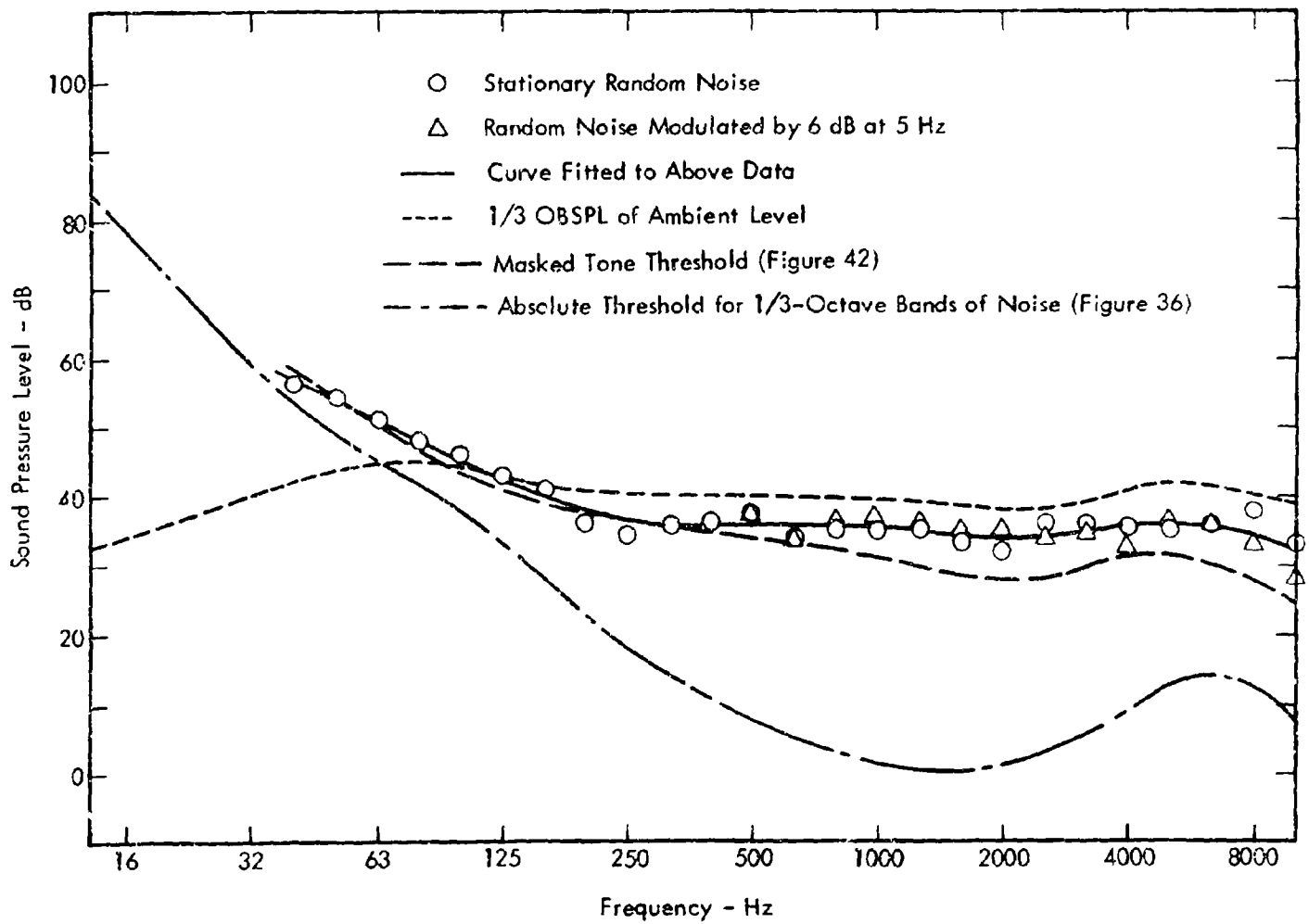

Figure 44. Masked Thresholds for 1/3-Octave Bands of Random Noise.

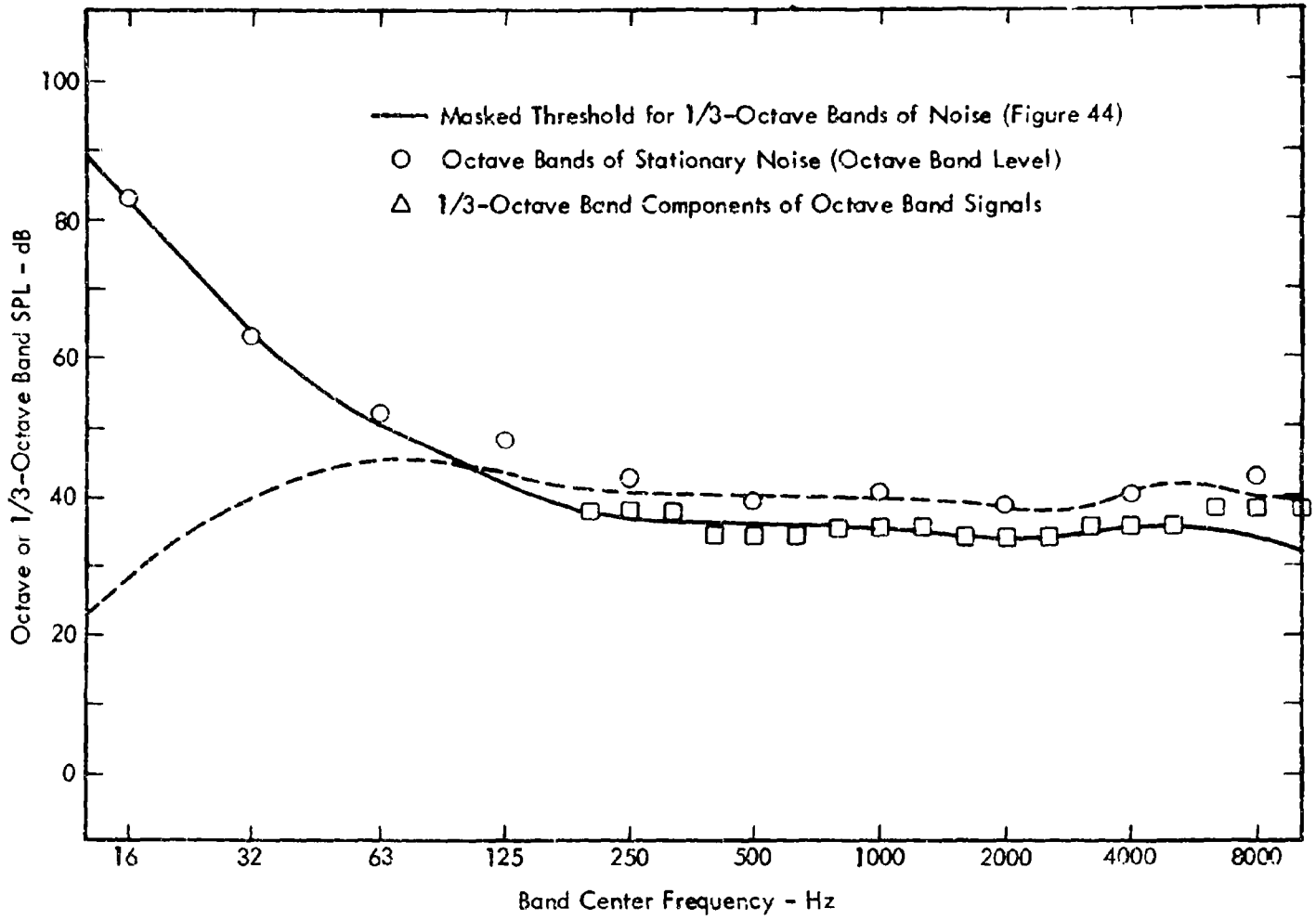

Figure 45. Masked Thresholds for Octave Bands of Noise.

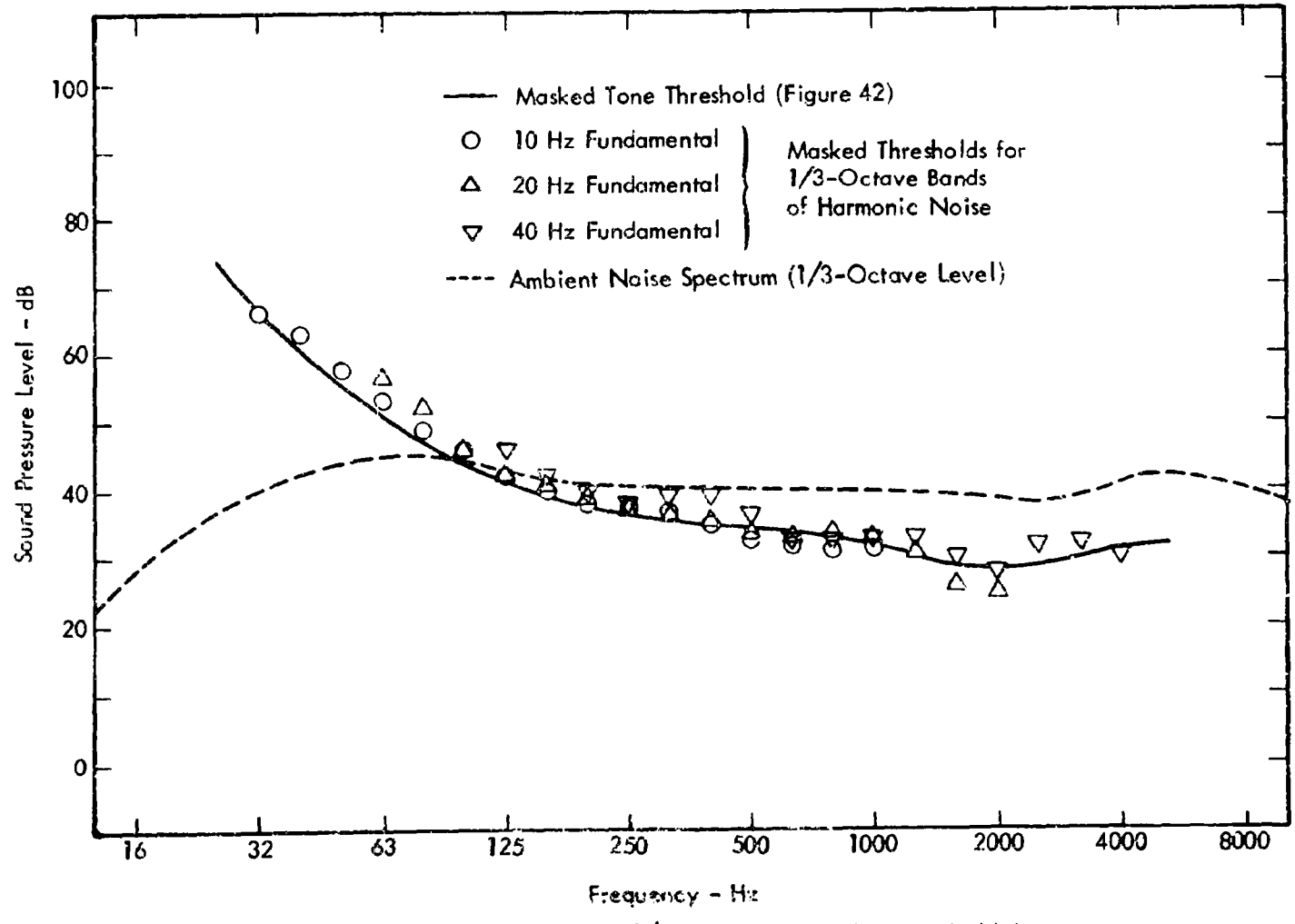

Figure 46. Masked Thresholds for 1/3-Octave Bands of Harmonic Noise.

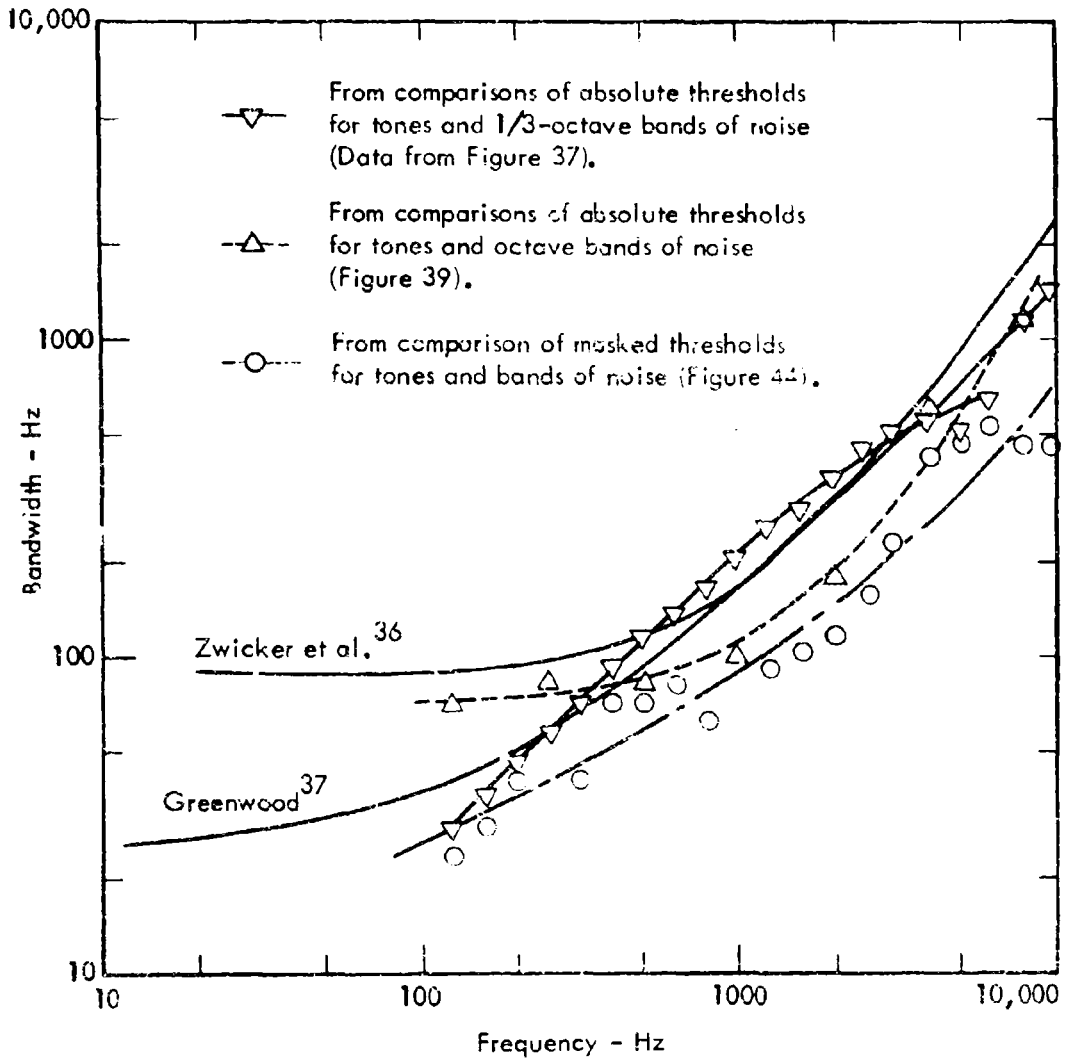

Figure 47. Comparisons of Critical Bandwidths Determined by Various Criteria.

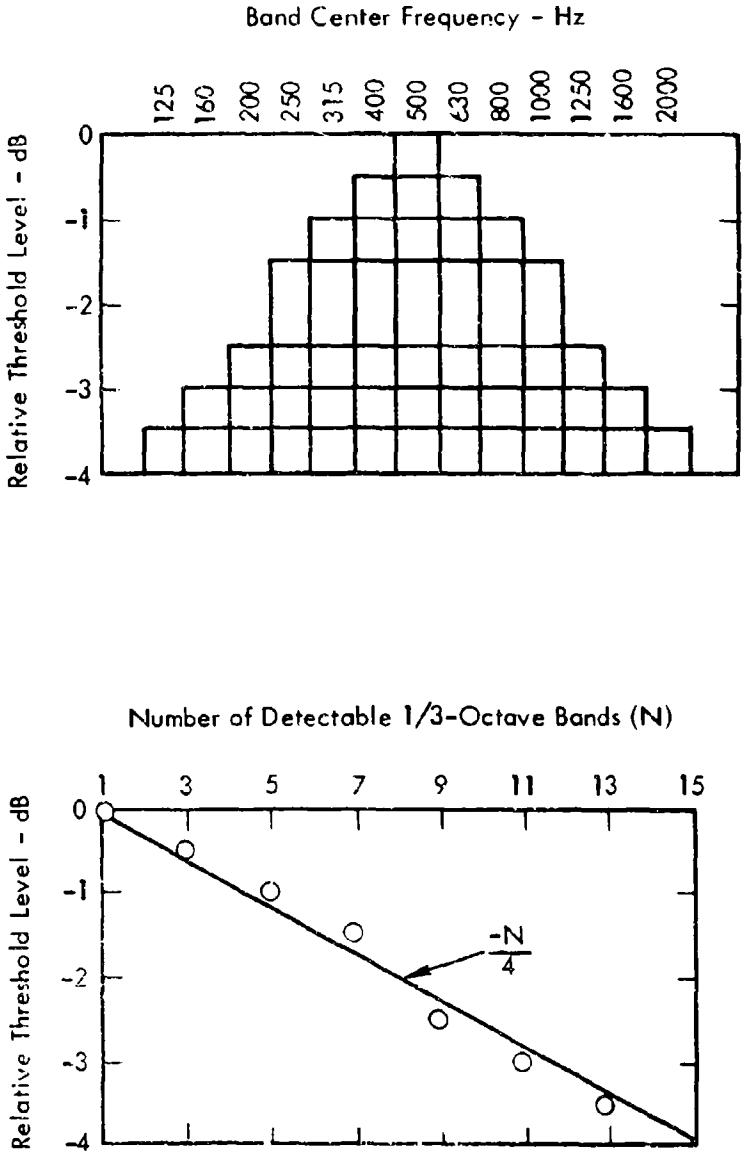

Figure 48. Depression of Masked Threshold by Multiple Band Detection.

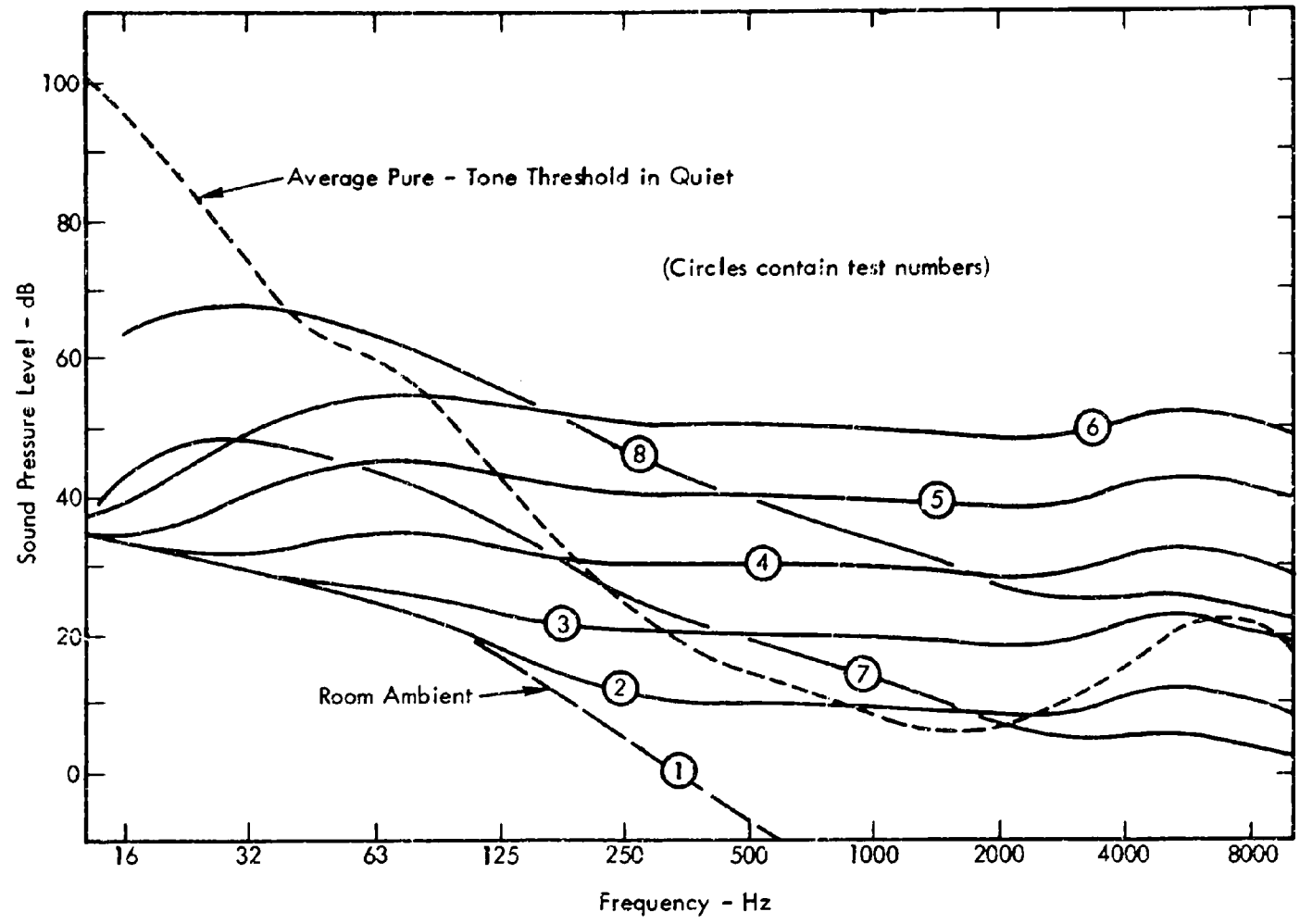

Figure 49. 1/3-Octave Band Level Spectra of Masking Noises Used in Validation Tests.

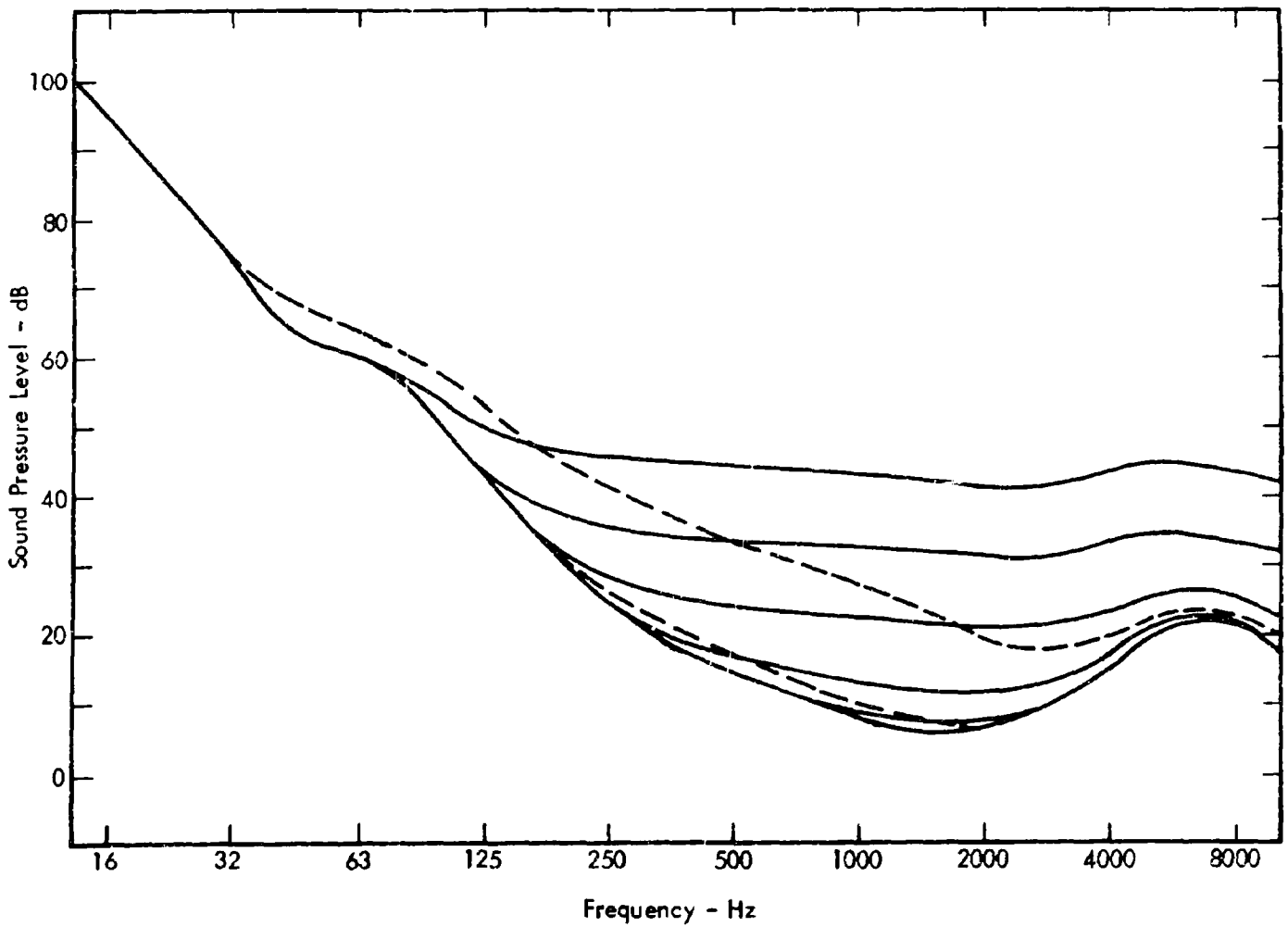

Figure 50. Combined Critical Band Audibility Thresholds Computed from Data of Figure 49.

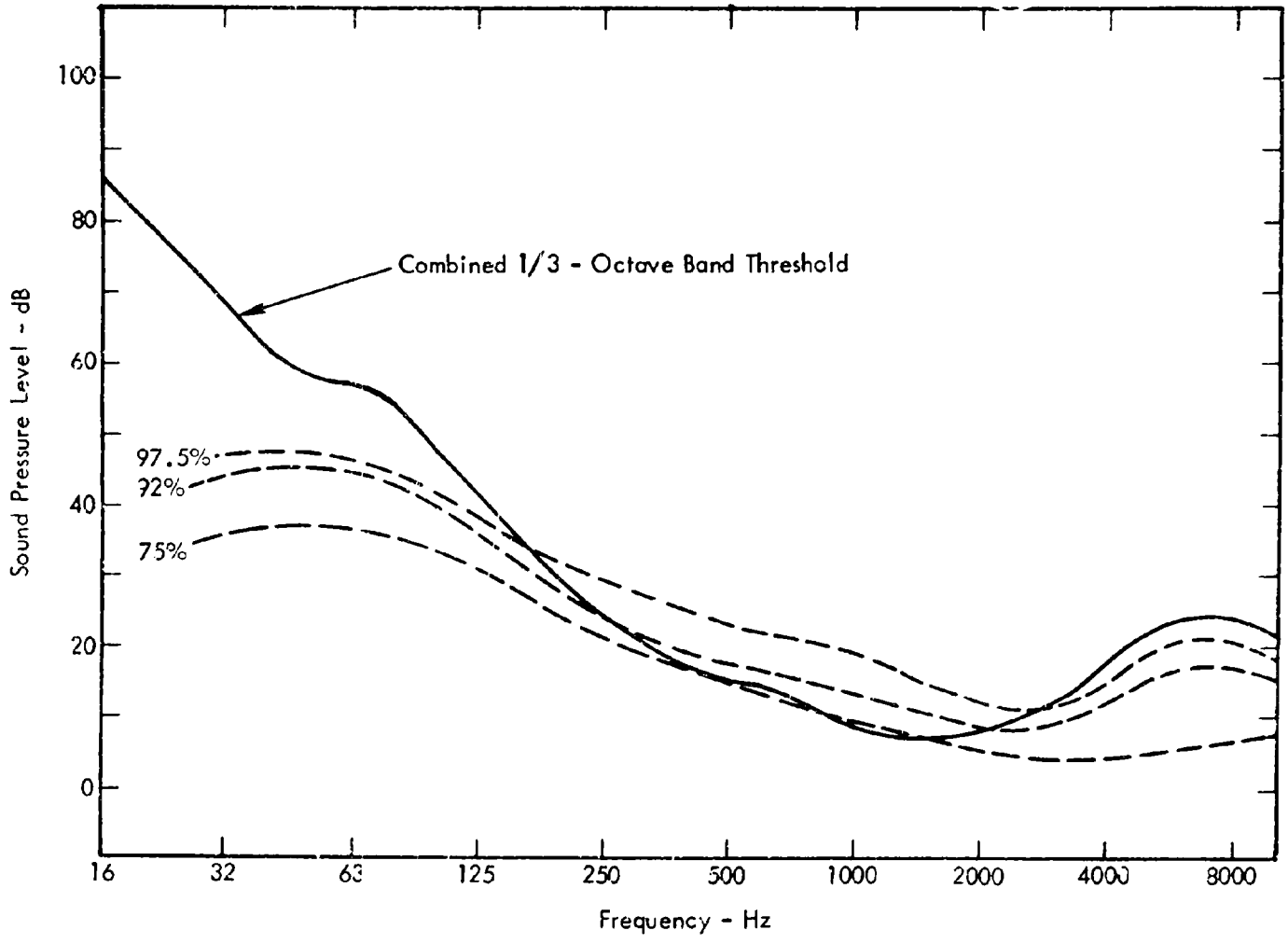

Figure 51. Percentile Distributions of 1/3-Octave Band Signal Levels at Threshold - Test 1.

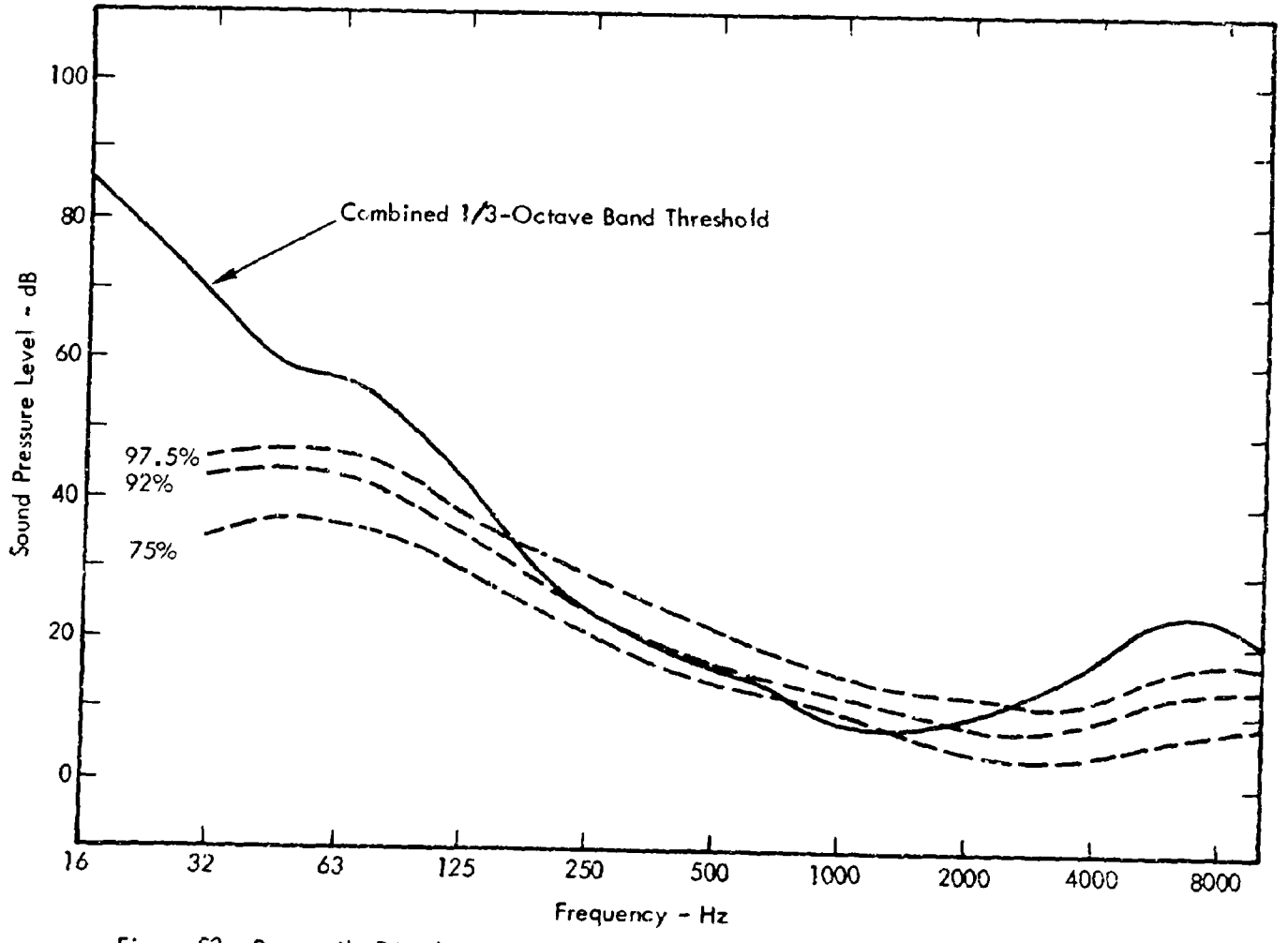

Figure 52. Percentile Distributions of 1/3-Octave Band Signal Levels at Threshold - Test 2.

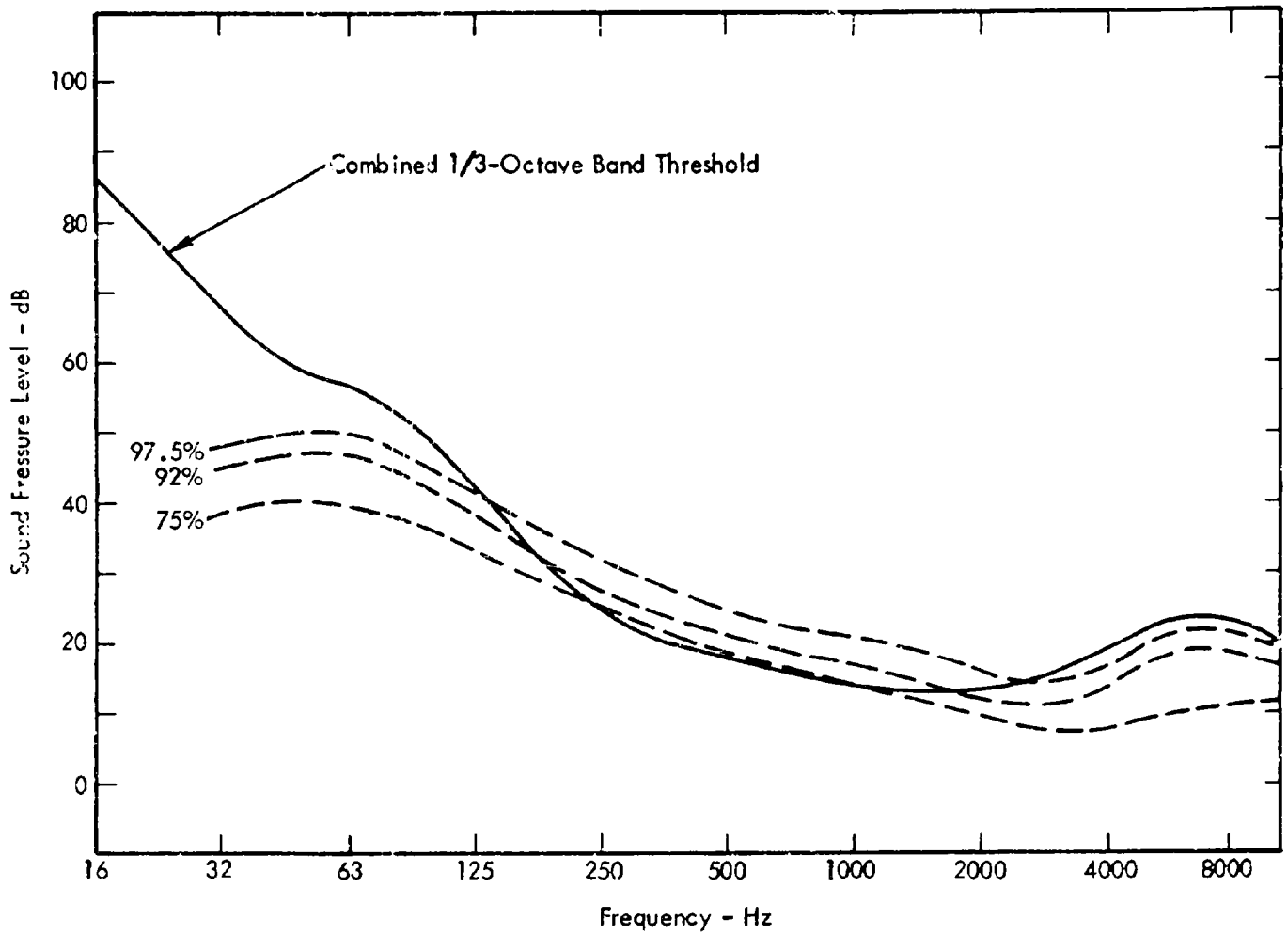

Figure 53. Percentile Distributions of 1/3 - Octave Band Signal Levels at Threshold - Test 3.

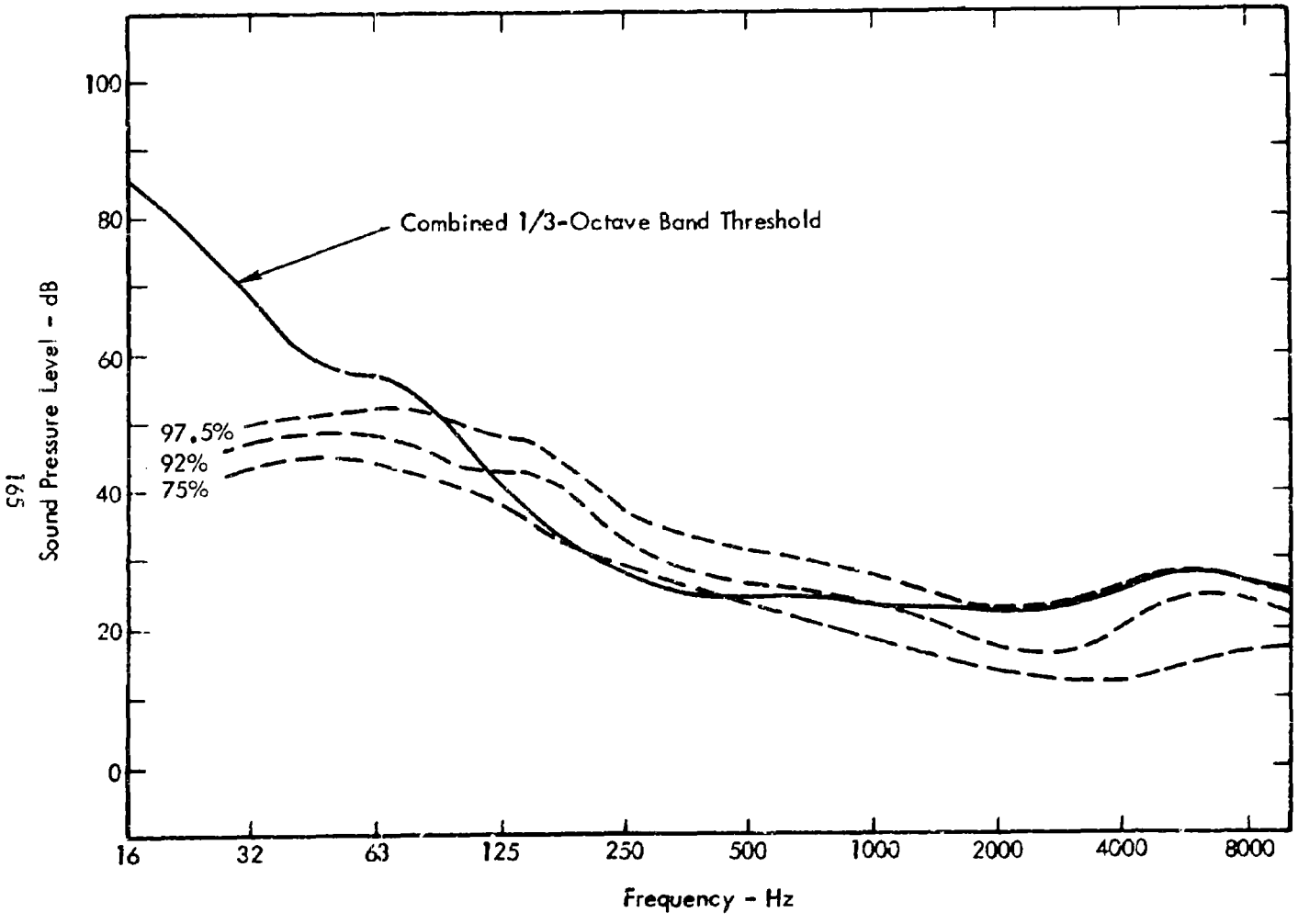

Figure 54. Percentile Distributions of 1/3-Octave Band Signal Levels at Threshold - Test 4.

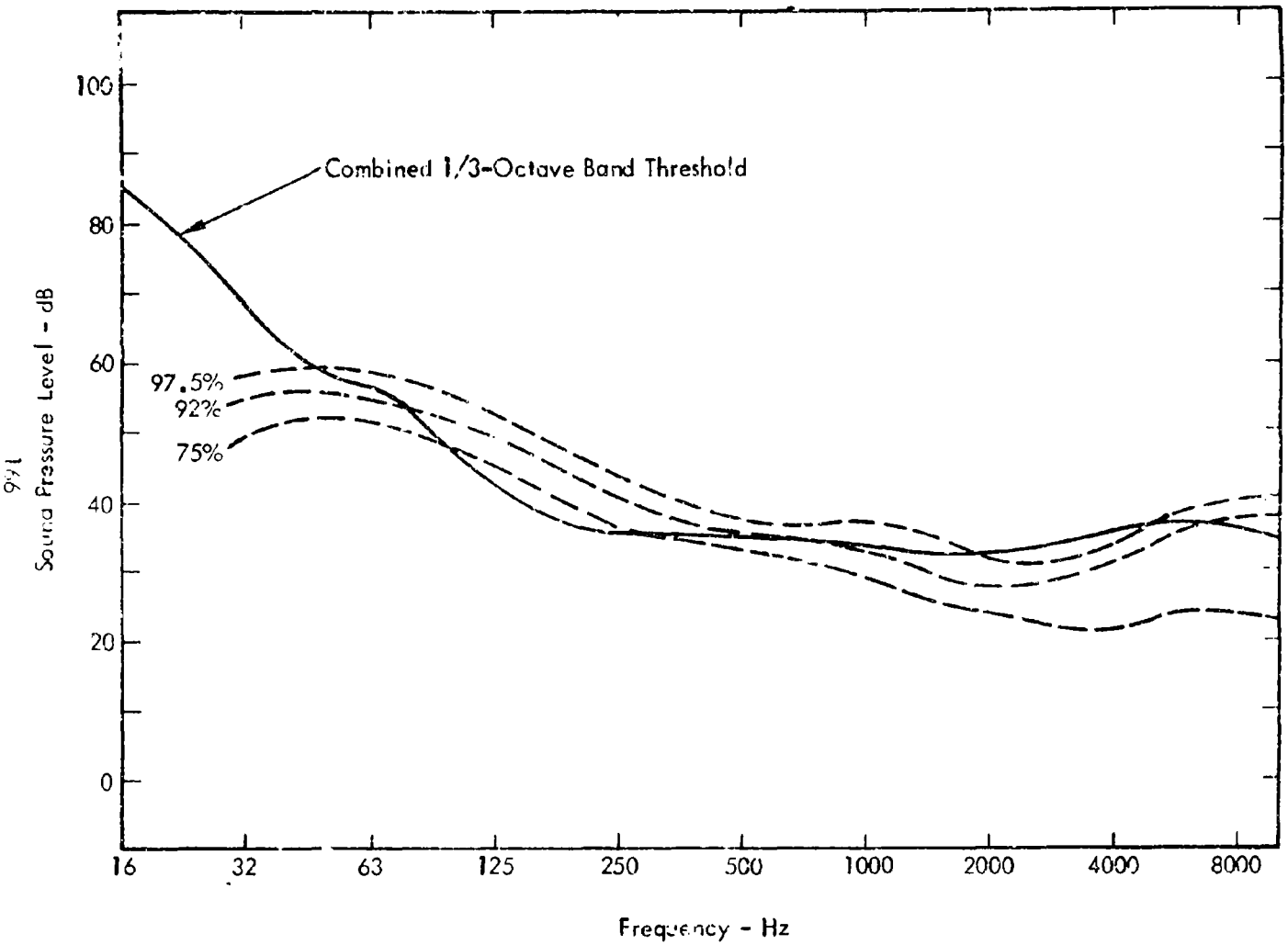

Figure 55. Percentile Distributions of 1/3-Octave Band Signal Levels at Threshold - Test 5.

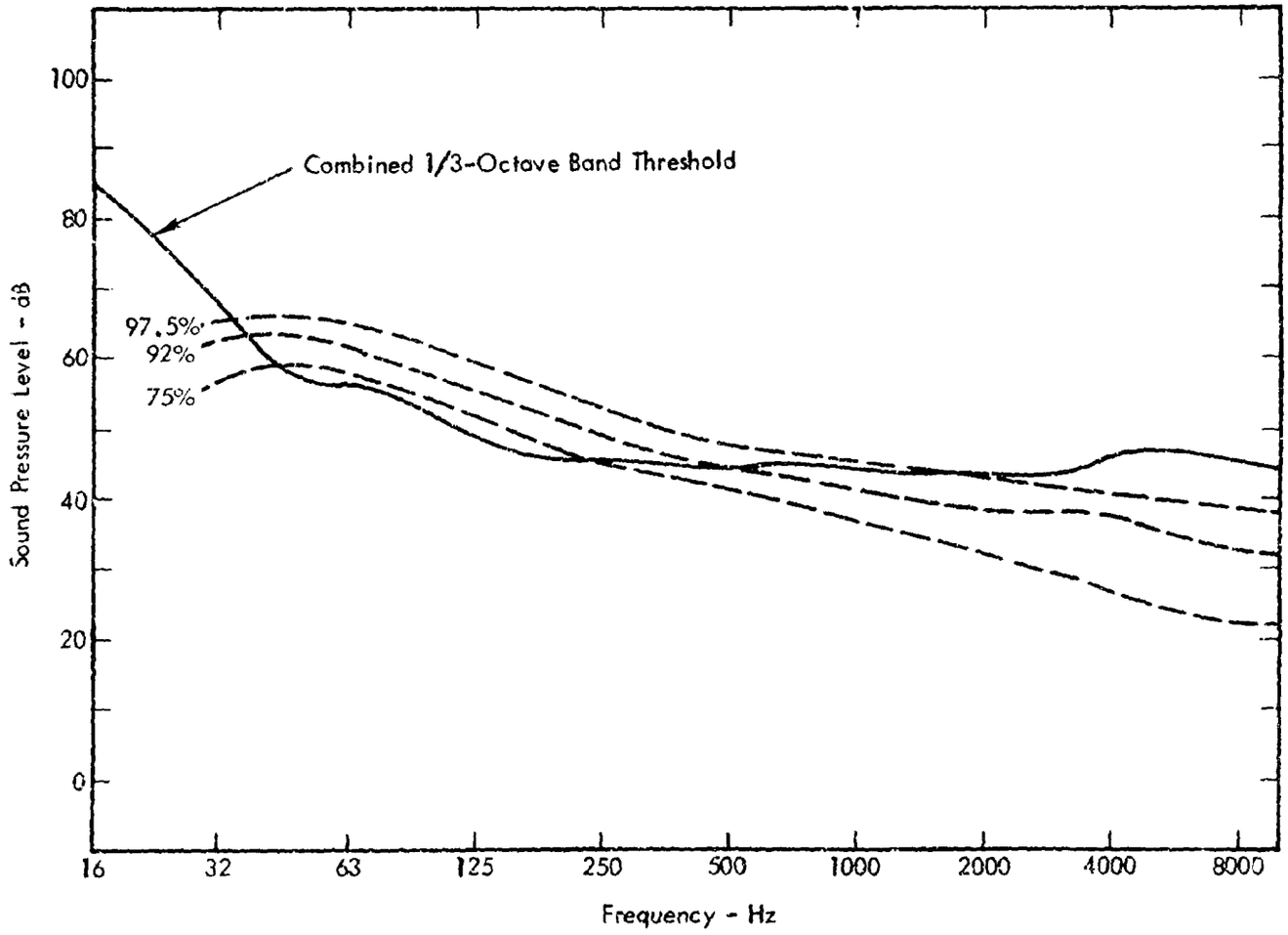

Figure 56. Percentile Distributions of 1/3-Octave Band Signal Levels at Threshold - Test 6.

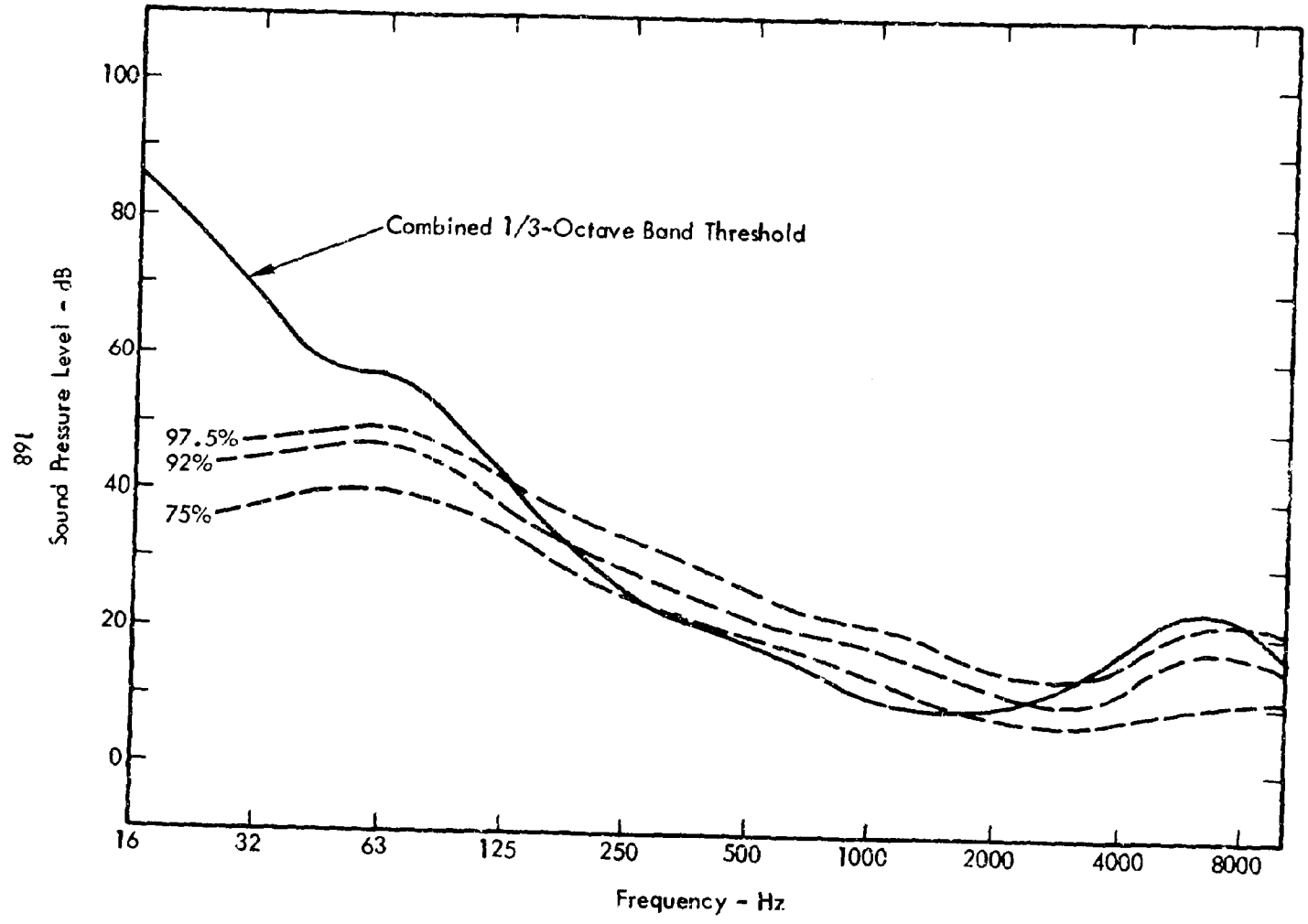

Figure 57. Percentile Distributions of 1/3-Octave Band Signal Levels at Threshold - Test 7.

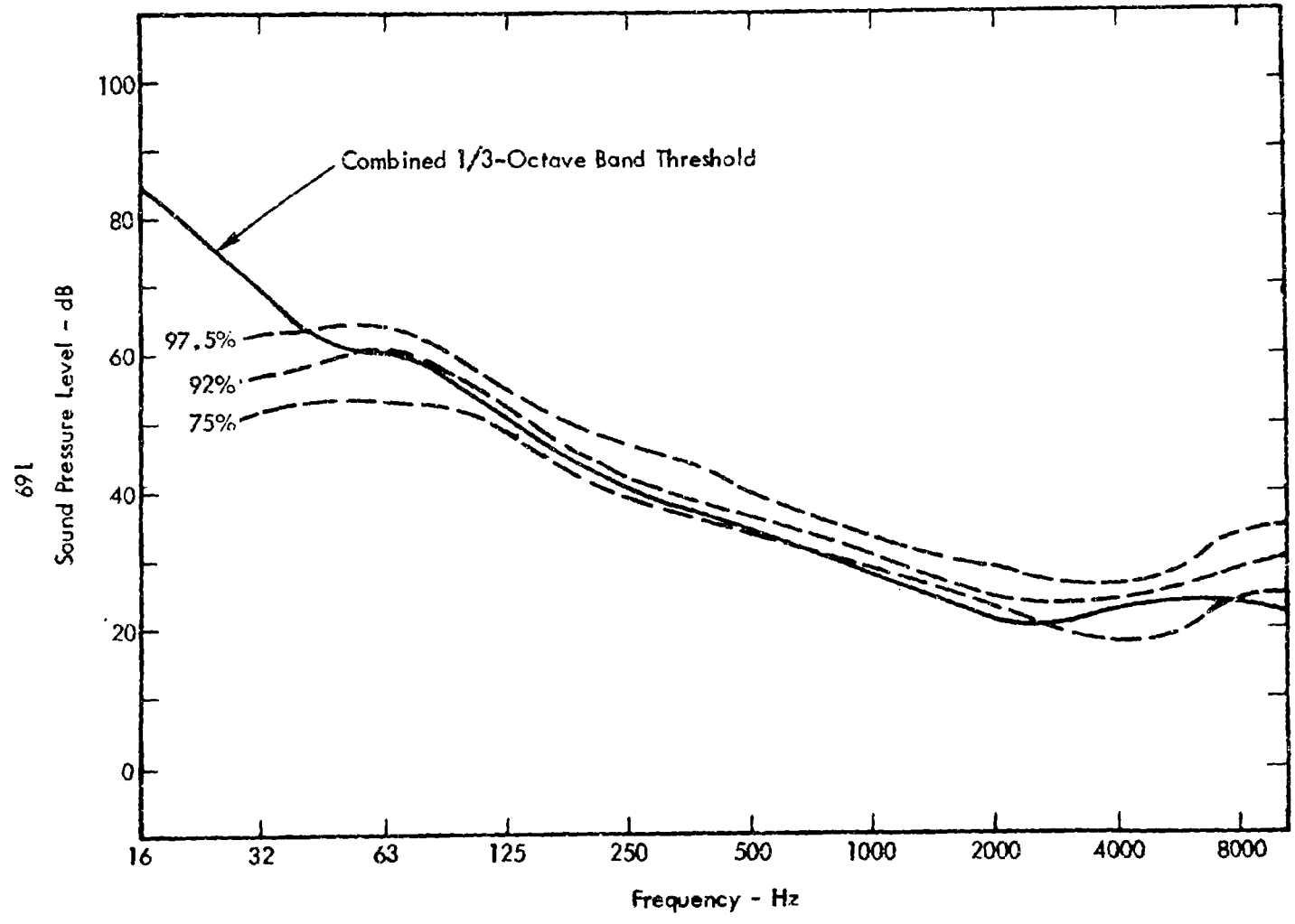

Figure 58. Percentile Distributions of 1/3-Octave Band Signal Levels at Threshold - Test 8.

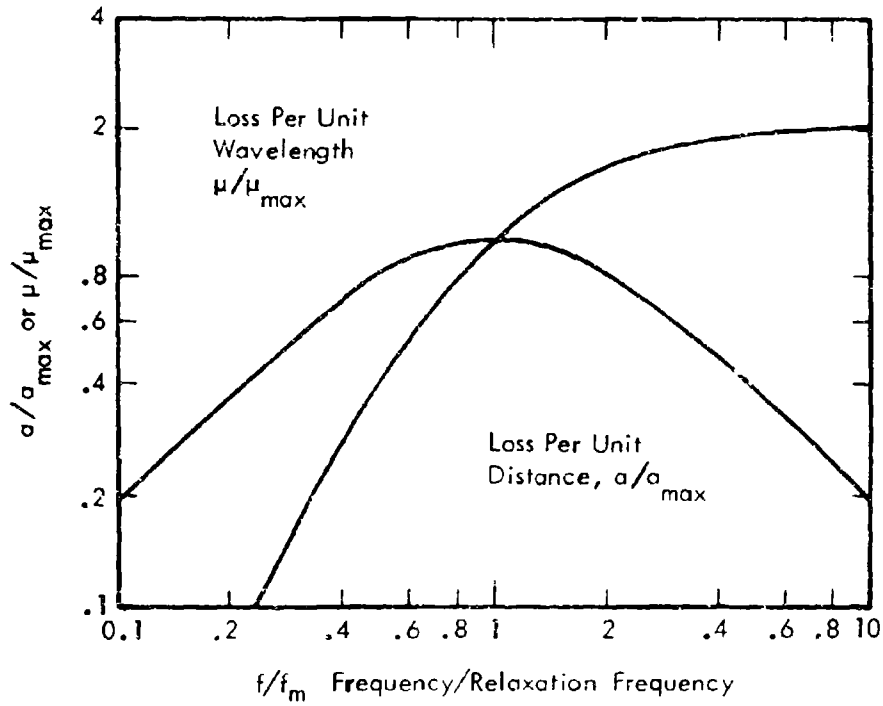

Figure 59. Variation in Normalized Relaxation Loss Coefficiency With Frequency Relative to Relaxation Frequency.

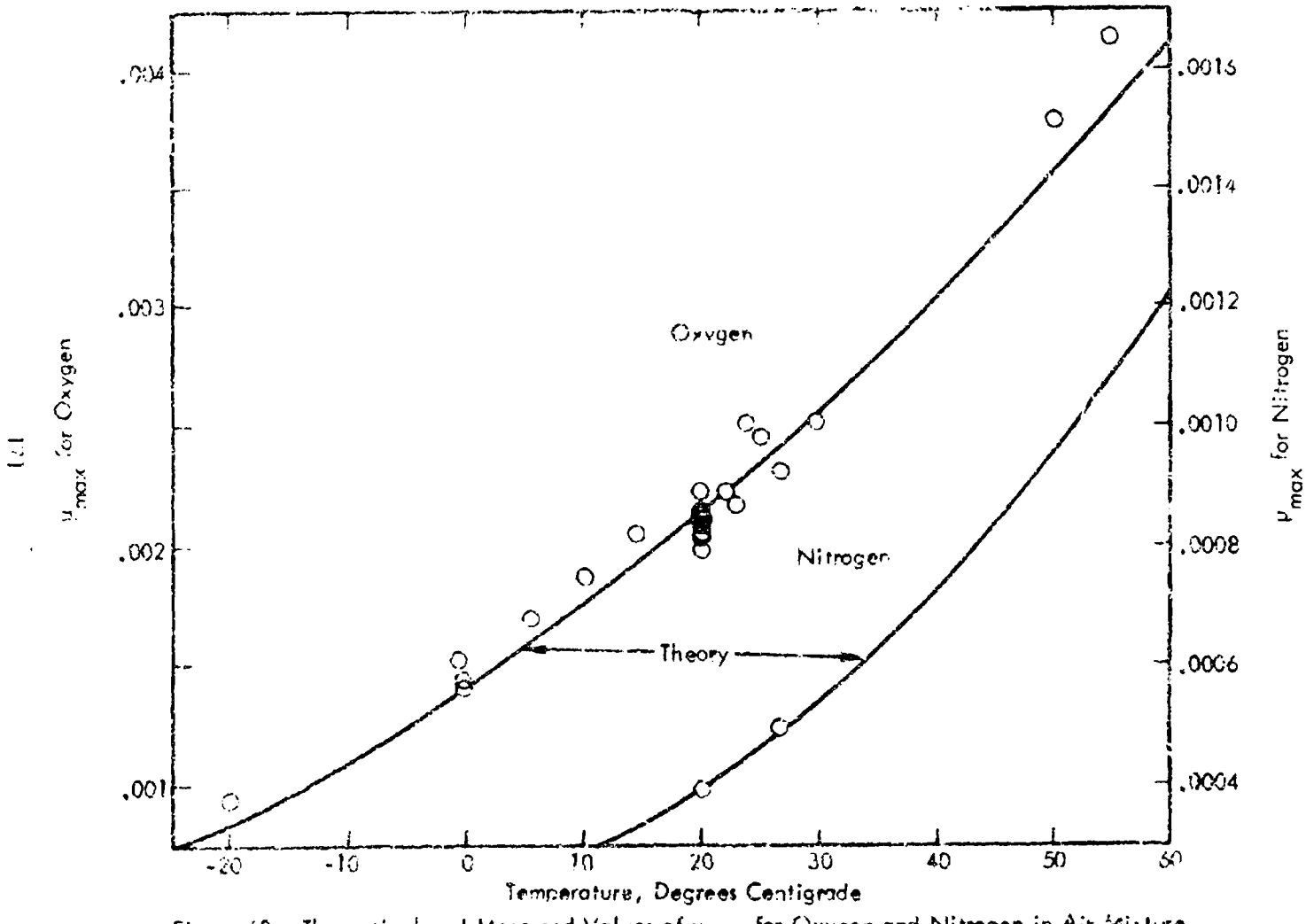

Figure 60. Theoretical and Measured Values of μ_{max} for Oxygen and Nitrogen in Air Mixture.

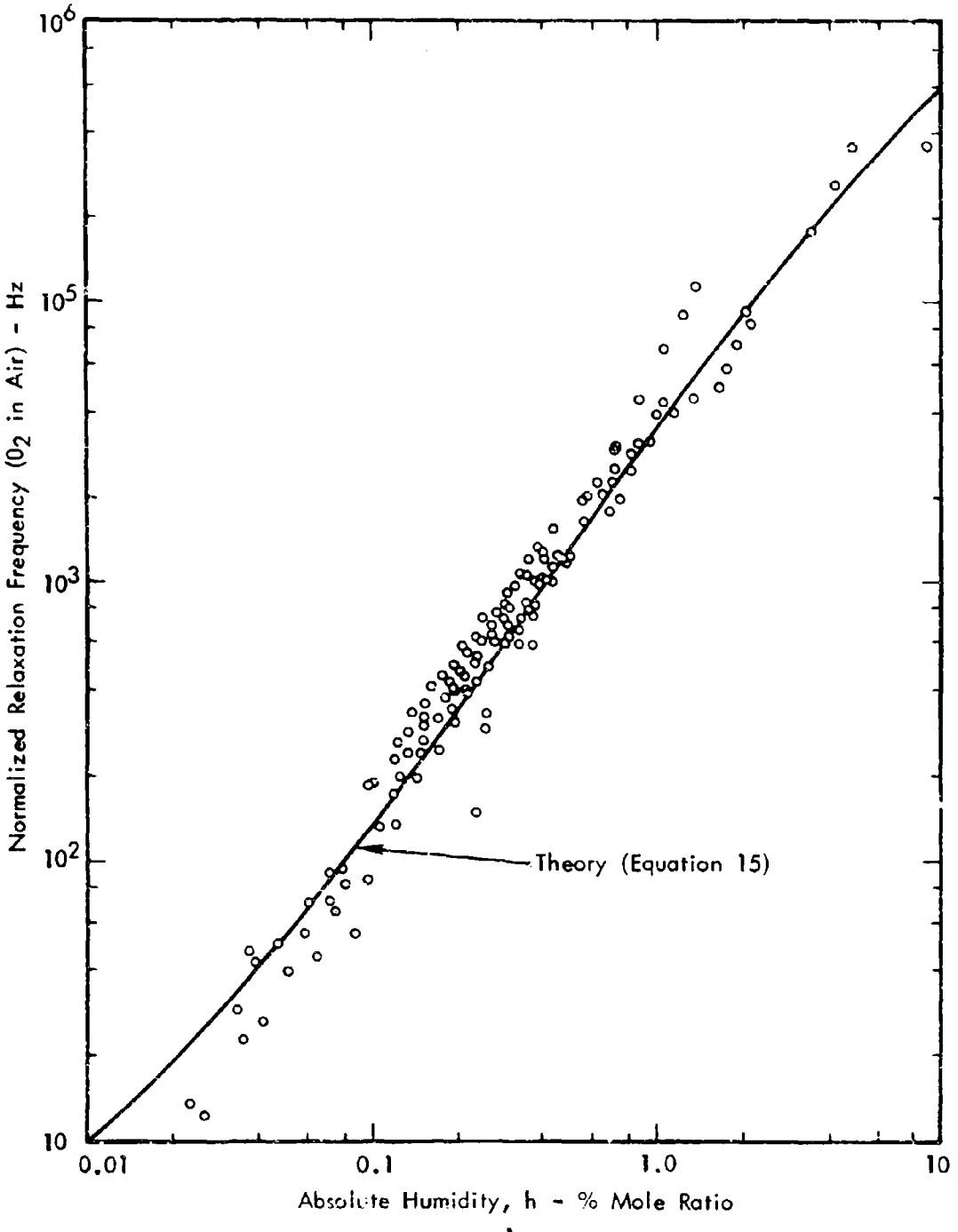

Figure 61. Measured Values of Relaxation Frequency for Oxygen in Air.

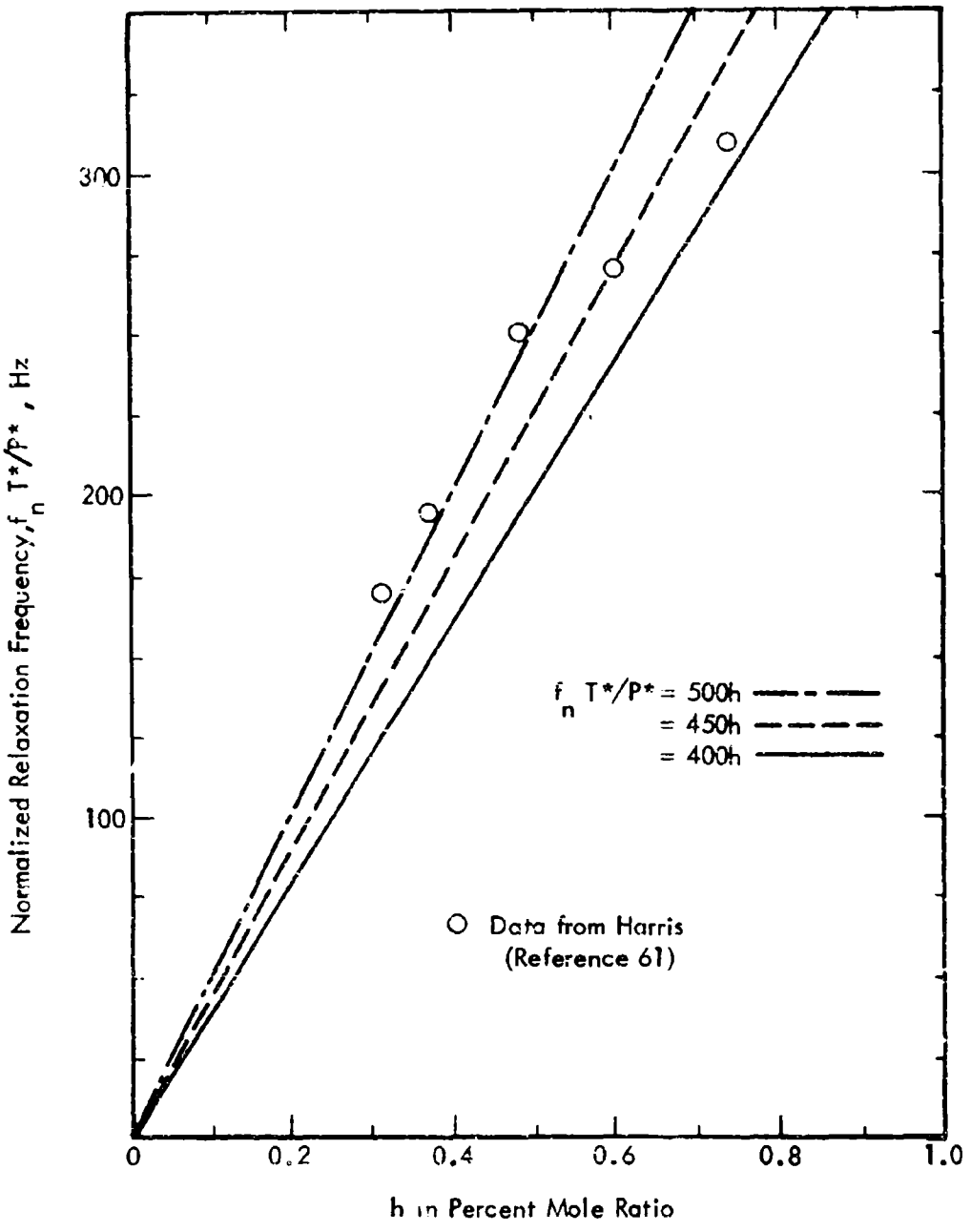

Figure 62. Relaxation Frequency of Nitrogen as a Function of Water Vapor Mole Ratio in Humid Air.

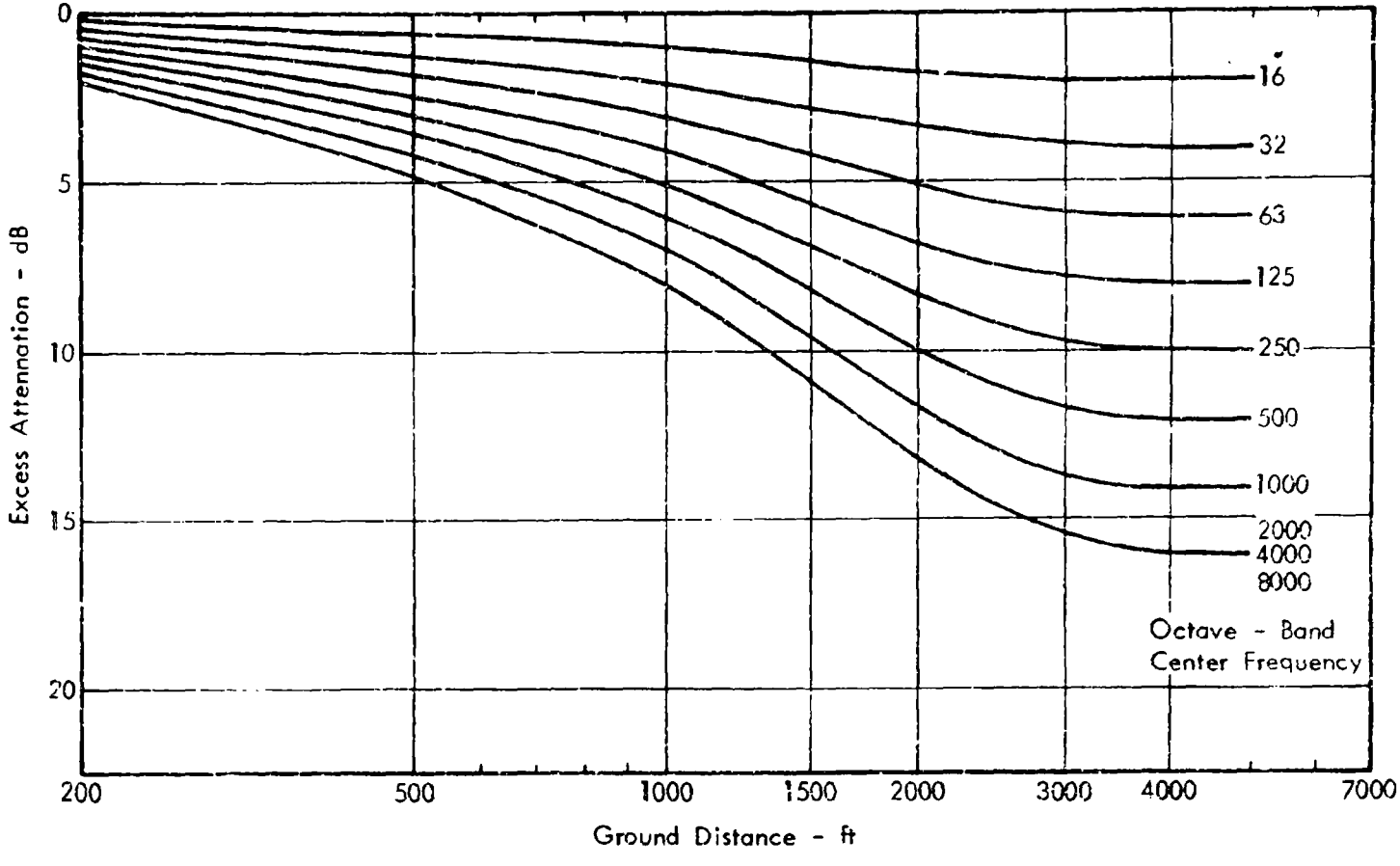

Figure 63. Excess Attenuation Due to Atmospheric Turbulence for Elevation Angles Less than 10°. (Adapted from Reference 80).

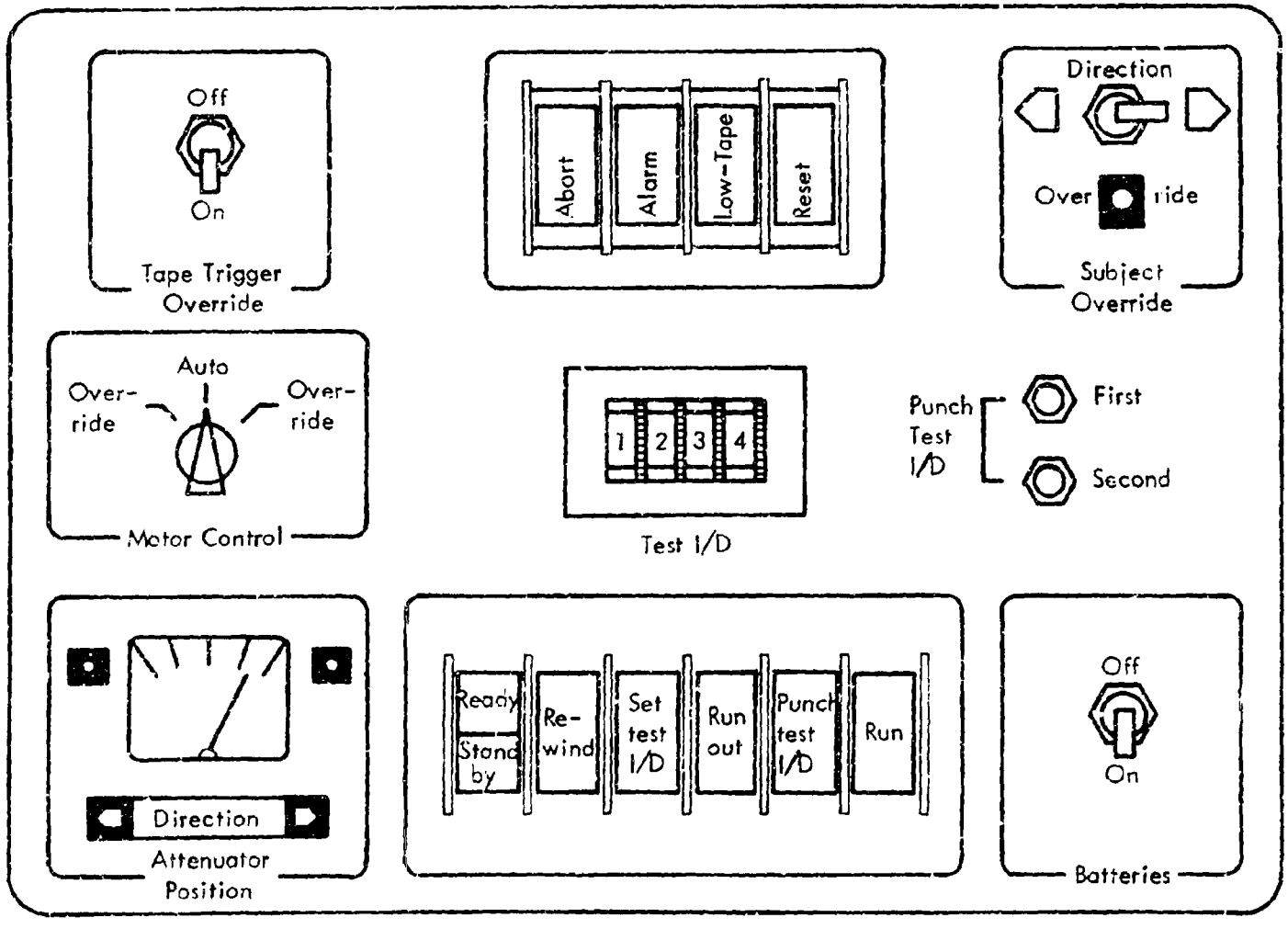

Figure 64. Data Acquisition System (DAS) Control Panel.

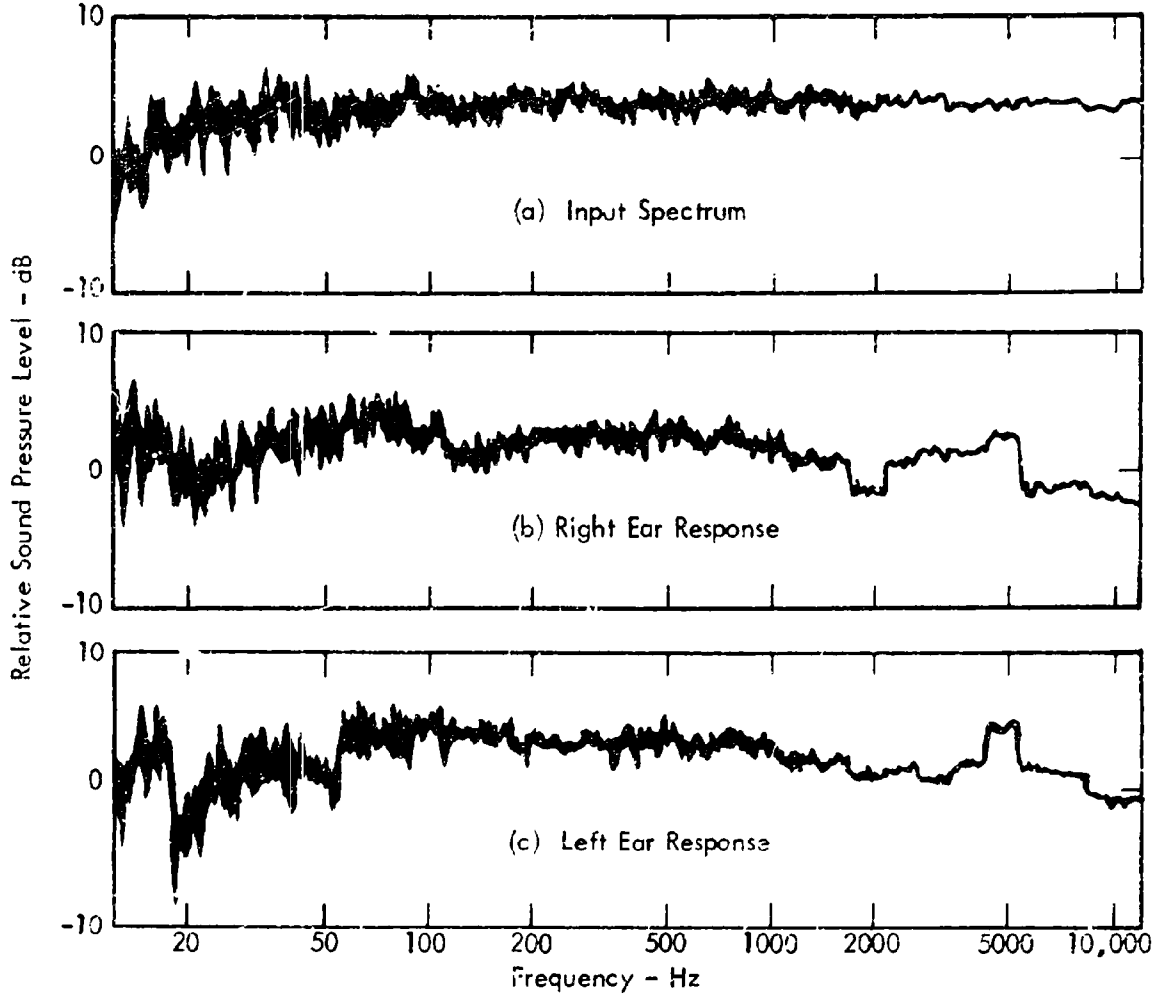

Figure 65. Response of System to Pink Noise Input (by 1/3-Octaves).

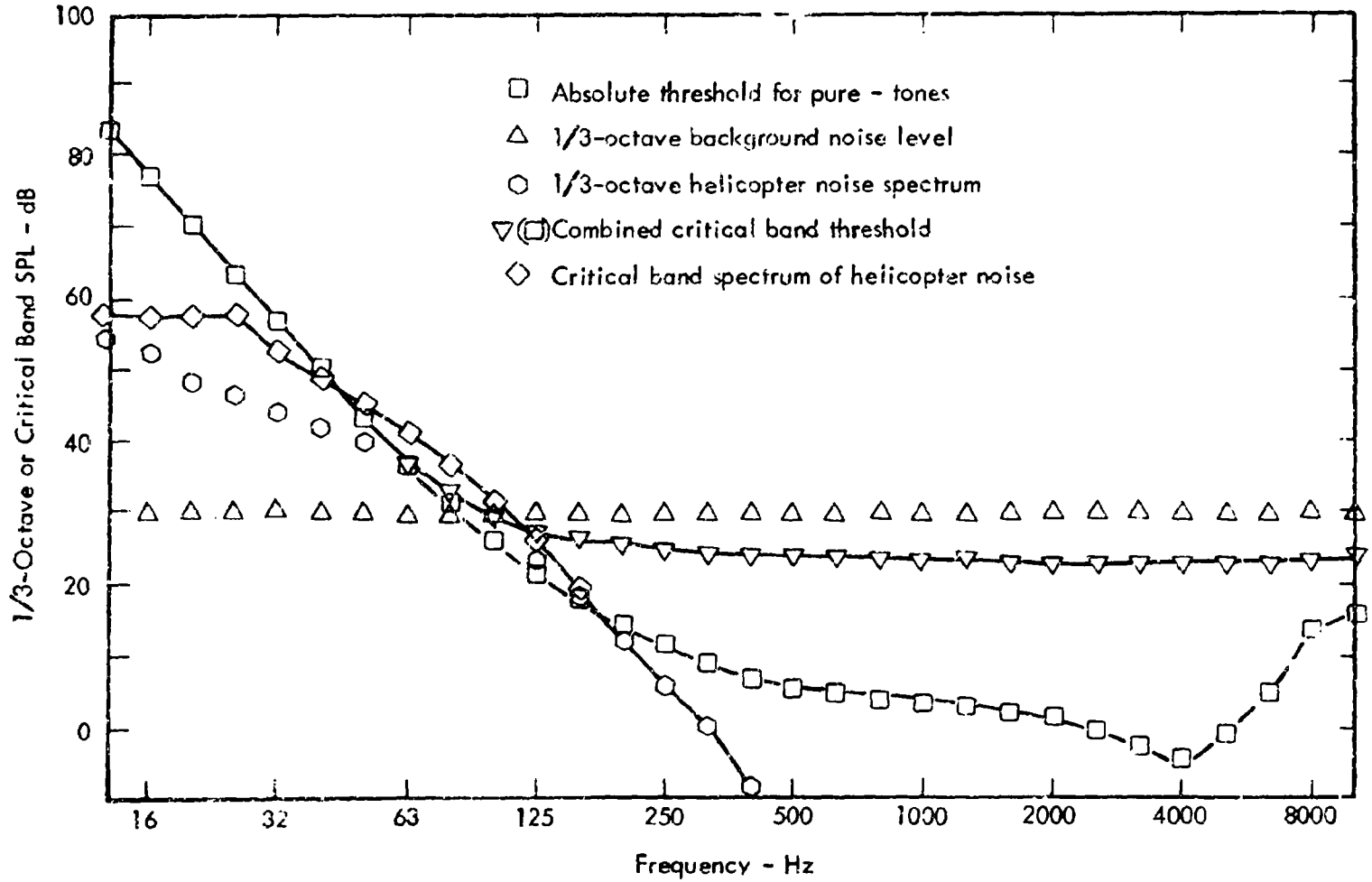

Figure 66. Example Calculation of Helicopter Audibility - Appendix III, Method A.

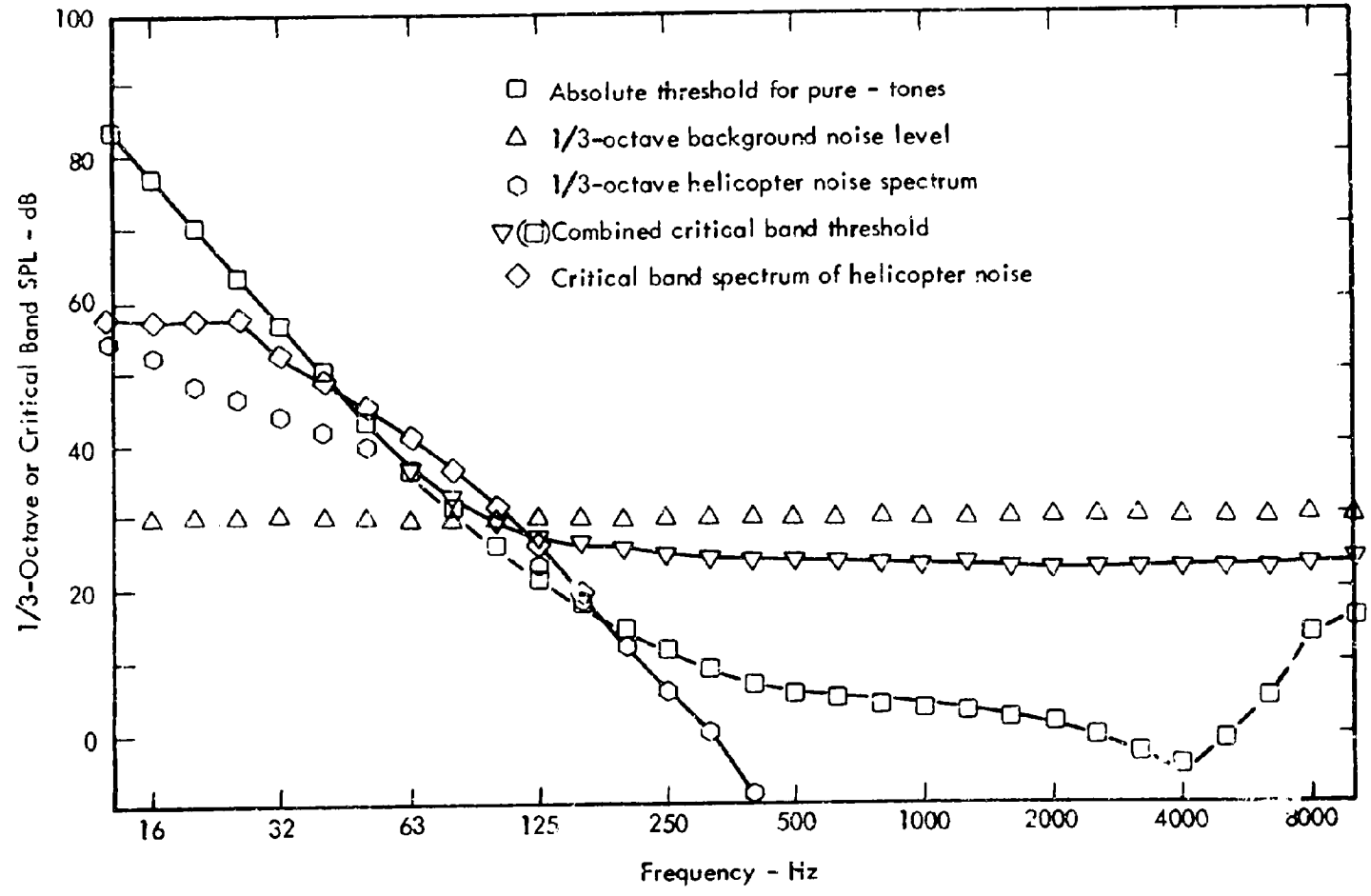

Figure 66. Example Calculation of Helicopter Audibility - Appendix III, Method A.